# Investigations into the Multiple Auditory Steady-State Response (MASTER) Technique In Humans

Michael Sasha John

A thesis submitted in conformity with the requirements
for the degree of Doctor of Philosophy
Institute of Medical Science
University of Toronto

# ABSTRACT

**Investigations into the Multiple Auditory Steady-State Response (MASTER) Technique in Humans**
Michael Sâsha John, Ph.D. Thesis March, 2001
Institute of Medical Science, University of Toronto

The Multiple Auditory Steady-State Response (MASTER) technique enables the rapid and objective assessment of hearing by statistically evaluating electrophysiological responses evoked by multiple tones which are presented simultaneously. The technique offers several advantages over transient stimuli techniques used to assess hearing. Firstly, since eight stimuli may be presented simultaneously, in the time normally required to evaluate one stimulus, MASTER provides a relatively rapid assessment of hearing. Secondly, the stimuli are more frequency specific than transient stimuli since steady-state stimuli contain spectral energy only at the carrier frequency and at the sidebands, which occur at spectral frequencies equal to the difference between the carrier and modulation frequency. Lastly, the technique reduces the necessity for expert evaluation of a subject's responses since these are evaluated objectively, statistically, and automatically by a computer program. The experiments presented here build upon the original work on the technique that occurred only a short time ago (Lins, 1995), and serve to form a sufficient foundation for the technique to start to be evaluated as a viable clinical tool. Chapter 1 demonstrates some limitations of the technique that should be considered when designing test stimuli. For example, in order to insure that simultaneously presented stimuli do not interact, they should be separated by at least one octave in normal hearing subjects. Chapter 2 provides a description of the theory, design, and implementation of a Windows based data acquisition system. In Chapter 3 the use of both amplitude and frequency modulated stimuli is examined. We show that by using both of these types of modulation the technique is more efficient, even at threshold intensities. In Chapter 4, the phase values of the responses are examined and a technique is proposed for accurately converting phases into latencies. As with amplitude, steady-state phase values are stable over time, show changes with intensity that are similar to those seen with transient stimuli, and are unchanged by the presentation of multiple stimuli. The work presented here suggests the MASTER technique can function as a useful clinical tool in objective audiometry, and suggests several directions that may be useful for future research. (349 words)

# ACKNOWLEDGEMENTS

While the work presented here was often difficult and sometimes even painful, it is important to remember that it is always an honor and a privilege to have the opportunity to engage in research. During my thesis research I have been supported by a Medical Research Council Studentship, which was provided by the Medical Research Council of Canada, which obtains its funding from taxes incurred by Canadians. Accordingly, I would like to thank Canadians, and the Canadian government for creating a society where science and education are still supported reasonably well: let us hope that this will continue in the future. Accordingly, I have tried to balance the investigations relating to basic science and physiology with attempting to advance a technique which seems very close to being ready to serve as a useful clinical tool in the near future. Hopefully, Canadians will soon get something useful back from supporting my research in this area.

I would also like to thank the Medical Research Council of Canada, James Knowles and the Baycrest Foundation for funding the research itself.

I would like to thank Terry Picton. Ideally, research should not occur in a vacuum. Sadly, I find that this is more often than not, the exception rather than the rule, especially when it comes to pursuing a Ph.D. Unlike many of my peers I had supervisor who acted as a constant source of support throughout the entire process. Terry Picton is one of the most hard working, thorough, smart, supportive, and fair scientists I have ever met, and it has been a great privilege and quite a bit of fun to work with him over the last 3 years.

The work in this thesis was also largely aided by the hard work of Otavio Lins, Bridget Boucher, Hilmi Dijani, and Patricia Van Roon, as well as the helpful advice provided by Martin Regan and Jos Eggermont.

Lastly, I would like to thank the data. Even a well-designed experiment will not yield the expected results if the physiology doesn't happen to work the way you think it does. In the words of Endel Tulving "In successful research you can be at odds with other scientists, in fact this is often good, but you can NEVER afford to be at odds with Mother Nature." The data in this thesis were often beautiful, told their story loudly, replicated very nicely, and contained few outliers. They were a pleasure to work with.

This thesis is dedicated to the incredible friends I have made while living in Toronto, to my fellow lab geeks, and to my housemates who have all given me a lifetime of memories over the last few years (most of them good, few of them sane). Of course, this thesis is also dedicated to my family (especially Josh-the-B-Guash-man), most of whom have acted as a constant source of support and with whom I still talk to every week.

...And, of course, to Katherine, A.K.A. "Huggy Buggy"

# TABLE OF CONTENTS

# LIST OF TABLES

## Chapter 1



## Chapter 3



## Chapter 4

# LIST OF FIGURES

## Introduction



## Chapter 1



## Chapter 2



## Chapter 3

## Chapter 4

# List of Abbreviations

| | |
|---|---|
| AD | Analog-to-digital |
| AM | Amplitude modulation |
| AM/FM | Simultaneous AM/FM modulation |
| ASSR | Auditory steady-state response (s) |
| CF | Center frequency (usually of an auditory fiber) |
| CN | Cochlear nucleus |
| CPU | Central Processor Unit |
| Cz | Signifies vertex scalp location in 10-20 system |
| DA | Digital-to-analog |
| dB | Decibel |
| df | Degrees of freedom |
| DMA | Direct memory access |
| DPOAE | Distortion Product oto-acoustic emission |
| EEG | Electroencephalogram |
| E or $\varepsilon$ | Epsilon (estimates covariance between measures) |
| ERP | Event related potential |
| EP | Evoked potential |
| FFT | Fast Fourier Technique |
| $F_c$ | Carrier frequencies |
| $f_m$ | modulation frequencies |
| FIFO | First-in-first-out buffer |
| Fisher LSD | Fisher's Least Significant Difference post-hoc test |
| FM | Frequency modulation |
| HL | Hearing level |
| Hz | Hertz |
| IAFM | Independent AM and FM modulation |
| IC | Inferior Colliculus |
| kHZ | Kilohertz (1000 Hz) |
| kOhm | 1000 ohms |
| MASTER | Multiple auditory steady-state response (s) |
| Mb | Megabyte |
| MHz | Megahertz |
| MM | Mixed Modulation (AM/FM at same modulation rate ) |
| ms | Millisecond (note: occasionally also 'msec') |
| MTF | Modulation transfer function |
| pa1 | File or Parameters associated with defining stimuli in the MASTER system |
| pa2 | File or Parameters associated with defining recording parameters in the MASTER system |
| PC | Personal computer |
| P-P | Peak-to-peak (measure of amplitude) |
| RAM | Random Access Memory |
| RMS | Root-mean-square (measure of amplitude) |
| SOC | Superior olivary complex |
| SPL | Sound pressure level |
| $T^2$ | Hotelling's $T^2$ test |
| V | Volts |
| VCN | Ventral cochlear nucleus |
| VI's | Virtual instruments |
| $\mu$V | Microvolts (1volt/1,000,000) |
| nV | Nanovolts |
| $\Delta f$ | Change in frequency |
| $\pm$ | above and below a given value |
| $\Sigma$ | Sum of components |

# Foreword

The idea of automatic and objective evaluation of electrophysiological activity is fascinating and immediately presents many wonderful challenges! My research has concerned automatic or computer-aided evaluation of brain activity for some years. In 1991 I finished an honor's thesis in the department of psychology at Reed College concerned with the automatic detection of deception using a technique which incorporated multiple stepwise discriminant analysis, in which the computer would somewhat automatically provide a probability estimate that a person was intentionally lying. During my graduate work at McGill, where I took my first course in signal processing and was introduced to MATLAB (possibly the greatest software program ever written), I began to build more sophisticated computer programs which evaluated brain activity using signal analysis techniques such as the FFT and the short-time FFT (which is similar to wavelet analysis). I also became interested in emerging areas such as adaptive neurostimulation, objective measurement of anesthetic depth, automatic source analysis of brain activity, objective and quantified measurement of responses to novel pharmaceutical compounds ("pharmaco-EEG"), and other areas which have led to several very interesting projects and even one or two patents.

While the research presented in this thesis continues to focus on objective methods of evaluating brain activity, it also marks the latest stage in my efforts towards becoming a fairly knowledgeable, well-rounded, and competent scientist. My past research gave me a foundation in cognitive evoked potentials, QEEG, EEG during rest, mental load, and sleep: in other words, I was concerned with the brain as a whole. My work on this thesis gave me the opportunity to focus on a specific primary sensory area for the first time. I have begun to understand how the cochlea, which I knew nothing about 3 years ago, performs various tasks which act to provide us with an incredibly sophisticated hearing machine. To be honest, when I started a thesis on this topic I did not do it out of interest in the area (after all, why study the keyboard when you can study the computer?). It was more like taking an acrid medicine: I did it because I thought that it would be good for me to move away from looking at the system as a whole and learn about a specific part. I did not think it would be fascinating. I was wrong.

# INTRODUCTION

*Overview of the Thesis*

The four chapters of this thesis cover a considerable amount of material. An overview is important, not only because it will give readers a general feeling for what will be presented here, but also because it will help to provide some understanding of the reasoning and processes that acted to shape the direction of the research and the questions that were asked. The progression of the chapters of this thesis reflects my increasing familiarity with the MASTER technique. Chapter 1 is the result of research that we conducted when I first came to Dr. Picton's laboratory in 1997. The research in this chapter was done using a specialized DOS based system that he had built in Ottawa using C for a programming language and customized data acquisition boards. Lins and Picton (1995), building upon some experiments which were done in the visual modality, and carried out over two decades earlier by David Regan (1970), had recently shown that multiple auditory steady-state potentials could be evoked by presenting several AM tones simultaneously. The work in Chapter 1 represents both their efforts to obtain a more concrete understanding of the technique and the evoked responses (in terms of the types of interactions that may occur between stimuli) and my efforts to figure out what they were up to and attempt to determine why it was sensible. In line with this research dynamic, much of this thesis is a combination of a tension between feeling that I knew enough about what we were doing to push the technique forward and feeling a bit hesitant, which would cause me to draw back, check our assumptions, approach the data slightly differently, and re-evaluate our ideas about the technique. By way of example, Figure 1-2 of Chapter 1 resulted from the concern about the validity of a dual method using both averaging and long FFT sweeps in order to provide optimum signal-to-noise levels in our recordings. The figure shows one of several tests that we carried out during this thesis work in order to check the basic processes of the technique. As a second example, we again tested the validity of this dual method, as well as our strategy for removing artifacts, as is seen in Figure 2-7. In Chapter 1, I also re-evaluated the finding made in Lins and Picton (1995) that only 4 stimuli should be presented to each ear. Was this limitation due to the carrier frequencies being too close together or was it a function

of closely spaced modulation frequencies? We found that up to 4 stimuli could be presented simultaneously provided that the carrier frequencies were separated by at least 1 octave (Tables 1-1, 1-2, and 1-4 of Chapter 1). Modulation frequencies of adjacent stimuli, it seemed, could be set very close to each other without decreasing the amplitudes of the responses (we put this finding to the test again in Chapter 4). Lastly, I examined both the 40 Hz range and the 80 Hz range since Lins et al. (1995) had previously shown that the responses above 80 Hz were not attenuated by arousal level or sleep, which was not the case for the stimuli in the 40 Hz range. By comparing the results of Tables 1-2 and 1-6 we found that the 80 Hz responses were attenuated less than those in the 40 Hz range when multiple stimuli were presented. Accordingly, in the research presented in the subsequent chapters of this thesis, we will always use modulation rates above 70 Hz. The reminder of the research in Chapter 1 primarily concerned an area with which I had very little experience: modeling of the data to explain interactions between stimuli. Initially, this was beyond my comprehension since I had never heard of things like tuning curves, excitation envelopes, or compressive rectification. This initial project, therefore, enabled me to obtain some familiarity with the mechanisms of the cochlea, to discover how one could approach figuring out how these mechanisms led to the recorded responses, and acted to give me my first real taste of the extraordinary complication, stunning simplicity, and unquestionable beauty of the auditory system.

The research in Chapter 1, effectively catapulted me into the world of the multiple auditory steady-state response (MASTER) technique. I now had a reasonable appreciation for the power of the technique and understood some of its strengths and weaknesses: it was time to get my hands a bit dirty. During the experiments of Chapter 1, I had regarded the data acquisition system in the laboratory as a sort of black box, where the stimuli were created and the responses evaluated through a set of very complicated processes. For several converging practical reasons, but also so that I could really understand the technique from the ground upwards, we decided it would be a good idea if I built a Windows based data collection system for using the MASTER technique. Chapter 2 describes the MASTER data acquisition system which was the result of about 8 months of programming and learning about buffering techniques, timing issues, data

transfer, and other headache-inducing topics. Indeed, the project enabled me to become well acquainted with the different areas of the MASTER technique from the generation of stimuli to the statistical evaluation of the responses. Importantly, creating a data collection system enabled the addition of several features lacking in the original system, such as the option of saving the raw data, so that it could be re-played or re-analyzed. This feature enabled our evaluation of data to become dynamic. In other words, results could be analyzed at different periods of the data collection. Consequently, we have been able to obtain the type of results seen in Figure 2-6, where response detection over time is shown, and this also enabled us to perform an in-depth evaluation of the percentage of false positives and false negatives that occurred as recording sessions progressed. The MASTER system also enabled us to explore the technique, by allowing us to easily alter recording parameters or even the way in which data was evaluated, and thereby let us rapidly confirm hypotheses and explore new areas. The data collected in this chapter was important not only because it served to validate our statistical methods and artifact techniques, but also because it led to the next set of experiments. A paper by Cohen et al. (1991) had previously demonstrated steady-state responses to stimuli that were both AM and FM were larger than responses evoked by AM alone. As can be seen in Figure 2-6, we extended these findings to the multiple stimulus case and showed that at 50 dB SPL, the stimuli that were both AM/FM produced responses that were about 130% larger than the responses to simple AM stimuli leading to response detection in about ½ the time required by the simple AM stimuli. Thus, in addition to evaluating 8 stimuli in the time it would normally take to evaluate 1, this study provided evidence that the test could be made even more rapid by using AM/FM stimuli.

Chapter 3 was the subsequent logical step due to the data collected in Chapter 2, and investigated, in more depth, the properties of the responses to stimuli that were AM, FM, or AM/FM combined ("mixed modulation" or MM). In the first part of the paper, we examined the responses to different depths of AM and FM and attempted to make some comparisons between the two types of responses both in terms of amplitude and phase. Importantly, we considered the responses in the context of the amplitude spectra of the AM and FM stimuli and introduced some basic principles which should enable readers to make more sense of the results. For example, the fact that 50% AM and 50% FM stimuli have such different spectral characteristics indicated that AM and FM depth

must be treated somewhat differently. After examining AM and FM separately, we examined MM stimulation. In much of the experiments in this chapter, in the case of MM, the AM and FM components occur at the same rate (as was the case in Chapter 2), causing only one response to appear in the amplitude spectrum. By changing the phase of the FM relative to the AM, we found that the MM response *seemed* to be the vector sum of the two separate responses. Using a very elegant (yet simple) model that was developed by Dr. Picton, we were then able to model the two responses and formally demonstrate that the response to MM stimuli could be understood as the simple vector addition of the response to AM and FM alone. Accordingly, the data collected in this chapter provided plausible evidence of the independence of these two processing systems. Another interesting finding of this chapter was that the MM augmentation was present not only at 50 dB SPL, but also at 40 SPL and 30 dB SPL. This finding indicated that MM stimuli should help facilitate obtaining responses near threshold, where the MASTER technique begins to encounter trouble and requires considerably larger amounts of data for the detection of responses (Herdman and Stapells, 2000). The last topic of Chapter 3 that will be touched upon here is the idea of independent AM and FM modulation (IAFM) for the same carrier frequency region: in other words, by modulating the AM and FM at two independent rates, two responses in the amplitude spectra of the EEG could be evoked. We were originally very excited by this finding because it raised the possibility of developing a new statistic that could make use of the two responses evoked in the same area of the cochlea. While our initial attempts did not suggest that this method would provide more rapid detection of responses than the MM approach (where AM and FM occur at the same rate), the IAFM method may still be very useful because it provides information about the processing of the two types of modulation in each frequency range.

The last set of experiments is contained in Chapter 4, which examines the phase of the steady-state response. Much of the data presented in this chapter were collected in 1998, but the analysis and interpretation of the data required close to 2 years. In the words of Dr. Picton, "phase is not easy." I have probably heard him say this over 100 times, and each time it rings more true. If I knew then what I know now of the non-linearities of the auditory system, I would never have kept plugging away at the data and somewhat naively asserting "this has to make sense, we just have to keep at it". In fact,

the subject still often confuses me and makes me question how I ended up in neuroscience rather than designing the new Bug for VW or opening a surf shop on the north shore of Waikiki. However, the effort paid off (we think), and the data seem to make sense most of the time.

The major reason that this topic was intriguing to me was that the phase of the steady-state response is always available: the FFT will always produce an amplitude value, which is related to the size of the response, and a phase value, which is related to the latency of the response. However, except for using phase in a statistical sense, as a means of detecting the presence of a steady-state response (Dobie, 1993) it is not much examined. There is good reason for this. Phase is inherently ambiguous because it is a circular measurement. Phase can be represented as an angle which defines a number of degrees or radians of a circle, and since a circle only has 360 degrees, the measure becomes troublesome if it is less than 0, or greater than 360 (see Figure 2 in Chapter 4). For example, 4 degrees of phase may in fact be 364, or 724!

Unlike the other chapters, the results of this chapter will not be summarized here with any detail since these should be approached very slowly. Yet, the rationale that prompted us to attempt to make sense of the phase data should be mentioned so that the reader understands why we felt justified in undertaking this task. The phase (latency) of the steady-state response was investigated because our preliminary data sets suggested that it was a viable parameter to be studied with the MASTER technique in that it had the minimum requirements. In other words, we quickly found that phase was stable over time (intra-subject), was similar between subjects, changed as expected due to changes in intensity (which had been shown in the case of latency for transient stimuli), and was not significantly different for single or multiple stimuli. It was trying to sensibly convert phase into latency that was the challenging aspect of the study.

It should be obvious that the types of experiments found in Chapter 4 would be far less feasible if we had presented each steady-state stimulus separately, since a tremendous amount of time would be required in order to collect the necessary data from each subject. For example, due to the issue of non-linear filters or "filter slopes" which has been raised by Bijl (Bijl and Veringa, 1985), when commenting upon the work of Diamond (1977), it was very important to collect data for each carrier frequency at each modulation rate. By consecutively presenting all our carrier frequencies at the same

modulation rate, we were able to circumvent any non-linearities which may exist in the auditory system at different rates of modulation. The MASTER technique allowed the data for this experiment to be collected in 2 hours rather than 16 (and that was only one of the seven studies presented in that paper). Another important point is that some of the experiments done in Chapter 4 would not have been sensibly formulated without the understandings obtained in Chapters 1-3. Each bit of new knowledge of the MASTER technique seems to increase its power and versatility. For example, since we were reasonably certain that modulation rates of adjacent carrier frequencies could be set closely without causing a reduction in amplitude of the responses, we separated adjacent modulation frequencies by only 0.24 Hz in the last experiment described in this chapter. The ability of the auditory system and the central nervous system to successfully produce one response at 159.912 Hz and another at 160.156 Hz is still awe-evoking to me. It seems that this chapter nicely combines with the rest of the evidence presented in this thesis to show the power of this technique, and to demonstrate that this is a relatively young method that may hold great promise within the near future.

Lastly, the projects in this paper would not have been possible or sensible without the elegant research of several dedicated scientists who provided important results by which ours could be contextualized and understood. The work with which I have become most familiar and which has acted to steer this thesis the most was the following: the early work of Galambos and Regan on steady-state evoked potentials; the work of Cohen and Rickards on combined AM/FM stimulation and steady-state stimulation of rates as high as 450 Hz; the studies of Valdes, Cohen, and Dobie on the evaluation of different statistical techniques for evaluating the response; the work of Møller, Khanna, Saberi, and Langner with respect to the ways in which the auditory system (post-cochlea) processes both AM and FM information and modulation in general; and the work of Jos Eggermont and Brian Moore who basically seem to publish articles on everything! Of course the work of Dr. Terry Picton and Otavio Lins, and their collaborators has obviously also acted as a strong pair of shoulders on which this thesis stands.

The MASTER technique is an interesting, powerful, and clinically useful method of objective audiometry which is generating increasing interest from the scientific community. Our system is currently used in eight other clinics/research laboratories around the world, and several more systems will be shipped over this upcoming summer.

The research in this thesis has provided a firm foundation for this technique and has hinted at what some of the next steps should be. Most of the work was a lot of fun. I hope learning about it serves a similar function for those who read these pages.

*Overview of the physiology*

This thesis focuses upon the development of a technique which permits the auditory system to be evaluated using different types of stimuli and several methods of data analysis. While the characteristics of responses that were obtained under various experimental manipulations are described in detail, a discussion of the origins of these responses is not taken up in depth. Further, much of the modeling contained herein emphasizes cochlear processes, rather than central mechanisms, when explaining the results. Indeed, many of our results may be explained by models that solely incorporate cochlear processes, thus avoiding the need to also examine the contributions of more central mechanisms. A consideration of central mechanisms may have resulted more in complicating our models by several orders of magnitude without necessarily providing a significantly better fit for the data. However, there *are* brains inside the heads of our subjects, and the electrical potentials that we are recording are generated at locations that are more central than the cochlea. Accordingly, some discussion of the specialized neuronal mechanisms that are related to the processing of modulated sounds is merited.

Auditory steady-state responses (ASSRs) are relatively simple stimuli which may be used to investigate how the auditory system processes complex real world sounds such as speech. The human auditory system is composed of many specialized structures which aid in the conversion of acoustic stimuli into meaningful neuronal representations. The processing of sound begins in the outer ear and moves centrally through the middle ear to the cochlea. The outer and middle ear serve mainly to conduct sounds from the air to the fluid-based system of the cochlea with little loss of energy. At this peripheral level the hearing system does not have specialized features for processing modulated tones rather than pure tone stimuli.

The more specialized processing of modulation, for example AM, occurs beginning at the level of the cochlea. As discussed by Lins et al. (1995), AM stimuli will produce responses in the cochlea that follow the modulation envelope due to the

rectification of the responses both at the level of the inner hair cells (for loud stimuli, e.g., >50 dB SPL) and at the synapse between the inner hair cells and the fibers of the primary afferent pathway (see Figure Intr-1). The responses of the inner hair cells are asymmetric and saturate in one direction more quickly than in the other. Accordingly, the inner hair cells will both compress and rectify a response at a loud intensity. Additionally, the responses at the level of the primary afferent fibers are always rectified, regardless of the intensity of the stimuli, because action potentials are only evoked by depolarization of the hair cells. Since only by movement of the hair cells in one direction causes their ion channels to open, leading to depolarization, only half of the acoustic waveform leads to neurotransmitter release and the resultant excitatory post-synaptic potentials of the primary auditory nerve afferents: hence, there is half-wave rather than full-wave rectification. Further the responses, both at the hair cell (i.e., membrane potentials of the cochlear microphonic) and in the cochlear nerve, saturate at higher intensity levels (see $2^{nd}$ and $4^{th}$ column of Figure Intr-1) leading to a compression of the final response transmitted by the auditory nerve fibers. In the processing of acoustic energy, the cochlea and primary afferent nerve fibers therefore act together to form a compressive half-wave rectification system. In a linear system, the frequency content of the output will be the same as that of the stimulus. Only in the case of a non-linearity (e.g., rectification) can a response contain energy at the frequency of modulation. Rectification is why our responses occur at the modulation frequencies.

In addition to compressive rectification, the neural representation of information about the AM envelope is often enhanced at the level of the cochlea and primary afferents. Intuitively, it seems sensible to expect the voltage responses of inner hair cells, in response to AM tones, should be a predictable function of the responses that occur to low frequency sounds. For example, both stimuli will be subject to the same rectification processes, low pass filtering, and peak or envelope detection resulting in the phase locking of synchronized activity in the cochlear nerve fiber (Smith, 1998). However, the output of the post synaptic cochlear nerve fiber is not merely a function between that neuron's static rate-intensity function and the intensity envelope of the AM tone. In fact, responses to modulated tones are often larger and extend to higher intensities than can be predicted from the static input-output relationship that is elicited by a pure tone presented

**Figure: Intr-1. Simple physiological model for the responses to AM stimuli.** The top row represents the events following the presentation of a low-intensity stimulus. The bottom row represents the events following the presentation of a high-intensity stimulus. The sequence of events is shown from left to right. The stimuli (first column), represented both in the time domain and in the frequency domain, pass through a function simulating the inner hair cells (second column). This asymmetric bi-directional compressing exponential function saturates faster when the input increases in one direction than in the other. The output of the inner hair cells (third column) passes through a function simulating the ganglion cells (fourth column). This function is a unidirectional compressing rectifier. The output of the ganglion cells, whose axons constitute most of the afferent axons of the auditory nerve, is shown in the last column. Rectification of the signal introduces a spectral component at the frequency of modulation (as well as at higher harmonics). This explains how auditory steady-state responses can have spectral power at the frequency of modulation when the stimulus has no power at this frequency (Regan, 1994). In a spontaneous firing neuron, the energy will exist in the inhibitory direction (below the x-axis). The model is quite simple and looks only at the hair cells and the auditory-nerve fibers. (from Lins et al, 1995. Reprinted with permission.)

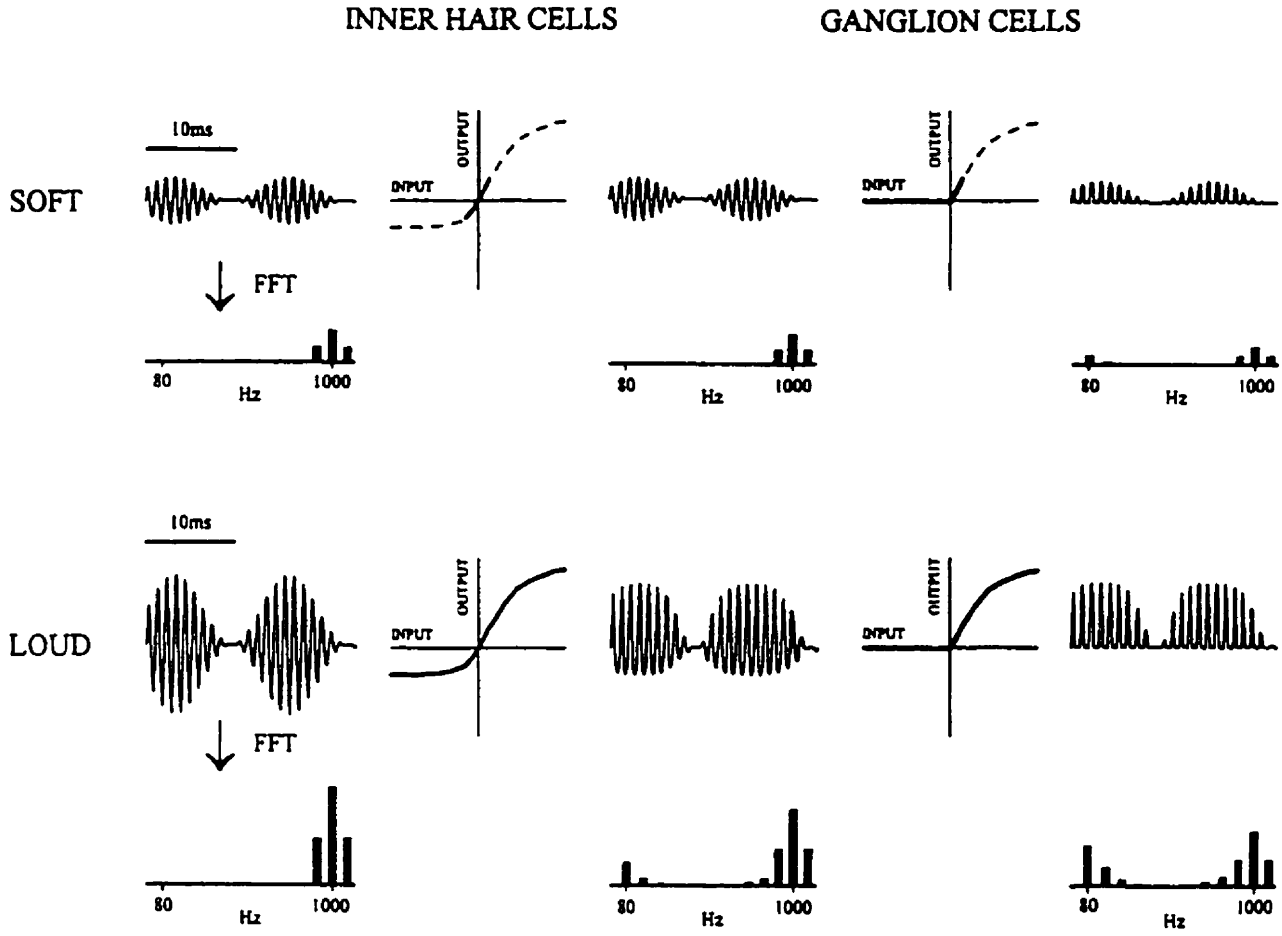
INNER HAIR CELLS
GANGLION CELLS
SOFT
LOUD
10ms
FFT
INPUT
OUTPUT
80
Hz
1000

at different intensities (Smith and Brachman, 1980). The enhancement of the modulated response with regard to the original modulated signal may occur due to rapid adaptation after an onset response (Cooper et al., 1993; Smith, 1998; Giesler, 1998). Another mechanism that may also play a role in the detection of a rapidly changing stimulus envelope relies on range fractionation. Several different types of primary afferent neurons encode the signals generated by the hair cells of the cochlea (e.g., cells with low or high spontaneous rates). Since information at different intensities is fractionated by types of neurons that enable the auditory system to encode over a large range of intensities (as reviewed by Geisler, 1998), the relatively quick stimulation of the different types of neurons caused by slope of the AM envelope may help to detect the rapid transitions of the AM envelope. Because the responses to AM are also enhanced more centrally at the levels of the cochlear nucleus and the inferior colliculus (Møller, 1972; Rees and Møller, 1983), modulated tones may evoke larger brainstem responses than pure tones of the same intensity and therefore, may be detected more rapidly.

A large part of this thesis also considers frequency modulation. The response of a fiber to the instantaneous frequency of an FM tone is identical to its discharge in response to a pure tone at the same frequency (Sinex and Geisler, 1981). Studies of the auditory nerve (Sinex and Geisler, 1981; Khanna and Teich, 1989ab) have shown that while AM responses follow the AM envelope, the FM responses may occur at both the modulation frequency and its second harmonic, although the prior response is primary. The processing of FM is somewhat complicated, but likely results from an FM to AM transduction. With respect to the activation of the inner hair cells as discussed above, the energy of an FM stimulus will be processed (and rectified) similarly to that of an AM signal at the level of the cochlea (Khanna and Teich, 1989b).

The coding of the rectified information about the modulated envelope at the level of the cochlear nerve relies mostly on the phase locking of primary afferent neurons to the modulation envelopes of the sound (as might be expected in the case of AM since discharge rates of primary neurons increase with increasing intensity of the stimulus, as occurs with the AM envelope). By evaluating the size of the phase locked neural responses as a function of modulation rate, a modulation transfer function (MTF) can be obtained. At the level of the auditory nerve, the MTFs for AM stimuli are reasonably flat up to the 1500 Hz rate at which point strong attenuation occurs (Joris and Yin, 1992).

As the auditory nerve fibers transmit the information about the modulated signal to the cochlear nucleus (CN), a second filtering process occurs, with many of the neurons of the CN exhibiting a bandpass response with respect to the modulation frequencies. Early on, Møller (1974) showed that CN neurons which process both AM and FM often demonstrate a preference for a particular rate of modulation, above and below which they decrease their firing rate (i.e., a bandpass). The MTFs of this region therefore assume the shape of an upside down "V", the apex of which is known as the best modulation frequency. The cochlear nucleus not only encodes modulation, but also seems to amplify the modulated signal, accentuating the peak of the response relative to the original modulated signal (Møller, 1972; Smith et al., 1985). The amplification of the AM envelope occurs in several specialized types of neurons. Frisina et al. (1990a) showed that in the ventral cochlear nucleus (VCN) the ability to encode amplitude modulation was best in onset neurons, followed by choppers, although the pimarylike and auditory nerve fibers also reproduced the modulated signal. The best modulation frequency of the different units explored by Frisina et al. (1990a) ranged from 180-240 for onset units and from 80-520 for choppers. The general trend in the amplitude of the steady-state response MTF is a decrease in amplitude with increasing modulation rate. However, this trend deviates from a pure decay by containing areas of larger response at the 40 Hz, 80 Hz, and 120 Hz ranges (Cohen et al., 1991). Possibly, this may be caused by a tendency for the best modulation frequency to occur at a majority of CN neurons near 40 Hz in humans, which could also lead them to fire at the $2^{nd}$, and $3^{rd}$ harmonics of this rate.

From the cochlear nucleus, the neuronal signals are transmitted to the superior olivary complex, and then to the inferior colliculus by way of the lateral lemniscus. A series of elegant experiments by Langer (e.g., Langer and Schreiner, 1988) have explored how AM is encoded, in the cat, at the level of the inferior colliculus. At the level of the inferior colliculus there exists a topographical order to neuronal populations demonstrating iso-frequency lamina to different best modulation frequencies which seem to be orthogonal to those for different carrier frequencies (Langer et al., 1998). Low pass filtering again occurs at lower intensity levels, while showing a bandpass at greater intensities.

Although there is a transduction of the FM signal into AM, the activation of the inner hair cells in response to an FM signal will occur at different latencies than would

occur for pure AM. In addition to the units, that have just been described, which process information about the periodicity of a stimulus, the brain has specialized neuronal systems that respond specifically to FM stimuli. Groups of neurons from the brainstem up to the cortex respond both to upward and downward glides, while many show a preference for upward glides (Tian and Rauschecker, 1994; Ricketts et al., 1998; Gordon and O'Neill, 1998). This preference is also seen in behavioral data (Demany and Clement, 1998) and electrophysiological data in response to transient FM sweep stimuli (Kohn et al., 1977). Preference to certain directions and certain rates of FM (but not AM) has also been shown, and there may be an interaction between rate and directional preference. For example, Møller (1977), and others (Zhao et al., 1997), have described FM responsive cells that produced responses to both upward and downward glides for modulation frequencies below 50 Hz, while these only responded to the upward glides at higher modulation frequencies. The preference for upward glides may be seen in steady-state responses as well. For example, in Chapter 3 we interpret our results as suggesting that larger steady-state responses occurred during upward glides of FM.

The origin of the auditory steady-state responses (ASSRs) is very likely dependent upon the rate of the modulation frequencies. Modulation frequencies in the 40 Hz range are generated both at the cortex and in the brainstem. Under anesthesia or sleep the cortical component disappears, while the smaller brainstem component of the response remains. Since the brainstem is located earlier in the auditory pathway than the cortex, this latter component is characterized by a shorter apparent latency (Lins et al., 1995). ASSRs evoked to rates of 80 Hz and above also have shorter apparent latencies than the 40 Hz steady-state response and are also likely generated in the lower and upper brainstem.

The origins of the transient evoked brainstem potentials are well known and their amplitudes and latencies are used to help detect disorders of the auditory system and central nervous system. Extensive reviews of anatomical basis of these brainstem potentials exist in the literature (Møller and Jannetta, 1985). Wave I is thought to be generated at the distal part of the auditory nerve due to the initiation of action potentials. Wave II occurs mainly at the proximal end of the auditory nerve although there may be a distal component. Wave III occurs at the cochlear nucleus, with a small component from the nerve fibers entering the nucleus. Wave IV occurs at the superior olivary complex

(SOC) with some contribution from the cochlear nucleus. The last peak we will discuss is the positively going wave V, which occurs at the lateral lemniscus, and which exists in animals (although this may show up as wave IV in animals -see review by Starr and Don, 1988) even after bilateral ablation of the inferior colliculus (IC), as has been shown by Wada and Starr (1983). As discussed in Chapter 4, the auditory steady state response can be reasonably predicted from the superposition of overlapping transient responses, even more so when appropriate refractory periods and multiple generators are incorporated into the modeled data (Gutschalk et al., 1999).

Another line of evidence that steady-state potentials are generated in the brainstem derives from the scalp topography of these responses which suggests a dipole in the brainstem which points towards the fronto-central cortex. If the responses at rates between 80 and 200 Hz were generated closer to the peripheral centers of the auditory system, such as occurs with wave I of the transient response, then a lateralization would be expected in the scalp topography (as occurs with wave I). In fact, this is not the case when using the mastoid, rather than the neck, as a reference: since the recorded responses are smaller rather than larger, as would occur with a dipole source near the ear which was oriented towards the Cz recording electrode.

Of the multiple components of the brainstem response it is most likely wave V, originating in the lateral lemniscus, that is the strongest contributor to the steady-state responses at the modulation frequencies which were used in the thesis. Wave V amplitude is not affected much by repetition rate of the stimulus and has routinely been evoked at rates comparable to those of our modulation rates (Jewett and Williston, 1971). In contrast, faster repetition rates have been shown to cause decreases in the amplitudes of the earlier components, possibly by means of forward masking (Kramer and Teas, 1982).

Additional evidence that the faster steady-state responses, such as the 80 Hz response, are generated in the same areas that produce the transient brainstem responses and prior to the level of the IC can be found in Chapter 3. In that chapter, we show that AM and FM are probably generated by independent neuronal populations. The reductions seen in individual responses evoked by AM and FM (modeled), when these stimuli are presented together in a mixed modulation stimulus, are small and can be reasonably explained by considering changes that occur in the energy of the stimulus, and

by cochlear mechanisms alone, rather than by any type of interference (i.e., interaction between responses that would lead to decreases of these responses) which might occur in the brainstem. At the level of the IC, information about modulation is being examined independently of the type of modulation or the frequency of the carrier and AM and FM responses would likely be processed by the same periodicity area (Langner et al., 1998). The fact that we did not see much interference in simultaneous presentation of AM and FM responses suggests that the potentials that we are recording are generated, to a large degree, in regions that occur earlier than the IC.

Other results discussed in this thesis also suggest that the steady-state responses are generated prior to the level of the IC. Langer and Schreiner (1988) found that a re-coding of information occurs at the IC which is more complex than at earlier levels of processing. At the CN the MTFs from entrained responses shows tuning to the modulation rate without demonstrating changes in discharge rate that increase with increasing modulation frequencies. In the IC, both the MTFs of the synchronized activity, as well as the mean discharge rate, varies with the modulation rate. Accordingly, at this level there is a change in the way that the modulation information has been encoded. In line with the above study, if the steady-state responses were being generated at the level of the IC, we may have obtained larger responses at higher rates of modulation. Since we found the opposite, where faster modulation rates tend to cause decreases in the amplitudes of steady-state responses, this may also be seen as supporting a generator prior to the IC.

The latency data provided in Chapter 4 provide mixed evidence that the steady-state responses could be generated in the brainstem source of wave V. Latencies from 16 to 21 ms were found in the case of the 80-100 Hz modulated tones, while the 150-190 Hz modulation rates produced latencies in the 7-12 ms range. While the wave V responses evoked by transient tone stimuli are generally later than the latencies generally associated with wave V to click stimuli, the latency estimates for the 80-100 Hz data are quite large to be easily reconciled with the latencies commonly obtained for the transient wave V. One characteristic of the data in the 80-110 Hz range is that the responses have slightly larger amplitudes than responses at other rates. The fact that these responses were characterized by both longer latencies and larger amplitudes than might be expected from a linear filter may be explained by the activation of a multi-synaptic circuit in response to

modulations in this range. Indeed, the phase data of Cohen et al. (1988) seem to suggest a transition in the phase trends that occur at these modulation rates compared to rates below 80 Hz. The 150-190 Hz modulation rates were chosen so that the superimposition of responses would be likely to cause transient responses in the 5.2 ms to 6.6 ms range (i.e., wave V) to overlap since this time range is equal to the periods of these modulation rates (e.g. 1000/190=5.2 ms). The 8-13 ms latency estimates obtained for these faster modulation rates were thus characterized by response latencies that were much closer with those associated with the wave V response that is evoked by transient tone stimuli.

*A final note on clinical relevance*

The MASTER technique offers many advantages to the clinical testing environment. Objective audiometry is useful when testing babies, or other individuals who may not be willing or able to give reliable behavioral responses to indicate their hearing abilities (e.g., thresholds). While oto-acoustic omissions are able to provide an indication that normal hearing levels exist at 30 dB SPL or more, they are not able to provide information related to threshold. Frequency-specific auditory brainstem responses using tone burst stimuli or single steady-state stimuli techniques can provide frequency-specific threshold information, but are relatively slow procedures. Hopefully, the MASTER technique can serve as a useful tool for objective audiometry since it can evaluate frequency-specific thresholds to multiple stimuli in the time normally required to test a single stimulus. Because steady-state responses are statistically assessed by the computer, rather than requiring a subjective and time consuming evaluation by a trained professional, less specialized training is required on the part of its users. The MASTER technique can be used not only to assess frequency specific thresholds, but can also provide information as to the sensitivity of the auditory system to various rates of stimulation, to types of modulation, and to depths of modulation.

The work in this thesis was done using control subjects with normal hearing levels. In the application of the MASTER technique to clinical populations several types of issues may arise. For example, with regard to the interaction of the multiple tones, it is possible that interactions between stimuli may occur due to the broader tuning curves, and lack of tuning "tips", that can be present in abnormal cochleas (Harrison, 1981). Picton et al. (1998) investigated the use of the MASTER technique in infants and

children for both aided and unaided hearing. While this initial utilization of the MASTER technique was able to provide valuable information in many cases, the authors found a case of aided hearing, where the physiological thresholds were lower in the case of high frequency stimuli when these were presented alone rather than in combination with other lower frequencies. A possible cause of the results produced by that subject may have been that the higher frequency tuning curves lacked the high sensitivity "tip" at the characteristic frequency of the hair cell and may have therefore been more susceptible to an interaction with low frequencies.

The interactions of several tones, as may occur in the MASTER technique with clinical populations, can also be seen as an advantage of the technique. For example, the responses to multiple stimuli may be similar to the sensitivity of these individuals to natural sounds, which will undoubtedly be comprised of complex mixtures of tonal frequencies. Moreover, by independently adjusting the volume of the MASTER tonal stimuli, automated procedures could be created relatively easily which could circumvent any problems which might occur due to presenting multiple stimuli at the same intensity level. Additionally, even if 3 rather than 4 tones were tested in a single condition (and the high frequency 4 kHz tone was tested alone) this would still save time for a full examination.

This thesis did not study clinical populations in its investigation of the MASTER technique since we were interested in laying a strong foundation with regard to understanding the characteristics of multiple steady-state responses. Early clinical studies indicate that the technique works well (Lins et al., 1996; Picton et al., 1998). The creation of a portable system will enable other researchers to help us to begin to use the system in clinical populations and to collect normative values in adults and infants. Considerable interest has been continuously shown by both our scientific and clinical colleagues. Accordingly, we are excited about now being in a position to find out quite a bit about how we may use AM, FM, MM, and IAFM stimuli to provide rapid and objective measures of various hearing disorders using the MASTER technique and system.

# CHAPTER 1

## MULTIPLE AUDITORY STEADY-STATE RESPONSES (MASTER): STIMULUS AND RECORDING PARAMETERS

A portion of this material has previously appeared in M.S. John, O Lins, B Boucher, and T W Picton (1998), *Multiple Auditory Steady-State Responses (MASTER): Stimulus and Recording Parameters.* Audiology (37); 59-82. *Reprinted with permission*

**Acknowledgements** This research was funded by the Medical Research Council of Canada. The authors would also like to thank James Knowles and the Baycrest Foundation for their support.

## ABSTRACT

Steady-state responses evoked by simultaneously presented amplitude-modulated tones were measured by examining the spectral components in the recording that corresponded to the different modulation-frequencies. When using modulation-frequencies between 70 and 110 Hz and an intensity of 60 dB SPL, there were significant interactions between two stimuli when the carrier-frequencies were closer than one half octave apart, with attenuation of the response to the lower carrier-frequency. However, there were no significant decreases in response-amplitude with four simultaneous stimuli provided the carrier-frequencies differed by one octave or more. Higher intensities (70 dB SPL) resulted in greater interactions between the stimuli than when low intensities (35 dB SPL) were used. Modulation-frequencies could be as closely spaced as 1.3 Hz without affecting the responses. Using broadband noise as a carrier instead of a pure tone resulted in a significantly larger response when the stimuli were presented at the same sound pressure level. At modulation-frequencies between 30 and 50 Hz, there were greater interactions between stimuli than at faster modulation-frequencies. These results support the following recommendations for using multiple stimuli in evoked potential audiometry: (i) The multiple stimulus technique works well for steady-state responses at frequencies between 70 and 110 Hz. (ii) Up to four stimuli can be simultaneously presented to an ear without significant loss in amplitude of the response provided the carrier-frequencies separated by an octave and the intensities are 60 dB SPL or less. (iii) Bandpass noise might serve as a better carrier signal than pure tones.

## INTRODUCTION

A steady-state evoked potential occurs when a repeating stimulus evokes an electrical waveform whose constituent frequency-components maintain constant amplitude and phase over prolonged time periods (Regan, 1989). Steady-state responses are produced when stimuli are presented at a rate sufficiently rapid that the response to any one stimulus overlaps the responses to preceding stimuli. After the first few stimuli, the recorded waveform assumes the periodic waveform of the steady-state response.

Auditory steady-state responses can be obtained using many different stimulus rates (Rickards and Clark, 1984). The most widely studied auditory steady-state response is evoked by stimuli presented at rates near 40 Hz (Galambos et al.,1981; Stapells et al 1984). This 40-Hz response can be used to assess hearing (Dauman et al.,1984; Rodriguez et al.,1986). However, the response decreases in amplitude considerably during sleep (Galambos et al., 1981; Linden, et al., 1985; Jerger et al., 1986), is dramatically attenuated during general anesthesia (Madler and Pöppel,1987; Plourde and Picton, 1990), and is difficult to record in infants (Stapells et al.,1988). The auditory steady-state response to stimuli presented at rates of 70-110 Hz (Cohen et al., 1991; Levi et al, 1993; Aoyagi et al., 1994) are two to three times smaller than those of the 40 Hz response. Nevertheless, these rapid responses are much less affected by arousal (Cohen et al., 1991; Levi et al, 1993; Lins et al., 1995), and are readily recorded in infants (Aoyagi et al.,1993; Rickards et al.,1994). The 70-110 Hz responses are therefore useful for objective audiometry in patients who cannot provide reliable behavioral responses (Rance et al.,1995; Lins et al.,1996).

Recording responses to many different stimuli at the same time would allow objective audiometry to obtain as much information about hearing as possible in as short a time as possible. Regan and Cartwright (1970) demonstrated that steady-state responses to several simultaneous visual stimuli could be recorded and analyzed independently if each stimulus was

modulated at a different rate (Regan, 1989). This was later shown to also be possible in the auditory modality (Lins et al.,1995; Picton et al.,1987; Regan and Regan, 1988). Multiple carrier-frequencies, each modulated by its own signature modulating-frequency, evoke multiple steady-state responses, each measured at the particular frequency at which the carrier is modulated. Recording multiple responses simultaneously in one session leads to a significant reduction in recording time since many responses can be recorded in the same time that it takes to record one. However, the multiple-stimulus technique is only more efficient than the traditional single-stimulus technique if any reduction in amplitude of the response caused by the simultaneous presentation of the stimuli is less than the reduction in the EEG noise provided by the increased time available for recording the responses. Lins and Picton (1995) demonstrated that there was no loss in the amplitude of the 70-110 Hz responses (at 60 dB SPL) provided that the carrier-frequencies were separated by an octave or were presented in separate ears. Lins et al.(1996) further demonstrated that audiometric thresholds could be reliably estimated from responses to eight simultaneous stimuli (four in each ear).

The **M**ultiple **A**uditory **S**teady-state **R**esponse (**MASTER**) technique therefore shows great promise for objective audiometry. This chapter investigates several parameters that may affect the amplitude of the responses when multiple auditory stimuli are presented simultaneously. The results can be considered from both physiological and clinical viewpoints. The first looks at the physiological interactions that occur in the cochlea and brain when two or more stimuli are presented simultaneously. The clinical view considers whether evoked potential audiometry is more efficient when recording multiple responses in a single epoch or recording single responses in multiple epochs, and determines the parameters within with such increased efficiency occurs.

## METHODS

### Subjects

The 30 subjects (11 female) were volunteers obtained from laboratory personnel, colleagues and friends. Their ages ranged between 15 and 52 years. All subjects were screened for normal hearing for pure tones (range 500-4000 Hz) at 30 dB HL. During the recordings the subjects sat in a comfortable reclining chair inside a quiet room. Since arousal affects the amplitude of the 40 Hz responses, subjects were asked to stay awake and read during the recording of these responses. However, since the 80 Hz response is unaffected by arousal (Cohen et al., 1991; Lins et al., 1995) subjects were encouraged to relax and fall asleep during the recording of these more rapid responses, in order to reduce the background noise levels in the EEG. Most subjects were able to sleep.

### Recording

Gold-plated recording electrodes were placed at the vertex and at the posterior midline of the neck just below the hair line (7-8 cm below the inion). The ground electrode was placed on the right side of the neck. The skin beneath the electrodes was abraded to ensure that inter-electrode impedances were below 5 kOhm at 10 Hz. EEG signals were collected using a bandpass of 10 to 300 Hz (6 dB/octave).

The timing for the analog-to-digital (AD) conversion was based on a 4 MHz clock. For recording the 70-110 Hz responses, conversion occurred every 5888 ticks of the clock (1.472 ms) at a rate of 679.35 Hz. This rate was exactly 1/32 the rate of DA conversion.

Recordings continued over multiple sweeps each lasting 12.058 seconds (8192 time-points). The number of sweeps varied with the experimental conditions so as to ensure a good signal-to-noise ratio: usually 48 or 64 when recording the smaller 80 Hz responses. Occasionally, when the noise levels were high, up to 96 sweeps were necessary. In order to allow reasonable artifact-rejection, the recording sweep consisted of 16 sections each lasting 753.66 ms. A section (rather than an entire sweep) was rejected if the section contained any

potentials with amplitudes greater than ±40 μV. If a section was rejected, that part of the recording sweep was filled in with the next recorded data. This procedure did not violate assumptions of stationarity because each section consisted of an integer multiple of the composite frequencies and started with identical phase. Between 0% and 20% of the data sections were rejected. If artifact-rejection was due to the presence of a large alpha rhythm rather than movement artifact, adjusting the artifact threshold to ±50 μV enabled the recording to proceed without an inordinate number of rejections. Each recording lasted from 7 to 20 minutes, depending on the number of rejections and the number of sweeps.

For recording the 30-50 Hz responses, the AD conversion rate was reduced by half. This led to sections and sweeps that were twice the duration of those described for the 70-110 Hz responses. Because of the greater signal to noise ratio for the slower responses, far fewer sweeps needed to be averaged and the recording time for obtaining a reliable response was halved.

**Auditory Stimuli**

The stimuli were generated digitally and converted to analog form with 12-bit resolution at a digital-to-analog (DA) rate of once every 184 clock ticks (0.046 ms) or 21,739.13 Hz. The analog waveforms were then low-pass filtered (48 dB/octave) at 4 kHz (10 kHz when the experiment used 4 kHz carrier-frequencies) to remove digitization noise and high-pass filtered at 200 Hz to remove any possible electrical artifact at the modulating frequencies. The stimuli were amplified to a calibration-intensity and then attenuated to achieve the desired dB level. The stimuli were presented to the subject through insert earphones. The stimuli were calibrated using a Brüel and Kjaer Model 2230 Sound Level Meter with a DB 0138 2-$cm^2$ coupler. Normal thresholds tested in a low-noise environment (Lins et al.,1996) were 28, 17, 18, and 18 dB SPL for carrier-frequencies of 500, 1000, 2000, and 4000 Hz. Unless otherwise noted the stimuli were presented to the right ear.

Each amplitude-modulated (AM) stimulus was created by multiplying together two sine waves. The sine wave with the higher frequency ($f_c$) was the carrier; the sine wave with the lower frequency ($f_m$) formed the modulating envelope. The full formula was:

$$a*\sin(2\pi f_c t+\theta_c)*(m*\sin(2\pi f_m t+\theta_m) + 1)/(1 + m)$$

where **a** was the amplitude of the carrier, **m** the amount of modulation (from 0.0 to 1.0), and $\theta_c$ and $\theta_m$ the phases of the two sine waves. With unit amplitude, 100% modulation, and zero onset-phases, the formula for the signal was thus

$$\sin(2\pi f_c t)*(\sin(2\pi f_m t) + 1)/2$$

The stimuli for multiple stimulation were formed by summing the individual amplitude-modulated stimuli. If the carrier-frequencies of the different stimuli were the same, the resultant compound waveform was equivalent to modulating one carrier tone at multiple rates. Figure 1 illustrates sample stimuli viewed in both the time and the frequency domain. The amplitude spectra plot the amplitudes at each frequency as the square root of sum of the squares of the real and imaginary components in the Fast Fourier Transform at that frequency. The figure also shows the effects of submitting the stimuli to half-wave rectification as a simple example of nonlinear processing (Regan and Regan, 1988; Regan, 1994). Half-wave rectification causes energy to show up in the spectrum at frequencies equal to the modulating frequencies and at other frequencies formed by adding or subtracting the modulation and carrier-frequencies and their harmonics (Regan, 1994).

The frequencies of both the carrier and modulation signals were adjusted so that there were an integer number of cycles within a recording section (753.66 ms). This allowed the sweeps to be linked together without acoustic artifact and allowed the sections to be interchangeable during artifact rejection. Thus, a carrier-frequency of 1000 Hz was adjusted to 1000.45 Hz so that 754 complete cycles occurred within each section, and a modulation-

*Please see next page for figure*

**Figure 1-1: Auditory steady-state time waveforms & amplitude spectra.** The upper tracings in this figure represent the temporal waveforms of the acoustic signals used in Experiment 2, which investigated the effects of increasing the number of different amplitude-modulated stimuli that were simultaneously presented. Below the time waveforms are shown the amplitude spectra. Each amplitude-modulated tone is represented by energy at the carrier-frequency and at sideband frequencies separated from the carrier by a distance equal to the modulating frequency. The lower half of the figure represents these signals after they have been rectified. The spectra are now displayed only in the low frequencies. Rectification causes energy to show up at the modulating frequency. The amount of energy decreases with an increase in the number of modulated signals present. With multiple stimuli, energy is also dispersed into various distortion-product frequencies. The amplitude range for the spectra of the original signals (0-1.0) is five times that of the rectified signals (0-0.2).

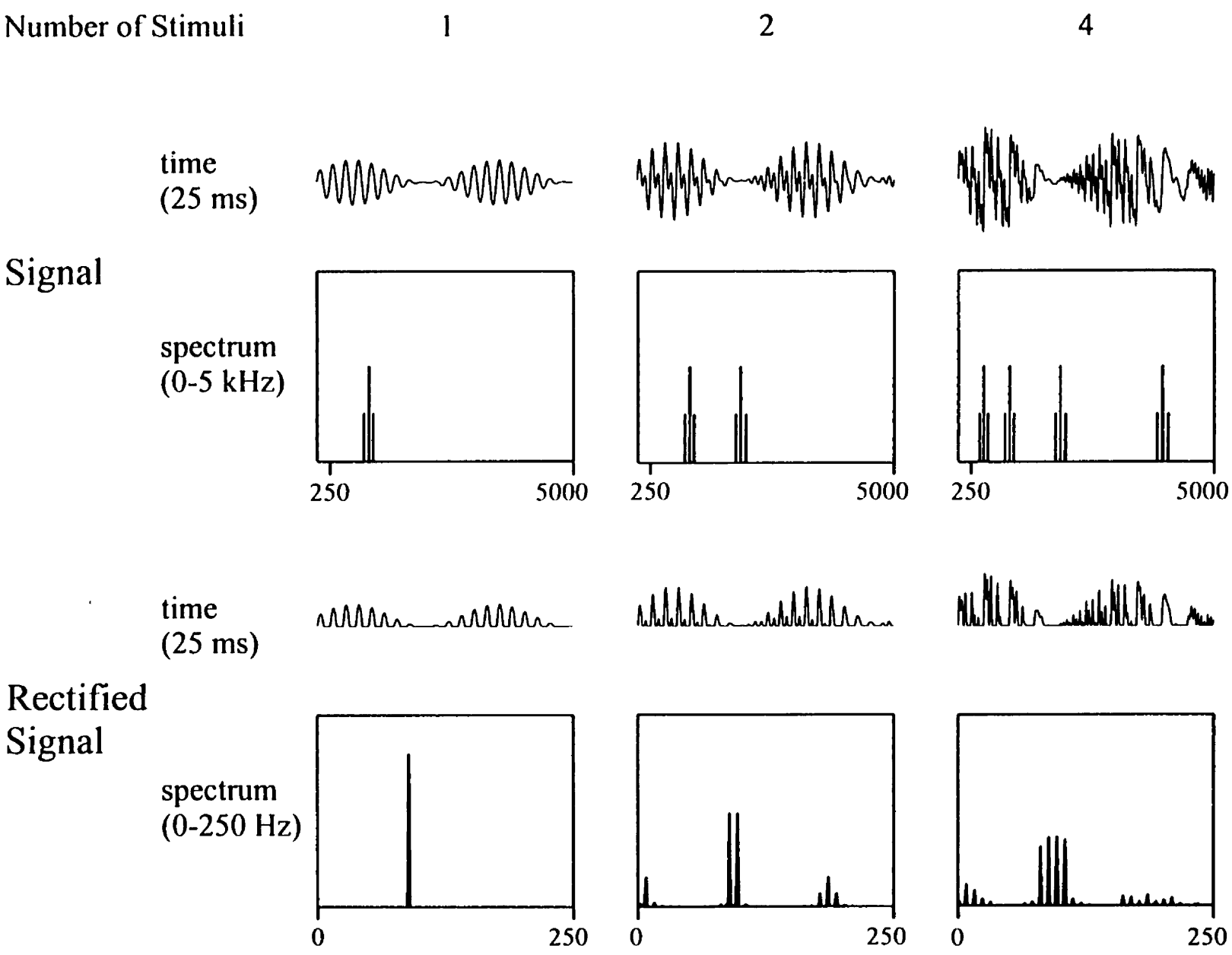
Number of Stimuli
1
2
4
time
(25 ms)
Signal
spectrum
(0-5 kHz)
250
5000
250
5000
250
5000
time
(25 ms)
Rectified
Signal
spectrum
(0-250 Hz)
0
250
0
250
0
250

*Please see next page for figure*

**Figure 1-2. Noise-reduction when recording steady-state responses.** The noise in a recording can be attenuated by either averaging responses together (as shown in the top half of the figure) or by increasing the duration of the sweep that is submitted to Fourier analysis (lower half of the figure). For each technique the time-domain waveform and the amplitude spectrum are shown. The amount of noise in a recording can be assessed by measuring the amplitude of the activity at frequencies different from that of the steady-state response. As can be seen, the noise level decreases by a factor of 2 with a four-fold increase in either the number of sweeps averaged (Na) or the number of points submitted to Fourier analysis (Ns). Simulated data were used to make this figure.

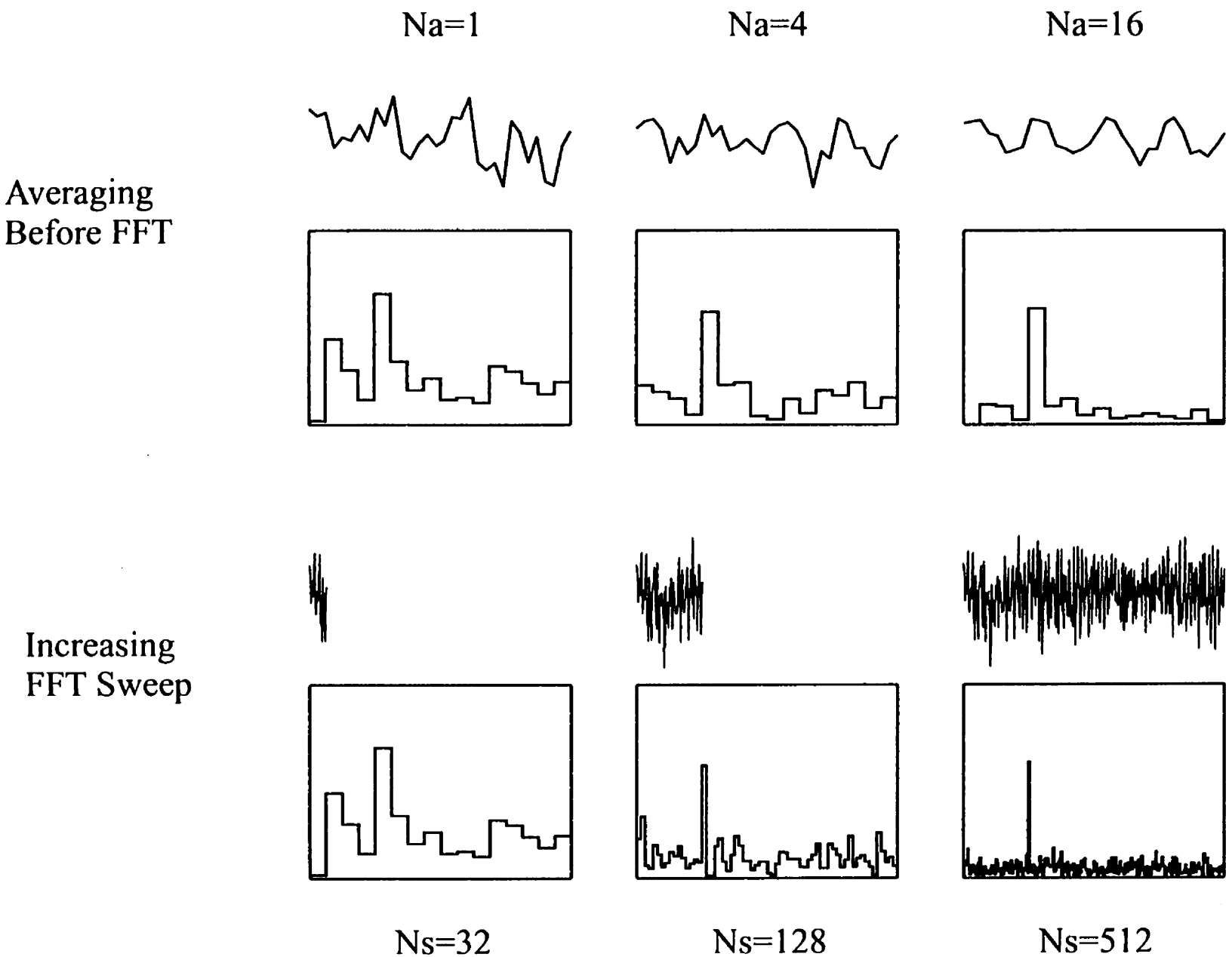
Na=1
Na=4
Na=16
Averaging
Before FFT
Increasing
FFT Sweep
Ns=32
Ns=128
Ns=512

frequency of 81 Hz was adjusted to 80.938 Hz. For simplicity, the carrier-frequencies are henceforth expressed without the decimal and the modulation-frequencies with only one decimal.

In some experiments, white noise served as a carrier stimulus. This was generated digitally using normally distributed random numbers and then amplitude-modulated by multiplying by a sinusoidal modulation-frequency. The resultant signal could be bandpass filtered using a 48-dB/octave filter. For the "narrow-band noise", both the high and the low cutoff frequencies were set to the same value. The roll-off slope of the filters then passed only those frequencies very close to the cutoff setting. The intensities of the stimuli were re-adjusted after filtering so that all stimuli had the same SPL.

**Analyses**

As shown in Figure 1-2, noise levels in recordings of the steady-state response can be reduced either by averaging in the time-domain or by increasing the duration of the data submitted to Fourier analysis. We used both techniques. The responses were initially analyzed by averaging together the recorded sweeps in the time-domain. The resultant 12.058-second (8192-timepoint) averaged sweep was then transformed into the frequency domain using a Fast Fourier Transform (FFT). An equivalent procedure would have converted each of the recorded sweeps into the frequency-domain and then averaged these together paying attention to both phase and amplitude ("coherent averaging"). The FFT converts the original amplitude-time waveform into a series of cosine waves with specific frequencies, each having its own amplitude and phase. The FFT represents these cosine waves as vectors on a two-dimensional plane. The X-Y coordinates are then commonly transformed into polar coordinates as amplitude and phase. The amplitude is the length of the vector ($\sqrt{X^2 + Y^2}$) and the phase is the rotation of the vector in relation to the X-axis as calculated by arctan (Y/X). The amplitudes reported in this chapter are baseline-to-peak amplitudes and the phases are cosine-onset phase. The specific frequencies

available from the FFT are integer multiples of the **1/(Nt)** resolution of the FFT, where **N** is the number of time-points and **t** is the time per timepoint. For our analyses the resolution of the FFT was 0.08293 Hz, and the resultant spectrum spanned from zero to 339.68 Hz (4096 x 0.08293).

**Statistical Evaluations**

The presence or absence of a response was assessed by the F-technique. This method evaluates if the response at the frequency of stimulation is different from the noise at adjacent frequencies (Lins et al.,1996; Wei, 1990; Zurek, 1992; Dobie and Wilson, 1996; Valdes et al., 1997). An FFT of the whole sweep yields a spectrum with a resolution of 0.083 Hz per FFT bin. The power at the signal frequency is comprised of both the signal power and the residual noise power. The F statistic computes the ratio between the power measured at the signal frequency and the average power in 120 neighboring frequency bins - 60 above and 60 below the signal frequency (i.e., about 5 Hz on each side of the signal) - used as an estimate of the background noise. When using the multiple-stimulus technique those frequencies at which another signal is present were excluded from this calculation. The significance of this F-ratio was evaluated against critical values for F at 2 and 240 degrees of freedom. This technique allowed us to continue averaging until a response was significantly different ($p<0.05$) from noise. We also measured the response in each of the 16 sections within a sweep and calculated the confidence limits of the 2-dimensional mean of these responses using the circular $T^2$ test (Victor and Mast J, 1991; Dobie and Wilson, 1993). This provided us with an estimate of the confidence limits but was not used for determining the signal to noise ratio.

The main analyses concerned changes in the amplitude of the response with the experimental manipulations. The statistical significance of these manipulations was assessed by repeated-measures analyses of variance (ANOVA). Post-hoc comparisons used the Fisher Least Significant Difference (LSD) test. The LSD was chosen since comparisons within a single set of

experimental recordings were often independent. Differences were considered significant at the $p<0.05$ level.

**Modeling**

In order to understand the results, we attempted to model the effects of different physical and physiological processes using parameters from the literature. The models used in this chapter derive from models discussed in prior research from our laboratory (Lins, et al.,1995; Lins and Picton, 1995). They are used informally to illustrate our interpretation of the data rather than formally to model all of the underlying mechanisms. Three main physiological processes were modeled.

(i) The first was the basilar membrane traveling wave activation pattern of a single tone (Robles et al.,1986). This included both the tip and the tails of the tuning curves. This process was used to describe which frequencies would activate a local region of the basilar membrane neurons.

(ii) The second was the nonlinear processing - compressive rectification - of the hair-cells. This process provides a mechanism for the nervous system to recognize the modulating frequency since a rectified signal contains energy at the modulating frequency that is not present in the unrectified acoustic signal (Lins et al.,1995; Regan and Regan, 1988; Regan, 1994). It also explains the interference that occurs when multiple modulated stimuli are presented simultaneously: decreased amplitude occurs at the modulation-frequencies (illustrated in Figure 1-1). This is in part related to the loss of energy caused by superposition of the different frequencies to form beats. However, in the cochlea this will only occur to the extent that the different frequencies wind up activating the same region of the basilar membrane. This effect would not be present when two carrier signals were of exactly the same frequency and phase. When the carrier-frequencies differ, the attenuation would be constant regardless of the frequencies, unless other distortion products overlap the modulation-frequency. On the basis of

simple rectification models (e.g. Figure 1-1) we assessed the interference effect of two stimuli as a 30% reduction from the amplitude produced by single stimulus. However, since the compression that occurs as the intensity increases might decrease this attenuation, we modeled the interference effect at about 20%. The resultant effect is thus a combination of the traveling-wave's distribution of a particular frequency to the region being examined and the nonlinear distortion.

(iii) A third process is the suppression that occurs when two tones occur together rather than singly. We modeled this as a large effect when the suppressing tone is of higher frequency and within an octave in frequency, and a smaller effect when the suppressing tone has a lower frequency. This follows the data available from studies of both auditory nerve fibers (Arthur 1971; Harris 1979) and basilar membrane motion (Cooper 1996) which shows that at moderate intensities high to low frequency suppression is more prominent.

We allowed each of these three processes to exert a multiplicative effect on the input. Any difference between the actual data and the model would then require further explanation. This model is explored in greater depth later in this chapter and also in appendix A.

## RESULTS

### Experiment 1: Interactions between two carrier-frequencies

The goal of this experiment was to determine the interactions between stimuli having different carrier-frequencies. How close together can the carrier-frequencies be before there is a significant attenuation of the response? What is the nature of this attenuation - does it follow a pattern that might be expected from mechanical masking caused by the traveling wave or are other mechanisms involved? Responses were recorded for combinations of two AM tones, each of which had an intensity of 60 dB SPL. A probe tone with a modulation-frequency of 80.9 Hz and a carrier-frequency of 1000 Hz was always present. A masker tone had a modulation

*Please see next page for figure*

**Figure 1-3: Interactions between tones with different carrier-frequencies.** This figure shows data from one subject in two experimental conditions. In the first condition (upper half of the figure) a probe stimulus with a carrier-frequency of 1000 Hz and a modulating-frequency at 80.9 Hz was presented together with a masker stimulus having a carrier-frequency of 750 Hz and a modulation- frequency of 96.9 Hz. In the second condition (the lower half of the figure) everything was the same except the carrier-frequency of the masker stimulus which was changed to 1350 Hz. On the left are shown the amplitude spectra obtained in each experimental condition. The responses to the probe and to the masker are recognizable at their modulation-frequencies. On the right of the figure the responses at these frequencies are given in polar plots in order to show the phase as well as the amplitude of the response. The figure demonstrates the basic findings, that when two stimuli are presented simultaneously the stimulus with the higher carrier-frequency causes attenuation of the stimulus with the lower carrier-frequency. These results are from a single subject.

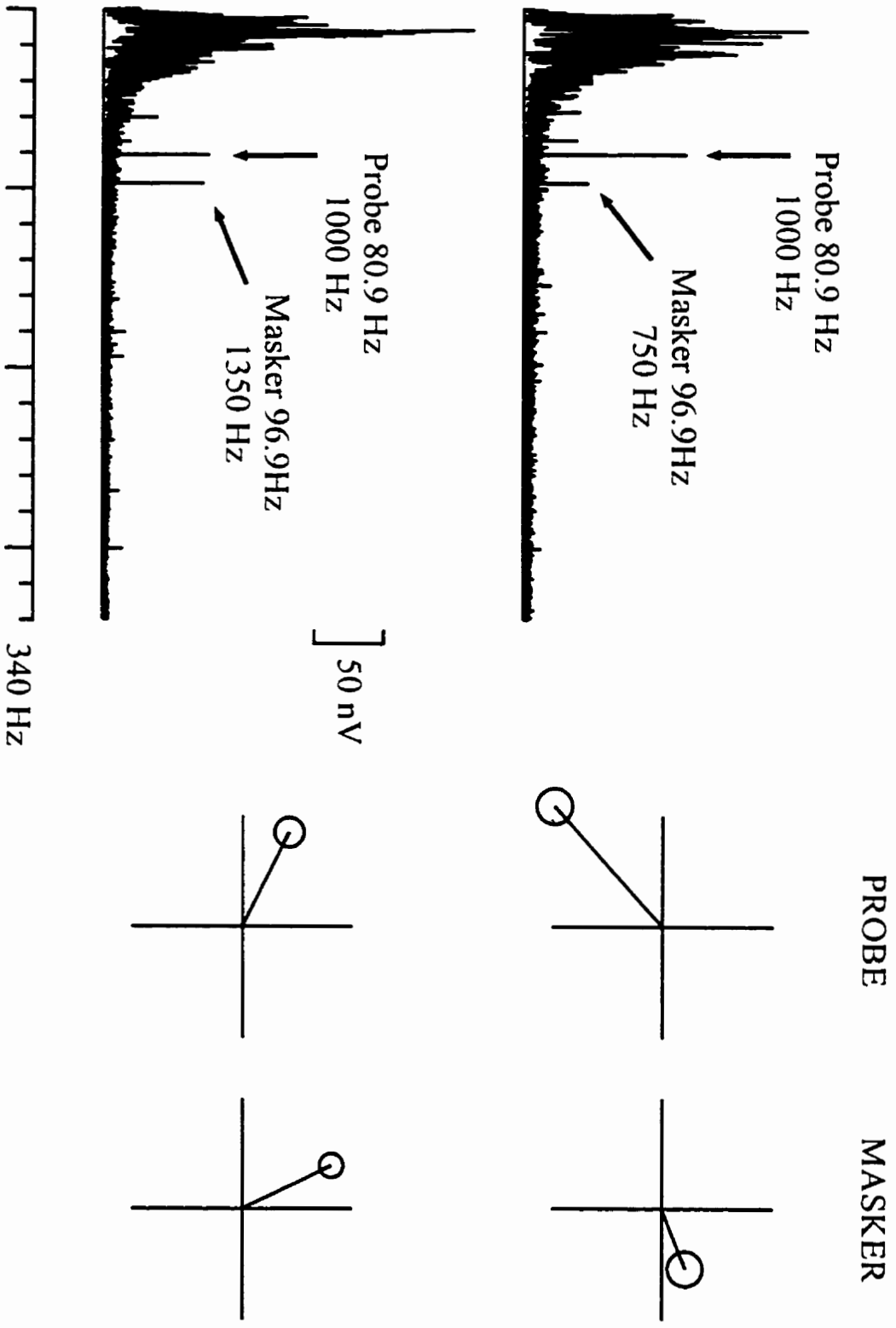
Probe 80.9 Hz
1000 Hz
Masker 96.9Hz
750 Hz
Probe 80.9 Hz
1000 Hz
Masker 96.9Hz
1350 Hz
50 nV
340 Hz
PROBE
MASKER

*Please see next page for figure*

**Figure 1-4. Carrier-frequency interactions.** These results graph the mean amplitudes for five subjects when a probe tone with a carrier-frequency of 1000 Hz was presented simultaneously with masker tones with carrier-frequencies that varied from 500 to 2000 Hz. The probe response (filled circles) shows the effects of maskers of varying frequency. The dashed line represents the magnitude of the response to the probe presented alone. The masker response shows the effect of the 1000-Hz probe when the masker had different frequencies. If the response alone has a similar amplitude across carrier-frequencies, and if the interactions are similar at different frequencies, the graph for the masker should be the left-right mirror image of the graph for the probe. On the left of the figure are shown the "least significant differences" ($p<0.05$) so that the significance of the changes in the graphs can be assessed.

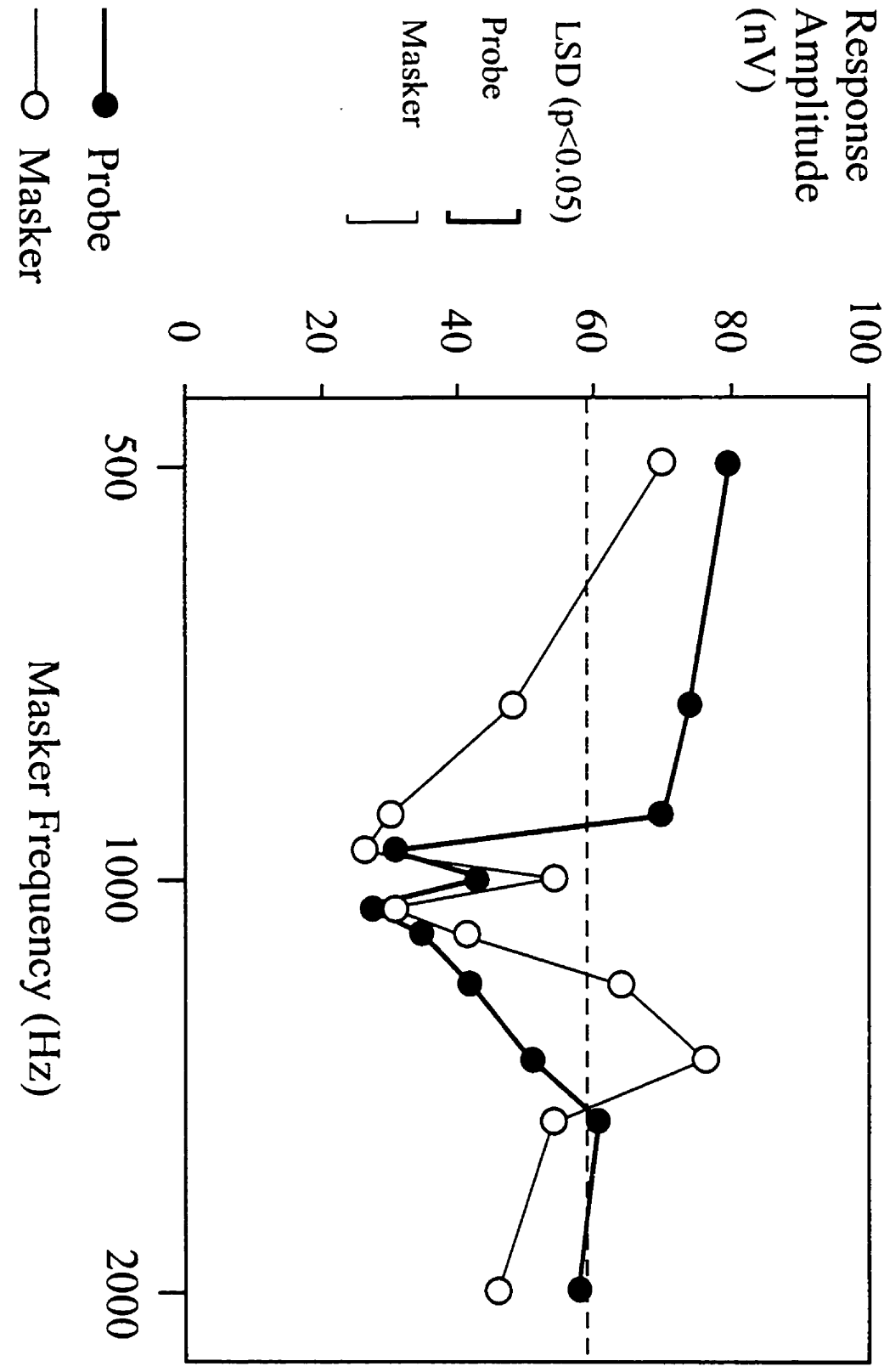
Response Amplitude (nV)
100
80
60
40
20
0
LSD (p<0.05)
Probe
Masker
500
1000
2000
Masker Frequency (Hz)
Probe
Masker

*Please see next page for figure*

**Figure 1-5. Carrier-frequency interactions using narrow-band noise stimuli.** This figure plots the amplitude-spectra for the grand-mean data from eight subjects when a probe with a center-frequency of 1000 Hz was presented alone and then simultaneously with a masker having center-frequencies between 660 and 1500 Hz. Only a portion of the spectra are plotted (60-120 Hz).

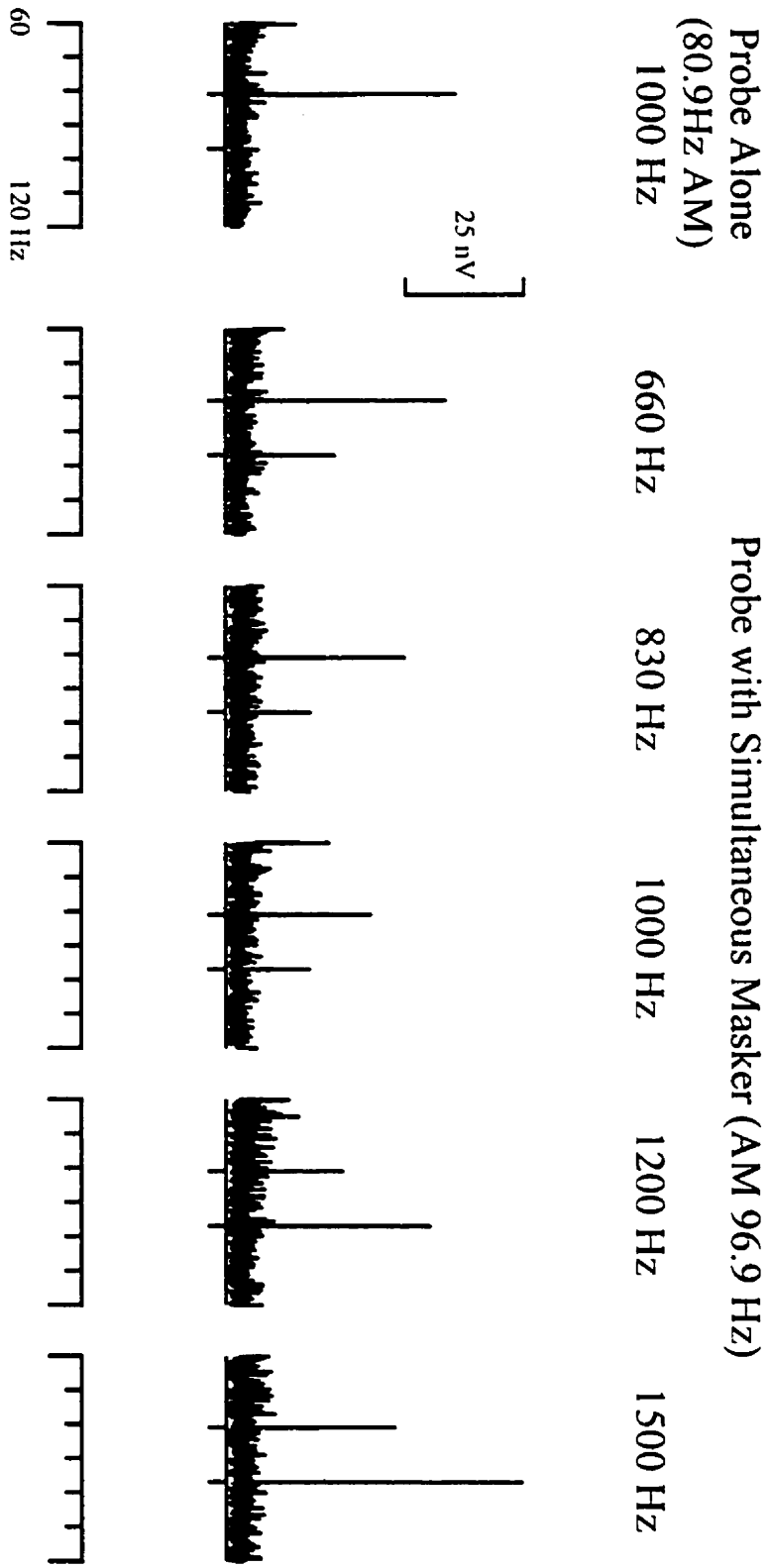
Probe Alone
(80.9Hz AM)
1000 Hz
Probe with Simultaneous Masker (AM 96.9 Hz)
660 Hz
830 Hz
1000 Hz
1200 Hz
1500 Hz
25 nV
60
120 Hz

*Please see next page for figure*

**Figure 1-6. Carrier-frequency interactions using narrow-band noise stimuli.** This graph plots the mean amplitude from the eight subjects involved in the experiment for which the spectra are given in the preceding figure. The graphing format is similar to that in Figure 1-4. The amplitudes in this graph are slightly larger than those shown in the spectra (Figure 1-5), since the measurements here were based upon averaging each subject's amplitude without respect to changes in phase from one subject to the next. On the left of the figure are shown the "least significant differences".

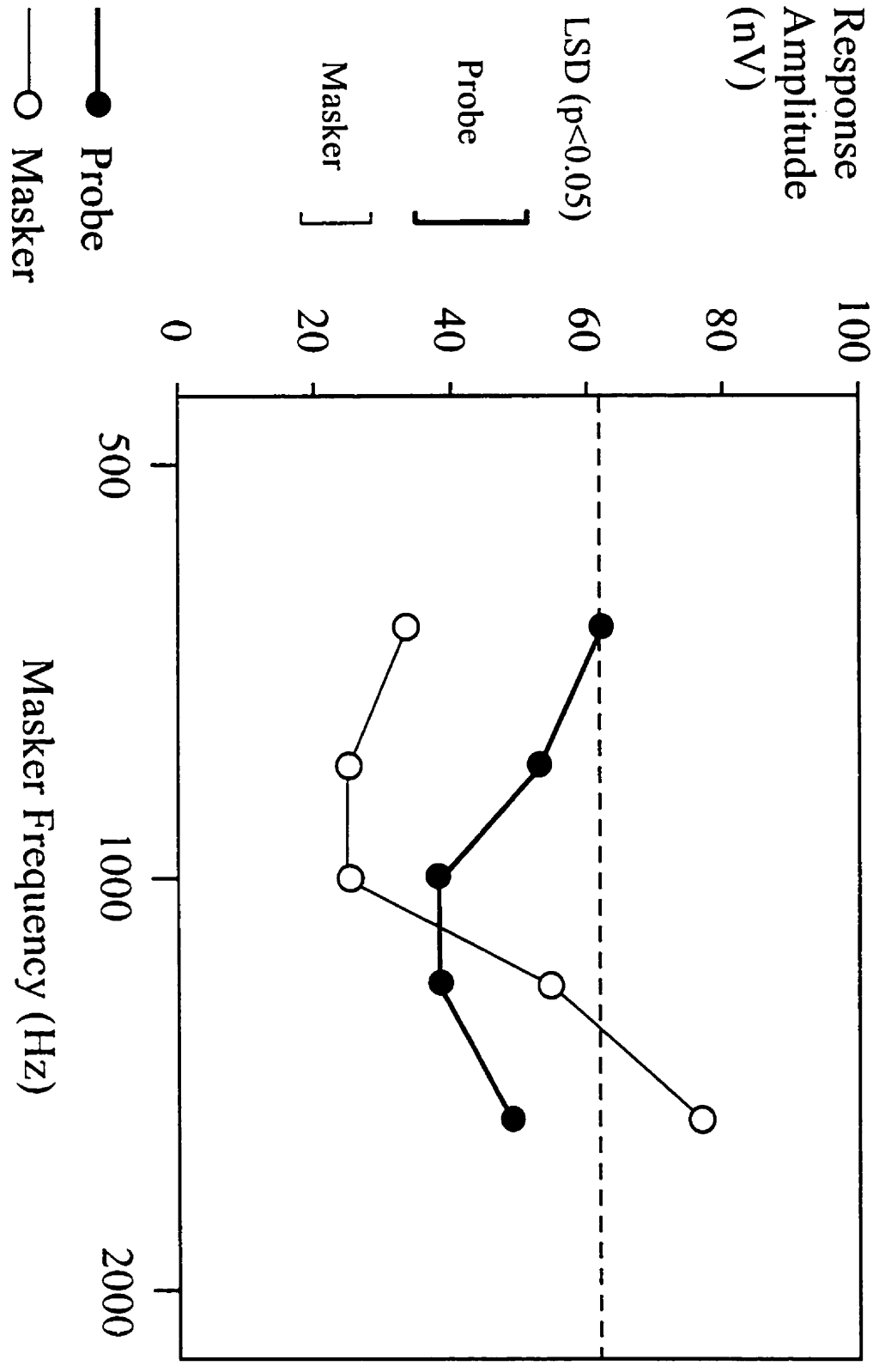
Response Amplitude (nV)
100
80
60
40
20
0
LSD (p<0.05)
Probe
Masker
500
1000
2000
Masker Frequency (Hz)
Probe
Masker

*Please see next page for figure*

**Figure 1-7. Modeled interactions between stimuli with different carrier-frequencies.** The upper part of this figure shows the 1000-Hz probe data reported in Figure 1-4 with each subject's data recalculated as percentages of their own response for the 1000-Hz stimulus presented alone. These results were then modeled using three separate components shown sequentially below these results. The first component represents the activation pattern of the traveling wave on the basilar membrane. The second component represents the attenuation of the response caused by nonlinear processing in the hair cell. This occurs when the two stimuli have different frequencies. The third component represents two-tone suppression effects from stimuli of higher frequencies, together with a small suppression-effect of stimuli at lower frequencies. The residual difference after these three components were modeled is shown at the bottom of the figure. This represents some unknown physiological process that appears to enhance the response if a masker is present, with greater effect when the masker has a lower frequency.

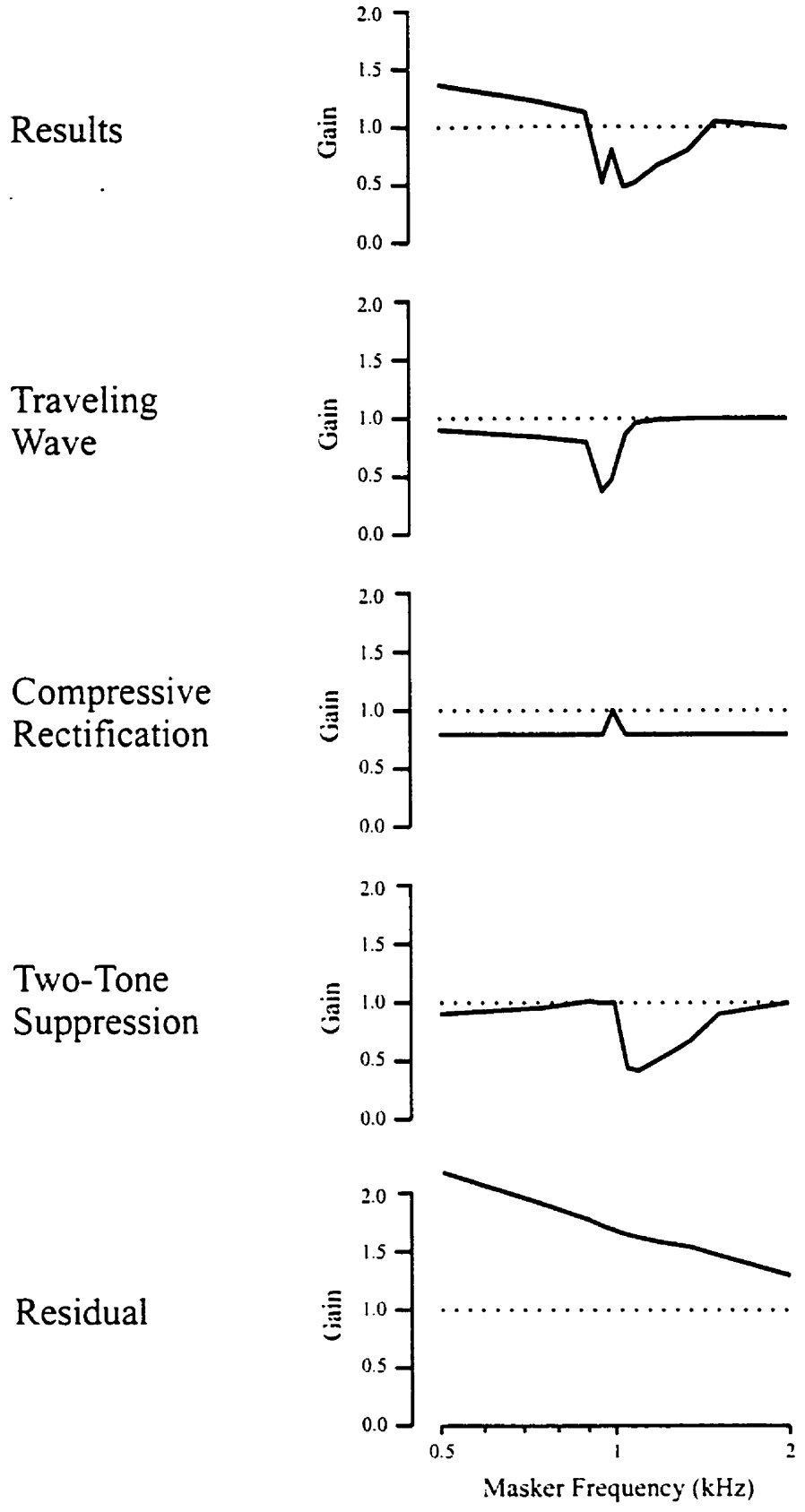
Results
Traveling Wave
Compressive Rectification
Two-Tone Suppression
Residual
Gain
2.0
1.5
1.0
0.5
0.0
0.5
1
2
Masker Frequency (kHz)

frequency of 96.9 Hz and a carrier-frequency that varied with the experimental condition: 0.5, 0.75, 0.9, 0.95, 1.0, 1.05, 1.1, 1.2, 1.35, 1.5 and 2.0 kHz. In a baseline condition the probe tone was presented alone. Five subjects (mean age 35, range 25-49, 1 female) participated in this experiment. Recordings were obtained on three separate days, with several data points repeated across days to ensure that the results were consistent from day to day. A subsidiary set of recordings with 8 (3 common to the initial experiment and 5 new) subjects (mean age 31, range 23-40, 4 female) used narrow band noise (with identical high and low cutoff-frequencies) instead of pure tones for both the probe and masker stimuli. For this experiment the masker stimuli had center-frequencies of 0.66, 0.83, 1, 1.2 and 1.5 kHz.

Sample results from the pure tone stimuli are shown in Figure 1-3 and the mean amplitudes can be found in Figure 1-4. The spectra for the mean waveforms and the mean amplitudes for the noise stimuli are graphed in Figures 5 and 6. The amplitude of the response to the probe (filled circles) varied significantly with the masker frequency ($F=12.7$;df 10,40;$p<0.001$ for the tonal data and $F=3.8$; df 4,28; $p<0.05$ for the noise data). The amplitude of the response to the masker (open circles) also varied with frequency ($F=6.2$;df 10,40;$p<0.001$ for the tonal data and $F=43.7$;df 4,28;$p<0.001$ for the noise data). Post-hoc tests showed three significant aspects of these patterns. First, as can be seen in Figure 1-4, the probe response when the masker was 500 Hz was significantly larger than the response when there was no masker. Second, the response when both the probe and masker tones had a frequency of 1.0 kHz was larger than when the masker had a frequency of 0.95 or 1.05 kHz. Third, as shown in Figure 1-6, the masker responses when the noise masker was higher in frequency than the probe were significantly larger than when the masker was equally lower in frequency (comparing frequencies on a logarithmic scale: 1.2 versus 0.83 kHz and 1.5 versus 0.66 kHz). A mirror-image pattern occurred for the probe amplitudes. Although the same comparisons were not available for the pure tones, the patterns were quite similar.

Figure 1-7 presents the results of modeling the physiological processes that might underlie the interactions noted in Figure 1-4. Three processes are considered: the traveling wave, the nonlinear processing of the hair cell, and two-tone suppression. Having modeled these processes, we are then left with an unexplained residual enhancement process, which decreases monotonically from lower to higher frequencies.

**Experiment 2: Multiple stimuli in the 70-110 Hz range**

Experiment 1 indicated no significant decrease in the responses for two simultaneous stimuli provided that the carrier-frequencies were separated by more than one-half octave. The second experiment examined whether this was true if more than two stimuli were presented simultaneously. Eleven subjects (mean age 29 years, range 15-36, 2 female) participated in this experiment. The stimulus combinations are shown in Table 1-1. Responses to a single 1000 Hz tone or a single 2000 Hz tone served as baseline measurements. These tones were then simultaneously presented with other tones to create combinations of 2, 4 or 8 tones. Two variants of the 4-stimulus condition were used: in one the carrier-frequencies were separated by one octave and in the other by a half-octave. All of the stimuli were individually calibrated to 60 dB SPL so that the combined stimuli had higher intensities. For example, the 8-tone combination stimulus had an intensity of 67 dB SPL.

Mean amplitudes and mean confidence limits (from the $T^2$ test) for the 11 subjects are given in Table 1-2. The amplitudes were analyzed for stimuli with carrier-frequencies of 1000 Hz and 2000 Hz in a two-way (carrier-frequency by condition) repeated-measures ANOVA. There was a significant main effect for condition ($F=13.1$; df 4,88, $p<0.001$) and a significant interaction between carrier-frequency and condition ($F=2.5$, df 4,88, $p<0.05$) but no significant effect of carrier-frequency. Post-hoc tests indicated a significant decrease in amplitude in the two conditions where the carrier-frequencies were separated by one-half octave.

*Please see next page for table*

**Table 1-1: Tone combinations for multiple stimuli.** The 6 different stimulus-combinations contained the carrier-frequencies indicated in the columns of the table. The modulation-rates for each carrier-frequency are indicated in the cells of the table. All tones were presented to right ear only.

## Table 1-1: Tone Combinations for Multiple Stimuli

| Carrier Frequency (Hz) | Modulation-frequency (Hz) | | | | |
|---|---|---|---|---|---|
| | Single stimulus | 2-stimulus | 4-stimulus | | 8-stimulus |
| 335 | | | | | 77.0 |
| 500 | | | 80.9 | | 80.9 |
| 710 | | | | 80.9 | 84.9 |
| 1000 | 88.9 | 88.9 | 88.9 | 88.9 | 88.9 |
| 1420 | | | | 96.9 | 92.9 |
| 2000 | 96.9 | 96.9 | 96.9 | 104.8 | 96.9 |
| 2840 | | | | | 100.8 |
| 4000 | | | 104.8 | | 104.8 |

*Please see next page for table*

**Table 1-2: Response amplitudes during multiple stimulation.** Responses elicited by the 70-110 Hz modulated stimuli are measured in nanovolts. First column presents the mean measurements for 12 subjects. Asterisks indicate that the amplitude was significantly (* $p<0.05$; **$p<0.01$) smaller than the response to the single stimulus at this carrier-frequency. The second column gives the average confidence limits ($p<0.05$). The third column presents the mean of the individual measurements expressed as a percentage of the response in the single-stimulus condition for each subject. The percentages in brackets are based on the mean measurements (in the first column). The fourth column gives the model percentages (see text).

## Table 1-2 Response Amplitudes During Multiple Stimulation

| Condition | 1kHz Response | | | | 2kHz Response | | | |
|---|---|---|---|---|---|---|---|---|
| | mean | conf | % | model | mean | conf | % | model |
| single stimulus | 70 | 19 | 100 | 100 | 75 | 20 | 100 | 100 |
| 2 stimuli | 64 | 24 | 95(91) | 85 | 72 | 26 | 108(96) | 110 |
| 4 stimuli - octave | 65 | 26 | 103(92) | 94 | 62 | 21 | 95(83) | 94 |
| 4 stimuli - ½-octave | 41** | 20 | 69(58) | 54 | 51** | 18 | 74(68) | 94 |
| 8 stimuli - ½-octave | 52* | 20 | 88(73) | 60 | 32** | 20 | 54(43) | 60 |

The interaction resulted from the 2000 Hz response being significantly smaller in the 8-stimulus condition than in the 4-stimulus condition with one-half octave separation, whereas the opposite occurred (but not significantly) for the 1000-Hz response.

From the results of the first experiment (paying particular attention to the narrow-band noise results), we constructed a simple model of the interactions. We estimated that each stimulus would attenuate responses to stimuli with carrier-frequencies a ½-octave lower or higher to 75% and 85% respectively, would attenuate responses to a stimulus with a carrier-frequency 1-octave lower to 85%, and would enhance responses to a stimulus 1-octave higher to 110%. Beyond one-octave we assumed no effect and we did not consider any iteration. In the 2-stimulus condition this model would predict that the 1000-Hz and 2000 Hz responses would be 85% and 110% of their baseline measurements. For the 4-stimulus 1-octave condition both responses should be 94%, since each stimulus is in the presence of stimuli 1-octave higher and lower. For the 4-stimulus ½-octave condition, the 1000 Hz response should be 54% (85%x75%x85%), and the 2000 Hz response should be 94% (110%x85%). For the 8-stimulus ½-octave conditions, the both responses should be 60% (110%x85%x75%x85%). This simple model fits the data reasonably well for all results except for the 2000 Hz response in the 4-stimulus ½-octave condition, which is clearly smaller than might have been expected.

**Experiment 3: Effects of intensity**

The results of the second experiment are the opposite of what would be predicted from masking profiles. Psychophysical studies have shown that low-frequency tones attenuate the response to high-frequency tones rather than vice versa (Egan and Hake, 1950; Moore, 1995). It is possible that our suprathreshold measurements might have been different from psychophysical masking effects which are usually obtained with near-threshold probe stimuli. We therefore decided to evaluate the multiple-stimulus technique using both high and low intensities (75 and 35 dB SPL). Single-stimulus baseline responses were obtained for 1000 and 2000 Hz tones amplitude-modulated at frequencies of 88.9 and 96.9 Hz respectively. Multiple-stimulus responses were then obtained when the two stimuli were presented simultaneously, and in a 4-

stimulus condition (with the addition of a 500 Hz tone modulated at 80.9 Hz and a 4000 Hz tone modulated at 104.8 Hz). Eight subjects (mean age 27 years, range 15-34, 5 female) participated in this study.

Illustrative results from one subject are shown in Figure 1-8. Table 1-3 presents the mean amplitudes from the 8 subjects. At 35 dB SPL there were no significant changes. The amplitudes of the responses were virtually identical when the stimuli were presented alone as when the stimuli occurred in combination. However, there were significant effects at 75 dB SPL (at 1000 Hz $F=13.5$; df 2,14; $p<0.001$; at 2000 Hz $F=17.2$; df 2,14; $p<0.001$). In the 2 stimuli condition, the 1000 Hz response decreased to 62% of its original value, while the 2000 Hz response remained relatively unaffected at 98%. When the 1000 Hz tone was presented with 3 other stimuli it decreased to 56% and the 2000 Hz decreased to 49%. These results are similar in pattern to those at 60 dB SPL although increased in amount. The decrease in the 2000 Hz response only occurs when a 4000 Hz stimulus is included in the stimulus combination. The results therefore support the conclusion from the previous experiments that a high-frequency tone attenuates the steady-state response to an amplitude-modulated low-frequency tone. The effects are larger at higher intensities.

**Experiment 4: Effects of modulation-frequency**

In the preceding experiments, the modulation-frequencies differed by a minimum of 4 Hz. The fourth experiment was designed to investigate the effects of further decreasing the difference between adjacent modulation-frequencies. A response to a single 1000 Hz tone modulated at a frequency of 84.9 Hz served as the baseline. This response was then recorded in the presence of a 2000 Hz tone modulated at 86.3, 87.6, 90.2 or 92.8 Hz (1.3, 2.6, 5.3 and 7.9 Hz separation), and then in the presence of both a 2000 Hz tone and a 500 Hz tone with modulations frequencies separated by the same amount (1.3, 2.6, 5.3 and 7.9 Hz) with the 500 Hz tone having

*Please see next page for figure*

**Figure 1-8. Simultaneous stimulation at different intensities.** This figure represents the responses obtained in one subject when 1, 2, or 4 stimuli were presented simultaneously at intensities of 75 dB SPL and 35 dB SPL. At 35 dB SPL there are no significant changes between the single-stimulus responses and the multiple-stimulus responses, although there is no clearly recognizable response to the 500 Hz stimulus (bottom line). At 75 dB SPL there is a significant decrease in the amplitude of the responses when stimuli of higher frequency are simultaneously present. The x-axis starts at 20 Hz, since the amplitudes of the lower frequencies were very large.

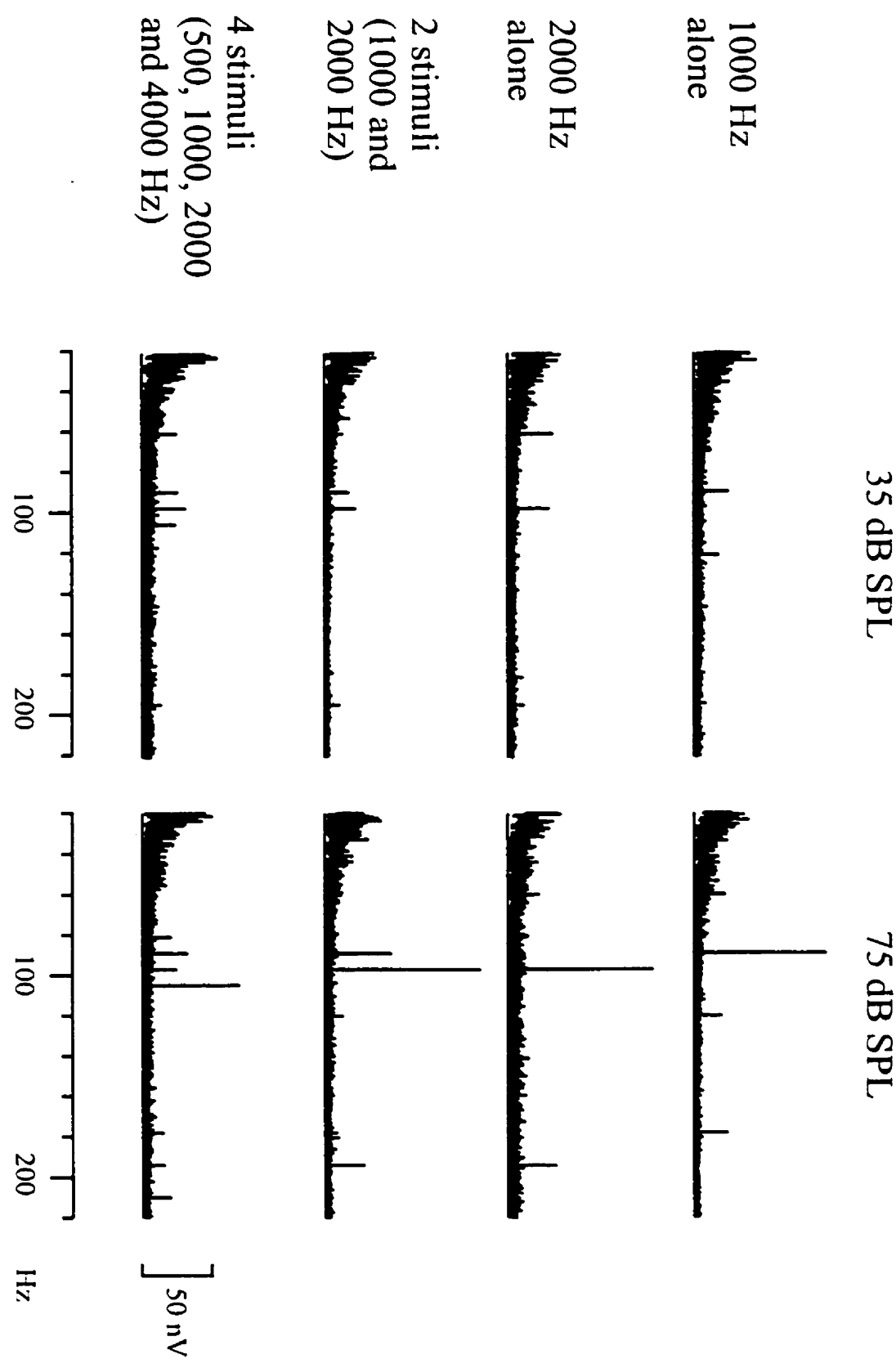
35 dB SPL
75 dB SPL
1000 Hz alone
2000 Hz alone
2 stimuli (1000 and 2000 Hz)
4 stimuli (500, 1000, 2000 and 4000 Hz)
100
200
100
200
50 nV
Hz

*Please see next page for table*

**Table 1-3: Effects of intensity on interactions between multiple stimuli.** The higher intensity 75 dB SPL data show an interaction between stimuli that is not seen in the lower intensity results. The attenuation caused by the addition of additional stimuli is also larger than that found for the 60 dB SPL results shown in Table 1-2.

**Table 1-3 Effects of Intensity on Interactions between Multiple Stimuli**

| Stimuli | Response Amplitude (nV) | | |
|---|---|---|---|
| | Alone | 2-stimuli | 4-stimuli |
| 1000 Hz 75 dB SPL | 157 | 97** | 88** |
| 35 dB SPL | 38 | 38 | 38 |
| 2000 Hz 75 dB SPL | 133 | 130 | 65** |
| 35 dB SPL | 38 | 42 | 35 |

** different from the response when the stimulus presented alone $p<0.01$

*Please see next page for table*

**TABLE 1-4: Spacing of the modulation-frequencies.** Average baseline response to the 1000 Hz stimulus (AM at 84.9 Hz) was 78 nV

## Table 1-4 Spacing of the Modulation-Frequencies

| | Response Amplitude (nV) | | | | | | | |
|---|---|---|---|---|---|---|---|---|
| Spacing | 1.3 Hz | | 2.6 Hz | | 5.3 Hz | | 7.9 Hz | |
| Carrier-frequency (kHz) | 1 | 2 | 1 | 2 | 1 | 2 | 1 | 2 |
| Two Stimuli (1000 and 2000 Hz) | 70 | 84 | 77 | 91 | 66 | 94 | 70 | 91 |
| Three Stimuli (500, 1000 and 2000 Hz) | 72 | 77 | 80 | 87 | 66 | 77 | 82 | 81 |

a lower modulation-frequency. Nine subjects (mean age 32, range 23-52, 4 female) participated in this experiment.

The mean amplitudes are given in Table 1-4. The results (for the 1000 Hz responses) were initially analyzed by comparing all the response amplitudes to those obtained when the 1000 Hz stimulus was presented alone. There were no significant differences ($F=1.5$; df 8,64; $p>0.1$). Next, the responses for the multiple-stimulus conditions were analyzed using a two-way (separation of modulation-frequency by number of stimuli) repeated-measures ANOVA. There was no significant effect of the number of stimuli and no significant interaction. However, there was a significant effect of separation ($F=4.6$; df 3,48; $p<0.01$). Post-hoc testing showed that only the reduction in the amplitude of the 1000-Hz response at separations of 5.3 Hz was significant. Since closer separations (1.3 and 2.6 Hz) caused no attenuation, and since the 2000-Hz responses was not similarly affected, we considered the effect as caused by chance.

**Experiment 5: Noise stimuli**

Most of the carrier signals in Experiments 1-4 were pure tones. Bandpass noise may offer advantages as a carrier signal since it is less susceptible to problems of harmonic interactions with the modulation-frequency. Since Experiment 1 had shown that narrow band noise stimuli could elicit reliable responses, we further explored the use of bandpass noise as a carrier stimulus. Noise that was filtered at three different bandpass settings (200-8000 Hz, 700-1400 Hz and 1000-1000 Hz), and a 1000 Hz pure tone were used as carrier stimuli. The intensity of each stimulus was adjusted to 60 dB SPL. Responses were recorded in 10 subjects (mean age 26, range 21-34, 5 female).

The mean amplitudes and their standard deviations are shown in Table 1-5. There was a highly significant effect of bandwidth on the amplitude of the response ($F=23.2$; df 3,27;

$p<0.001$), with the response to the broadband stimulus being significantly larger than any of the other responses.

**Experiment 6: Multiple stimuli in the 30-60 Hz range**

Steady-state responses recorded using stimulus-rates near 40 Hz have also been used as an objective test of hearing (Dauman et al., 1984; Rodriguez et al., 1986). Previous results have shown that the 40-Hz response was reduced to 78% (Picton et al., 1987) or 66% (Lins et al., 1996) when two stimuli with the same carrier-frequency but different modulation-frequencies were used. However, interactions between stimuli with different carrier-frequencies have not been studied. In order to obtain a relevant baseline to which various experimental conditions could be compared, we recorded the response to a single 1000 Hz probe tone that was amplitude-modulated at 42.7 Hz. The amplitude of this steady-state response was then compared to the amplitude of the same response when the tone was presented in various tone combinations, as summarized in Table 1-6. Each of the tones had an intensity of 60 dB HL. Thirteen subjects (mean age 27 years, range 23-50 years, 3 female) participated in this experiment.

The results from one subject are shown in Figure 1-9 and the mean amplitudes across the subjects are shown in Table 1-6. The average amplitude obtained during the baseline recording, in which a single 1000 Hz was presented to the left ear only, was 0.34 μV. By comparing this baseline value to the subsequent amplitudes of this response, when the 1000 Hz tone was presented in combination with other tones, a percentage was formed. An ANOVA comparing the amplitudes among the baseline measurements and conditions 2-8 showed that the difference in the response amplitudes across the various stimulus manipulations was significant ($F=11.5$;df 7,84; $p<0.001$]. Post-hoc Fisher LSD comparisons indicated a significant decrease in amplitude from the baseline measurement when two tones were presented to the same ear at the same frequency (1000 Hz), when four tones were presented to the left ear (condition 7), and when 8

*Please see next page for table*

**Table 1-5: Bandpass noise as carrier stimulus.** While the broad band stimulus evokes a significantly larger response than the 1000 Hz pure tone, the one-octave noise and the narrow band noise produce slightly smaller responses, though this was not significant.

## Table 1-5 Bandpass Noise as Carrier Stimulus

| Carrier Stimulus | Response Amplitude (nV) |
|---|---|
| 1000 Hz Pure Tone | 90±55 |
| Broad Band Noise (200-8000 Hz) | 138±53** |
| One-Octave Noise (700-1400 Hz) | 85±39 |
| Narrow Band Noise (1000-1000 Hz) | 71±46 |

** Significantly different from pure tone response ($p<0.01$)

*Please see next page for figure*

**Figure 1-9. Modulation-frequencies in the 30-50 Hz range.** These results show the amplitude spectra for one typical subject in four of the conditions of Experiment 5. On the right of the figure are shown the polar plots of the responses for the stimulus, with a carrier-frequency of 1000 Hz and a modulation-frequency of 42.7 Hz in each of the four conditions. As can be seen, there is significant attenuation of the response when stimuli are presented simultaneously and this attenuation increases with the number of stimuli.

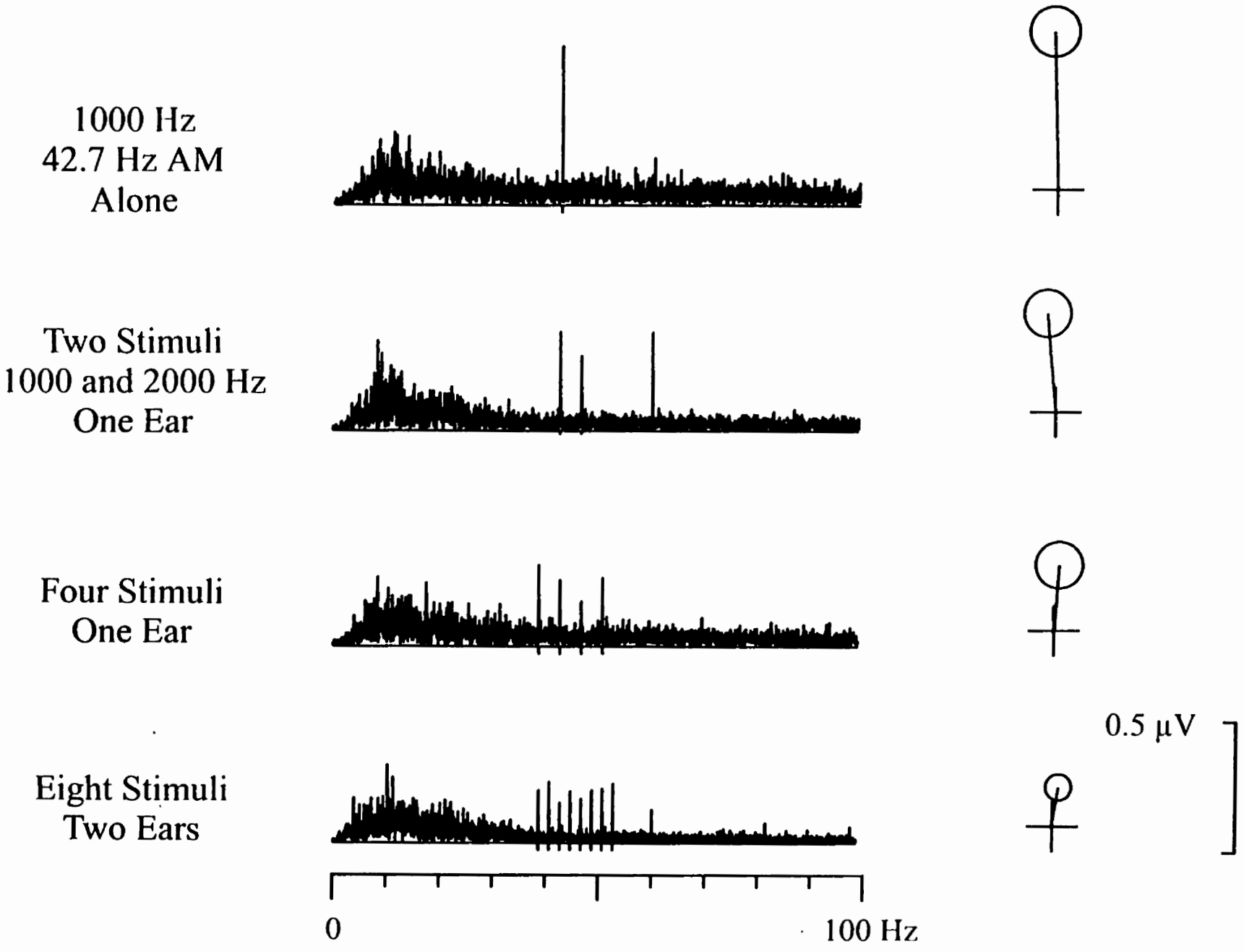
1000 Hz
42.7 Hz AM
Alone
Two Stimuli
1000 and 2000 Hz
One Ear
Four Stimuli
One Ear
Eight Stimuli
Two Ears
0.5 µV
0
100 Hz

*Please see next page for table*

**Table 1-6: Multiple stimuli modulated in the 30-50 Hz range.** The upper part of the table shows the stimulus combinations 1 to 8 which were comprised of carrier-frequencies and modulation rates as indicated by the "•" symbol. The lower part of the table (below the double line) shows the measurements of the response to the stimulus with a carrier-frequency of 1000 Hz and a modulation-frequency of 42.7 Hz. The significance represents the statistical comparison between the amplitude in the multiple-stimulus condition and in the baseline condition (the 1000 Hz stimulus presented alone).

## Table 1-6: Multiple Stimuli Modulated in the 30-50 Hz Range

| | Carrier Frequency | Modulation Frequency | Condition 1 | 2 | 3 | 4 | 5 | 6 | 7 | 8 |
|---|---|---|---|---|---|---|---|---|---|---|
| Left Ear | 500 | 38.7 | | • | | | | | • | • |
| | 1000 | 42.7 | • | • | • | • | • | • | • | • |
| | 1000 | 44.7 | • | | | | | | | |
| | 2000 | 46.7 | | | • | | | | • | • |
| | 4000 | 50.7 | | | | • | | | • | • |
| Right Ear | 500 | 40.7 | | | | | | | | • |
| | 1000 | 44.7 | | | | | • | | | • |
| | 2000 | 48.7 | | | | | | • | | • |
| | 4000 | 52.7 | | | | | | | | • |
| **Measurement** | | | | | | | | | | |
| **Mean Amplitude (μV)** | | | 0.23 | 0.36 | 0.30 | 0.36 | 0.31 | 0.33 | 0.23 | 0.15 |
| **Significance ($p<0.05$)** | | | * | | | | | | * | * |
| **Standard Deviation** | | | 0.09 | 0.14 | 0.09 | 0.14 | 0.10 | 0.12 | 0.07 | 0.07 |
| **% of Baseline (0.34 μV)** | | | 66 | 104 | 87 | 104 | 89 | 95 | 66 | 44 |

tones were presented to the two ears (condition 8). The other post-hoc comparisons were not significant, although the pattern of the results is very similar to that noted in Experiment 1: the 1000 Hz response was smaller when the stimulus was combined with a 2000 Hz tone and larger when combined with a 500 Hz tone.

## DISCUSSION

The experiments described in this chapter were initially designed to test the limits of using multiple simultaneous stimuli when recording steady-state responses. Our previous studies (Lins et al., 1996; Lins and Picton, 1995) had shown that the MASTER technique was very promising. Although the results of the present experiments confirmed most of our impressions about the technique, some of the results were different from what we had expected. For example, the two-tone interactions were opposite to what we had expected from our understanding of masking. Factors that might be considered when the actual differs from the predicted are that nonlinear processing is occurring, or that the predictive models are not taking into account all active processes. Since nonlinearities are essential for recording the response to amplitude-modulated stimuli, we shall start our discussion here.

### Non-linearities

The cochlea functions in a very nonlinear manner (Dallos, 1973; Green, 1976). The hair-cell responds preferentially to movement of the hairs in one direction. In addition, the responsiveness saturates with increasing amplitude of the stimulus. The cochlear transfer function can therefore been described as a compressive rectification with a direct current offset

A sinusoidally amplitude-modulated pure tone contains energy at three frequencies (Figure 1-1) - the carrier-frequency plus two other frequencies separated from the carrier by the modulation-frequency (Regan, 1994). This signal contains no energy at the modulation-

frequency. However, a nonlinear distortion of this signal will result in energy at frequencies equal to the sums and differences of the frequencies present and integer multiples of these frequencies. Prominent among these "distortion products" or "combination tones" will be the modulation-frequency. Non-linearities in the cochlea thus provide the basis for the detection of envelopes. Without the distortion, there is no energy at the envelope frequency.

Nonlinear distortions should be distinguished from linear effects which also occur between combinations of tones. The combination of two tones of different frequencies results in a tone whose amplitude beats at a frequency equal to the difference between the frequencies of the two tones. Nonlinear distortion of beating stimuli will result in energy at the beat-frequency (see top of Figure 1-10). Beats are simpler in their frequency content (two frequencies) than sinusoidally amplitude-modulated tones (three frequencies) and can elicit the same envelope-following responses as sinusoidally modulated tones (Dolphin et al., 1994).

Multiple sinusoidally amplitude-modulated tones contain multiple frequencies, all of which can participate in the formation of distortion products when submitted to nonlinear distortion. The resultant response will show energy at each of the modulation-frequencies and also at frequencies formed by various combinations of the modulation-frequencies and carrier-frequencies.

A problem arises when these other distortion products overlap with the modulation-frequency distortion-products and attenuate the modulation-frequency response. The 8-stimulus response in Figure 1-10 (middle row) shows an example: two of the modulation-frequencies have been attenuated by such overlaps. This can often be avoided by judicious choice of modulation and carrier-frequencies (using as many prime numbers as possible). However, this strategy becomes difficult with multiple stimuli and with the requirement for integer cycles of both carrier and modulation-frequency through a recording sweep.

*Please see next page for figure*

**Figure 1-10: Nonlinear distortions.** This figure illustrates the effects of simple nonlinear processing (rectification) on some of the stimuli used in the experiments. The spectra at the center of the figure represent the frequencies present in the signal before nonlinear processing. The spectra at the right show the effects of rectification on these signals. These spectra show only the low-frequency regions (0-250 Hz). The amplitude scales are arbitrary but equivalent within an example. When the carrier-frequencies are very close together (top example) there are multiple distortion-products. One of these (asterisk) is at difference between the two carrier-frequencies (the beat frequency). Others (arrows) are at the modulation-frequencies. When eight amplitude-modulated tones are presented simultaneously (middle example), there is more attenuation of two of the modulation-frequencies (arrows) compared to the others caused by overlapping higher-order distortion products. The bottom example shows the response to amplitude-modulated noise. In the rectified response, there are low-level distortion-products at all frequencies and one large response at the modulation-frequency.

| Carrier | Modulation |
|---|---|
| 1000 | 80.9 |
| 1050 | 96.9 |
| 335 | 77.0 |
| 500 | 80.9 |
| 710 | 84.9 |
| 1000 | 88.9 |
| 1420 | 92.9 |
| 2000 | 96.9 |
| 2840 | 100.8 |
| 4000 | 104.8 |
| Noise (700-1400) | 80.9 |

Signal

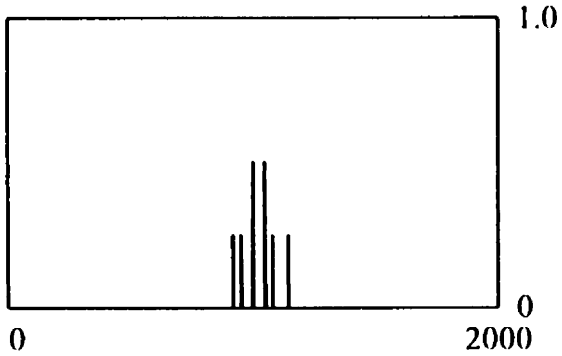


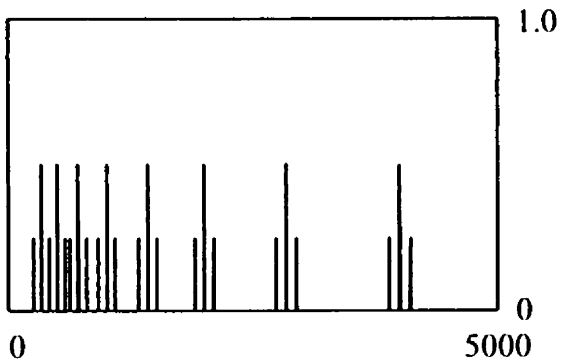


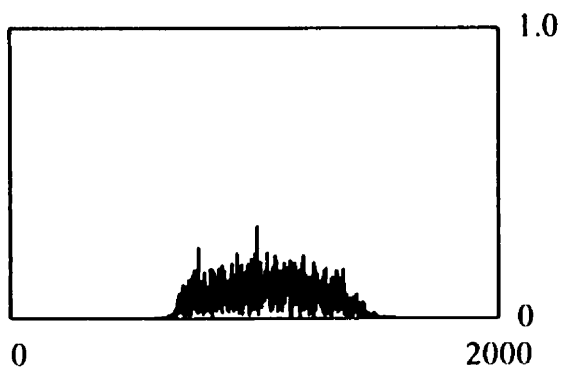


Rectified Signal

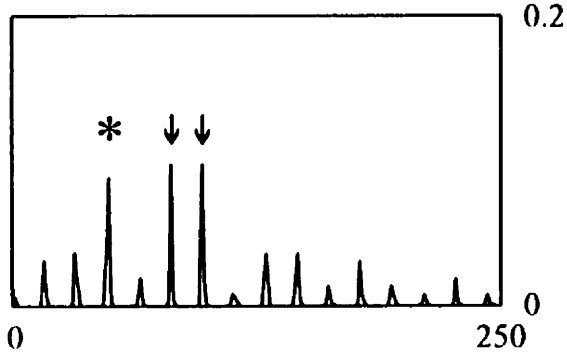


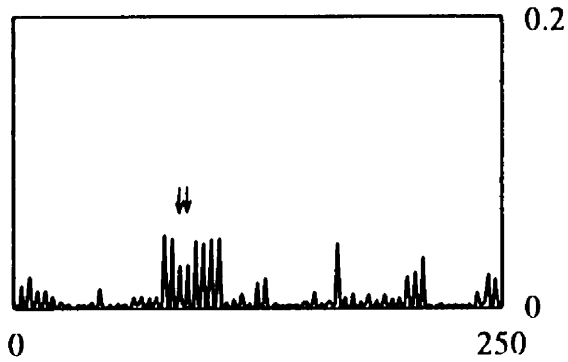


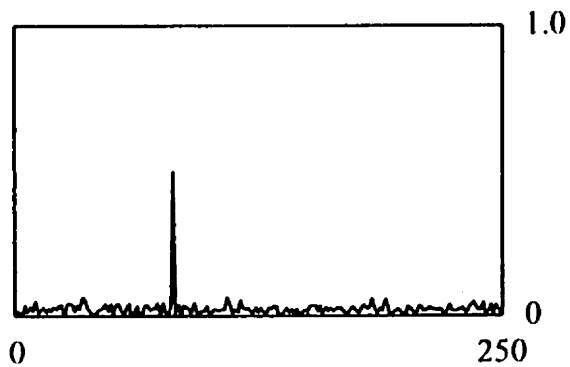

Using noise instead of a pure tone as the carrier signal might circumvent this problem. Since noise consists of multiple frequencies, the number of distortion products is increased. However, the energy at each of the distortion products is lower (Figure 1-10, bottom example). Furthermore, these will tend to cancel if the noise changes from sweep to sweep, since averaging will further decrease the amplitude of these distortion products. We had initially not considered noise as a stimulus, due to a concern that phase variability would attenuate the amplitude of response. However, phase is minimally affected by carrier-frequency provided that modulation-frequency is held constant (Cohen et al., 1991; Lins et al., 1995). A travelling-wave delay of 1 ms would translate to a 36-degree change in phase for a modulation-frequency of 100 Hz. As shown in Experiment 5, an amplitude-modulated broad-band noise elicits a large response that may prove useful in rapid screening of hearing. An amplitude-modulated narrow-band noise elicits a response that is similar to that elicited by a tone with fewer problems of overlapping distortion products.

**Interactions between Stimuli**

The results shown in Figure 1-4 have important implications for models of auditory processing. When two amplitude-modulated tones are presented simultaneously and when the carrier-frequencies are separated by less than one-half octave, the envelope-response to the low-frequency carrier is attenuated more than the response to the high-frequency carrier. This result is the opposite of what might be expected from the extensive literature on masking (Egan and Hake, 1950; Moore, 1995; Delgutte, 1990; Delgutte, 1996). Nevertheless, the results were quite robust across repeated recordings, and similar findings occurred for both narrow-band noise stimuli and pure tones. Furthermore, the results of Experiments 2 and 3 both clearly show that high-frequency tones attenuate low-frequency tones. Dolphin and Mountain (1993) reported very similar results when studying the response of the gerbil to a sinusoidally amplitude-modulated "probe" tone in the presence of an "interfering" pure tone. Interfering tones with frequencies

higher than the probe attenuated the response more than interfering tones of lower frequency. Dolphin and Mountain (1993) related their findings to two-tone suppression. Accordingly, we incorporated this process when modeling our results (Figure 1-7). In the modeling, we attempted to explain as many of the findings as possible by what happens in the cochlea and auditory nerve. By the time the steady-state responses are generated in the brainstem and cortex, many other physiological processes may have exerted an effect. Nevertheless, the earlier effects have to be accounted for:

***(i) Traveling wave:***

If the activation patterns of two stimuli overlap, the hair cells located in the area of overlap will respond to the interactions between the two stimuli in that area. Because of the non-linearities of the hair cell transduction process, the response to two tones presented simultaneously will be smaller than the sum of the responses to the same tones presented alone. The decrease will depend on the differences between the frequencies of the mask and the probe, and on the relative amplitudes of the two tones at one region of the basilar membrane. The relative amplitudes will depend on the asymmetrical activation pattern of the traveling wave (Robles et al., 1986; Rhode and Robles, 1974; Yates, 1995).

***(ii) Compressive Rectification***

If the masker tone has a slightly different frequency than the probe tone the amplitude of the response to the probe is less than when the masker has the exactly the same frequency and phase as the probe tone. This explains the notch in the interaction curve at 1000 Hz. Such a notch is not present for the noise stimuli since we were adding together two different filtered noises at 1000 Hz and not identical stimuli. When the masker and the probe have different frequencies, the compressive rectification (Russell and Sellick, 1978; Patuzzi and Sellick, 1983) that occurs at the level of the hair cell will attenuate the response to the modulation-frequencies from what would occur when the signals are presented alone.

***(iii) Suppression***

Two-tone suppression occurs when the response to one tone is reduced due to the presence of a second tone (Rupert et al., 1963; Nomoto et al.,1964; Sachs and Kiang, 1968; Ruggero, 1992). Two-tone suppression is a cochlear phenomenon since it persists even after sectioning the auditory nerve central to the site of recording (Kiang et al., 1965). At moderate intensities, the suppression is greater when the suppressing tone is higher in frequency (Arthur et al., 1971; Harris, 1979; Cooper, 1996).

***(iv) Residual***

After modeling these three components, we were still left with an unexplained residual effect. This represents an amplification that is larger for maskers with lower frequencies. It is generalized over a wide range of frequencies, unlike either the travelling wave or two-tone suppression. This effect is present in most of our data although it is not present in some (e.g. the noise probe data in Figures 5 and 6). It is probably a small effect that may or may not be recognizable in the recording noise. What might it represent? Some process of enhancement would appear necessary to counter the attenuation of the modulation-frequency response when multiple AM tones are combined and submitted to distortion (e.g., the lower set of spectra in Figure 1-1). Unless the intensities are high, there is no such attenuation of the response provided the carrier-frequencies are an octave or more apart. Accordingly, there may be some facilitatory process within the brain stem - "synchrony enhancement" - whereby the presence of one tone increases the envelope detection of another tone.

**Numbers and Noise**

The advantage of the MASTER technique is that information is obtained about many stimuli in the time usually taken to measure the response to a single stimulus. A similar approach has been proposed for recording oto-acoustic emissions: the simultaneous presentation of multiple pairs of stimuli, each pair eliciting distinguishable distortion-product emissions

(Zurek and Rabinowitz, 1995). The advantage of simultaneous stimulation for the evoked potentials persists as long as the MASTER amplitudes are about the same amplitude as when the stimuli are presented alone. If the responses decrease in amplitude, the extra time necessary to obtain an equivalent signal-to-noise ratio must be balanced against the increased information obtained because of the multiple responses.

Noise is reduced by a factor equivalent to $1/\sqrt{T}$ where T is the time spent either in averaging or in increasing the duration of the sweep submitted to Fourier analysis (Figure 1-2). Since recording N responses using single-stimulus techniques would require N times the amount of time to obtain information about N stimuli, the multiple stimulus technique remains more efficient than the single-stimulus technique provided that the amplitude reduction in the response is less than $1/\sqrt{N}$. Thus a 4-stimulus MASTER technique remains better than a single-stimulus technique provided that MASTER amplitudes are reduced no less than 50%. If the MASTER amplitude divided by the single-stimulus response amplitude is A, the time to obtain the same signal-to-noise ratio using the single-stimulus technique compared to the time for the MASTER technique is $N(A^2)$.

As can be seen in Table 1-2, the MASTER technique for the 70-110 Hz responses is significantly more efficient than the single stimulus technique when 4 stimuli are presented at 60 dB SPL to one ear provided the carrier-frequencies are an octave apart. When the carrier-frequencies become as close as one half octave the MASTER technique is only slightly more efficient (8 stimuli) than or no different (4 stimuli) from the single-stimulus technique. However when the intensity was increased to 75 dB SPL (Table 1-3), the efficiency of the MASTER technique is not significantly different from the single-stimulus technique. This is caused by the greater interactions between stimuli at this high intensity. Nevertheless, despite these interactions, the efficiency is still not less than the single-stimulus technique.

Using a slightly different stimulus technique ("beats" as described in the initial section of this discussion), Dolphin (1996) found in gerbils a slight decrease in amplitude when increasing the number of stimuli but this decrease did not eliminate the increased efficiency of recording with simultaneous rather than single stimuli. These results are similar to our results in human subjects at intensities above 60 dB SPL where the multiple stimulus technique does reduce the amplitude of the responses.

Using the MASTER technique with responses in the 30-50 Hz range is not as promising (Table 1-5). The response amplitudes at 60 dB SPL when using 2, 4, and 8 simultaneous stimuli (87, 66, 44%) are only slightly greater than the threshold for increased efficiency (71, 50, 36%). Greater interactions between stimuli may expected at these slower modulation rates, compared to the faster rates since these are primarily generated in the auditory cortex. While the brainstem structures often act to disentangle and analyze the various components of a sound stimulus, as the information moves to the higher levels, where reintegration of the original sound occurs, greater interactions tend to occur. It may therefore not be worth the trouble to record these responses using the MASTER technique since other problems affect the multiple-stimulus technique in addition to the attenuation of the response. In particular, the responses to the various distortion products may increase the background noise.

**Discrimination of Modulation-frequencies**

Provided the Fourier analysis has a sufficient resolving power, the modulation-frequencies for different carrier signals can be very close together. Experiment 4 shows that making modulation-frequencies as close as 1.3 Hz does not attenuate the response. In terms of the audiometric applications of MASTER, this provides considerable freedom in choosing the modulation-frequencies. It terms of physiology, it indicates that the separation into carrier-frequencies occurs before the recognition of the envelope. Different cells are probably mediating

the envelope-responses to the different carrier-frequencies. No interaction between the different modulation-frequencies would therefore occur if the modulations are confined to different carrier-frequencies. Certain cells in the cochlear nucleus ("onset chopper", "chopper" and "pauser/buildup" units) show a particular sensitivity to amplitude-modulation (MØller, 1974; Frisina et al., 1990a; Frisina et al.,1990b; Rhode and Greenberg, 1992). The spectral sensitivity of these cells is similar to that of the afferent fibers in the auditory nerve. The auditory system therefore appears to perform an initial frequency analysis (in the cochlea) and subsequently considers the envelope within the analyzed frequency-bands. The modulation transfer functions in these cochlear-nucleus cells have a low-pass shape: responses occur at all modulation-frequencies below an upper cut-off. By the time the information has reached the inferior colliculus, many of the modulation transfer functions approximate band-pass filters, with the neurons responding to modulation-frequencies within set ranges (Langner and Schreiner, 1988). In the medial geniculate, some neurons respond to particular modulation-frequencies independently of the spectral content of the carrier-stimulus (Preuss and Muller-Preuss, 1990). At this level, but not before, there might be some interactions between closely spaced modulation-frequencies.

**Caveats**

Increasing the intensity of the stimuli may decrease the efficiency of the MASTER technique. We originally thought that increasing the intensity would bring about the classic masking effects whereby the response to a high-frequency tone would be attenuated by the concurrent presence of a low frequency tone. Increasing the intensity of the stimuli to 75 dB SPL did increase the interactions between the stimuli. Indeed, the responses when four stimuli are presented simultaneously at this intensity are sufficiently attenuated that it is no longer clearly more efficient to record the responses simultaneously. However, the pattern of the interactions

followed the same pattern as seen at moderate intensities with the attenuation being greater for the lower frequency tones.

It is difficult to predict what might occur in patients with hearing impairment due to cochlear dysfunction. The tuning curves of the auditory nerve fibers coming from a hearing-impaired cochlea are quite different from normal auditory nerve fibers. The tip of the tuning curve is often attenuated, absent or distorted (Kiang et al., 1976; Dallos and Harris, 1978). In these pathological auditory nerve fibers, the response that occurs to a single-stimulus at its characteristic frequency might not occur in the presence of other stimuli of lower frequency that activate the response area of the cell and thereby mask its response to stimuli at its characteristic frequency. Certain discrepancies can therefore exist between the pure tone audiogram obtained using single-stimuli and the responses obtained using multiple-simultaneous stimuli. However, since everyday sounds contain multiple frequencies, it is possible that MASTER may provide a better representation of actual hearing than the responses to single stimuli.

Steady-state responses are evoked by tones that last from seconds to minutes. This differs from the intermittent stimuli used in normal behavioral testing and in most other evoked potential techniques. Two potential problems should therefore be considered. First, high-intensity stimuli might cause a temporary threshold shift. Second, there might be adaptation of the responses over time. Indeed, some of our subjects noted that the 35-dB 2000 Hz tone occasionally became inaudible. Both of these problems would be reduced if the recordings stopped as soon as a response was recognized as significantly different from the background noise, rather than, as in our experiments, persisting for approximately ten minutes (chosen to provide highly reliable recordings).

Alternatively, the occasional inability to hear the 2000 Hz tone may have been due to minor amounts of adaptation, since the low intensity stimuli (e.g., 35 dB SPL) may have been at, or even below, either the subject's behavioral threshold, physiological threshold, or both. The

intensity levels that are needed to evoke steady-state responses at the lower and higher carrier frequencies (for example, below 1000 Hz and above 3000 Hz) are higher. Accordingly, when using the MASTER technique for audiometric purposes, investigators should be aware of the minimum threshold intensities (as a function of frequency) that can evoke responses.

The sinusoidally amplitude-modulated tone is highly restricted in its frequency content. Acoustically it is much more frequency-specific than other stimuli used in evoked potential audiometry. The degree of this frequency-specificity will need to be checked using appropriate masking procedures (Stapells et al., 1993). AM tones will not be any more place-specific than pure tones: an amplitude-modulated tone will activate regions of the basilar membrane from the stapes to the area most responsive to the carrier-frequency in a manner very similar to a pure tone. These stimuli will therefore cause a spread of activation towards the higher frequencies. Audiometry using the MASTER technique, like behavioural audiometry with pure tones, is frequency-specific but not place-specific. Masking techniques to render the responses place-specific as well as frequency-specific (Stapells et al., 1993) cannot easily be used when multiple stimuli are presented simultaneously.

We recorded the responses only between the vertex and the neck. This montage is probably optimal for the 80-Hz responses. However, since the 40-Hz responses are generated, in-part, from within the auditory cortex, it is possible that other montages may have provided better recordings, particularly for certain carrier-frequencies. It is also possible the at signal-to-noise levels could have been more efficiently reduced if recordings from more than one electrode-combination were considered.

**Recommendations for the MASTER Technique**

Although the physiological interactions are quite complex, the audiometric implications of these results are reasonably clear. The MASTER technique works well for steady-state

responses at frequencies between 70 and 110 Hz. At least four stimuli can be simultaneously presented to an ear without any significant decrease in the response, provided the carrier-frequencies separated by an octave and the intensities are 60 dB SPL or less. It is possible we might use six simultaneous stimuli at each ear, as long as the stimuli are separated by octaves: 250 Hz, 500 Hz, 1 kHz, 2 kHz, 4 kHz and 8 kHz. Previous studies have suggested that 4 stimuli can be presented to each ear (for a total of 8 stimuli) without loss in amplitude (Lins et al., 1996). Thus the time to record the responses can be reduced eightfold. Caution must be exercised in interpreting the responses at higher intensities where greater interactions may occur between the simultaneous stimuli. Lastly, because of the problems of overlapping distortion products, bandpass noise might be a better carrier signal than pure tones.

# CHAPTER 2

## MASTER:

## A WINDOWS PROGRAM FOR RECORDING MULTIPLE AUDITORY STEADY-STATE RESPONSES

A portion of this material has previously appeared in M. S. John and T. W. Picton (2000) *MASTER: A Windows Program for Recording Multiple Auditory Steady-State Responses.* Computer Methods and Programs in Biomedicine (61), p 125-150. *Reprinted with permission*

## Abstract

MASTER is a Windows-based data acquisition system designed to assess human hearing by recording auditory steady-state responses. The system simultaneously generates multiple amplitude-modulated and/or frequency-modulated auditory stimuli, acquires electrophysiological responses to these stimuli, displays these responses in the frequency-domain, and determines whether or not the responses are significantly larger than background electroencephalographic activity. The operator can print out the results, store the data on disk for more extensive analysis by other programs, review stored data and combine results. The system design follows clear principles concerning the generation of acoustic signals, the acquisition of artifact-free data, the analysis of electrophysiological responses in the frequency-domain, and the objective detection of signals in noise. The instrument uses a popular programming language (LabVIEW) and a commercial data acquisition board (AT-MIO-16E-10), both of which are available from National Instruments.

## 1] Introduction

This chapter discusses the general principles underlying the Multiple Auditory Steady-State Response (MASTER) technique and describes a data collection system we designed for using the technique. As discussed in Chapter 1, the MASTER technique provides a rapid and objective assessment of hearing, which is based upon the statistical evaluation of the electrophysiological responses evoked by multiple auditory tones presented simultaneously. These auditory steady-state responses can be recorded from the human scalp intermixed with the other activity in the electroencephalogram (EEG). As shown in Figure 1-2, a combination of averaging and frequency-analysis can be used to distinguish the responses from the background EEG activity.

After reading Chapter 1, the reader should now be familiar with the basics of the technique. Eight continuous tones can be presented (four to each ear) and each tone is sinusoidally modulated at a unique frequency. The detection of the interwoven responses becomes possible after the electrophysiological data are transformed into the frequency domain. The response to each tone is then identified at the specific frequency at which the tone was modulated. The technique thus evaluates the responsiveness of the human auditory system to several different tonal frequencies in the same time it would take to record one response if each stimulus was presented separately.

Additionally, some advantages of the actual application of the technique should now be obvious. Electrophysiological responses to sounds are useful when patients are unable or unwilling to give accurate or reliable behavioral responses (Dobie, 1993). This occurs in newborn infants, young children, comatose or anesthetized patients, patients who have difficulty communicating because of neurological or psychiatric disorders, and patients who may be feigning hearing loss. The auditory steady-state responses have several advantages over other electrophysiological procedures for assessing audiological responsiveness. For example, data can be obtained from either awake or sleeping subjects since arousal state has minimal effect on the steady-state response to stimuli presented at rates of 70 Hz or faster (Cohen et al., 1991; Lins and Picton, 1995). Responses were found to be rapidly obtained by presenting four simultaneous stimuli in each ear (a total of eight stimuli), provided the carrier-frequencies ($f_c$) are separated by

at least one half-octave and the modulation-frequencies ($f_m$) are separated by at least 1.3 Hz (Lins and Picton, 1995; Chapter 1, Table 1-2). Moreover, because the stimuli are sinusoidally modulated tones, the stimulus energy contains less spectral "splatter" than transient stimuli such as tonepips.

The MASTER system, which includes both software and hardware, can be used with a PC running Windows95 to collect and analyze auditory steady-state responses. While the system was primarily designed to facilitate research with the auditory steady-state responses it may also be used by clinicians and audiologists to assess hearing in patients who require objective audiometry. Accordingly, it is our hope that over the next several years many types of users will be able to use the system both clinically and experimentally. Accordingly, in this chapter we hoped to provide future users with a good understanding of the system design which follows clear principles concerning the generation of acoustic signals, the acquisition of artifact-free data, the analysis of electrophysiological responses in the frequency-domain, and the objective detection of signals in noise.

## 2| Background

Human auditory steady-state responses were first recorded by Galambos et al. (1981), using stimuli presented at rates near 40 Hz. Subsequent studies showed that steady-state responses may be recorded over a wide range of other stimulus rates (Rickards and Clark, 1984; Lins et al., 1995). Since the 40 Hz responses fluctuate with the level of arousal (Linden et al., 1985), faster rates (>70 Hz) may be preferable for audiometric purposes because the responses at these rates are little affected by arousal (Cohen et al.,1991; Lins and Picton, 1995). Combining both amplitude-modulation (AM) and frequency-modulation (FM) produces larger auditory steady-state responses than either type of modulation alone (Cohen et al., 1991). Steady-state responses can be statistically distinguished from the background electroencephalographic activity in which they normally occur by means of several frequency-domain techniques (Picton et al., 1987; Victor and Mast, 1992; Zurek, 1992; Dobie and Wilson, 1996; Valdes et al., 1997). The idea of presenting several stimuli at once was first investigated over three decades ago by Regan and his colleagues (Regan and Heron, 1969; Regan et al., 1970) who showed that steady-state responses elicited by several simultaneously presented visual stimuli could be recorded and

analyzed independently as long as each stimulus was presented at a different rate. More recently, Lins and Picton (1995) extended these findings into the auditory modality and recorded responses to multiple amplitude-modulated tones.

One of the most important applications for the auditory steady-state responses is in assessing hearing in newborn infants. Oto-acoustic emissions can provide a rapid screening test for hearing impairment but cannot determine the severity of the hearing loss. Auditory steady-state responses perform well in this context (Rickards et al., 1994; Rance et al., 1995; Lins et al., 1996; Rance et al., 1998) and protocols are being developed to monitor the treatment of the detected hearing impairment (Picton et al., 1998). Accordingly, we decided to develop a system which would use standard hardware and a flexible programming system, thus allowing easy modifications of a general steady-state response program according to evolving techniques.

After reviewing various data acquisition platforms, we chose to create our programs using LabVIEW™ from National Instruments. LabVIEW is a graphical programming language which lets the user create "virtual instruments" (VIs) that look and act like real instruments (Poindessault, 1995; Johnson, 1997) and which is tailored to work with a large number of data acquisition cards. LabVIEW is attractive because it contains a vast number of functions which enable system control and data acquisition. Other researchers have used it to build systems for data acquisition and analysis in neurophysiology (Budai et al., 1993; Nordstrom et al., 1995)., cardio-vascular research (Davis et al., 1997), clinical audiology (Kunov et al., 1997), neurosurgical monitoring (Bardt et al., 1998), and intraoperative monitoring (Heyer et al., 1995). We also chose LabVIEW because it operates in a Windows95 environment which supports communication between programs (e.g. for evaluating data in spreadsheet-programs), and because it allows the program to be easily modified for different protocols through the interface of the Windows operating system. For the data acquisition board we chose National Instruments AT-MIO-16E-10 board, which provides 2 channels of digital-analog (DA) conversion (12 bit resolution), and 16 channels of analog-digital (AD) conversion (also 12 bit resolution). The present system uses only one of the AD channels because we have not yet finished developing techniques to evaluate multiple channel recordings. Prior to the development of the MASTER system, we used a more rudimentary program written in C, the major drawbacks of which were the lack of real time-processing and display, the need for custom-built interface-boards, and the lack of user-friendliness due to the non-Windows environment.

## 3] Overview of The MASTER Technique

A steady-state evoked response is a repetitive evoked potential "whose constituent discrete frequency components remain constant in amplitude and time over an infinitely prolonged time period" (Regan, 1989). In actual practice, an auditory steady-state response may be elicited by presenting an auditory stimulus at a rate that is sufficiently rapid to cause the brain's response to any one sound stimulus to overlap the response to the preceding stimulus. This technique results in a response containing frequencies at the rate of stimulation and/or at harmonics of this rate. The sinusoidal modulation of the amplitude or frequency of a continuous carrier-frequency may also be used to evoke steady-state responses (Rickards and Clark, 1984; Kuwada, et al., 1986; Picton, et al 1987). Because the modulation-frequency evokes the responses these have also been called the envelope-following response (Dolphin et al., 1994).

The MASTER technique presents multiple tones, each of which are modulated at a unique frequency. The compressive rectification which occurs in the cochlea causes each tone to evoke a response at the frequency by which it is modulated (Lins et al., 1995). Because the scalp-recorded activity contains superimposed responses to the multiple components of the stimulus, it is difficult to distinguish the individual responses in the time domain. However, if the data are converted into the frequency domain using a Fast Fourier Transform (FFT), the amplitude and phase of the response to each stimulus can be measured at the specific frequency at which the tone was modulated.

As well as identifying responses at particular stimulus-modulation frequencies, MASTER also evaluates a noise estimate that is derived from neighboring frequencies in the spectrum at which no stimulation occurred. If there were no response, the power at the modulating frequency would be within the range of the power at these neighboring frequencies. An F-ratio can estimate the probability that the amplitude of the modulation-frequency of a stimulus (the signal) is either within the distribution of amplitudes at the neighboring frequencies (the noise), or exceeds it (Zurek, 1992; Dobie and Wilson, 1996; Valdes et al., 1997; Lins et al., 1996). When this probability is less than 0.05, the response is considered significantly different from noise, and the subject is considered to have heard the tone that was modulated at that frequency.

In general, as more data is collected the signal-to-noise ratio increases. Several approaches are used in order to increase the signal to noise ratio of the recorded data. Averaging

together repeated recordings or "sweeps" reduces the level of activity in the recording that is not time-locked to the stimuli. Selectively rejecting recordings wherein the noise level is particularly high (usually because of non-cerebral potentials or "artifacts") prior to averaging also increases the efficiency of the averaging process (Picton et al., 1983). Artifact rejection protocols are set up in MASTER to operate only on individual sections of the recording sweep or "epochs." Increasing the duration of the activity submitted to the FFT increases the frequency-resolution of the analysis. Provided the stimulus frequencies are precisely locked to the recording period, increasing the sweep duration thus reduces the noise level, by distributing the power across more FFT bins, without affecting the amplitude of the response since it is represented within a single FFT bin (Chapter 1, *Figure 1-2*).

When converting time series data into the frequency domain the amount of data submitted to the FFT becomes an issue. The specific frequencies available from an FFT operation are integer multiples of the **1/(Nt)** resolution of the FFT, where **N** is the number of time points and **t** is the time between each data point. During data collection a series of data sections or "epochs" are collected. In the experiments that will be discussed in this chapter the digitization of the electrophysiological signals occurred at 1000 Hz and the buffer had a length of 1024 points. Therefore, each epoch lasted 1.024 seconds. Because submitting single epochs to the FFT analysis would produce a frequency resolution of only 0.98 Hz, the individual epochs are linked together to form longer data windows termed "sweeps". By using 16 epochs in each sweep, data windows of 16,384 time-points were created, producing a frequency resolution of 1/(16*1.024*.001) or .061 Hz in the amplitude spectrum which spanned from zero to 500 Hz (the Nyquist frequency).

Not all the data that was collected was submitted to the FFT routine. Artifact rejection was accomplished by rejecting any epoch containing a voltage value that exceeded ±50 μV. If an epoch was rejected, the next epoch which was not rejected was used in its place when linking the epochs of data into sweeps. This procedure does not cause discontinuities to occur in the recorded response because each of the stimuli which evoked the responses were constructed so that each epoch contained an integer multiple of the modulation and carrier-frequencies and started with identical phases. More detailed discussions of the processes of stimulus generation and artifact rejection occur later in this chapter (see section 5.2 and 5.5).

In general, as more data is collected the signal-to-noise ratio is improved. We have shown

*Please see next page for figure.*

**Figure 2-1: MASTER system.** The system includes software running on a PC which operates a data-acquisition board. The DA outputs of this board are sent via a connection box to an audiometer which acts to control the intensity and the transduction of the stimuli to the subject. A pre-amplifier is needed to amplify the subject's electrophysiological responses to a level appropriate to the AD input. The program begins with a Main screen which shows the various options which are available to the user. Choosing any button invokes another screen dedicated to the selected option. When the specific task of that screen is completed, the user is returned to the Main screen.

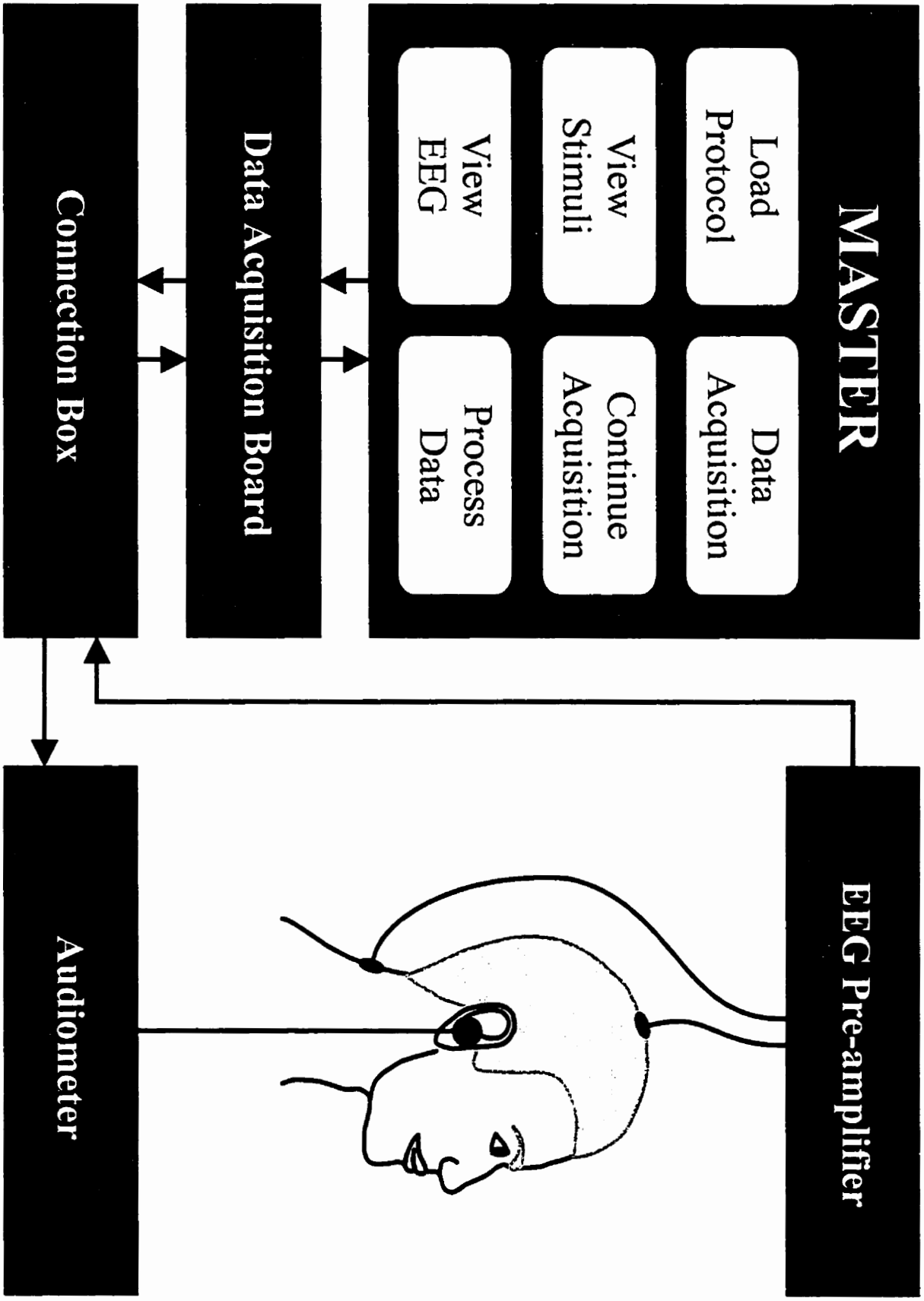
MASTER
Load Protocol
Data Acquisition
View Stimuli
Continue Acquisition
View EEG
Process Data
Data Acquisition Board
Connection Box
Audiometer
EEG Pre-amplifier

that the signal-to-noise ratio can be reduced with similar efficiency by either averaging the data in the time domain or using the data to increase the duration of the sweep which will be submitted to FFT analysis (Chapter 1, *Figure 1-2*). We use both techniques. When enough data for an entire sweep is obtained, an FFT analysis computes the spectrum. When the next sweep is collected it is added to the prior sweep in the time domain and the result is again submitted to FFT analysis. This is more efficient than combining the spectra, which would require vector averaging, in order to consider phase as well as amplitude. The responses are then evaluated using the previously described F-ratio technique. When the F-ratio of a response at a particular modulation-frequency is significant at $p<0.05$ then the subject is considered to have heard the carrier-frequency. This technique therefore offers a rapid and objective method to test hearing.

## 4] System Description

In addition to the digital signal processing that occurs in the MASTER system, recording the auditory steady-state responses requires analog signal conditioning for both the auditory and the electroencephalographic signals. The current MASTER system is relatively inexpensive because it relies upon other instruments, which already exist in most laboratories and audiology clinics, to amplify and filter these signals (Figure 2-1). In addition to the software the system includes a connection box which contains a series of input and output connectors and several resistor bridges for voltage-attenuation. For example, the voltage signals (±10 volts) from the DA outputs of the board are attenuated by a factor of 10 at two of the terminals so that they may be connected to the "tape input" of a clinical audiometer. This audiometer enables the operator to adjust the intensity levels of the stimuli and to select the transducer (e.g., earphone, free field speaker, bone conduction vibrator, etc.). For the data presented in this chapter, a Grason-Stadler Model 16 Audiometer was used. Additionally, the electrical activity recorded from the scalp (usually in the range of ±20 μV) must be amplified before reaching the AD input of the data acquisition board. For the data presented in this chapter, we used a small, battery-operated EEG amplifier (Model P55, Grass Instruments) with a gain of 10,000, a high-pass filter of 1 Hz and a low-pass filter of 300 Hz (-3 dB points, 6 dB/octave).

### *4.1 Main Screen*

When a user starts the MASTER program the Main screen appears (Figure 2-1). The left side of the screen contains buttons for establishing the experimental protocol and ensuring proper system performance, and the right hand side concerns options for the collection and analysis of data.

Although the figures in this chapter appear in black and white, the actual screens use a simple color scheme to designate the functions of various components. For example, three shades of blue are used: a light blue to indicate information which is important to the operation of the screen; a dark blue for buttons that evoke various operations within the program; and a middle blue for the background. White lettering is used to provide descriptive labels for the parameters displayed in the screens. Three highlight colours are also used: yellow to highlight spectral data values at the modulation-frequencies, and to indicate controls that can manipulate the processing of the recorded data; red to display cautionary information (such as illegal values); and green to signify that given parameter value is acceptable.

### *4.2 Load Protocol Screen*

Pressing the "Load Protocol" button invokes a screen for defining experimental parameters (Figure 2). This screen contains controls that allow the user to generate various types of stimuli (top section of screen) and configure AD and DA operations (bottom section). Control values can be modified by mouse-clicking on the arrows that are adjacent to each control value, by entering the values directly from the computer's keyboard, or by loading a set of stored values from disk. Since there are numerous parameters for any given experiment, the user will commonly load values stored in text files that have ".pa1" or ".pa2" filename extensions, e.g. "default.pa1." To create new protocols the user can adjust the parameters and then store them in a new file by pressing the "write data" button (the use of long file names is supported under LabView). Both reading and writing from disk are done using standard Windows dialogue boxes for file operations (e.g., "Open File"). Since pa1 and pa2 files are text files, the user can also modify the parameters for an experiment using a standard text editor. However, it is generally safer to edit parameters from within the MASTER program to ensure

*Please see next page for figure.*

**Figure 2-2: Load Protocol screen.** The top of this screen is used to define up to eight stimuli which may be either amplitude-modulated, frequency-modulated or both. The stimuli defined for the left ear are typical of what would be used to record responses. The stimuli defined for the right ear are only to illustrate important aspects of the stimuli, which are displayed in Figure 2-3. The lower part of this screen enables the user to change parameters related to recording the responses.

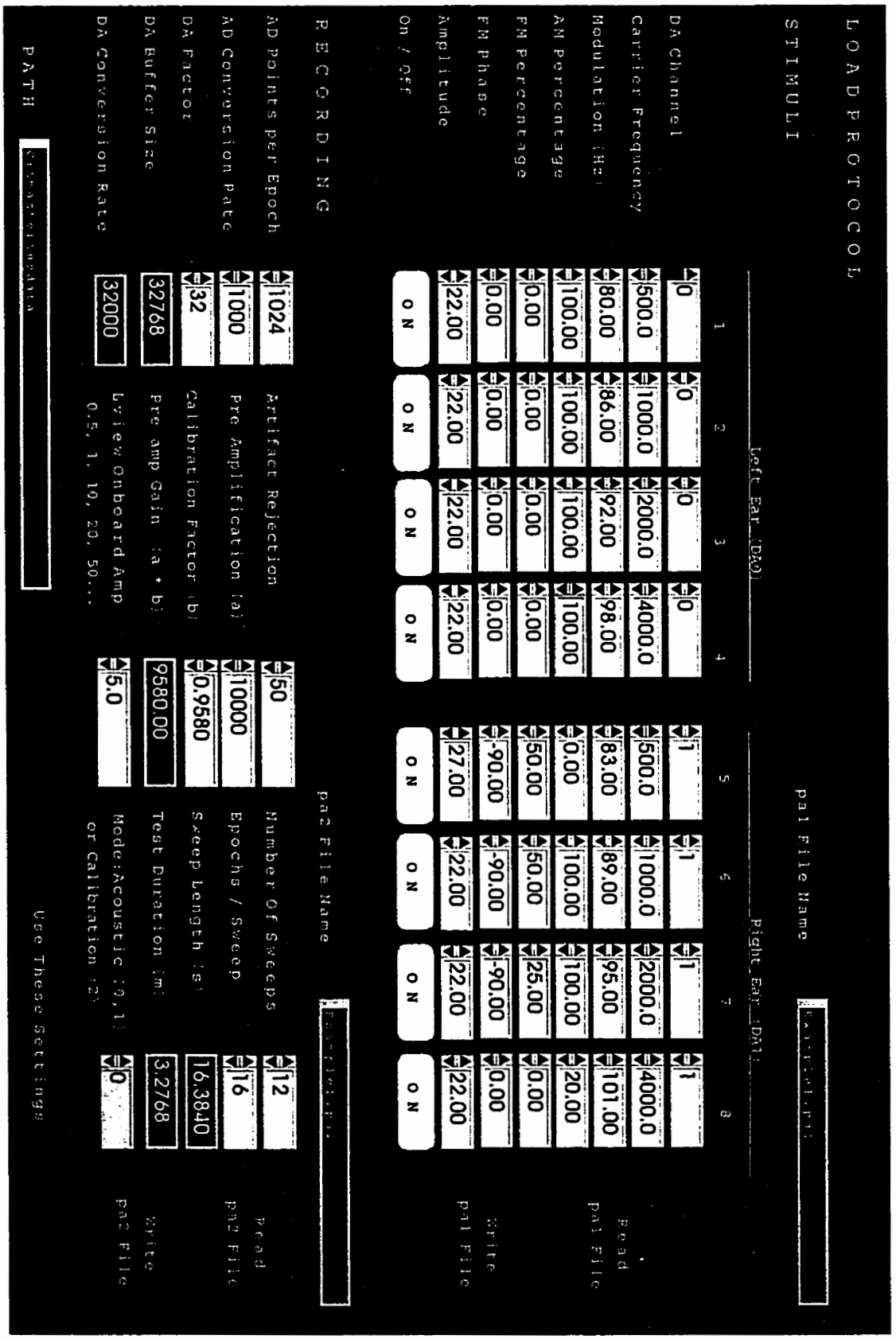
LOAD PROTOCOL
STIMULI
pal File Name
Left Ear (DA0)
Right Ear (DA1)
1 2 3 4 5 6 7 8
DA Channel
Carrier Frequency
Modulation (Hz)
AM Percentage
FM Percentage
FM Phase
Amplitude
On / Off
ON
Read pal File
Write pal File
RECORDING
pa2 File Name
AD Points per Epoch
AD Conversion Rate
DA Factor
DA Buffer Size
DA Conversion Rate
Artifact Rejection
Pre Amplification (a)
Calibration Factor (b)
Pre amp Gain (a * b)
Lview Onboard Amp
0.5, 1, 10, 20, 50...
Number Of Sweeps
Epochs / Sweep
Sweep Length (s)
Test Duration (m)
Mode:Acoustic (0,1)
or Calibration (2)
1024
1000
32
32768
32000
50
10000
0.9580
9580.00
5.0
12
16
16.3840
3.2768
0
Read pa2 File
Write pa2 File
PATH
Use These Settings

that "illegal" values are not chosen. Many of the parameters must conform to certain principles so that processes like the synchronous timing of the AD and DA conversions occur successfully.

As is indicated by the controls located in the top section of the screen, the MASTER system is currently configured to present a maximum of eight stimuli. The most common testing protocol utilizes four stimuli in each ear since previous research has shown that using a greater number of stimuli can decrease the amplitude of the responses (Chapter 1, *Table 1-1*). This typical setup is indicated by the titles on the screen which indicate which stimuli will normally be presented to the left and right ear. However, in principle, the software can present up to eight stimuli in one ear if none are presented to the other ear. For each stimulus the user defines the following options:

- **DA Channel:** determines the DA channel to which the stimuli are sent (0 is for the DA0 output which usually goes to the left ear, and 1 is for DA1 output which goes to the right ear).
- **Carrier-frequency:** determines the center frequency of the stimulus, usually between 0.5 and 8 kHz.
- **Modulation-frequency:** determines the frequency of the modulation envelope, between 80 and 200 Hz for the rapid auditory steady-state responses, or near 40 Hz for the middle latency steady-state responses.
- **AM Percentage:** determines the amount of amplitude-modulation expressed as a percentage (0-100%) according to the formula $\mathbf{100(a_{max}-a_{min})/(a_{max}+a_{min})}$ where $\mathbf{a_{max}}$ is the maximum amplitude of the signal and $\mathbf{a_{min}}$ the minimum amplitude. When $\mathbf{a_{min}}$ is zero the amount of modulation is 100%.
- **FM Percentage:** determines the amount of frequency-modulation expressed as a percentage (0%-100%) according to the formula $\mathbf{100(f_{max}-f_{min})/f_c}$ where $\mathbf{f_{max}}$ is the maximum frequency of the signal, $\mathbf{f_{min}}$ the minimum frequency, and $\mathbf{f_c}$ the carrier-frequency. For example, when a carrier-frequency of 1000 Hz is frequency-modulated at 20% the frequency moves between 900 and 1100 Hz, i.e. ±10%. The other term used to describe FM is $\mathbf{\Delta f}$ which is the excursion between the middle frequency (the carrier) and either $\mathbf{f_{max}}$ or $\mathbf{f_{min}}$. In this example, $\mathbf{\Delta f}$ is 100 Hz or 10% of the carrier-frequency.

- **FM Phase:** determines the phase (in degrees) of the frequency-modulation relative to the amplitude-modulation so that changes in the frequency of the stimuli can occur either in-phase or out-of-phase with those of the AM. Since the maximum frequency will occur at 180° sine phase, and the maximum amplitude will occur at 90°, a phase setting of -90° will ensure that the tone that is both amplitude- and frequency-modulated will reach maximum frequency at the same time as it reaches maximum amplitude (see Figure 2-3).
- **Amplitude:** determines the amplitude of the stimulus expressed as a percentage of the maximum voltage allowed by the output buffer (±10 volts). Since the stimuli within each ear are added together, when 4 stimuli are used each of the 4 stimuli should be defined to use no more than 25% of the total range.
- **On/Off:** determines if the stimulus will be presented to the subject. This control allows the operator to select a subset of the stimuli for presentation.

The lower half of the screen enables the user to set the experimental parameters for the data acquisition and output buffers. The left column permits the user to modify the AD and DA conversion rates and the buffer sizes. After a sampling rate is chosen, the user chooses the size of the AD buffer. For optimal computational performance (i.e. using the Fast Fourier Transform rather than a slower discrete Fourier transform) the number of points in the AD buffer should be set equal to a power of two. While the LabVIEW routines for spectral analysis will perform correctly even if the number of points is not a power of two, the computational time is significantly longer. The duration of a buffer is a function of the number of points in the buffer and the rate at which the buffer is filled or emptied. In the example shown in Figure 2-2, where the number of points in the buffer is set to 1024 and the input conversion rate is set to 1000 Hz, it will take 1.024 seconds for the buffer to become filled. Each time the data buffer is filled, one epoch of the recording is completed. When choosing AD conversion rates, the operator must consider the range of frequencies that are present in the incoming data. In order to prevent aliasing, the AD conversion rate should be greater than twice the highest frequency in the input. Thus, when the low-pass filter of the pre-amplifier is set to 300 Hz, the AD conversion rate should be at least 600 Hz.

It is essential that the AD and DA buffers have an identical duration (in this example

1.024 seconds) so that the input and output buffers remain synchronized during the recording. In order to make the duration of these two buffers identical, the parameters for the DA operations are calculated as a function of the AD parameters. Accordingly, the operator enters a "DA factor." In the example shown in Figure 2-2, the operator has chosen a DA factor of 32, giving a DA buffer size of 32,768 points and a DA rate of 32,000 Hz. If one wishes to view the spectrum of the stimuli using the View Stimuli screen, it is helpful to make the DA factor a power of two so that the FFT algorithm can be used to rapidly calculate the spectrum (provided the size of the AD buffer is also a power of 2). The screen uses the convention that numbers derived from other inputs (e.g., the DA buffer size which is computed as a function of the AD buffer size and the DA factor) are shown in light blue on a dark blue background.

Normally we use a maximum carrier-frequency of 8 kHz in our audiometric testing procedures and a DA rate of 32 kHz, since this will present the stimulus without significant distortion. Increasing the D/A rate above 32 kHz is not permitted because of the speed limitations of the AT-MIO-16E-10 board. The screen provides a warning in the form of a flashing red indicator if the numbers entered are not possible given the clock resolution and/or the processing speed of the board. These red indicators occur if the DA conversion exceeds 32 kHz or if the rate of either the AD or DA conversion is not an integer fraction of the board's 20 MHz clock rate. The operator can then change the entered values until the red light is turned off. Because the MASTER system may be used with different boards in the future, the software has not been programmed to automatically adjust the values chosen by the user based upon the limitations of the current board

The central column contains controls which enable the user to modify parameters which affect the acquisition and scaling of the electrophysiological data. The artifact rejection level determines the value which must be surpassed in order for a recording epoch to be rejected. The amplification factor and calibration factor are used so that the data can be scaled and displayed in the proper units. The AT-MIO-16E-10 data acquisition board has its own onboard amplification which can be adjusted to a factor of 0.5, 1, 5, 10, 20, 50 or 100. The range of the AD conversion after the onboard amplifier is ±5 V. The optimal configuration occurs when the pre-amplification and on board amplification are set so that the full 12-bit range of the input buffer is used to represent the incoming analog signal. When the pre-amplification is set at 10,000, typical EEG

signals which are ±20 μV (peak-to-peak) becomes ±200 mV. Using an onboard gain of 5 increases the incoming signal to ±1 V which reproduces the signal well without clipping. The clipping occurs at ±5 V after the onboard amplification, equivalent in this case to ±100 μV in the EEG.

The two top controls in the third column enable the user to determine the amount of data that will be collected and the number of data epochs which will be used to compose each data sweep. By increasing the number of epochs that are concatenated together to form a sweep, the operator will increase the frequency-resolution of the FFT. The spectral analysis will utilize the FFT if the result of multiplying the number of epochs per sweep and the number of points in each epoch produces a number of points which is a power of two (e.g., 16,384). If the number of points is not a power of 2, the program will run and the amplitude and phase of the responses will still be calculated correctly but the program will use a discrete Fourier transform, rather than zero padding the data and using the FFT. In order to maintain a reasonable speed of processing, we therefore recommend that both the number of points in an epoch and the number of epochs in a sweep be set to powers of 2.

Since the currently defined AD epoch will last 1.024 seconds and each sweep has been set to contain 16 epochs, each sweep will last 16.384 seconds. Further, since the user has indicated that 12 sweeps will be collected, 192 epochs will be collected, causing the recording session to last about 3.2 minutes. If the user wishes to increase the frequency-resolution of the amplitude spectrum by using a sweep containing 32 rather than 16 epochs, the program would automatically adjust all the parameters and internal computations in accordance with this change.

The last control of the third column determines the type of stimuli that will be used during the recording period. The user selects whether the stimuli are presented according to one of three modes. In Mode 0 the stimuli have a constant root-mean-square amplitude, while in Mode 1 the stimuli will have a constant peak-to-peak amplitude. Mode 2 presents stimuli consisting of only the modulating frequencies (without any carrier-frequencies) which are used to calibrate the EEG amplifier (see sections 5.2 and 5.6).

Like the stimulus parameters, the recording parameters may also be saved in, and loaded from, text files. The files for the recording parameters have the filename extension "pa2". The use of separate pa1 and pa2 files allows users to mix and match different parameters for stimuli

and recording. For example, one might wish to use the same stimuli with two different pre-amplifiers, or with different AD conversion rates. Lastly, at the bottom of the screen is a control which allows the operator to enter a path that determines the directory where the parameter files are stored and where the raw data, and results obtained during the recording, will be stored.

### *4.3 View Stimulus Screen*

The acoustic stimuli used in the MASTER program are carrier-frequencies that may be either amplitude-modulated, frequency-modulated, or both. Figure 2-3 illustrates the stimuli that were generated according to the control values displayed in the experimental parameter screen in Figure 2-2. In the left ear, there are four individual carrier-frequencies ($f_c$), each of which is amplitude-modulated at a unique modulation-frequency ($f_m$). These four are added together to create the stimulus that will be presented to the left ear. The time course of this stimulus (for the first 50 msec) can be seen in the upper graph of the right hand column.

---

*Please see next page for figure*

**Figure 2-3: View Stimulus screen.** Up to eight stimuli can be displayed here and summed together to create the stimulus that will be presented to a subject. Note that only the first 50 milliseconds of each stimulus are shown. The top right hand graph shows a digital representation of the stimulus that was created by adding the first four stimuli in the left hand column, each of which has been amplitude-modulated at 100% as is indicated by the parameters shown in Figure 2-2. Under this waveform is the amplitude spectrum of the stimulus showing four peaks in the spectrum corresponding to each of the carrier-frequencies together with flanking side-bands related to the modulation. In order to show the spectra more clearly, the x-axis of the graph has been changed so that extends only to 6 kHz rather than the usual 10 k Hz. The four stimuli presented to the right ear demonstrate what occurs when combining AM and FM. The first stimulus is only frequency-modulated. The phase is set at $-90^{\circ}$ so that the peak frequency occurs at the same time as the peak amplitude would have occurred if the stimulus were amplitude-modulated (this stimulus can be compared to the first stimulus in the left ear which also has a carrier-frequency of 500 Hz and which is modulated a little more slowly). The second and third stimuli in the right ear are both AM and FM. Because the largest amplitude occurs at the highest frequency, the spectrum is not centered on the carrier-frequency but is shifted upward. This shift is very clear for the second stimulus which is 50% FM, but is more subtle for the third stimulus which is only 25% FM. The fourth stimulus shows a 20% AM stimulus. The amount of modulation is sufficiently small that the side-bands are below the lower limits of the y-axis. The "buffer checks" indicates that the right ear stimulus exceeds the buffer. Even though the sum of the amplitudes (27+22+22+22) is less than 100, the peak amplitudes of the AM stimuli (the second and third in particular) have been increased to maintain the RMS intensity. Unless the stimuli are changed the DA converter will clip.

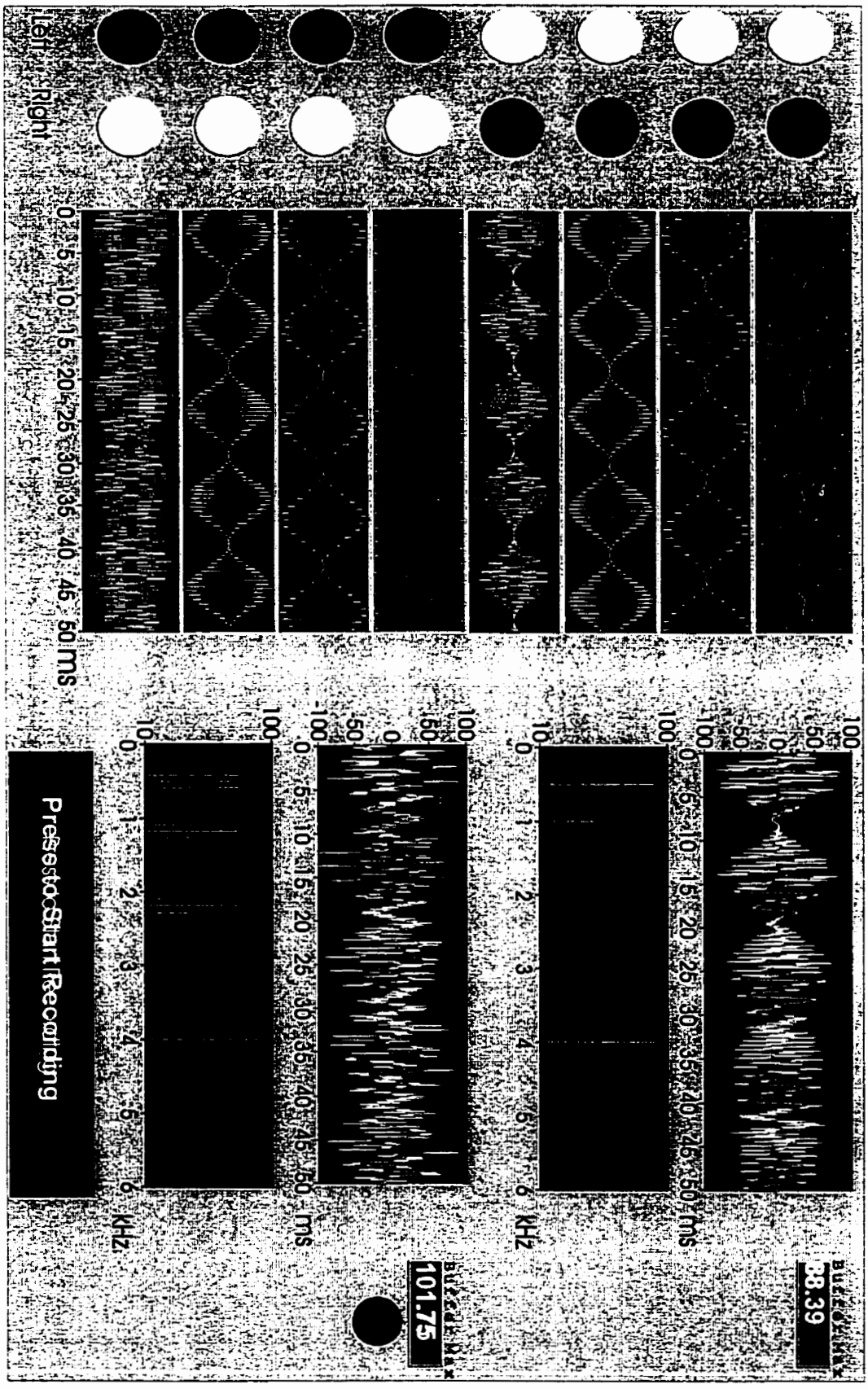
Left
Right
0 5 10 15 20 25 30 35 40 45 50 ms
Preset to Start Recording
100
50
0
-50
-100
0 5 10 15 20 25 30 35 40 45 50 ms
10
0
0 1 2 3 4 5 6 kHz
100
50
0
-50
-100
0 5 10 15 20 25 30 35 40 45 50 ms
10
0
0 1 2 3 4 5 6 kHz
Buffer Max
38.39
Buffer Max
101.75

Below that is the amplitude spectrum which indicates that the stimulus is comprised of the original four carrier-frequencies, each with two side-bands at $f_c \pm f_m$. To the right of these plots is an indicator showing the results of a buffer check. The output buffers are defined so that they can output values ranging from ±100 (which produces the full ±10 volt range of the output buffer). Since the maximum value of the stimulus which is to be presented to the left ear is 88.39 this stimulus can be successfully represented in the buffer. However, the stimulus constructed for the right ear exceeds the maximum. Since all values over 100 would be clipped at 100, the right-ear stimulus would be significantly distorted if used in an actual experiment. Because peak-to-peak amplitudes of the stimuli may be altered to maintain a constant RMS in Mode 0, this buffer check is non-trivial (illustrated in Figure 2-3).

In the figure the left ear stimuli are typical of what might be used to evoke auditory steady-state responses. The stimuli defined for the right ear were created for demonstration purposes only and would not be used in an actual experiment. The first stimulus is a carrier-frequency that is frequency-modulated at 50%. The second stimulus is a carrier with 100% amplitude-modulation and 50% frequency-modulation. The phase of the frequency-modulation has been set to –90° in order to align the maximum frequency of the stimulus with the maximum amplitude. In the third stimulus 100% AM and 25% FM (phase still –90°) were used. The fourth stimulus shows only 20% AM and no FM.

### *4.4 View EEG Screen*

Before beginning a recording session a user will normally choose to view the incoming electrophysiological data. Pressing the View EEG button, located in the bottom left corner of the Main screen, will invoke a simple screen which displays the subject's EEG. On this screen, the user can change the x and y scales, or the A/D rate, to observe the quality of the incoming EEG signal For instance, the user may increase the sampling rate to 2000 Hz, or more, to ensure that a slow frequency is not due to the aliasing of a high frequency.

### *4.5 Data Acquisition Screen*

Figure 2-4 shows the screen used during data acquisition. The data which is displayed in the figure was obtained from a recording session which presented stimuli to both the left and right ear. In the upper left section of the screen is a chart labeled "EEG" which displays the incoming electrophysiological signal. Its y-axis spans ±100 μV and its x-axis automatically adjusts to show the all the data points of the current epoch (with the number of points rounded down to the nearest 100). If a user wishes to display fewer time points of each sweep, the x-axis values are configurable, and may be changed by clicking on the value with the mouse and entering a new value from the keyboard. The horizontal lines that appear at ±60 μV on this chart show the artifact-rejection limits (these are red on the computer screen). If the current epoch contains values which exceed these limits, it is rejected, i.e. not averaged and not stored in the raw data file.

In the upper right of the screen is a graph of the amplitude spectrum of the average response. The amplitude ($a$) is measured as the base-to-peak amplitude of the cosine wave – $a \cdot \cos(2\pi f)$ - provided by the FFT. The data submitted to the FFT is the average response of the subject and is obtained by adding each recorded sweep to a running sum and dividing this by the number of sweeps collected. Therefore, this display is updated each time enough artifact-free data epochs have been collected to add an additional sweep to the average. The x-axis normally spans from 0 to 200 Hz, while the y-axis is automatically scaled according to the highest amplitude value. The axes may also be configured by the user by clicking the mouse on a value on the axis and inputting a new value from the keyboard. Additionally, because the lower frequencies usually have higher amplitudes than higher frequencies, the user can click on the button labeled "Auto" to change it to "A>70". In this mode, the scaling will set the maximum of the y-axis to the maximum amplitude of frequencies above 70 Hz. The X-scaling button can also be used to change the frequency-range of the spectrum. On the computer screen the amplitudes of the spectrum which occur at frequencies corresponding to the modulation-frequencies are highlighted in yellow. In Figure 2-4, 6 of the 8 spectral peaks corresponding to the modulation-frequencies are clearly larger than the background activity.

Below the displays of the EEG and the amplitude spectrum of the average sweep are several indicators which allow the operator to monitor, and in some cases control, the data acquisition.

*Please see next page for figure.*

**Figure 2-4: Data Acquisition screen.** The incoming EEG is monitored in the upper left graph. This figure was obtained by reading data from a disk-file, the name of which is presented at the top of the graph. The spectrum of the average responses is shown in the upper right graph. The frequencies in the spectrum corresponding to the modulating frequencies are highlighted. For this figure the y-axis of the spectrum was changed to show so that both the responses and the residual EEG spectrum are easily visible. The normal options are to set the y-axis automatically to the maximum value (which would make the responses small) or to the maximum value above 70 Hz (which would clip the lower frequencies). Another option would be just to display the spectrum above 80 Hz (X-scaling button). A line noise peak can be seen at 60 Hz (in order to avoid phase distortion we chose not to use any analog notch-filtering). Responses can be recognized between the frequencies 80 and 100 Hz. There are also smaller peaks recognizable at the second harmonics (between 160 and 200 Hz). In the lower half of the screen are shown polar plots of the responses to each of the stimuli. Responses to six of the eight stimuli being presented to the subject have become significant after only about 2 minutes of recording. The significance of the response can be seen visually by seeing whether the circle incorporates the intersection of the axes, or by checking the probability of the F-value (F). The responses to 500 and 750 Hz have not reached significance.

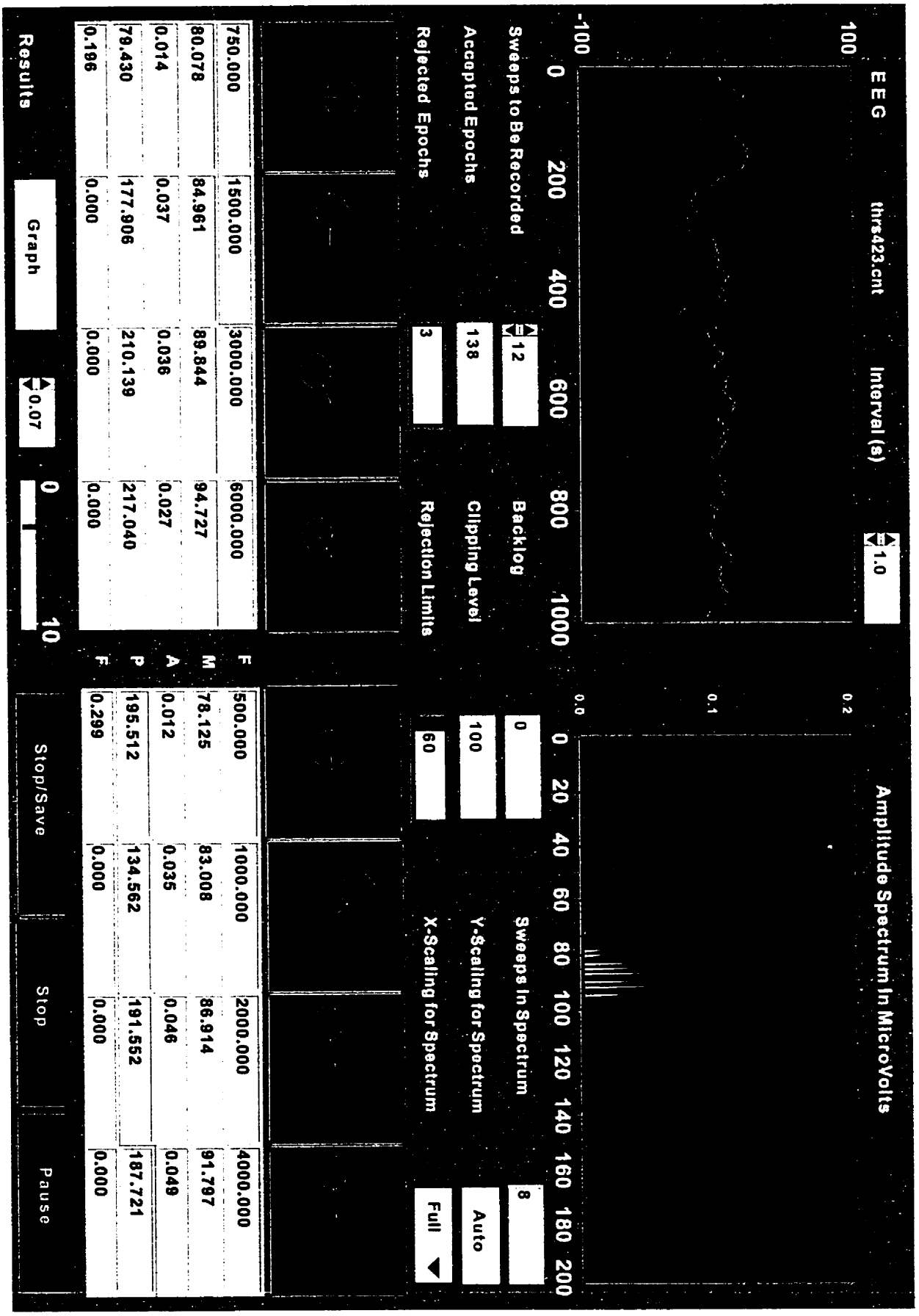
EEG
thrs423.cnt
Interval (s)
1.0
100
-100
0
200
400
600
800
1000
Amplitude Spectrum In MicroVolts
0.2
0.1
0.0
0
20
40
60
80
100
120
140
160
180
200
Sweeps to Be Recorded
12
Backlog
Sweeps In Spectrum
8
Accepted Epochs
138
Clipping Level
Y-Scaling for Spectrum
Auto
Rejected Epochs
3
Rejection Limits
X-Scaling for Spectrum
Full
Results
Graph
0.07
0
10
Stop/Save
Stop
Pause
750.000
1500.000
3000.000
6000.000
80.078
84.961
89.844
94.727
0.014
0.037
0.036
0.027
79.430
177.906
210.139
217.040
0.196
0.000
0.000
0.000
F
M
A
P
F
500.000
78.125
0.012
195.512
0.299
1000.000
83.008
0.035
134.562
0.000
2000.000
86.914
0.046
191.552
0.000
4000.000
91.797
0.049
187.721
0.000

- **Sweeps to be Recorded:** indicates the number of sweeps required for a complete recording. This is a control as well as an indicator. During data collection the operator can thus increase or decrease the number of sweeps according to how well the responses are being recognized.
- **Accepted Epochs:** indicates the number of epochs that did not exceed the rejection threshold.
- **Rejected Epochs**: signifies the number of epochs that exceeded the rejection criteria. Rejected epochs do not enter into the averaging and are not stored with the raw data.
- **Backlog:** shows the amount of data left over in the software buffer after it has been read. If this number intermittently deviates from zero, or becomes very large for only a moment, then the experimental protocol may be near the memory and processing capability of the computer (see section 5.1 for details).
- **Clipping Level**: indicates the level at which the AD converter clips the EEG signal. This information is useful for setting the artifact-rejection limits (which should be less than the clipping level), and for checking that the amplifier settings are correct.
- **Rejection Limits:** indicates the current threshold for rejection. This value can be changed online during the experiment to adjust to different states of the subject.
- **Sweeps In Spectrum:** indicates the number of sweeps in the current average response, which has been submitted to the FFT routine to give the displayed spectrum.
- **Y-Scaling:** This button determines whether the y-scale of the spectrum display depends on the whole spectrum or just that part of the spectrum greater than 70Hz.
- **X-Scaling:** This button determines whether the x-scale of the spectrum display starts from zero, from 80 Hz or from 160 Hz.

The lower half of the figure displays the evaluations of each responses both graphically and numerically. The left four graphical polar plots represent the responses produced by stimuli presented to the left ear. Each plot shows the magnitude of the response as a vector which

extends from the origin outward. The phase of the response (relative to the phase of the modulating frequency) is represented as the angle between the line and the x-axis. The 95% confidence interval for the noise is represented by a circle centered at the end of the vector. As long as the circle does not include the origin, a response lies outside of the 95% noise estimate. In other words, there is only a 5% chance that there is no real response and that the measurement occurred by chance.

This display is based on that used in the Hotelling's $T^2$ test (Picton et al., 1987; Victor and Mast, 1992) which assesses the variability of the average response by making multiple measurements of the response in subsections of the recording. In the $T^2$ technique the circle indicates the confidence limits of the mean measurement. The F-test is different because it measures confidence limits of the activity recorded at frequencies other than the signal (i.e., a noise estimate). The diagram might therefore more properly show the circle around the origin and the vector of the response either exceeding or not exceeding the radius of the circle, respectively, for significant or non-significant responses. However, because the $T^2$ and the F-test yield equivalent results (Dobie and Wilson, 1993), the display uses the plotting convention of the $T^2$ test since this makes it visually easier to see the significance of the response. In this record, the first four graphs indicate that a significant response has occurred for carrier-frequencies at 6000, 3000, and 1500 Hz, while the 750 Hz tone (far left) does not produce a response than is significantly different from background noise levels. The second 4 responses due to stimuli presented in the right ear indicate that the 500 Hz failed to produce a significant response. The failure of the 500 and 750 Hz tones to evoke a significant response is not unexpected because in some subjects about 6 minutes of recording is required for these frequencies to produce significant responses. The scaling of these plots can be changed using either the sliding control or the digital control located at the bottom of the screen.

The responses are also described numerically in the eight columns of numbers located below the polar plots. The left four columns show the current results for the left ear stimuli, while the right four contain data for the right ear. The results for each response are displayed using 5 values: Carrier-frequency, Modulation-frequency, Amplitude of the response, Phase of the response, F-ratio level of significance for that frequency. The first two values of each column describe the stimuli and therefore remain constant, the last three values change as the recording progresses.

The user may choose to change the polar graphs to a simpler representations of whether or not the response is significant. Depressing the button labeled "Graph" under the tabulated results replaces each of the polar plots with a colored circle. A green circle means that the probability that the response occurred by chance is less than 5%. An orange circle means that the probability is 5-10%, while a red circle indicates that is more than 10%. The ability to change the display online demonstrates an attractive feature of LabVIEW which does not exist in other programming languages. LabVIEW offers the ability to toggle the state of any component of a screen from visible to invisible. This is a powerful feature because entirely different screens can be created for users of different skill levels (e.g., scientist, clinician, student), with each of the screens still using the same source code.

In the lower right corner of the screen are three buttons which can be used to halt the operation of the program. The button labeled "Stop" is used to halt the entry of new data into the recording, while the input and output buffers continue their operation. This can be used if the data acquisition needs to be halted in the middle of a recording session, as might occur if the user needs to reattach an electrode to subject's scalp because it fell off before the end of the testing procedure. When the problem has been fixed, the user can then choose "Continue Acquisition" from the Main screen (Figure 2-1) and the subsequently collected data will be appended to the data that was already collected. The button labeled "Stop/Save" will stop all input and output operations, clear the input and output buffers, and save any data that has been collected prior to that point. This can be used if the user feels that enough data has been collected and wants to continue on to another recording.

Two features of this screen are only available during the playback of data from disk and are not available during data collection due to the synchronization requirements of the input and output buffers. The "Pause" button is used to halt the program only when reviewing data from a recording that had been previously stored to disk. Additionally, a control labeled "Interval" which is located above the chart of the incoming EEG data is used during data review. This control determines how long each data epoch is displayed on the screen before the next epoch is read from disk.

### *4.6 Process Data Screen*

After the data has been acquired and stored, the operator may wish to combine these data sets across subjects or across replications within one subject. The Process Data screen allows the operator to work on data sets which have already been recorded. Three different subscreen options are available through this screen: "Review", "Combine" and "Log Results."

The "Review" features are used to examine data that have already been recorded, and to print out hardcopy figures. The figures are organized in a similar manner to the way the data are presented on the Data Acquisition screen, except that graph of the incoming EEG is omitted and the spectrum of the average data is expanded to fill its place. The screen also allows the operator to choose the number of responses that are graphed, and to enter comments about the data.

The "Combine" routines support either the averaging or subtracting of previously recorded data sets (Figure 2-5). A user may wish to average data because, for instance, the results from a short recording session may not show a significant response even though the subject might hear the stimulus. This is usually due to the fact that the noise has not been sufficiently reduced by averaging and still obscures the responses. The results from several recording sessions must therefore be combined in order to demonstrate a significant response. As discussed earlier, computing the average of spectral results is accomplished by averaging the time series waveforms from the different files, and then re-computing the amplitude spectrum.

Sweep-weighted averaging is commonly used when combining different data sets obtained from a single subject using the same stimuli. Weighting is used because the average waveform from each recording session may have been generated from different numbers of sweeps. For example, the user might have increased the number of sweeps in one of the sessions in order to gain slightly more data. In this situation, each sub-average should be weighted during averaging by the number of sweeps in that sub-average. For two sets of data $\mathbf{X_1}$ and $\mathbf{X_2}$ based on $\mathbf{N_1}$ and $\mathbf{N_2}$ sweeps respectively, each time point ($\mathbf{i}$=1 to the size of the sweep) in the sweep-weighted average is

$$(X_{1i}N_1 + X_{2i}N_2)/(N_1 + N_2)$$

and this is then stored as the average of $N_1+N_2$ sweeps. These calculations are performed using double precision in order to attenuate the effects of round-off error if the sum becomes large.

*Please see next page for figure*

**Figure 2-5: Process Data screen.** This screen illustrates how stored data can be combined. The operator selects what type of processing to be done. Then he or she enters the name of the file where the processed data should be stored and gives the processing a sequence number. The files to be processed are selected from those present in the path and entered in the listing on the lower right. Once everything is set up, the operator presses the "Process Files" button. The screen shows the set up to perform a weighted average of the data in two files and to put the average data in Cond1.avg, and then to perform a weighted average of three files and to put the average data in Cond2.avg.

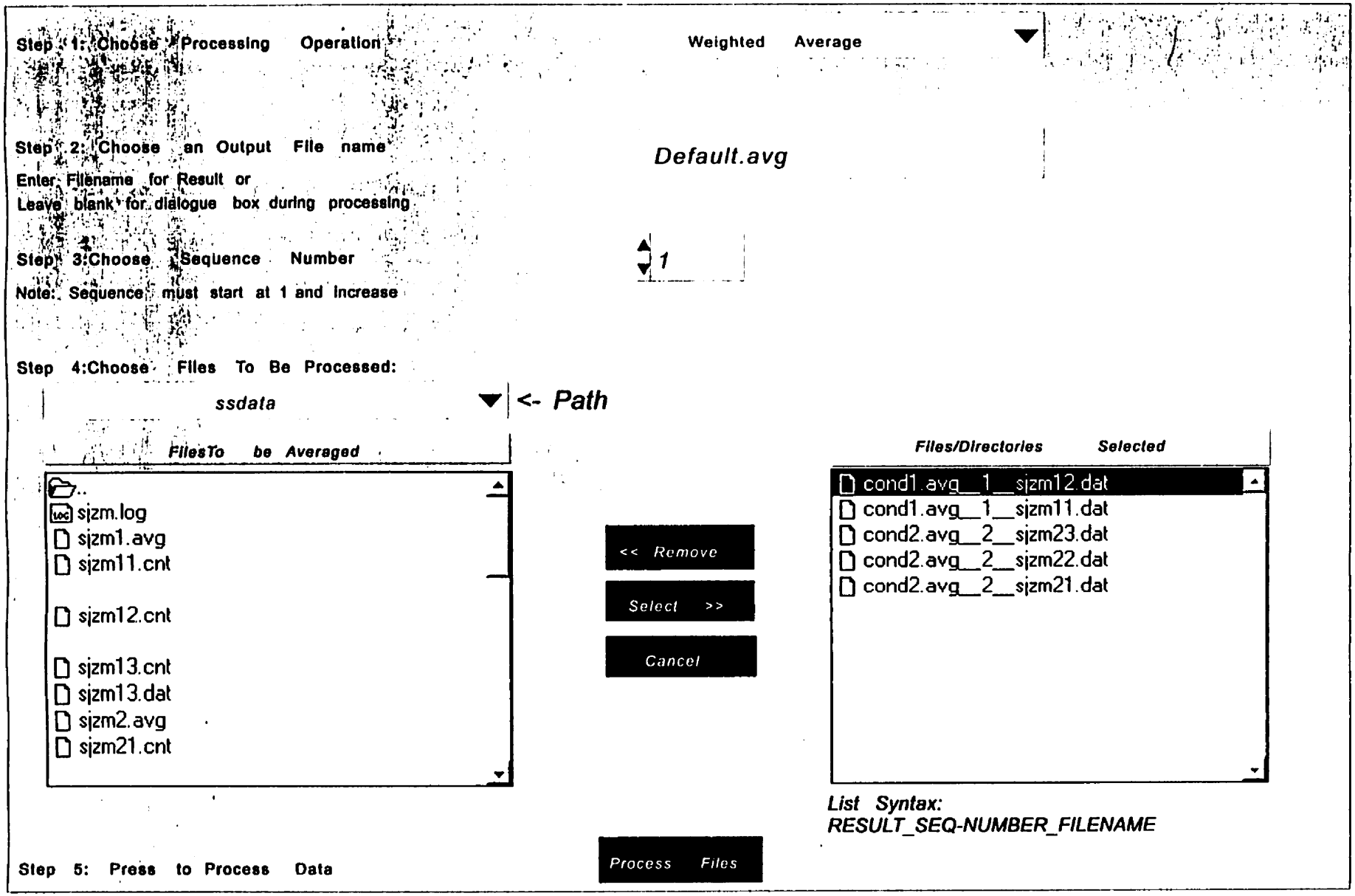
Step 1: Choose Processing Operation
Weighted Average
Step 2: Choose an Output File name
Default.avg
Enter Filename for Result or
Leave blank for dialogue box during processing
Step 3:Choose Sequence Number
1
Note: Sequence must start at 1 and increase
Step 4:Choose Files To Be Processed:
ssdata
<- Path
FilesTo be Averaged
..
sjzm.log
sjzm1.avg
sjzm11.cnt
sjzm12.cnt
sjzm13.cnt
sjzm13.dat
sjzm2.avg
sjzm21.cnt
<< Remove
Select >>
Cancel
Files/Directories Selected
cond1.avg__1__sjzm12.dat
cond1.avg__1__sjzm11.dat
cond2.avg__2__sjzm23.dat
cond2.avg__2__sjzm22.dat
cond2.avg__2__sjzm21.dat
List Syntax:
RESULT_SEQ-NUMBER_FILENAME
Step 5: Press to Process Data
Process Files

Alternatively, the operator may opt for non-weighted averaging when combining data across subjects in order to weight each subject equally. Merely because more data may have been collected for a particular subject does not mean that this set of data should contribute more to the average. For non-weighted averaging, the formula for combining two averages is simply

$$(X_{1i} + X_{2i})/2$$

and this is stored as the average of 2 "sweeps". The convention for the number of sweeps is arbitrary. By using the number of subjects for the number of sweeps, files can easily be distinguished as a weighted average rather than a non-weighted average. Furthermore, using the number of subjects allows one to later average together non-weighted averages using sweep-weighted averaging. For example, the average of the first eight subjects can be combined with the average of the next two subjects using weighted averaging to obtain the average of ten subjects with each subject equally weighted.

Subtracting responses may be necessary when evaluating the effects of masking. The derived response technique, for example, sequentially subtracts responses recorded using masking noise at decreasing high-pass cut-off frequencies to determine the responses to the frequencies between the cut-off frequencies (Don et al., 1979). Subtraction must be done using un-weighted calculations. Furthermore, there is no division following the subtraction. When the diminuend is **X1** and the subtrahend is **X2**, the result of the subtraction (the difference) is

$$X_{1i}-X_{2i}$$

and this is stored as the average of 1 "sweep". Again, the convention is arbitrary.

The screen controlling the routines for averaging and subtracting are organized so that the operator inputs the required information step by step. The first step is to choose the type of processing to be used (weighted averaging, non-weighted averaging, or subtraction). The second step is to enter the name of a file for storing the results of the processing. The third step is to give the processing a sequence number. This number should be 1 if only one set of files is to be processed. The fourth step is to select the files for processing. For averaging, any number of files can be selected, but for subtraction only two files can be selected (first the minuend and second the subtrahend). The selected files are then listed using the syntax "results file - sequence number - file to be processed". Multiple repetitions of the process can be set up by circling

through steps 2 to 4 and adjusting the sequence number each time. Figure 2-5 shows the screen that will lead to two separate weighted averages, the first based on two data sets and the second based on three.

The Log Results routines allow users to export a summary of the experimental results to a file that can be used in another software application (e.g., for statistical analysis). Different methods for sorting the data can be chosen and data from different subjects and recording sessions may be logged together into a single ASCII file. The user may sort the data for a subject or a set of subjects in order of carrier-frequency, modulation-frequency, stimulus number, or ear of presentation. Log files therefore provide a convenient method of sorting data for report generation and statistical analysis of the results.

## 5] Computational Methods and Theory

The MASTER techniques were developed according to clear principles concerning the generation of stimuli, data collection, artifact rejection, and response analysis. Violation of any of these principles would cause the system to work either inefficiently, or not at all. This section describes some details of the programming that embodies these principles. Real data were used to illustrate the different principles.

### *5.1 Synchronizing the AD and DA Conversion*

AD and DA conversion must be perfectly synchronized. The basic unit within the MASTER technique is the epoch. An epoch of data is created every time the input buffer is filled. If the input and output buffers are exactly the same duration and they are started together, then it follows that they will both end at the same time. During continuous recording the buffers will continue to start and end at the same times, thereby ensuring that each recorded epoch is evoked by exactly the same stimuli. Every epoch should therefore contain responses with identical phase and amplitude which can be added together, removed due to artifact rejection, re-ordered, or re-sampled without changing the responses.

The MASTER system performs synchronized data input and output using a subroutine based upon a VI that is provided with LabVIEW version 5.0 ("Simul AI/AO buffered Trigger (E-

series MIO.vi)"). This VI synchronizes the start of signal acquisition and stimulus presentation using a digital pulse that is sensed by the PFI0 pin (programmable function input) which acts as a start trigger for both the DA and AD buffer conversion operations. The original VI required that the trigger be externally generated. Because we desired the program to start on its own, MASTER causes the board itself to generate a pulse on the GPCTR0_OUT pin (general purpose counter) which we have hardwired to PFI0. After the AD and DA buffers have been initialized and after the DA buffer has been filled with values which will produce the acoustic stimuli, simultaneous AD and DA conversion is initiated using the internally generated pulse. Although LabVIEW provides users with routines which use software timers (that rely on the CPU clock) for initiating the AD and DA operations, these were not used because they produce variable delays of more than 1 ms between the two buffers depending upon system performance demands. This modified VI permits MASTER to acquire and generate data simultaneously with no drifts in timing since both AD and DA operations are started by the same pulse and then controlled by the same hardware clock.

The MASTER software uses a circular buffering technique for both DA and AD buffers. This means that after the last point in the buffer is sent out or filled, the next value will be read or written to the first point in the buffer. During operation, while the output regenerates the same buffer of data, the input data is constantly changing, which requires that the data is transferred from the buffer to the computer before new data is written in its place. The "Simul AI/AO buffered Trigger (E-series MIO).vi" also contains a "scan backlog" indicator which shows the number of data samples that remained in the buffer after the transfer subroutine has executed. If the backlog value increases steadily, then the data are not being read fast enough to keep up with the acquisition, and the newly acquired data may overwrite unread data, which would cause the program to halt and display an appropriate error message. This important feature can indicate that the computer speed is not fast enough or the amount of RAM insufficient for the protocol that the user has designed.

As each AD conversion is completed, the value is transferred into a first-in-first-out (FIFO) buffer. Because the FIFO can collect up to 512 values before any information is lost the computer can ignore the incoming information for a time equal to the product of the FIFO size times and sampling rate. LabVIEW software routines manage data transfer between the FIFO on the board and the direct memory access (DMA) buffer which has been defined in the computer's

memory. While data are transferred from the FIFO into a part of the DMA buffer, the CPU is removing data from another part of the DMA buffer and processing it (storing it on disk or averaging it with the previously recorded data). This setup obviates the need for the traditional use of a double buffer. However, the acquisition parameters and DMA buffer size must be chosen so that the LabVIEW routines are able to transfer data out of the DMA buffer fast enough to keep up with the rate at which the FIFO is transferring new data into the buffer. If not, unread data in the FIFO will be overwritten, and the user would be alerted by the MASTER program that an error had occurred. The DMA buffer must be large enough to inhibit the FIFO from overwriting itself, while not being so large as to affect the RAM needs of the CPU. The input DMA buffer has been set at 16,384 values which is 16 times the values that are read using inputs of 1024 points each, since this is the default number of points used in data acquisition in the MASTER program.

The timing of both the AD and DA conversions is determined by counters that wait through a specified number of ticks of the clock on the AT-MIO-16E-10 board. Since this is a 20 MHz clock, the time between successive AD and DA conversions (i.e., 1/conversion rate) must be an integer multiple of 50 nanoseconds. The timing will drift during the experimental session if this 50 nanosecond requirement is not met, and will cause the buffers to become desynchronized. The program therefore permits A/D rates such as 500 or 1000 Hz, but does not allow 3000 Hz (Figure 2-2). The DA rate also has to be an integer multiple of 50 nanoseconds. For example, using 1000 Hz for the AD timing and a DA factor of 32 leads to a DA timing of or 31,250 nanoseconds (1/32 kHz), which is 625 clock ticks. If the DA factor were set to 30 rather than 32, the required timing for the DA conversion (30 kHz) is not an integer value of the clock ticks. The DA timing would be rounded off to an integer and the DA and AD conversion would become unsynchronized. If the user enters a value in these controls that produces illegal AD or DA values then a red warning indicator appears on the screen next to the illegal value (s).

### *5.2 Stimulus Generation*

The parameters entered in the Load Protocol screen (Figure 2-2) define the stimuli. The processes by which these stimuli are generated rely on a set of formulae that are reviewed in the following paragraphs. More intensive discussions of these formulae are available in Hartmann (1997) and Stanley (1982).

Dividing the AD buffer size by the AD rate gives the epoch time (**s**), e.g., 1.024 seconds. The DA conversion time (**t**) is equal to the reciprocal of the DA rate. Prior to constructing the stimuli, the stimulus parameters provided by the operator are altered slightly based upon **s** to prevent acoustic artifacts. During data acquisition the values in the DA buffer are continuously converted into analog signals. The DA buffer operates in a circular fashion, which means that after the last value is output from the buffer, the conversion process begins again from the beginning of the buffer. In order for the transition, from the last point in the buffer to the first point of the buffer, to occur without acoustic artifact, an integer number of cycles for all modulation-frequencies and carrier-frequencies must occur within the length of the buffer. Therefore, the frequencies provided by the operator for both carrier and modulation signals are adjusted to give an integer number of cycles within the buffer using the equation:

$$f=(\mathrm{int}(sf'))/s$$

where **s** is the buffer duration in seconds, **f** is the actual frequency to be used, **f'** is the frequency input by the user and **int** is a function returning the closest integer. For example, a modulation-frequency of 85 Hz is adjusted to 84.961 Hz when **s** is equal to 1.024 seconds. As well as enabling the DA sweeps to be linked together without acoustic artifact, this also ensures that the frequency of the response is exactly equal to one of the discrete frequencies measured by the FFT.

The other parameters defined in the Load Protocol screen are then also adjusted in order to simplify the calculations. First, the modulation indices $m_a$ and $m_f$ are calculated from the percentage modulation values entered for amplitude-modulation $m'_a$ and frequency-modulation $m'_f$ (rows 4 and 5, respectively, in Figure 2-2):

$$m_a = m_a'/100$$

$$m_f = (m_f'/100)(f_c/(2f_m))$$

Note that the index for frequency-modulation varies with both the carrier-frequency and the modulation-frequency. This is necessary for the calculations, which depend on manipulating the phase of the carrier signal at the modulation-frequency. The use of a percentage of the carrier-frequency to define the amount of frequency-modulation is not common and is open to ambiguity: is the numerator the total amount of frequency change from maximum to minimum

or just the change from the carrier to either the maximum or minimum frequency ($\Delta f$)? In keeping with previous papers in this field (Cohen et al.,1991; Picton et al., 1987), we define the percentage frequency-modulation as one hundred times the difference, between the maximum frequency and the minimum frequency, divided by the carrier-frequency. Thus, a 1000 Hz signal that is 20% frequency-modulated will range between 900 and 1100 Hz.

The amplitude value is adjusted so that a value of 100 equals one half of the range of the ±10 volt DA buffer:

$$a=10a'/100$$

where **a'** is the amplitude input by the user. The LabVIEW DA conversion routines convert these voltages into the actual levels used in the converter, which has a 12 bit resolution (4098 levels or 72 dB) and a minimum level difference of 48 mV.

A frequency-modulation term is calculated to adjust the phase and thus the instantaneous frequency of the signal:

$$P = m_f \sin(2\pi f_m t i + \theta\pi/180)$$

where $f_m$ is the modulation-frequency, **t** is the time per address in the sweep in seconds, and $\theta$ is the phase difference between the frequency- and amplitude-modulations expressed in degrees.

The MASTER program provides three different modes of stimulation. Mode 0 calculates stimuli which maintain their root-mean-square (RMS) pressure constant across the different amounts of amplitude-modulation (Viemeister, 1979; Sheft and Yost, 1990). Mode 1 calculates stimuli with a constant peak intensity. Mode 2 (for calibration) uses just the modulating frequency. The stimulus (**s**) is thus calculated according to one of the following formulae:

**Mode 0 (constant RMS):** $s(i) = a(1+m_a \sin(2\pi f_m t i)\sin(2\pi f_c t i+P))/(1+m_a^2/2)^{1/2}$

**Mode 1 (constant peak):** $s(i) = a(1+m_a \sin(2\pi f_m t i)\ \sin(2\pi f_c t i+P))/(1+m_a)$

**Mode 2 (calibration):** $s(i) = a(\sin(2\pi f_m t i))$

The MASTER technique combines all the individual stimuli for one ear into a single

waveform. The traveling wave separates a complex stimulus into its component frequencies with the higher frequencies activating the more proximal portions of the basilar membrane. Since the cochlea allocates the different carrier-frequencies to different regions of the basilar membrane, each carrier-frequency then evokes a separate response. The response occurs at the modulation-frequency specific to that particular carrier tone (Lins et al., 1995).

For each ear, the AT-MIO16-E10 board uses a 12-bit DA buffer which extends over a range of ±10 volts. Because the individual stimuli are summed together to obtain the final stimulus, the combined stimulus contains amplitudes which vary with the algebraic sum of the specific peaks and troughs of the individual stimuli. This combined stimulus will almost always contain amplitudes that are larger than the individual stimuli. The MASTER system defines the amplitude of its stimuli in terms of a "percentage of buffer". In order to keep the combined stimulus within the range of the DA converter the amplitudes of the individual stimuli should not generally exceed 100/N, where N is the number of stimuli within one ear. When N is 4 the individual stimuli are then represented with only 10-bit accuracy, and the combined stimulus is represented with the full 12-bit accuracy. Individual stimuli can be represented with a resolution as low as 6 bits and still evoke reliable responses, but at lower resolutions the acoustic waveforms are significantly distorted.

In order to ensure that the amplitude of the combined stimulus does not exceed the maximum value that the buffer can represent, the program checks the maximum amplitude and produces a warning if the maximum is exceeded (see Figure 2-4, right ear stimuli). The buffer check routines become non-trivial when using Mode 0, because although the user might define, for example, four stimuli, each of which has an amplitude that is 25% of the buffer, the amplitude correction factor (for constant RMS) may modify the signals so that they have considerably larger peak values. The summation of these new stimuli may then greatly exceed the buffer maximum, causing significant distortion when these values are clipped at the maximum value during DA conversion.

*5.3 Choice of Stimuli: AM and AM/FM stimuli*

MASTER allows the user to present stimuli using either AM or FM, or both. The advantage of using both AM and FM has been explored by Cohen et al.(1991), who demonstrated that larger responses (gains varying between 1.28 and 2.17 for different frequencies) could be obtained using both AM/FM stimuli over those obtained using either AM or FM alone. In their study, Cohen et al. (1991) suggested aligning the maximum frequency of the FM with the maximum amplitude of AM. This choice is supported by studies which have shown that evoked potentials respond preferentially to transitions from slower to faster frequencies (Maiste and Picton, 1989; Kohn, et al., 1978). We have extended Cohen's finding from single stimulus recordings to the multiple stimulus case. Four stimuli were presented at 50 dB SPL to the left ear (0.5, 1, 2, and 4 kHz) and four others to the right ear (0.75, 1.5, 3, and 6 kHz). The stimuli were modulated at frequencies that varied from 85 to 95 in 2.5 Hz increments with the higher carrier-frequencies in one ear having higher modulation-frequencies. The stimuli were modulated by either AM only (modulation depth 100%) or combined AM and FM (modulation depths of 100% and 25% respectively). The effect of recording-time on the number of significant responses was investigated in eight subjects using 16.384 second sweeps and averaging 12 of these sweeps (just over 3 minutes of data). The difference between AM and AM/FM stimuli can be seen in the bottom of Figure 2-6. The responses to the AM/FM stimuli were significantly larger in amplitude (average gain of 1.35) than the responses to the AM stimuli (main effect of modulation type $F=18.8$; df 1,7; $p<0.01$; no significant interaction with carrier-frequency). The time required for testing depends upon how rapidly a significant signal-to-noise ratio can be attained. Since the responses to AM/FM stimuli are significantly larger than the response to AM stimuli, the testing time can be shortened by using AM/FM stimuli. By the sixth sweep, 75% of the AM/FM responses (on average 6 out of the 8) are significantly different from noise. The responses to the AM stimuli do not reach this level of significance until after twelve sweeps have been collected.

The two carrier-frequencies that did not produce reliable responses in the three-minute period were 0.5 kHz and 6 kHz. These responses generally display smaller amplitudes than for

*Please see next page for figure.*

**Figure 2-6: Combined AM/FM stimuli.** The upper half of the figure shows the change in the responses and the estimated noise levels as the number of sweeps averaged increases from 1 to 12. For these graphs, the results for the AM and AM/FM stimuli have been combined to show the effect of carrier-frequency. For simplicity only the data from the right ear are used. The recorded amplitude drops slightly over the first few sweeps because unaveraged EEG noise contributes to the measurements in these sweeps. The response to the 6000 Hz carrier is smaller than the other responses. The upper right of the figure shows the effect of averaging on the estimated noise (background EEG). The noise decreases by the square root of the number of trials. In order for the F-test to be significant, the response has to be about 3 times the estimated background noise. Comparing the upper two graphs shows that the response to 6000 Hz carrier is not significantly different from noise even after 12 sweeps have been averaged. The lower left half of the figure shows the comparison between AM and AM/FM stimuli, with the data collapsed across carrier-frequency. The lower right half of the figure shows the percentage of stimuli that are judged significant as the averaging proceeds. The AM/FM stimuli clearly become significant faster than the AM stimuli. The increase in amplitude caused by the AM/FM modulation results in between seven and eight responses rapidly becoming significant within the three-minute recording period. These data were collected from eight subjects.

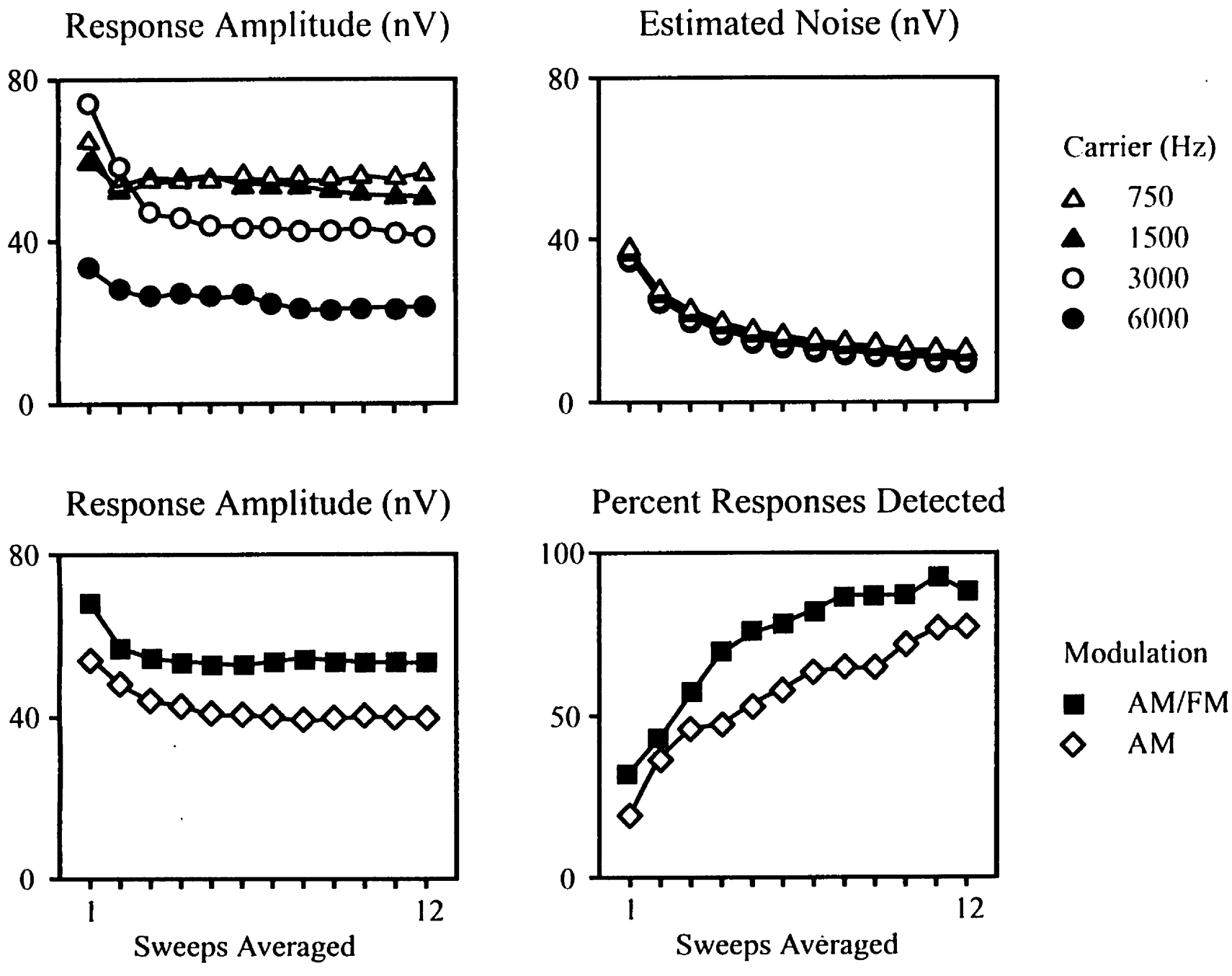
Response Amplitude (nV)
80
40
0
Estimated Noise (nV)
80
40
0
Carrier (Hz)
750
1500
3000
6000
Response Amplitude (nV)
80
40
0
1
12
Sweeps Averaged
Percent Responses Detected
100
50
0
1
12
Sweeps Averaged
Modulation
AM/FM
AM

the other carrier-frequencies (Lins et al., 1995, and as can be seen in Chapter 4) and often require twice that amount of time before they become significant. The different amplitudes of the responses for different carrier-frequencies are shown for the right ear stimuli in the upper part of Figure 2-6. There is only a slight reduction in the estimated noise (calculated as the mean amplitude in the 60 frequency bins above and the 60 frequency bins below the response frequency) with increasing carrier-frequency (and increasing modulation-frequency).

### *5.4 Detection of Steady-State Responses.*

The F-test enables the program to automatically provide the probability of whether a signal is present at the frequency of stimulation. This test derives historically from Fisher (1929), who described a test used by Schuster (1898) to investigate hidden periodicities in meteorological phenomena. This approach has recently been used to examine whether a response is present in recordings of the oto-acoustic emissions (Zurek, 1992). The assumption is that the activity in the adjacent frequency-bins is random with a mean of zero and equal variance in the real and imaginary dimensions. The ratio of signal power (the sum of the squares of the response in the two orthogonal dimensions) to the sum of the powers in N adjacent bins is distributed as F with 2 and 2N-1 degrees of freedom (Wei, 1990, p. 259, equation 12.1.8 noting that n equals 2N+2). Since we are not subtracting out the mean, we used 2 and 2N degrees of freedom (cf. Lins et al.,1996 and Zurek, 1992). The F-ratio may be computed using:

$$\frac{(x_s^2 + y_s^2)/2}{\left(\sum_{i=1}^{J} x_i^2 + \sum_{i=1}^{J} y_i^2\right)/(2J)}$$

in which **x** is the sine term of each polar vector and **y** is the cosine term, and **J** is the number of vectors which are used in the summation operation. We used **J** of 120 (60 measurements on either side of the signal). Because the sum of the squares of these sine and cosine terms equals the square of the amplitude, the equation reduces to:

$$120 a_s^2 \; / \; (\sum_{i=1}^{120} a_{ni}^2)$$

where $a_s$ is the amplitude at the signal being tested and $a_{ni}$ is the amplitude at each of the **i** adjacent frequencies.

When 120 bins of the FFT are used in the estimate of the noise, the ratio may be referenced to the F-ratio value for 2 and 239 degrees of freedom. The 120 values for the noise estimate are those which are adjacent to the modulating frequency (60 on either side), omitting those frequencies at which another response might occur. Valdes et al.(1997) found that the F-test performs as well as other techniques such as Hotelling's $T^2$ test (Picton et al., 1987; Victor and Mast, 1992) or the Rayleigh test which only looks at phase (Lütkenhöner, 1991).

The F-ratio procedure assumes that the noise is equally distributed across the frequencies. The noise would then be equally distributed across the FFT-bins. The amplitude of the EEG decreases (approximately exponentially) with increasing frequency (as can be seen in the amplitude spectrum in Figure 2-2). This could lead to an over-estimation of the noise levels and a more conservative test. In order to assess this, we empirically checked the performance of the F-ratio on real data from the experiment described in the preceding section. Using one recording (12 sweeps) from each of 8 subjects we analyzed 400 frequencies to obtain the number of false positives (i.e., those showing amplitudes larger than expected from the distribution of the adjacent 120 frequencies at $p<0.05$). The samples were obtained from consecutive frequencies starting at 72.99 Hz and increasing to 97.96 Hz, in 0.061 Hz increments (and omitting the frequencies containing responses). In order to evaluate the responses at the selected modulation-frequencies, the value at each frequency was compared to the 120 adjacent frequencies (60 above and 60 below). The data were also examined in the same way that they are evaluated online during a testing session: the first sweep (16.384 seconds of the record) was submitted to an FFT analysis and the number of false positives were calculated, then the average of the first and second sweep was analyzed, and so on, until all 12 sweeps of the record had been averaged and evaluated. Across all subjects, and for all the sweep sub-averages in the data set, the average number of false positives was 4.33% with a maximum of 6.25% and a minimum of 2.75%. The statistic is therefore slightly conservative when used with real data. There was no trend for the number of false positives to increase or decrease as the recording duration was increased. This

means that the testing procedure was reliable even for very short recording sessions: false positives were not more common after only one sweep was analyzed than after 12 sweeps. Rapid recordings are therefore not prone to increased false positives.

The F-ratio technique was also evaluated using a Kolmogorov-Smirnov test which checks whether a sample of results comes from a particular distribution (Press, 1992). We used this test to compare the cumulative distribution of the probabilities from the F-test against the expected monotonic increase from 0 to 1.0. None of the cumulative distributions were significantly different ($0.14<p<0.89$) from the expected straight line.

A statistical problem not addressed in the present program derives from the number of statistical tests performed as the recording proceeds (Schuster, 1898). It is possible for the operator to stop the test at any time that a desired significance level is reached. If the operator makes this decision every time the current sweep average is analyzed, the significance level resulting from the F-test is incorrect because multiple tests rather than a single test have been performed. In our laboratory we avoid the problem of repeated measurements by always collecting a set amount of data and only evaluating the response significance at the end of the recording period. However, we are beginning to work on algorithms which will allow the test to be stopped once the required level of significance has been attained. These algorithms will take the factor of repeated measures into consideration.

### *5.5 Artifact Rejection*

When data windows or "sweeps" of various lengths are submitted to the FFT routine, they produce a frequency resolution of $1/(Nt)$, where $N$ is the number of sample data points and $t$ is the time between each sample. The longer the sweep the better the frequency resolution. For our analyses we have used sweeps varying in duration from about 12 to 65 seconds. When a subject produces high-amplitude artifacts from non-cerebral generators such as movement or muscle, it has become routine in the analysis of evoked potentials to exclude these data from the analysis. However, if an entire sweep was rejected due to an artifact that lasted only 300 ms, the testing procedure could become very long. If we build each sweep by linking together shorter epochs, artifact rejection does not consume too much time. Accordingly, when a data epoch

contains artifact, it is not appended to the ongoing sweep, and the next artifact-free epoch is inserted instead.

The concatenation of temporally discontinuous epochs of data causes the recorded data to be nonstationary. However, this characteristic does not affect the spectral energy at the frequencies of stimulation since these frequencies are integer multiples of the epoch rate (the reciprocal of the epoch's duration). However, the spectral energy in the recorded data and which was not integer multiples of the epoch rate will be dispersed by the nonstationarity into frequencies $Nf_e$-$f_x$ where $f_x$ is the frequency of interest, $f_e$ is the epoch rate, and N is integer. This is illustrated in the top half of Figure 2-7.

In order to examine how significant these nonstationarities might be, we considered both modeled and real data using a 500 Hz AD rate, a buffer duration of 1024 ms and a total sweep duration of 16.384 seconds. Nonstationarities were modeled by reversing the order of the epochs in the averaged sweep to give a "jumbled" sweep (causing a jump to occur between each epoch and its neighbor). The top two lines of Figure 2-7 illustrate the effects of nonstationarity on a signal that is not an integer multiple of the epoch rate (0.977 Hz). The top row shows only a portion of the time data in order to illustrate the nonstationarities, one of which occurs at 1024 ms. The second row shows a portion of the spectra for the normal sweep and the jumbled sweep. We also modeled the effects when a signal at an integer multiple of the epoch rate occurs in random noise. The signal remains the same but the noise spectrum is changed (at all the frequencies that are not multiples of the epoch rate). However, there is no change in the estimate of the noise amplitude over a range of frequencies. In the case of the actual EEG data, there is a greater energy at low frequencies than at high. The nonstationarity could then cause a redistribution of the lower noise frequencies toward the higher. This could then increase the background noise levels estimated from the activity adjacent to the frequencies of the stimuli. In order to assess this we combined a synthetic response (at 9.8 Hz) with real EEG background noise (third row of the figure). There is indeed a very small increase in the background activity near the response.

*Please see next page for figure.*

**Figure 2-7: Effects of nonstationarities in the data.** The upper half of this figure shows the effects of inserting nonstationarities into a simple sine wave. The sine wave had a frequency of 11.11 Hz, which does not give an integer number of cycles in the recording epoch of 1.024 ms. The nonstationarities were induced by jumbling the order of the 16 epochs which composed a full sweep. There is then a sudden jump in phase at the transitions from one epoch to the next. An example is shown at the upper right at 1.024 ms into the sweep (two arrows). The spectrum of the jumbled signal shows energy at $\mathbf{Nf_e-f_x}$ where **N** is integer, $\mathbf{f_e}$ is the epoch rate (0.977 Hz) and $\mathbf{f_x}$ is the frequency of the sine wave. The maximum peak occurs at 11.35 Hz which is when N=23 (given the proviso that the measured frequency has to be an integer multiple of the frequency resolution for the whole sweep of 0.061 Hz). The third line of the figure shows what happens when EEG noise is jumbled. A modeled signal at exactly 10 cycles per epoch (9.8 Hz) was mixed with the EEG. Jumbling the epochs caused no change in this signal. The nonstationarities change the spectrum of the EEG background. As well as random changes in the microstructure of the spectrum, there is some spread of energy from the lower frequencies to the high. The bottom line shows what happens when a recording of four simultaneous responses in the 75-100 Hz frequency-range is jumbled. There is no change in the responses (arrows). The nonstationarities change the microstructure of the background EEG spectrum. Because the spectrum is relatively flat in this frequency region, however, there is no significant change in the general estimate of the background noise across frequencies.

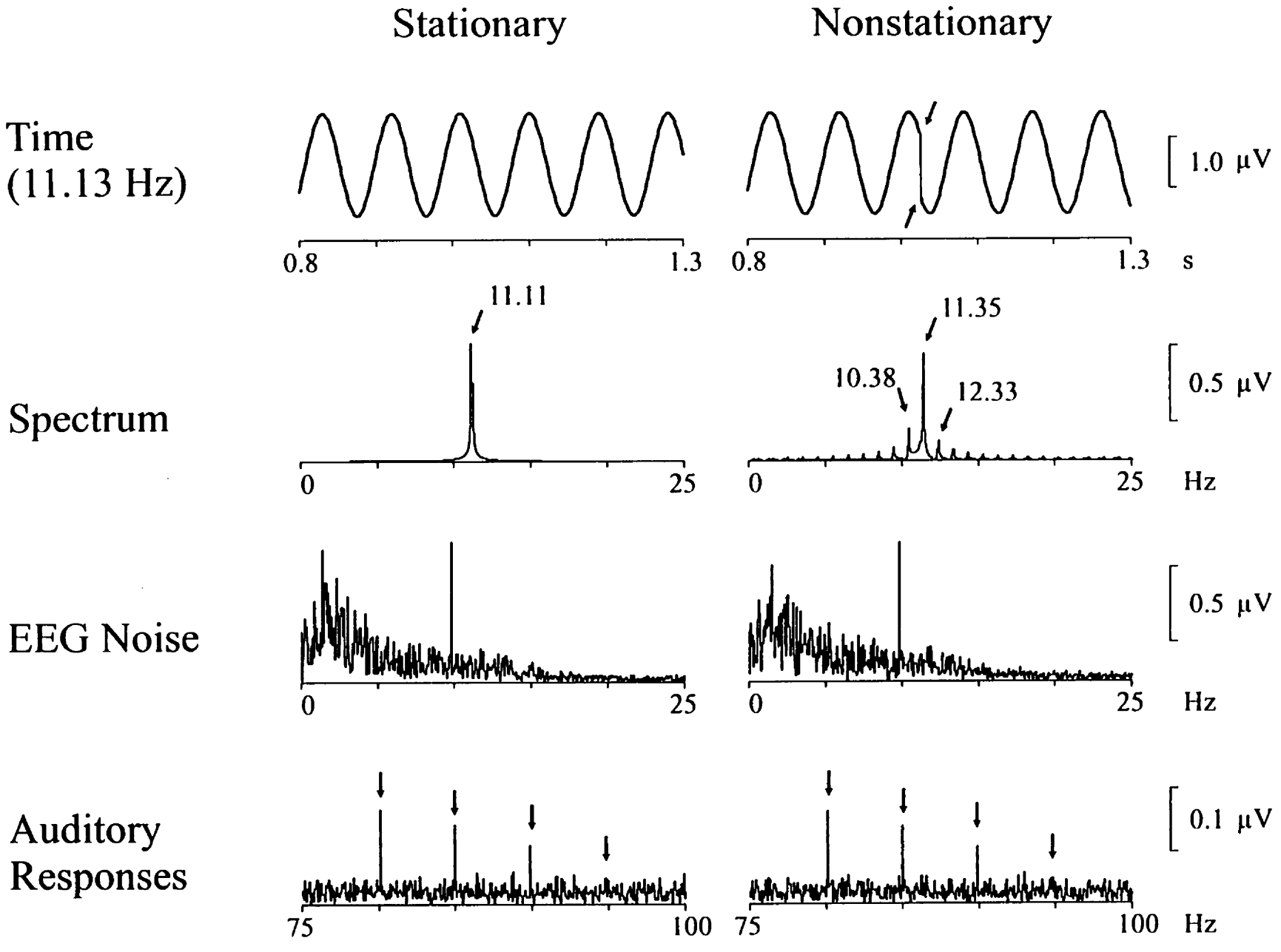
Stationary
Nonstationary
Time
(11.13 Hz)
1.0 µV
0.8
1.3
s
Spectrum
11.11
11.35
10.38
12.33
0.5 µV
0
25
Hz
EEG Noise
0.5 µV
0
25
Hz
Auditory
Responses
0.1 µV
75
100
Hz

At the frequencies most commonly used for recording the auditory steady-state responses, the falloff in EEG amplitude with increasing frequency is small. The bottom row of Figure 2-7 shows the amplitude spectrum of an original recording using four simultaneous stimuli at modulation rates of 80.1, 85.0, 89.8 and 94.7 Hz. The amplitudes of the four responses were 1.30, 0.92, 0.78 and 0.43 μV, with F-ratio probabilities less than 0.0001 for the first three responses and 0.0323 for the fourth response. While the spectrum of the jumbled sweep demonstrated minor changes in its pattern, the amplitudes at the frequencies of stimulation remain unchanged. Despite the change in the microstructure of the spectrum, there were no changes in the F-ratio probabilities before the third decimal place for any of the eight subjects examined. Therefore, while there was a small redistribution of the noise energy, this is not significant for the procedures we are using to detect responses (at least in the case of these relatively high modulation-frequencies). The implementation of a windowing procedure for each epoch as it is concatenated into the sweep could reduce this effect. However, the effect seems too small to warrant the use of such windowing and the amplitude recalibration it would entail.

### *5.6 Calibration Procedures*

All data acquisition instruments must have calibration procedures so that the operator can check the accuracy and reliability of the measurements. In order to perform AD calibration, the user selects Mode 2 in the Recording Protocol screen. The program will then present "stimuli" which are only the modulation-frequencies of the stimuli that are normally used. During calibration one of the DA channels is connected to the input of a million-to-one attenuator of the connection box whose output is sent to the EEG pre-amplifier. This setup enables the user to quantify both the amplitude and phase effects that the electronic circuitry would produce on the recorded steady-state responses. If the signals are at an amplitude of 25%, the amplitude presented from the DA output is ±2.5 volts and the responses should show an amplitude of 2.5 μV in the amplitude spectrum display. The calibration factor can be adjusted until this is true. We usually start the calibration procedure with the calibration factor equal to 1.0 since this allows an easier estimation of the calibration factor. If the calibration procedure is performed using different modulation-frequencies, the recorded activity will show changes across these frequencies related to the analog filters in the pre-amplifier. Both the amplitude and phase of the

signal may change with frequency. At present we do not change the calibration factor with the frequency of the response and we therefore recommend that the filter settings should not be too close to the modulation-frequencies or show too high a slope. As well as checking the pre-amplifier, the calibration procedure also allows the user to ensure that the DA and AD buffers are synchronized over time, since no change in phase or amplitude of the spectral peaks at the modulation-frequencies should occur during calibration. In practice, whenever a new paradigm is developed, it is generally a good idea to calibrate the system.

Calibration of the acoustic stimuli is also necessary. The analog signals are sent from the DA port through a ten-to-one attenuator in the connection box and then to the tape input of the audiometer. This instrument accepts an external input with a +/-1 volt range which it then amplifies, attenuates to the chosen decibel level and directs to the selected transducer (e.g., EarTone 3A ear-inserts or TDH headphones). Although the MASTER system enables 4 stimuli to be played in each ear, the DA calibration procedure should be performed on single stimuli. Using a sound pressure level meter (e.g., Brüel and Kjaer model 2230) and the appropriate coupler (e.g. a DB0138 2-$cm^2$ coupler in the case of insert earphones) the sound pressure level (SPL) of each single stimulus is measured. Across-frequency adjustments in intensity can be made by changing the amplification of the tape input (monitored on the audiometer's Vu-meter). Frequency-specific adjustments can be made (with due consideration to the resolution of the 12-bit DA converter) by changing the amplitudes of the stimulus on the Load Protocol screen.

## 6| Data Storage

At the termination of a recording session the results are automatically saved to a disk file having a ".dat" filename extension. Additionally, the user is given the option of saving the raw data as well (using a ".cnt" filename extension to denote the continuous recording). The raw data for a 3 minute recording at an AD rate of 1000 Hz requires about 1.6 Mb (180*1000*9 bytes). Files that store results of data processing such as averaging (".avg"), subtraction (".sub"), or summarization (".log") are also labeled by a unique filename extension. Unless the user specifically chooses a binary format, all data files are written in ASCII format which can be easily viewed using a word-processor or imported into analysis programs such as MATLAB™ or Excel™. All files contain a header, which displays the information defined in the pa1 and pa2

files, so that the experimental protocol used during data collection can be immediately ascertained. Software for reviewing raw data files is provided with the MASTER system. This is exactly the same as the software for online recording except that the "Record" button in the Main screen enables the user to load data from disk rather than collecting it from the hardware buffers.

## 7] Performance Issues

Since MASTER runs under a Window's operating environment, users are able to benefit from the same features that are common to most Windows based applications. For example, whole screen images can be sent to a network printer or copied and pasted into a graphics program. Alternatively, a user can copy any of the specific components of a screen by clicking the right mouse button while the cursor points to an object and then choosing "copy". The selected image can then be pasted into a graphics program. Additionally, as with other Windows-based programs, several programs may be executed concurrently while MASTER is run. The user may therefore run customized analyses on the data files as soon as they are collected. Running extensive analyses during actual data collection is, however, not recommended due to memory demands. While communication with other programs is possible using the ActiveX™ or dynamic data exchange (DDE) functionality of LabVIEW ™ this feature is not used at the present time by the MASTER program since raw data can be stored to disk, and MASTER already provides extensive real time analysis of the data. Unlike other Windows-based programs, the screen displays for MASTER may not be easily resized. MASTER automatically runs on a full screen setting (800 by 600 pixels) so that the only other screen component is usually the Window's Taskbar. While the current version of LabVIEW ™ supports resizing for different screen resolutions, we are aware of complaints that this feature has shown problems on some systems. Accordingly, MASTER warns the user if the computer's display is set incorrectly.

Our system runs easily on a Pentium 166 with 64 Mb RAM. Attempts to run the system on computers with only 32 Mb RAM have occasionally run into problems. Because of the inclusion of the "Backlog" indicator on the main data collection screen, users are warned if the experimental protocol begins to overload the resources of the system.

## 8| Conclusion

The MASTER system is a Windows based instrument for the real-time collection and analysis of auditory steady-state responses. We have designed it to be flexible, intuitive, and user-friendly. The system will quickly allow new researchers to study auditory steady-state responses without having to build and subsequently test their own programs. Further information, electronic copies of articles and abstracts from our laboratory and from other investigators using the Master system, demonstration software, and a tutorial are available at http://www.rotman-baycrest.on.ca/users/sasha_j/master.html.

**This page intentionally left blank.**

# Chapter 3

## Multiple Auditory Steady-State Responses to AM, FM, & MM Stimuli

A portion of the material in this chapter has also been included in the following:

John, M. S., Deimtrijevic, A., Van Roon, P. and Picton, T. W. *Multiple auditory steady-state responses to AM and FM stimuli*. Audiology and Neuro-Otology (2000, In Press). *Reprinted with permission.*

Deimtrijevic, A., John, M. S., Van Roon, P. and Picton, T. W. *Human Steady-State responses to tones independently modulated in both frequency and amplitude*. Ear and Hearing (2000, In Press). *Reprinted with permission.*

Some of the data were also presented at the TromsØ meeting of the IERASG, June, 1999.

## ABSTRACT

Multiple auditory steady-state responses were recorded using tonal stimuli that were amplitude-modulated (AM), frequency-modulated (FM) or modulated simultaneously in both amplitude and frequency (termed "mixed modulation", or MM). When the MM stimuli combined 100% AM and 25% FM (12.5% above and below the carrier frequency) and the maximum frequency occurred simultaneously with maximum amplitude, the MM response was about one third larger than the simple AM response. This enhancement was evident at intensities between 50 and 30 dB SPL and at carrier frequencies between 500 and 4000 Hz. Responses to MM stimuli are therefore more rapidly detected than responses to simple AM or FM stimuli. The AM and FM components of an MM stimulus generate independent responses that add together to give the MM response. Since AM responses generally occur with a slightly later phase delay than FM responses, the largest MM response is recorded when the maximum frequency of the MM stimulus occurs just after the maximum amplitude. Independent amplitude- and frequency-modulation (IAFM) of a carrier using two different modulating-frequencies (one for AM and one for FM) elicits separate AM and FM responses that are relatively independent of each other.

## INTRODUCTION

The modulation of one or more parameters of a sustained auditory stimulus has long been used to study auditory processing (reviewed by Hartmann, 1998; Zwicker and Fastl, 1990). The ability to detect changes in frequency or intensity can be evaluated by determining the threshold at which a frequency-modulated (FM) or amplitude-modulated (AM) sound can be distinguished from an unmodulated sound. At low modulation rates AM is distinguishable from FM but at rates above a "critical modulation frequency" (about 80 Hz), they become virtually identical in terms of the perceptual experience and the threshold at which they can be perceived.

The processing of AM is probably largely mediated through regions of the cochlea with characteristic frequencies slightly higher than the carrier-frequency (Zwicker and Fastl, 1990). This occurs because of the increasing asymmetry of the cochlear excitation pattern with increasing intensity. In support of this idea, Zwicker (1962) used stimuli which combined both AM and FM, which he called "mixed modulation" (MM). When the AM and FM components of the MM were in phase (i.e., the highest frequency occurring at the highest amplitude), the sensation of modulation was greater than when they were out of phase.

The processing of FM remains less well understood. FM might simply move the locus of activation back and forth on the basilar membrane, thus stimulating each region that it passes through in a similar manner to an AM stimulus. This simple view does not require any interaction between regions or any specific FM transduction mechanism. Because of the asymmetry of the cochlear excitation pattern, regions of the cochlea with characteristic frequencies lower than the carrier-frequency should be most sensitive to FM (Zwicker and Fastl, 1990). However, this does not explain why it is easier to perceive up-going changes in frequency (also known as an "upward sweep" or "upward glide") than equivalent down-going changes (Demany and Clement, 1998).

Physiological studies might help disentangle some of the mechanisms involved in processing modulated stimuli. Studies of the auditory nerve (Sinex and Geisler, 1981; Yates, 1987; Khanna and Teich, 1989ab; Smith, 1998) have indicated that fiber discharges follow the modulation-frequency. While FM responses may be at both the modulation-frequency and its second harmonic, the response at the modulation-frequency is the primary response. Individual

fibers of the primary auditory nerve fire at twice the frequency of FM when the carrier-frequency is at the characteristic frequency of the fiber, and at the modulation-frequency when the carrier-frequency is above or below the characteristic frequency (Khanna and Teich, 1989b). For any given FM sound, the sound will be different from the characteristic frequency of the majority of responding hair cells, causing the output of the cochlear system to occur mainly at the modulation-frequency. Furthermore, FM is subjectively experienced at the modulation-frequency rather than at the second harmonic.

Moving centrally from the auditory nerve, systems exist that respond to modulation independently of the frequency of the carrier, providing for the "spectral integration of periodicity information" (Langner et al., 1998). Psychophysical evidence for these types of systems can be seen in the interference effects that occur when subjects attempt to detect one modulated carrier in the presence of another modulated carrier (Yost and Sheft, 1989; Wilson et al., 1990). The perceptual detection of modulation is likely mediated by central systems that combine information from all auditory nerve fibers (Møller, 1972; Saberi and Hafter, 1995; Moore and Sek, 1994; Sek and Moore, 1996). These systems could use both spectral and time-based cues to evaluate the modulation envelopes (Edwards and Viemeister, 1994; Moore and Sek, 1996).

Specialized neuronal systems exist to process FM stimuli. Selective adaptation studies suggest systems specific to the processing of AM and FM (Kay and Matthews, 1972; Gardner and Wilson, 1979; Tansley and Regan, 1979; Tansley and Suffield, 1983). Studies of the central auditory nervous system show neurons that respond specifically to one direction of FM (Whitfield and Evans, 1965; Erulkar et al., 1968; Møller, 1974; Phillips et al., 1985; Mendelson et al., 1993). Some of these mechanisms may play a role in our experiencing FM at the first harmonic. For example, in the cerebral cortex, neurons tend to respond to upward rather than to downward sweeps, although this varies with the rate of frequency change (Tian and Rauschecker, 1994; Ricketts et al., 1998; Gordon and O'Neill, 1998). Møller (1977), and others (Zhao et al., 1997), have found that FM responsive cells produced responses both to upward and downward glides for modulation-frequencies below 50 Hz, and only to the upward glide for higher modulation-frequencies. The existence of a separate physiological system for the processing of frequency changes has been supported by the distinctive neuronal morphology of the FM-

responsive neurons in the inferior colliculus (Poon et al., 1992).

Human evoked potentials have been used to study the response of the auditory system to modulation for AM, FM and MM stimuli. Upward glides evoke larger and earlier N1-P2 responses than downward glides (Spoor et al., 1969; Jerger and Jerger, 1970; Kohn et al., 1978; Maiste and Picton, 1989). Auditory steady-state responses can be evoked by sinusoidal AM across a wide range of modulation-rates (Rickards and Clark, 1984). Picton et al. (1987) showed that FM as well as AM stimuli could evoke steady-state responses for modulation-frequencies near 40 Hz.

Auditory steady-state responses to tones modulated at frequencies between 80 and 100 Hz are useful in objective audiometry (Lins et al., 1996; Rance et al., 1995; Rickards et al., 1994). Multiple auditory steady-state potentials can be recorded to simultaneously presented stimuli without significant loss in the amplitude of any of the responses, as long as the carrier-frequencies of the component stimuli are separated by at least an octave in each ear (Lins and Picton, 1995; Dolphin, 1997; Chapter 1, see Table 1-1). In addition, statistical techniques to assess whether a response is present or not (Victor and Mast, 1991; Lins et al., 1996; Dobie and Wilson, 1996; Valdes et al., 1997) allow the procedure to be "objective" (Dobie, 1993) both for the examiner who is interpreting the responses as well as the subject who is providing them.

Optimizing the stimulus parameters to make the test more rapid would facilitate the use of auditory steady-state responses in objective audiometry. Using modulation rates above 70 Hz results in little, if any, decrease in response amplitude when the subject is asleep (Lins and Picton, 1995; Cohen et al., 1991). These rates therefore provide more reliable responses than rates near 40 Hz, where the response is significantly decreased during sleep (Levi et al., 1993; Linden et al., 1985) although still recognizable (Dobie and Wilson, 1998). Cohen et al. (1991) showed that MM tones produced significantly larger responses than simple AM tones. We extended the findings of Cohen et al. (1991) into the multiple stimulus case by simultaneously presenting 4 MM stimuli in each ear at 50 dB SPL, and found that the MM response amplitudes were increased by an average of 30% over the AM responses (see Chapter 2, *Section 5.3*). As averaging progressed, the MM responses became recognizable twice as rapidly as the AM responses.

The studies presented in this chapter investigated the human steady-state responses to AM, FM, and MM stimuli in order to learn more about how these types of stimuli are processed in the auditory system and to see how we might best use these responses to test hearing. First, some of the similarities and differences between the responses to AM and FM stimuli were explored. Second, we looked for interactions between stimuli by using various combinations of AM and FM stimuli. Third, we determined whether MM could augment the amplitude of the steady-state responses at intensities near threshold. Fourth, the relative phases of AM and FM in the MM stimulus were systematically modified to study both the clinical utility and the physiological mechanisms of the MM enhancement. Fifth, the relative latencies of the AM and FM responses were estimated. Lastly, we presented stimuli with AM at one rate and FM at another rate ("independent amplitude and frequency modulation" or IAFM) in order to obtain two responses for each carrier-frequency.

## METHODS

### Subjects

The 42 subjects (25 female) who participated in these studies were between the ages of 18 and 47 years (mean age was 27). The subjects were volunteers obtained from laboratory personnel, colleagues, and friends. Twenty-two subjects participated in more than one experiment. In each experiment roughly half of the subjects were chosen from each gender. All subjects were screened for normal hearing at 20 dB HL across all the frequencies (500-6000 Hz) used in the experimental conditions

### Auditory Stimuli

Stimuli consisted of sinusoidal tones each having a carrier-frequency of $\mathbf{f_c}$ , which was sinusoidally modulated at a unique rate. The AM stimuli were created by modulating the amplitude (**a**) of the stimulus. The depth of AM ($\mathbf{m_a}$) was defined as the ratio of the difference between the maximum and minimum amplitude of the signal to the sum of the maximum and minimum amplitude. The minimum amplitude of a 50% AM tone is thus one-third the maximum amplitude. The FM stimuli were formed by modulating the phase of the carrier-frequency. The

depth of FM ($m_f$) was defined as the ratio of the difference between the maximum and minimum frequencies to the carrier-frequency. When a 1000 Hz carrier is FM at 25%, the frequency varies from 875 Hz to 1125 Hz, (a deviation ±12.5% from the carrier-frequency of 1000 Hz).

The formula used for generating the stimuli (s) was based on the formulae of Chapter 2, and was:

$$s(i) = a(1+m_a\sin(2\pi f_{am}ti))\ \sin(2\pi f_c ti+(m_f f_c/(2f_{fm}))\ \sin(2\pi f_{fm}ti+\theta\pi/180))/(1+m_a^2/2)^{1/2}$$

where i is the address in the D/A output buffer, t is the time per address at which digital-to-analog (DA) conversion occurs, θ is the difference in phase between AM and FM, and $f_{am}$ and $f_{fm}$ are the modulation-frequencies for AM and FM, respectively. The term $m_f f_c/(2f_{fm})$ represents the "modulation index" for FM (usually denoted by ß), and the final divisor is used to maintain a constant root-mean-square amplitude across the different amounts of amplitude-modulation (Viemeister, 1979). If $m_f$ equals zero the stimulus becomes a simple AM tone. If $m_a$ equals zero the stimulus becomes a simple FM tone. If $f_{am}$ (the modulation-frequency for AM) equals $f_{fm}$ (the modulation-frequency for FM), the stimulus is simultaneously modulated at the same rate for both amplitude and frequency (i.e., "mixed modulation" or MM). The phase of the modulations as determined by the formula is such that when θ is -90 degrees and $f_{am}$ equals $f_{fm}$, the maximum frequency occurs at the same time as the maximum amplitude. This is caused by the fact that the FM is created by altering the rate of change of the frequency (via the instantaneous phase) rather than the frequency. The formula could have been simplified by making the initial two trigonometric terms 'cos' instead of 'sin', thereby aligning the amplitude and the frequency when θ is 0 degrees (cf., Hartmann and Hnath, 1982; Ozimek and Sek, 1987). For simplicity's sake and since the relative phase is arbitrary, we shall henceforth state that the relative phase is 0° when the maximum amplitude coincides with the maximum frequency. In Experiment 6, $f_{am}$ and $f_{fm}$ were different and the stimulus was a single carrier amplitude-modulated at one rate and frequency-modulated at a different rate: "independent amplitude- and frequency-modulation" (IAFM). Figures 3-1, 3-2 and 3-3 illustrate different types of stimuli used in our experiments.

*Please see next page for figure*

**Figure 3-1. AM and FM Stimuli.** The time waveforms of the stimuli and their corresponding spectra are shown on the left and right sides of the figure, respectively. The first stimulus is a pure sine wave and shows a single spectral peak at the frequency of the carrier with no sideband energy. The second stimulus is 100% AM, and shows a spectral peak at the carrier-frequency ($f_c$) and 2 sidebands at $f_c+f_{am}$ and $f_c-f_{am}$. These sidebands are each ¼ the amplitude of the unmodulated carrier, and the carrier has been reduced to ½ its original amplitude. The next stimulus is 50% AM. Here the sidebands are smaller than for the 100% AM stimulus. The fourth stimulus is 50% FM. This stimulus has a large number of sidebands because the frequency of the stimulus roves across a wide range. The largest sidebands appear at $f_c+2f_{fm}$ and $f_c-2f_{fm}$. The fourth stimulus is 20% FM. The frequency changes are difficult to see in the time-waveform. This stimulus has similar primary sidebands to the 50% AM stimulus but shows a smaller amount of energy at the carrier and an additional two small sidebands which are separated from the carrier-frequency by twice the modulation-frequency. The sixth waveform is an MM stimulus with the maximum frequency occurring at the same time in the waveform as the maximum amplitude. The spectral peaks are asymmetrical around the carrier-frequency with the sidebands at higher frequencies showing a greater amplitude than homologous sidebands at lower frequencies.

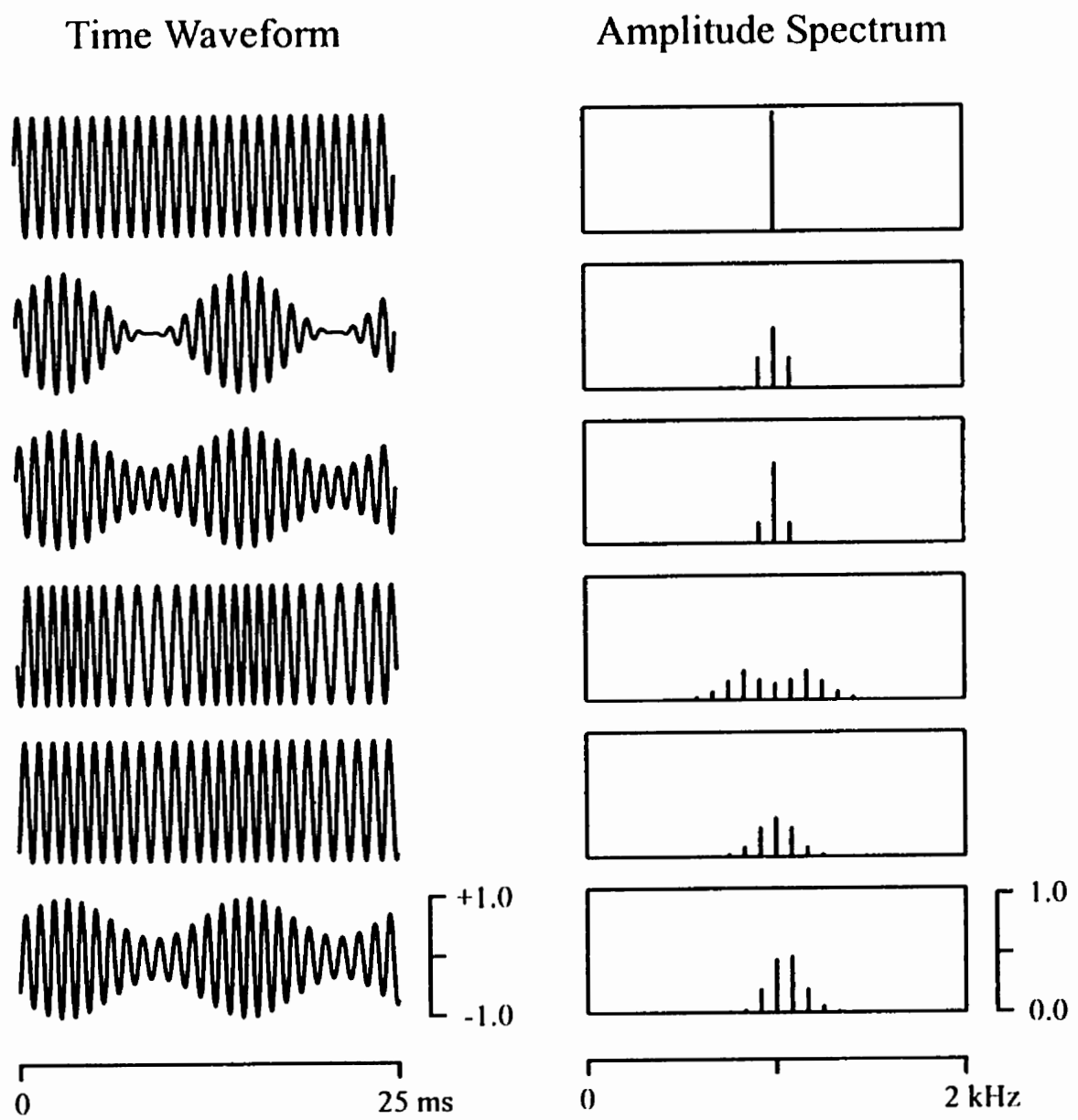
%AM
%FM
Time Waveform
Amplitude Spectrum
0
0
100
0
50
0
0
50
0
20
50
20
+1.0
-1.0
0
25 ms
1.0
0.0
0
2 kHz

*Please see next page for figure*

**Figure 3-2. Mixed Modulation (MM) with different phases of FM.** While the phase of the AM was always zero, the relative phase of the FM was adjusted so that it was 0, 90, 180 or 270 degrees. The relative phase was set so that at 0 degrees the maximum frequency occured at the same time in the waveform as the maximum amplitude. For illustration purposes, the time waveforms were created using 50% FM since this makes it easier to see the actual changes in the carrier-frequency. In addition to the spectra corresponding to the 50% FM, the spectra for 20% FM are also shown since several of the experiments used FM in the 10-25% range. Both sets of spectra show clear asymmetries around the carrier-frequency ($f_c$) when the phase is 0 or 180 degrees. In these two cases the frequency content has shifted above or below the carrier, respectively.

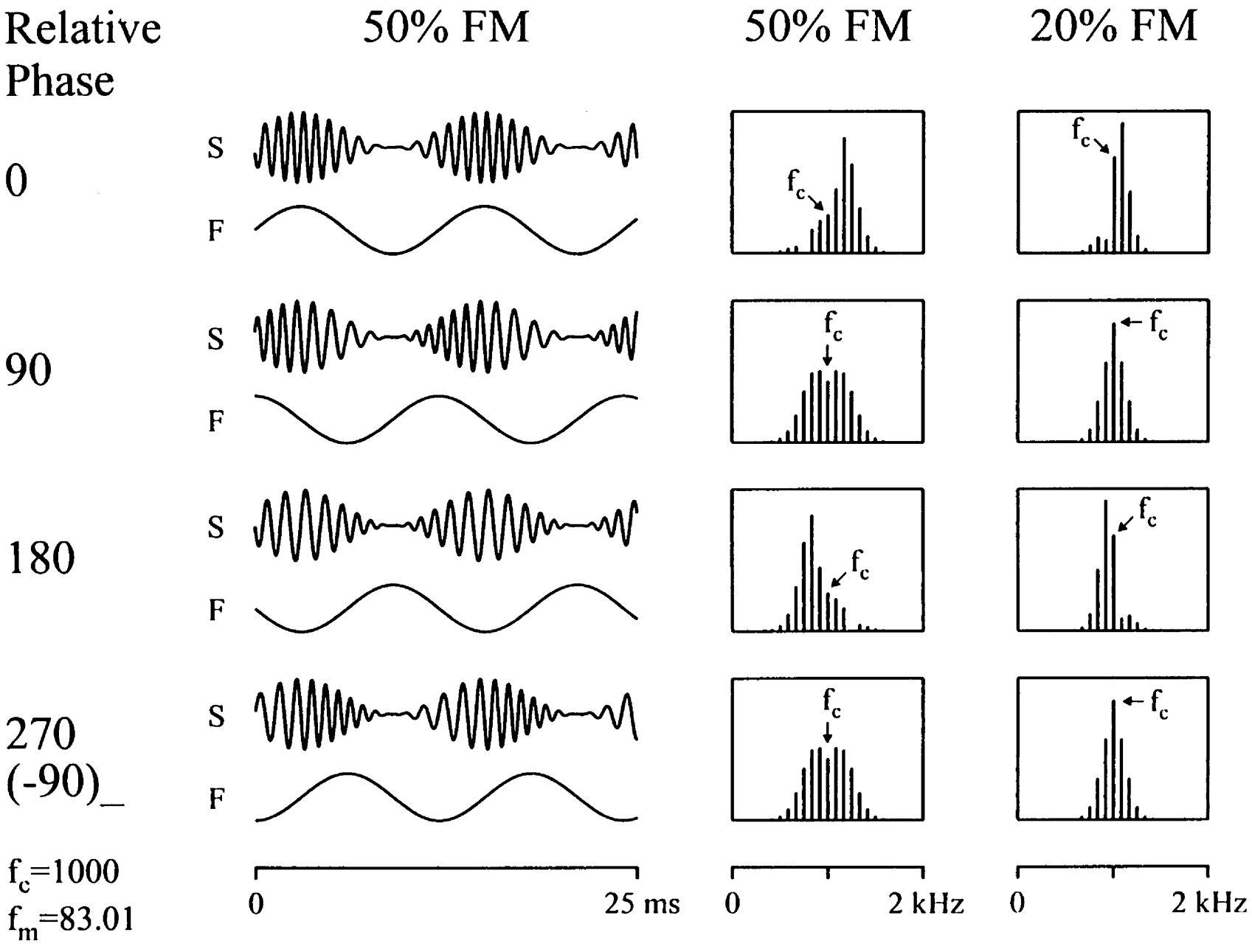
Relative Phase
50% FM
50% FM
20% FM
0
90
180
270
(-90)
S
F
$f_c$
$f_c$=1000
$f_m$=83.01
0
25 ms
0
2 kHz
0
2 kHz

*Please see next page for figure*

**Figure 3-3. Independent amplitude and frequency-modulation (IAFM).** The upper part of the figure shows the time waveforms for a stimulus with a carrier-frequency of 1000 Hz that is 50% AM and 20% FM. The AM occurs at 84.96 Hz, which is slightly faster than the FM, which occurs at 83.01 Hz. The graph in the middle of the figure shows the instantaneous frequency of the sound. As time progresses the maximum frequency shifts increasingly later with respect to the maximum amplitude (see arrows). The lower part of the figure shows the amplitude spectrum of the stimulus over a small range of frequencies near the carrier-frequency. There are two closely spaced sidebands on each side of the carrier, one representing the FM and the other representing the AM (indicated by arrows). There are other small components in the spectrum, which derive from combinations of the two modulating frequencies and the carrier.

50% AM with
$f_{am}$ of 84.96 Hz
20% FM with
$f_{fm}$ of 83.01 Hz

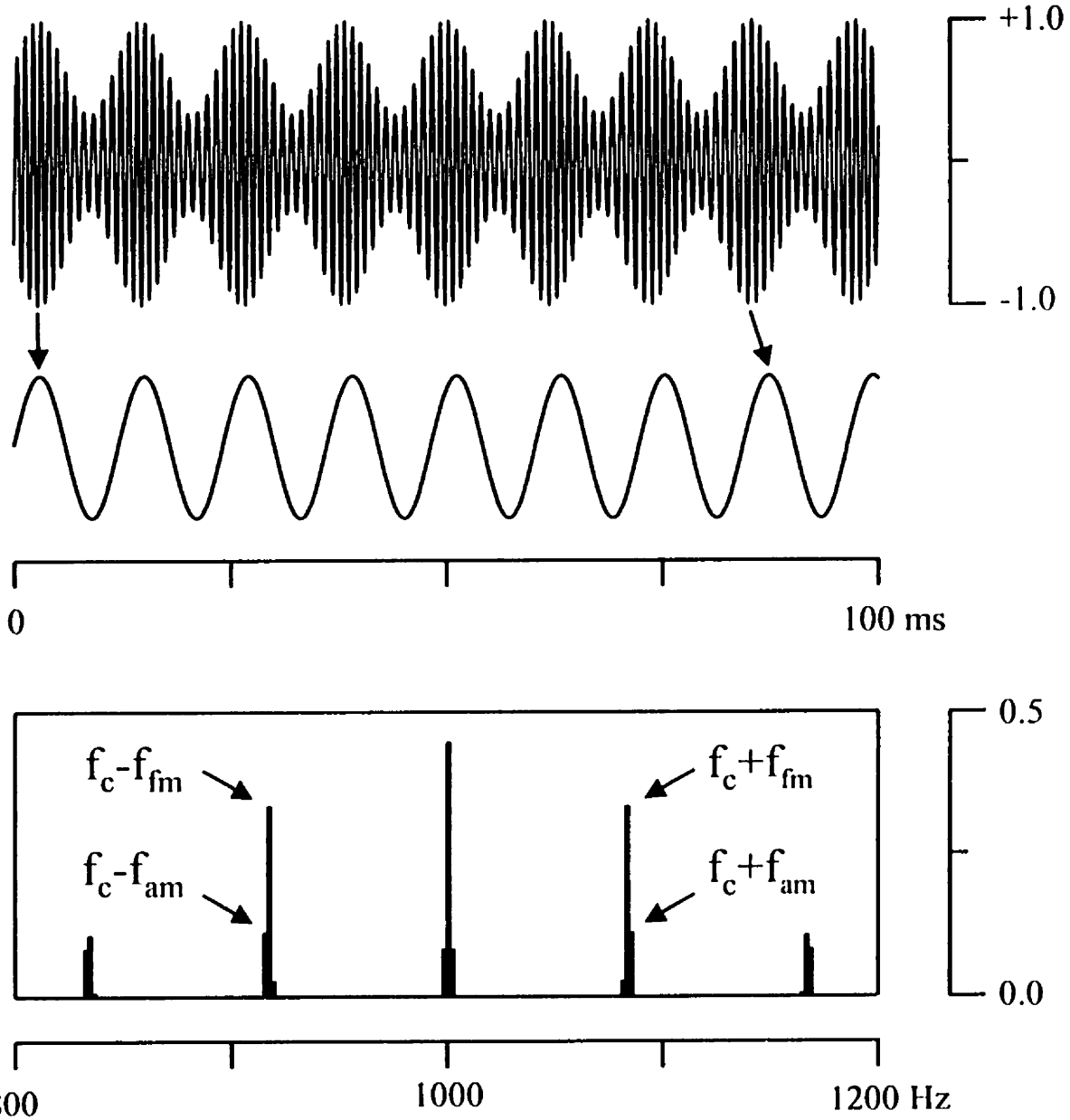

Previously we have shown that up to 4 stimuli can be presented to each ear as long as adjacent stimuli are separated by at least 1 octave (Chapter 1, *Table 1-1*). Accordingly, in most of the experiments in this chapter (those using at least 4 simultaneous stimuli in one or both ears) we used either a "500 Hz octave series" which contained 500, 1000, 2000, and 4000 Hz tones or a "750 Hz octave series" which contained 750, 1500, 3000, and 6000 Hz tones. For the experiments in this chapter that presented all of the different 8 tones simultaneously, the 500 Hz octave series was presented to the right ear and the 750 Hz octave series was presented to the left ear. The right ear stimuli were modulated at 78.13, 83.01, 86.91, and 91.80 Hz and the left ear stimuli were modulated at 80.08, 84.96, 89.84, and 94.73 Hz. The highly specific frequencies were due to the requirement for an integer number of cycles of a stimulus within each recording epoch of 1.024 s (Chapter 2, *sections 5.2, 5.5*). For MM stimuli, the AM and FM for each carrier-frequency occurred at the same rate; in other words, for the 500 Hz tone, both the AM and FM occurred at 78.13 Hz. For the IAFM stimuli we modified the MASTER data acquisition system (described in Chapter 2) to use one set of modulation-frequencies for AM and another set for FM (e.g., the 500 Hz carrier had an AM at 78.13 Hz and an FM at 80.08 Hz). In the remainder of this Chapter the modulation-frequencies will be reported with only single digit precision.

The digitally generated auditory stimuli were converted to analog form at a rate of 32 kHz using 12-bit precision. The analog waveforms were routed to a Grason-Stadler Model 16 audiometer where they were amplified to a calibration-intensity and then attenuated to achieve the desired intensity levels (60, 50, 40, or 30 dB SPL). The stimuli were presented either through TDH-50P headphones, calibrated with a Bruel and Kjaer Artificial Ear Type 4152, or through Eartone 3A insert earphones calibrated with a DB 0138 coupler. Both transducers have a relatively flat intensity response of ±3 dB SPL for tones under 4000 Hz, while the 6000 Hz response is decreased by about 5 dB SPL (headphone) or 20 dB SPL (ear insert). The insert earphones were not used if the experiment included carrier-frequencies of 6000 Hz. For simplicity, the attenuation of the 6000 Hz tone is not documented in the figures and tables.

**Recordings**

Electrophysiological responses were collected from a gold-plated Grass electrode located at Cz and referenced to the posterior neck (7-8 cm below the inion). An electrode placed over

the clavicle served as ground. All electrode impedances were under 5 kOhm at 10 Hz. Recordings occurred in a quiet testing chamber with the subjects lying in a reclining chair. Because sleeping subjects produce less background noise, we asked our subjects to attempt to sleep during the experimental session. All subjects slept through most of the experiments. The responses were amplified using a Grass P50 battery-powered amplifier with the low pass filter set at 300 Hz, a highpass setting of 1 Hz, and a gain of 10,000. The notch filter was turned off.

The MASTER data acquisition system which was described in Chapter 2 collected most of the data using an AD conversion rate of 1 kHz with 12-bit precision. Consecutive data epochs of 1.024 seconds were linked together to form sweeps of 16.384 seconds which were then submitted to an FFT to produce an amplitude spectrum with a resolution of 0.061 Hz. When an epoch contained electrophysiological activity over ±90 μV, it was rejected and the next acceptable epoch was used to build the sweep. In each recording period 16 sweeps (approximately 4 minutes of data) were averaged together. In most of the experiments described in this chapter, three recording periods were obtained and averaged together during each condition for each subject. Accordingly, approximately 13-15 minutes (depending upon the amount of rejected data) was required to collect data for each condition. However, if the F-ratio for the average response for a condition did not reach a significance level of $p<0.05$ for several of the stimuli (as might occur due to a noisy recording), an additional recording was collected and the average response was then based on 4 separate recording periods. In Experiments 1 and 2 we used an older version of the MASTER acquisition system with slightly different parameters (Chapter 1).

The MASTER system uses the FFT amplitude spectrum to evaluate the evoked response data in the frequency domain. The components of the spectrum corresponding to the frequencies of the stimuli each had a specific amplitude and phase. The amplitude of each response was computed from the square root of the sum of the squares of the real and imaginary components, with the calculation adjusted to give the baseline-to-peak amplitude of the sine wave. The onset phase of the response was computed as the angle between the response vector and the real axis. This phase was adjusted (e.g., converted from sine to cosine) so that it would equal zero when the response waveform was identical to the stimulus envelope. In order to make the phase more understandable in terms of the latency of the response, this measurement was converted to "phase

delay" by subtracting it from 360 degrees. This is the same as measuring the angle in a clockwise rather than anti-clockwise direction. Phase measurements were adjusted across the experiments by subtracting an acoustic delay of 0.9 ms when using ear inserts (and tubes) rather than headphones. The intricacies and ambiguities of measuring the phase of steady-state responses are discussed extensively in Chapter 4

Latencies were estimated from the phase delays measured at multiple modulation-frequencies (Experiment 5) in two ways. A traditional measure known as "apparent latency" (Regan, 1966) or "group delay" (Goldstein et al., 1971) was calculated by estimating the slope of the phase delay versus modulation-frequency graph and dividing this slope by 360. In addition, the latency was directly estimated using the "preceding cycles" technique (Chapter 4, *figures 4.2, 4.5*), which calculates the best fit across the different modulation-frequencies for different numbers of stimulus cycles preceding the response.

**Statistical Evaluations of Responses**

In order to determine if the FFT components at the stimulus modulation-frequencies were different than background EEG activity, the value at each of these frequencies was compared to the 120 adjacent frequencies (60 bins above and 60 below the stimulus frequency, or ±3.7 Hz, excluding those frequencies at which other stimuli were modulated) using an F-ratio (Zurek, 1992; Lins et al., 1996; Dobie and Wilson, 1996; Valdes et al., 1997). As discussed in earlier chapters, comparing this ratio against the critical values for F at 2 and 240 degrees of freedom gives the probability of a response being within the distribution of the background noise.

IAFM stimuli evoked two independent responses for each carrier-frequency, one for the AM response at the frequency $\mathbf{f_{am}}$ and one for the FM response at the frequency $\mathbf{f_{fm}}$. Two independent F-tests provided separate probability levels for each of these responses. These were then combined in order to yield the probability of a response being evoked by a particular carrier-frequency. This is akin to the meta-analytic procedure, or "Stouffer method", used when assessing the overall probability of an effect across two separate experiments (as described in Rosenthal, 1991, p. 68-70). The equivalent values on the standard normal distribution (Z-scores) for each of the probabilities were added, the resultant value was divided by the square root of 2 to

give a combined Z-score, and the probability of this value was obtained from the standard normal distribution. For example, if the two probabilities are 0.11 and 0.09 (neither significant at $p<0.05$), the Z-scores for each of these probabilities are 1.23. and 1.34, and the final Z-score of (1.23+1.34)/1.41 or 1.82 is associated with a probability level of 0.03 (Rosenthal, 1991, p. 70).

As in the earlier chapters, the amplitude data obtained in the experiments presented in this chapter were evaluated using repeated measures analyses of variance ANOVA, with Greenhouse-Geisser corrections where appropriate. Because many of the post-hoc comparisons occurring in a single experiment were independent (e.g., were due to activation of different regions of the cochlea), Fisher Least Significant Differences (LSD) were used. Phase data were evaluated using appropriate tests for circular data (Fisher, 1993). Differences were considered significant when $p<0.05$.

### Experimental Design

Since multiple experiments are reported in this chapter, the experimental designs for each particular experiment are provided with the results. The experiments presented here are of two types. Experiments 1, 2 and 3 concern the applied use of AM, FM and MM stimuli in determining thresholds for either modulation depth or intensity. Experiments 4, 5 and 6 were designed primarily to investigate the physiological processes that underlie the MM response.

## RESULTS

### Experiment 1: Different Amounts of AM and FM

Eight subjects participated in this experiment. Five levels of modulation were tested for both AM and FM stimuli. The carrier-frequency was always a 60 dB SPL 1000 Hz tone and the modulation-frequency was 82.3 Hz. The AM depths were 100, 50, 20, 10, and 5%. The FM depths were 50, 20, 10, 5, and 2%. The mean amplitudes, vector-averaged phases and incidence of significant responses at each modulation depth are shown in Figure 3-4. The 50% FM tone

*Please see next page for figure*

**Figure 3-4. Depth of modulation.** The left and right sides of the figure show the mean measurements for the AM and FM stimulus, respectively. The top of the figure plots the amplitudes of the responses and the average noise levels (dashed lines), from which the responses were distinguished. The 20% FM evoked a response with a similar amplitude to the response evoked by the 50% AM stimuli. The middle of the figure shows the normalized vector-averaged phases of the responses. The phase data are only plotted for depths of modulation wherein 4 or more subjects showed a significant response amplitude (and were calculated only from the data for these subjects). The phase did not change significantly at different levels of modulation. The bottom of the figure shows the percentage of responses that reached a significance level of $p<0.05$.

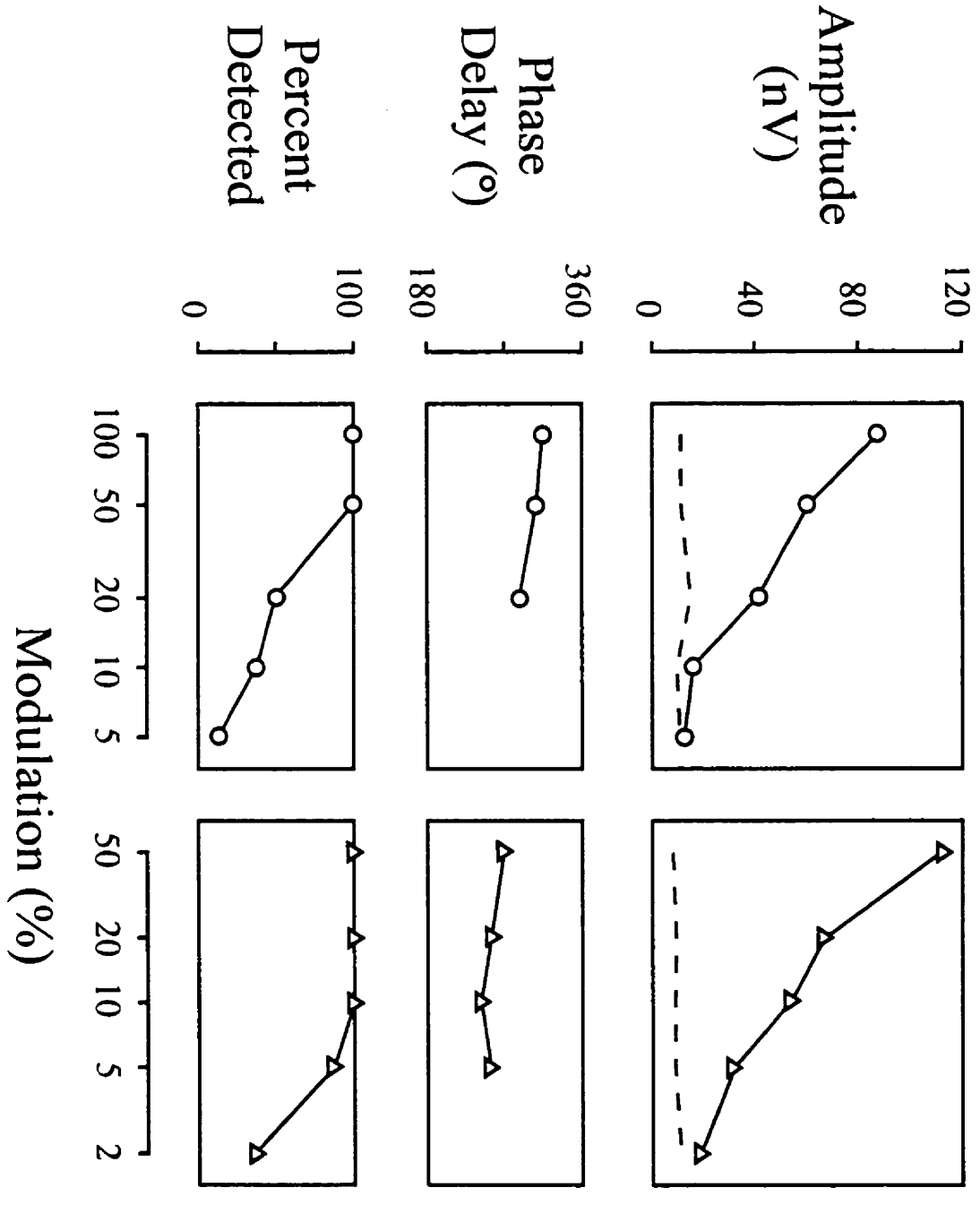
AM
FM
Amplitude (nV)
120
80
40
0
Phase Delay (°)
360
180
0
Percent Detected
100
0
100 50 20 10 5
50 20 10 5 2
Modulation (%)

produced a response that was larger than the response at 100% AM. There was no effect of modulation depth on the phase delay of either response. The phase delay of the response to the 50% AM stimulus was 47 degrees later than the phase delay for the 20% FM stimulus (a response with a similar amplitude). This difference was significant using nonparametric statistics (Fisher, 1993, p.114: $\chi^2$=4.0, df=1, p<0.05). The average behavioral discrimination limens for detecting modulation in these stimuli were 5.7% (SD 1.0) for AM and 1.4% (SD 0.4) for FM (equivalent to a modulation index of 0.085 for FM). The physiological response was detectable in 50% or more of the subjects at 20% AM and at 5% FM, i.e. at about 10 dB above threshold for both AM and FM.

**Experiment 2: Possible Interactions between AM and FM.**

Eight subjects participated in this experiment in order to evaluate the effects of simultaneously recording responses to two modulated stimuli. AM and FM tones were presented alone or in combination with other AM or FM tones. The modulation-frequency was 82.3 Hz for the 1 kHz carrier and 88.9 Hz for the 2 kHz carrier. In addition, an MM response was recorded at 1 kHz with zero phase delay between the AM and the FM, i.e. with the highest frequency occurring at the highest amplitude. The conditions can be seen in Table 3-1, which also shows the mean amplitudes of the 1 kHz response (for simplicity the 2 kHz responses are not shown). A repeated measures ANOVA of the 1 kHz responses indicated a main effect for modulation type (F=7.85; df=5,9; p<.001) with the MM responses significantly larger than the other types of response: 28% larger than the simple FM response (p<.01) and 51% larger than the simple AM response (p<.01). The 1 kHz responses at 100% AM and 25% FM were not statistically different. The response amplitudes did not change significantly when the modulated stimulus was presented in combination with an AM or FM stimulus at 2 kHz.

Although the AM response was unaffected by the presence of other stimuli, a repeated measures ANOVA of the 1 kHz FM responses to stimuli presented either alone and in combination indicated a main effect (F=10.82; df=3,9; p<.001) with the two tone responses being significantly smaller than responses to stimuli presented alone. In a separate analysis it was found that the 2 kHz FM tone was also reduced when presented with a 1 kHz AM tone. Thus,

**Table 3-1: Interactions between stimuli (Experiment 2)**

| Stimulus (Carrier 1kHz) | Other Stimuli | Amplitude (nV) | Phase Delay (°) |
|---|---|---|---|
| 100 % AM | none | 70±33 | 177 |
| | 2 kHz 100 % AM | 66±30 | 204 |
| | 2 kHz 25% FM | 69±30 | 193 |
| 25% FM | none | 83±27 | 145 |
| | 2 kHz 25% FM | 66±24 | 146 |
| MM (100% AM, 25% FM) | none | 106±49 | 184 |

while responses to AM stimuli do not decrease when presented with other AM or FM tones, FM responses show a consistent decrease of about 20% when presented with other FM or AM tones. The additional stimuli did not significantly affect the phase delay of the response. Once again the phase delay of the response to the 100% AM stimulus was later than the phase delay for the 25% FM stimulus. The MM response had a phase delay similar to that of the AM response.

**Experiment 3: Multiple AM and MM stimuli**

Eight subjects participated in each of the 2 paradigms of this experiment. In order to assess the effects of multiple MM stimulation across a lower range of intensities, we created stimuli that were either 100% AM or MM (100% AM and 25% FM). The MM stimuli were created so that the maximum frequency coincided with the maximum amplitude. Eight stimuli were presented simultaneously, four to each ear. Stimuli were presented at 50, 40, and 30 dB

*Please see next page for figure*

**Figure 3-5: Effects of MM on stimuli at different intensities.** For the data plotted in the upper half of the figure, the stimuli were 100% AM and 25% FM (±12.5% deviation from carrier-frequency). At 50, 40 and 30 dB SPL, the amplitudes were 30%, 49%, and 28% larger for responses evoked by MM compared to those evoked by AM. The increased amplitude for MM was evident at all intensities and frequencies except for 6 kHz. The bottom half of the figure shows the results (from a different group of 8 subjects) when the stimuli were 100% AM and 10% FM (±5% deviation from carrier-frequency). Amplitudes were 20%, 7%, and 8% larger for responses evoked by MM stimuli compared to AM only stimuli. While 10% FM may be useful in increasing response amplitude at 50 dB SPL, this effect is not evident at lower intensity levels.

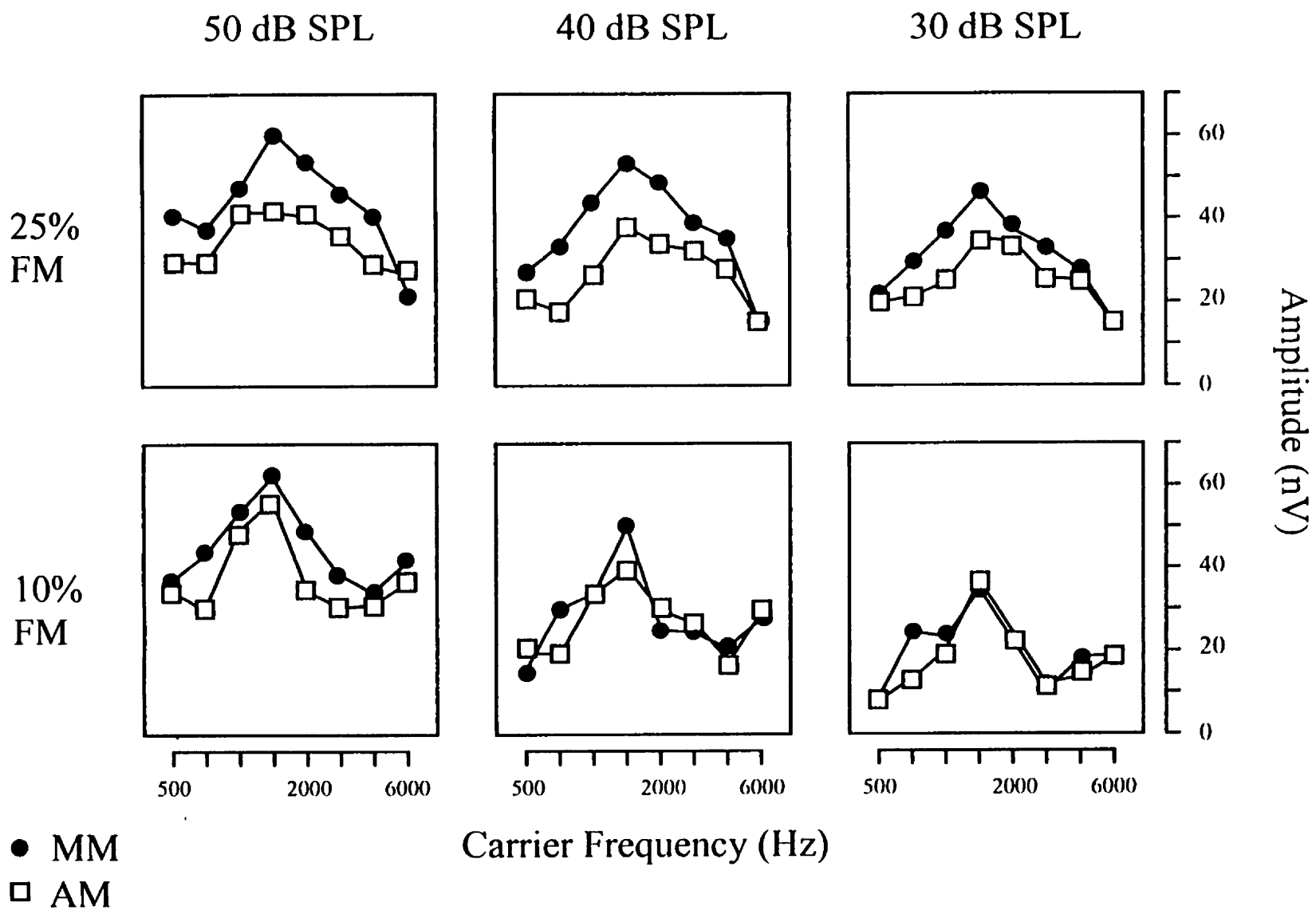
50 dB SPL
40 dB SPL
30 dB SPL
25% FM
10% FM
60
40
20
0
Amplitude (nV)
500
2000
6000
MM
AM
Carrier Frequency (Hz)

SPL during 3 separate recording conditions. The results of this experiment can be seen in Figure 3-5. A repeated measures ANOVA (modulation type x intensity x carrier-frequency) indicated a main effect for modulation type ($F=62.1$; $df=1,7$; $p<.001$) with the MM responses significantly larger than the AM responses. Main effects were also found for intensity ($F=47.0$; $df=2,14$; $p<.001$; $\epsilon=.54$) with the more intense stimuli evoking larger responses, and carrier-frequency ($F=8.3$; $df=7,49$; $p<.001$; $\epsilon=.41$) with the response being larger at the middle frequencies. The only significant interaction was found between modulation type and carrier-frequency ($F=3.7$; $df=7,49$; $p<.05$; $\epsilon=.60$) because the 6000 Hz response failed to be larger for the MM than the AM stimuli. The lack of any significant interaction between modulation type and intensity level indicates that the enhanced amplitudes of the MM stimuli persisted across all three intensity levels. The average MM responses were 35%, 50%, and 30% larger than the AM responses at 50, 40, and 30 dB SPL, respectively.

The phase delays of the responses are shown in Table 3-2. Only the results at the higher intensities are shown, since some of the measurements at 30 dB did not reach significance. The main finding was that for the carrier-frequencies of 1 kHz and higher, the delays were consistently later for the AM stimuli than for the MM stimuli. For both AM and MM stimuli, the phase delays consistently increased with decreasing intensity, with a change equivalent to about 0.7 ms for each 10 dB decrement. As expected, there was a general decrease in phase delay with increasing carrier-frequency (translating to a decrease in response latency), although these relative changes may have been slightly exaggerated since the modulation-frequencies also increased with increasing carrier-frequencies.

The larger size of the MM response compared to AM response at 25% FM made its detection more rapid indicating that the time for the test could be reduced by about a third even at 30 dB. This can be seen in Figure 3-6, which shows the percentage of significant responses that were evident at 30 dB after different amounts of averaging. The time saved can be estimated by the horizontal distance between the curves.

**Table 3-2: Phase delays of AM and MM responses (Experiment 3 with 25% FM in MM)**

| Type | Intensity (dB SPL) | Carrier-frequency (Hz) | | | | | | | |
|---|---|---|---|---|---|---|---|---|---|
| | | 500 | 750 | 1000 | 1500 | 2000 | 3000 | 4000 | 6000 |
| AM | 50 | 275 | 248 | 227 | 229 | 211 | 214 | 207 | 207 |
| | 40 | 283 | 302 | 270 | 251 | 224 | 225 | 226 | 208 |
| MM | 50 | 271 | 272 | 240 | 221 | 201 | 182 | 182 | 176 |
| | 40 | 299 | 302 | 269 | 237 | 212 | 200 | 194 | 182 |

*Please see next page for figure*

**Figure 3-6. Time for detecting the responses to MM.** Data in each graph are from 8 subjects. The graphs show the percentage of the responses, out of 8 different carrier-frequencies (4 in each ear), that reached significance as the number of sweeps averaged increased from 1 to 12. Each sweep contains about 16 seconds of data. The stimuli were presented at 30 dB SPL. The left graph shows data collected for 100% AM and for the MM stimulus with 25% FM. The right graph displays the results (from different subjects) when the FM component of the MM was 10%. MM clearly speeds up the detection of the responses when the FM component is 25% but not when the FM is only 10%.

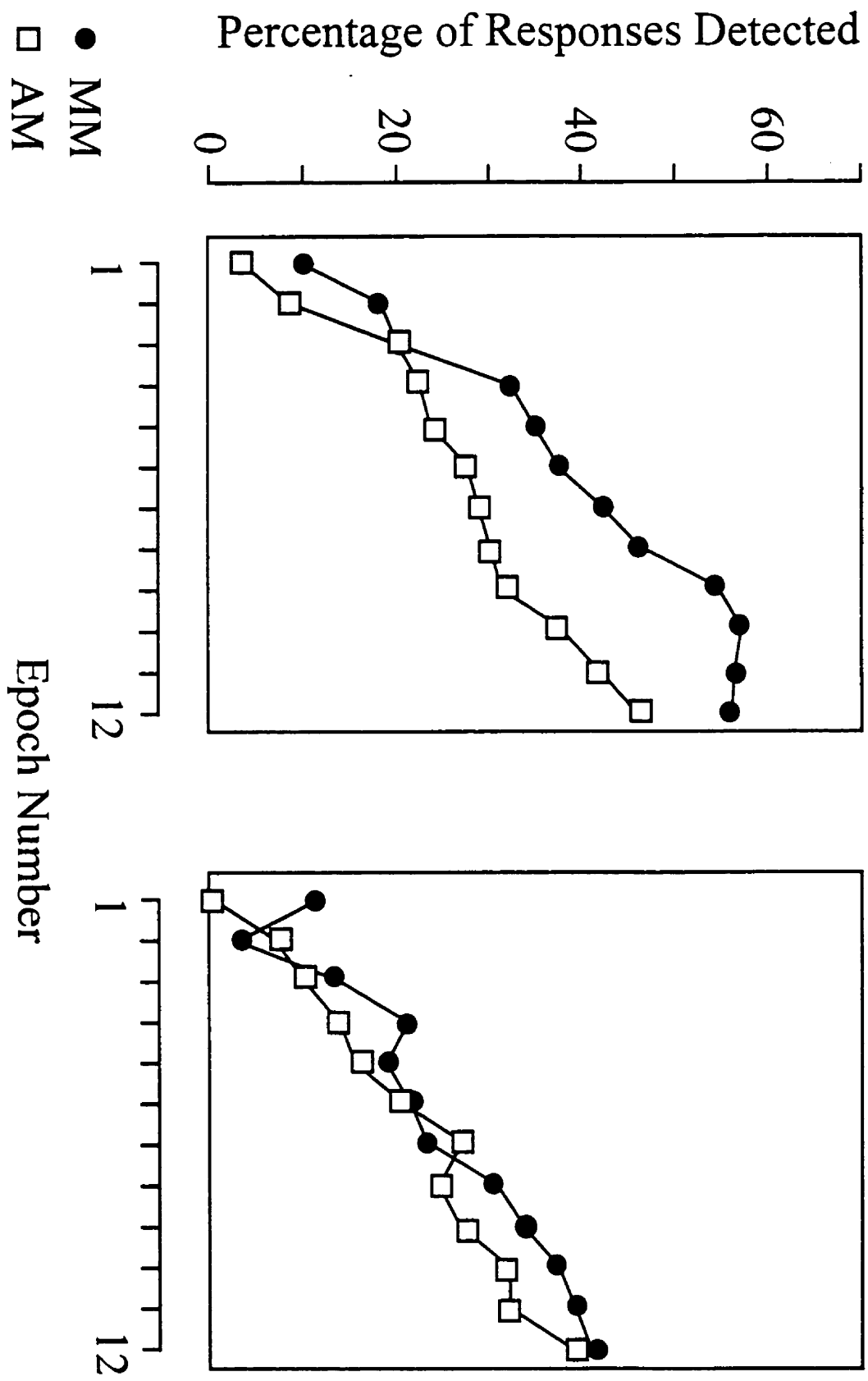
Percentage of Responses Detected
0
20
40
60
MM
AM
25% FM
10% FM
1
12
1
12
Epoch Number

A second paradigm using an FM depth of only 10% was carried out on a different group of eight subjects in order to see whether the technique could utilize MM stimuli with greater frequency-specificity. The results for this experiment can be seen in the lower part of Figure 3-5. The MM enhancement is clearly less for 10% FM than for 25% FM. A repeated-measures ANOVA identical to that used in Experiment 2 showed main effects for modulation type ($F=7.8$;$df=1,7$; $p<.001$; $\epsilon=1$), intensity level ($F=45.5$; $df=2,14$; $p<.05$; $\epsilon=.70$), and carrier-frequency ($F=12.6$ ;$df=7,49$; $p<.001$; $\epsilon=.39$). Unlike the first paradigm, the interaction between modulation type and carrier-frequency failed to reach significance. The average MM responses were 20%, 3%, and 12% larger than the responses to the AM stimuli at 50, 40, and 30 dB SPL, respectively.

**Experiment 4: Changing the FM phase in the MM stimulus**

Ten subjects participated in each of the 2 paradigms of this experiment. An examination of the phase results of Experiments 2 and 3 showed that the MM response often had a phase delay that was shorter than that of the AM response, as though it were tending toward the shorter phase delay of the FM response. This suggested that the MM response might be the result of the vector addition of independent AM and FM responses. The largest MM response would then occur when the phase of the FM stimulus relative to the AM stimulus causes the two components of the MM stimulus evoked responses to be in phase. Accordingly, we decided to investigate the effects of changing the relative phase between AM and FM in the MM stimuli. The stimuli in our first paradigm used the same carrier and modulation-frequencies as in Experiment 3, but were presented at only 50 dB SPL. In order to determine if changing the phase of the FM affected the amplitude of the MM response, four different relative phases (0, 90, 180 and 270°) were used in the MM stimuli in four separate conditions. The responses to simple AM and FM stimuli were also recorded, for a total of six experimental conditions in this paradigm.

The results are shown in Figure 3-7. A repeated measures ANOVA (modulation type x carrier-frequency) showed main effects for modulation type ($F=21.11$; $df=5,55$; $p<.001$; $\epsilon=.41$) and carrier-frequency ($F=7.23$; $df=7,77$; $p<.01$; $\epsilon=.38$), and a significant interaction ($F=4.22$; $df=35,385$; $p<.01$; $\epsilon=.15$) due to the divergent response seen at 6000 Hz. Fisher LSDs indicated

that MM with FM phases set at 0 (or 360) and 270 (or -90) degrees evoked significantly larger (10% and 25%, respectively) responses than the AM only condition. MM with FM phases of 90 and 180 degrees evoked responses that were significantly smaller than the simple AM response. The pure AM response was significantly larger than the pure FM response. The effects of stimulus phase were consistent for every carrier-frequency except 6000 Hz.

The possibility that the MM response represents the vector addition of the AM and FM responses is illustrated diagrammatically in Figure 3-8. The relative phase ($\varphi$) between the AM and the FM responses can be estimated by fitting a baseline-offset sine wave to the data obtained for the MM stimuli using different phases between the AM and FM components. This can be done using either an FFT analysis or an iterative least-mean-square fitting of a sine wave. The amplitude of the sine wave represents the FM component in the MM response, and the amount of baseline-offset represents the amplitude of the AM component. Each response may be decreased a little by the presence of the other. The FM response might be decreased due to the AM envelope, and the AM response might be decreased due to the loss of synchronization of nerve fibers as would occur with changes in frequency. Alternatively, the two responses might both be reduced by overlap of common neural generators. The results of this analysis (Table 3-3) indicated that the MM response could be reasonably represented as the vector addition of separate AM and FM responses, with the AM response amplitude reduced by about 10%, and the FM response amplitude reduced by about 21%. The estimated phase difference was very similar to the actual phase difference.

*Please see next page for figure*

**Figure 3-7. Effects of FM phase on the MM response.** The four upper graphs show the amplitudes separately for the different carrier-frequencies. The left graphs in this figure compare response amplitudes for stimuli that were evoked by AM or FM alone, while the right graphs show the response amplitudes for the MM stimuli with different phases of FM relative to the AM. The data obtained at 0° are re-plotted at 360°. The responses for the 4 lower carrier-frequencies are shown separately from those for the 4 higher carrier-frequencies so that the individual values can be seen more easily. The bottom set of graphs shows the mean amplitudes across all carrier-frequencies. The dotted line shows how the data can be fit using the technique illustrated in Figure 3-8. For all carrier-frequencies except 6000 Hz the MM response is larger when the phase is 270 or 360 degrees than when it is 90 or 180 degrees.

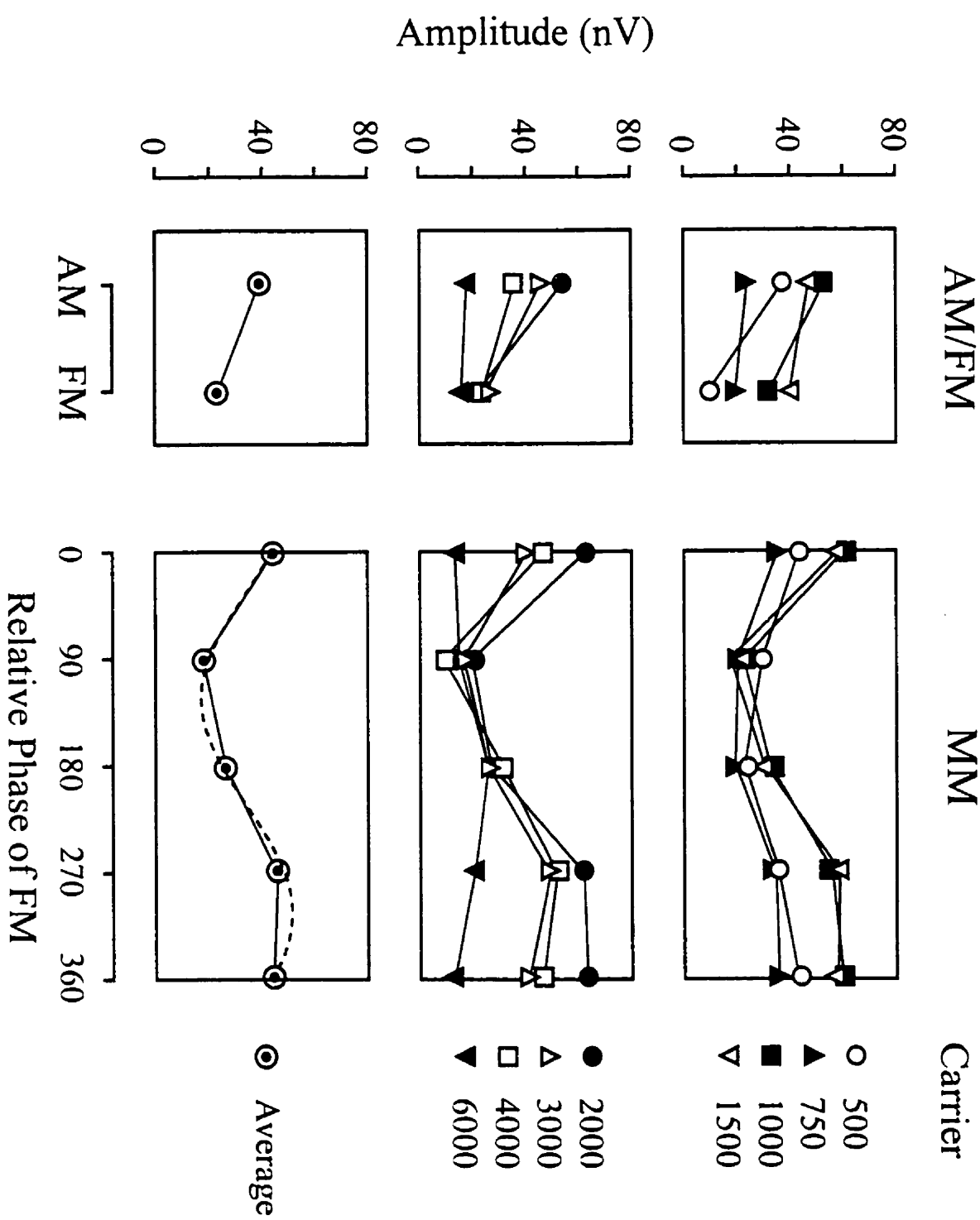
Amplitude (nV)
AM/FM
MM
Carrier
500
750
1000
1500
2000
3000
4000
6000
Average
AM
FM
0
40
80
0
90
180
270
360
Relative Phase of FM

*Please see next page for figure*

**Figure 3-8. Analysis of mixed modulation responses.** This figure shows diagrammatically how the MM response can be considered as the vector addition of independent responses to the AM and FM components of the stimulus. The left diagram shows the vector addition on a polar plot. The AM response is shown as the vector originating at zero. Added to this is an FM response vector of smaller amplitude and with a different phase. These responses (vectors) were evoked by stimuli that had the same phase, i.e. the relative phase between AM and FM stimuli was zero. The relative phases of the responses would be altered by changing the relative phase of the FM stimulus. Increases in the phase of the FM stimulus will rotate the FM response vector clockwise. The response to MM is shown as the dotted-line vector. The FM and AM response vectors will line up to produce the largest MM response when the relative phase between AM and FM equals $\varphi$. The right side of the figure illustrates how $\varphi$ can be derived using the MM amplitudes obtained when the relative phase between the AM and FM stimuli is varied. The amplitudes are fit with a sine wave having a baseline-offset. The size of the baseline-offset is equivalent to the amplitude of the AM response and the amplitude of the sine wave is equivalent to the amplitude of the FM response. The maximum MM amplitude (dotted line) occurs when the relative phase between AM and FM equals $\varphi$.

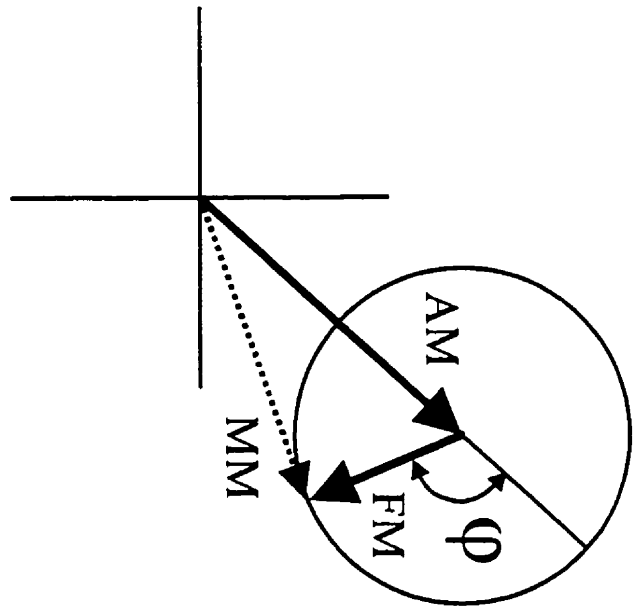
AM
MM
FM
φ

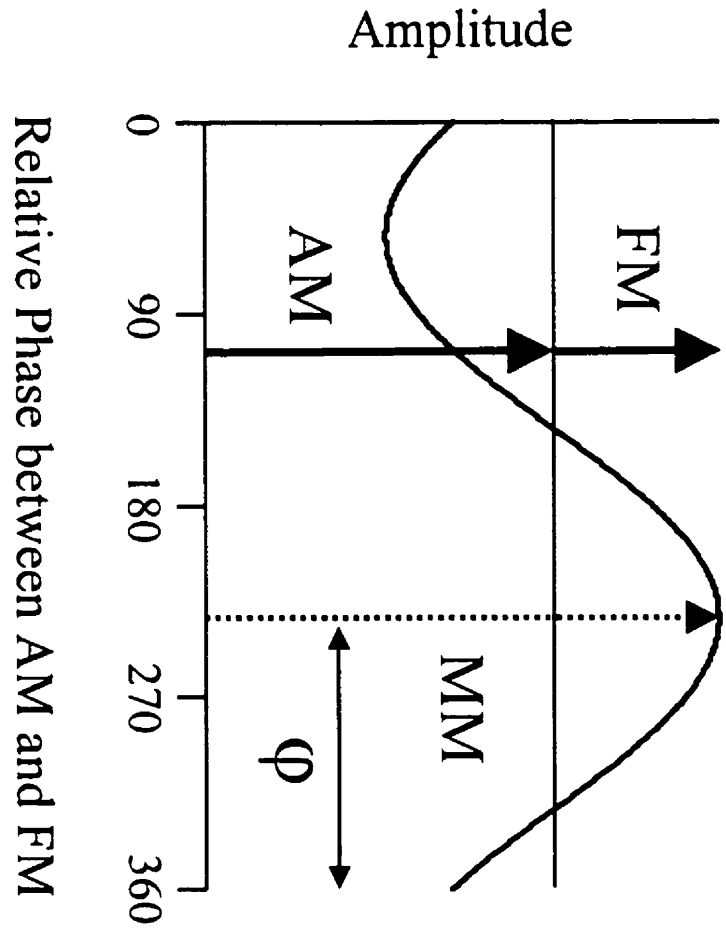
Amplitude
Relative Phase between AM and FM
0
90
180
270
360
AM
FM
MM
φ

**Table 3-3: Effects of combining AM and FM**

| 1 Carrier Frequency (Hz) | 2 AM amp. (nV) | 3 AM phase delay | 4 FM amp. (nV) | 5 FM phase delay | 6 MM AM amp. | 7 percent AM alone | 8 MM FM amp. | 9 percent FM alone | 10 estim. phase diff. | 11 actual phase diff. |
|---|---|---|---|---|---|---|---|---|---|---|
| 500 | 37 | 232 | 10 | 267 | 32 | 86 | 11 | 114 | -13 | 35 |
| 750 | 24 | 223 | 19 | 206 | 27 | 111 | 11 | 57 | -42 | -17 |
| 1000 | 54 | 214 | 32 | 175 | 42 | 78 | 22 | 68 | -49 | -39 |
| 1500 | 47 | 201 | 39 | 140 | 41 | 87 | 24 | 61 | -55 | -60 |
| 2000 | 53 | 176 | 23 | 115 | 43 | 80 | 28 | 120 | -49 | -61 |
| 3000 | 45 | 185 | 25 | 143 | 33 | 73 | 18 | 73 | -64 | -41 |
| 4000 | 36 | 186 | 24 | 113 | 35 | 98 | 22 | 91 | -68 | -73 |
| 6000 | 17 | 239 | 15 | 31 | 18 | 107 | 7 | 45 | -153 | -208 |

The data in columns 1-5 are obtained from the experiment, while data in columns 6-10 are derived from the model illustrated in Figure 3-8. Using this model, the data in column 6 represent the estimated response to the AM component of MM. The data in column 7 shows the estimated amplitude as a percentage of the actual amplitude of the AM responses alone (column 2). Columns 8 and 9 show similar data for the estimated FM responses. The data in column 10 show the phase differences between AM and FM responses that would produce the maximum amplitude of the MM response, as predicted by the model. The actual differences in phase delay between the AM and FM responses (column 5 minus column 3) are given for comparison in column 11 and are very close to those predicted for carrier-frequencies from 750 and 4000 Hz.

Since the results indicated that the MM response was generally largest when the phase difference between the AM and FM components was between 270 (-90) and 0 degrees, a second paradigm was studied (with a different set of 10 subjects) to check this range more closely. Accordingly, the stimuli were the same as in the first part of the experiment except they had relative phases of 0, 135 270, and 315 degrees. Our prediction was that the 315 degree condition would produce the largest responses while the 135 condition should produce the smallest. An additional fifth condition presented AM only stimuli to provide a baseline. The five conditions were tested at both 30 and 50 dB SPL. Average results across the two ears are shown in Figure 3-9 for the 50 dB SPL condition. The largest response occurred when the phase was 315 degrees. The optimum phase ($\varphi$) for the MM stimulus at 500, 1000, 2000 and 4000 Hz, calculated using the techniques shown in Figure 3-8, resulted in the following estimations: -293, -58, -40 and -48 degrees at 50 dB SPL, and -220, -37, -42 and -98 degrees at 30 dB SPL.

**Experiment 5. Latency estimates for AM and FM stimuli**

Eight subjects participated in this experiment. The preceding experiments had consistently indicated that the AM responses occurred with a later phase delay than the FM responses. Since phase delay is not directly transformable to latency, we decided to estimate the latencies of AM and FM responses by recording the same responses at different rates (see Chapter 4, *Figure 4-5*). The carrier-frequencies were a 500 Hz octave series and the stimuli were either 20% FM (left ear) or 100% AM (right ear). The FM rates (left ear) were 80.1, 85.0, 89.8, and 94.7 Hz and the AM rates (right ear) were 78.1, 83.0, 86.9, and 91.8 Hz. Each carrier was presented at each modulation-rate across four recording conditions. Stimuli were presented at 50 dB SPL using insert earphones. The vector-averaged phase delays for these subjects are shown in Figure 3-10. Table 3-4 shows the latencies estimated both by calculating the apparent latency and by determining the number of preceding cycles. The AM response generally occurred later than the FM response. The preceding-cycles technique indicated that both kinds of response were preceded by one cycle of the stimulus (see Chapter 4, *Figures 4-2, 4-5).*

*Please see next page for figure*

**Figure 3-9. Effects of FM phase on the MM response.** This figure shows the average results obtained in the second part of Experiment 4. MM responses were obtained using stimuli with FM phases of 0°, 45°, 270°, and 315°. The data are plotted in the same way as in Figure 3-7 so that the amplitudes obtained with the 0° phase are also re-plotted at 360°. For each carrier-frequency, the data have been fit with a sine wave according to the logic illustrated in Figure 3-8.

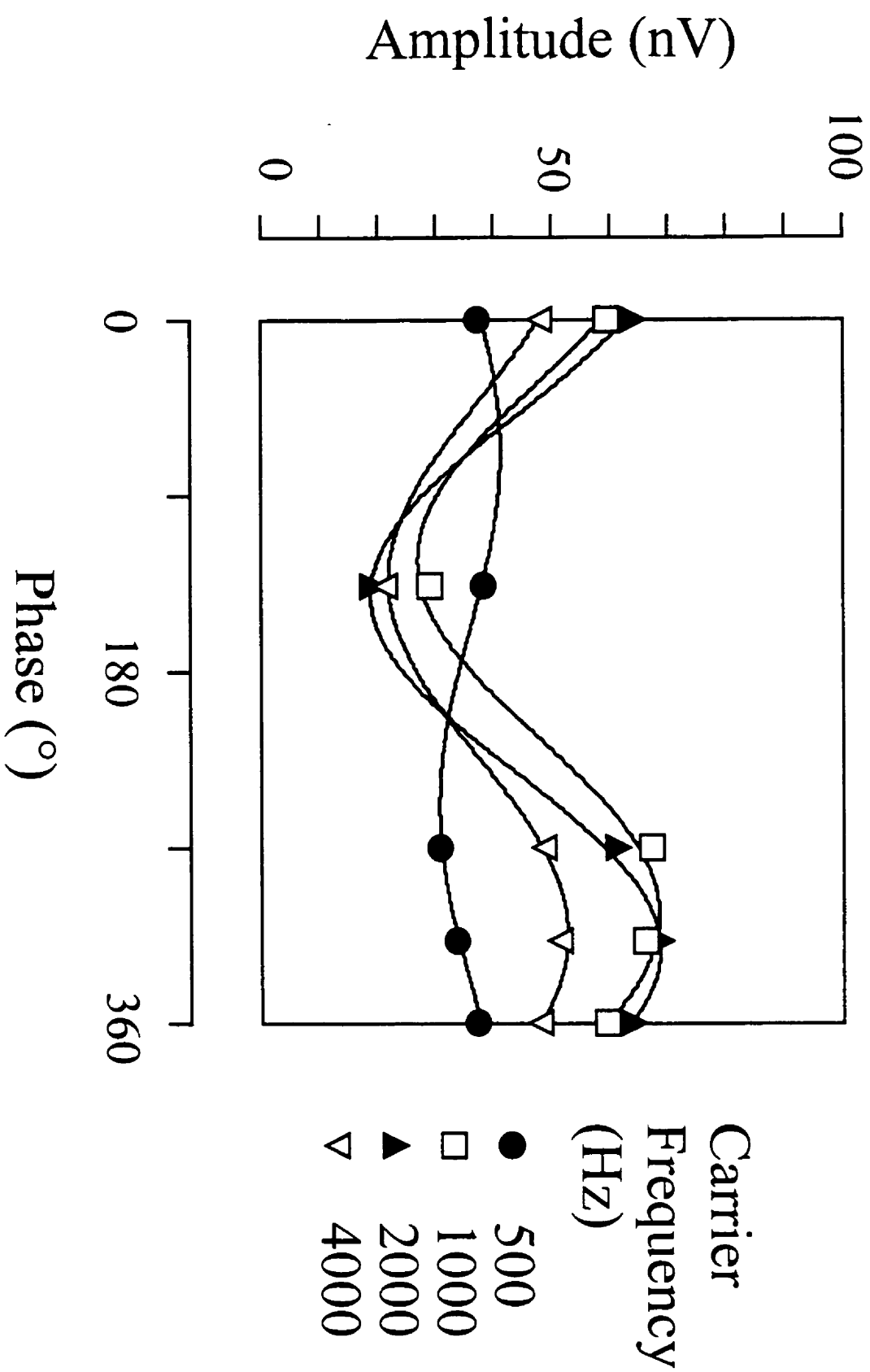
Amplitude (nV)
0
50
100
Phase (°)
0
180
360
Carrier Frequency (Hz)
500
1000
2000
4000

*Please see next page for figure*

**Figure 3-10. Latencies of the AM and FM responses.** This figure shows the average phase delays obtained for FM and AM stimuli recorded during Experiment 5. The phase delay increases with increasing modulation rate in an approximately linear fashion. An "apparent latency" can be calculated by measuring the slope of the phase versus modulation rate.

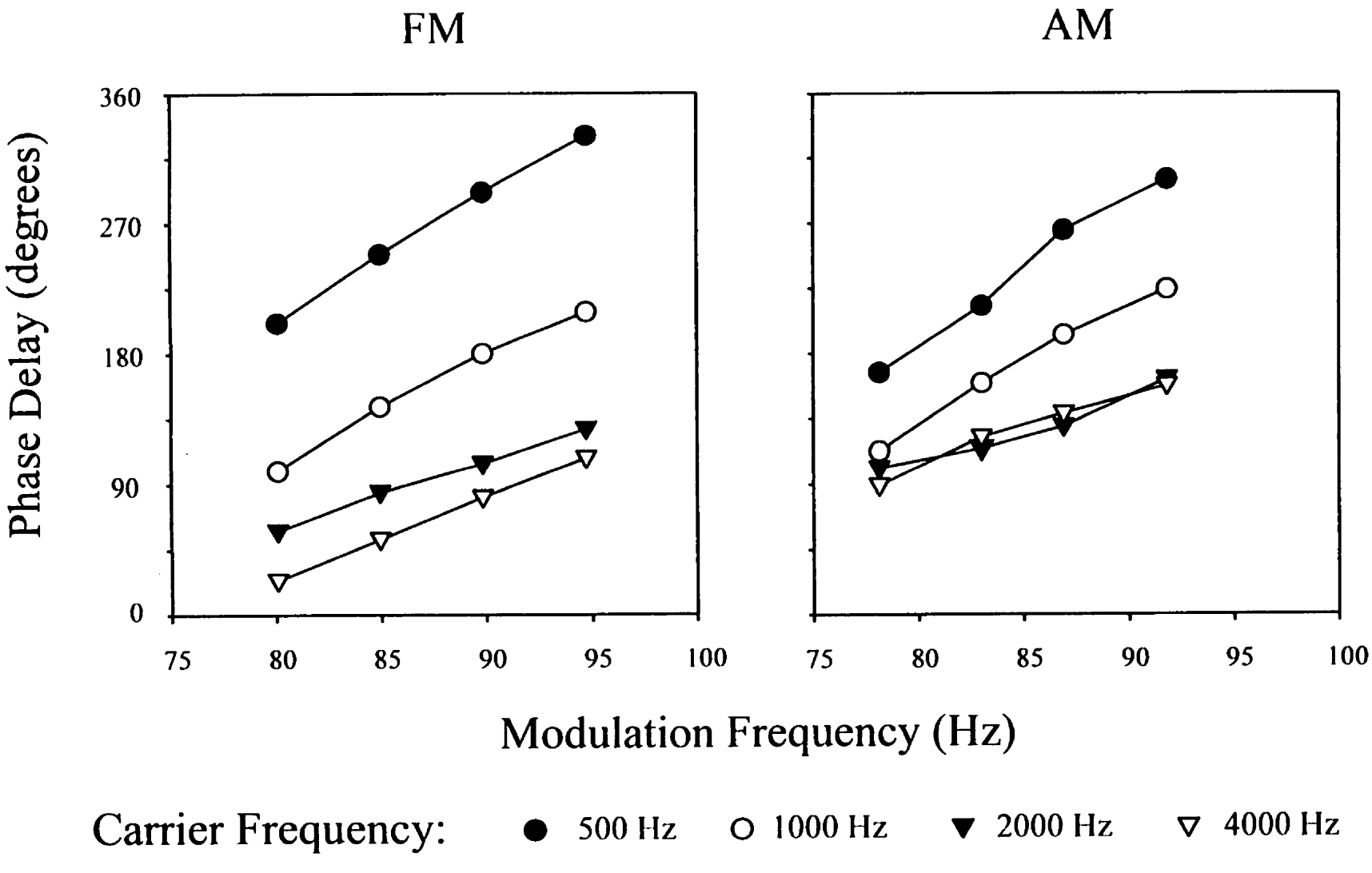
FM
AM
Phase Delay (degrees)
360
270
180
90
0
75
80
85
90
95
100
Modulation Frequency (Hz)
Carrier Frequency:
500 Hz
1000 Hz
2000 Hz
4000 Hz

**Table 3-4. Estimated latencies (ms) for AM and FM responses.**

| | 100% AM Response | | 20% FM Response | |
|---|---|---|---|---|
| Carrier | Apparent Latency | Preceding Cycles Technique | Apparent Latency | Preceding Cycles Technique |
| 500 | 30.9 | 19.5 | 27.6 | 19.9 |
| 1000 | 24.8 | 17.4 | 22.4 | 16.4 |
| 2000 | 15.4 | 15.9 | 12.3 | 14.4 |
| 4000 | 13.1 | 15.9 | 18.0 | 13.5 |

**Experiment 6: Independent amplitude and frequency-modulation (IAFM)**

Ten subjects participated in each of the 2 paradigms of this experiment. In the first paradigm, the stimuli consisted of the 750 Hz octave series, which was presented to the left ear at 50 dB SPL using the same modulation rates that were used in Experiments 3 and 4. Four types of stimuli were used: AM, FM, MM, and IAFM. The FM was always 20%. The AM was set at either 100% or 50% for the AM and IAFM stimuli, thus giving a total of 6 recording conditions. The relative phases of all FM stimuli were 90 degrees. The maximum frequency in the MM condition thus occurred one quarter of a cycle before the maximum amplitude (cf. Figure 3-2, second stimulus). Accordingly, in this paradigm the responses to MM should generally be smaller than the responses to AM (cf. Figure 3-7).

Sample data from one subject are shown in Figure 3-11. The eight stimuli that were presented to one ear clearly produce eight corresponding spectral peaks in the IAFM response. The mean amplitudes of the AM, FM and IAFM responses are shown in Figures 3-12. For carrier-frequencies of 750 and 1500 Hz, the amplitudes of the response to the AM component of the IAFM response were smaller than the amplitudes of the response to AM alone. The amount of reduction is similar for both 100% and 50% AM. For the same carrier-frequencies, the response to the FM component of IAFM is greatly attenuated, when AM is 100%, compared to when FM is presented alone, but not much when the AM is 50%. The response to the MM stimulus was, as expected from our choice of phase, smaller than the response to either FM alone or AM alone. Table 3-5 shows that the amplitudes and phases of the MM response were close to what would be predicted from vector-addition of the separate AM and FM responses (with some additional reduction in the amplitude).

*Please see next page for figure*

**Figure 3-11. Multiple auditory steady-state responses.** This figure shows the responses obtained in one subject for some of the conditions of Experiment 6. On the left of the figure are shown the responses viewed in the frequency domain. Only part of the amplitude spectrum is shown. At the frequencies of the stimuli (indicated by arrowheads) the amplitudes measured in the spectrum are higher than the background noise level. On the right of the figure the polar plots of the responses at each of the modulation-frequencies are shown. The circles represent the confidence limits of the noise. If the zero point is not included in the circle, the response can be considered as significantly ($p<0.05$) different from the background noise. The first set of responses represent those obtained in response to 100% AM. The middle responses are those obtained using 20% FM. The bottom set of responses represent the responses when a single carrier-frequency was independently modulated in both amplitude and frequency (IAFM). These responses tend to be slightly smaller in amplitude than those obtained when only one type of modulation occurred. The phases are quite similar. Note that the phase angle between the vector and the horizontal axis represents the "onset phase" when measured counter-clockwise and the "phase delay" when measured clockwise.

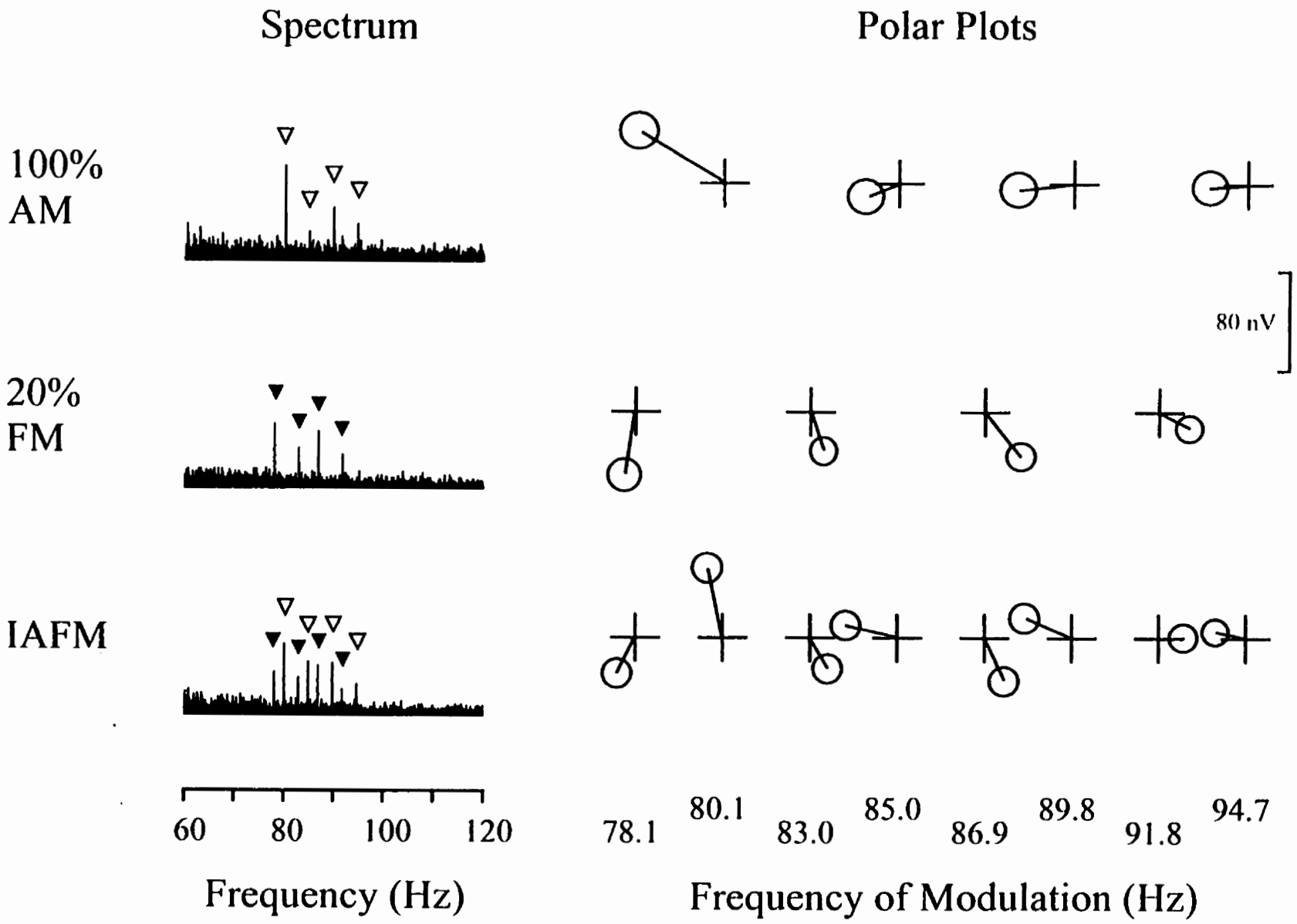
Spectrum
Polar Plots
100%
AM
20%
FM
IAFM
80 nV
60
80
100
120
Frequency (Hz)
78.1
80.1
83.0
85.0
86.9
89.8
91.8
94.7
Frequency of Modulation (Hz)

*Please see next page for figure*

**Figure 3-12. Response to independent amplitude and frequency-modulation (IAFM).** This figure compares the amplitudes of the responses to stimuli that were simply modulated in amplitude or frequency to the same responses when the modulations occurred together in the same stimuli. The amplitude of the response to AM is shown on the left graph and to FM on the right graph. The amplitudes decreased for the IAFM stimuli, with the decrease being larger for the lower carrier-frequencies.

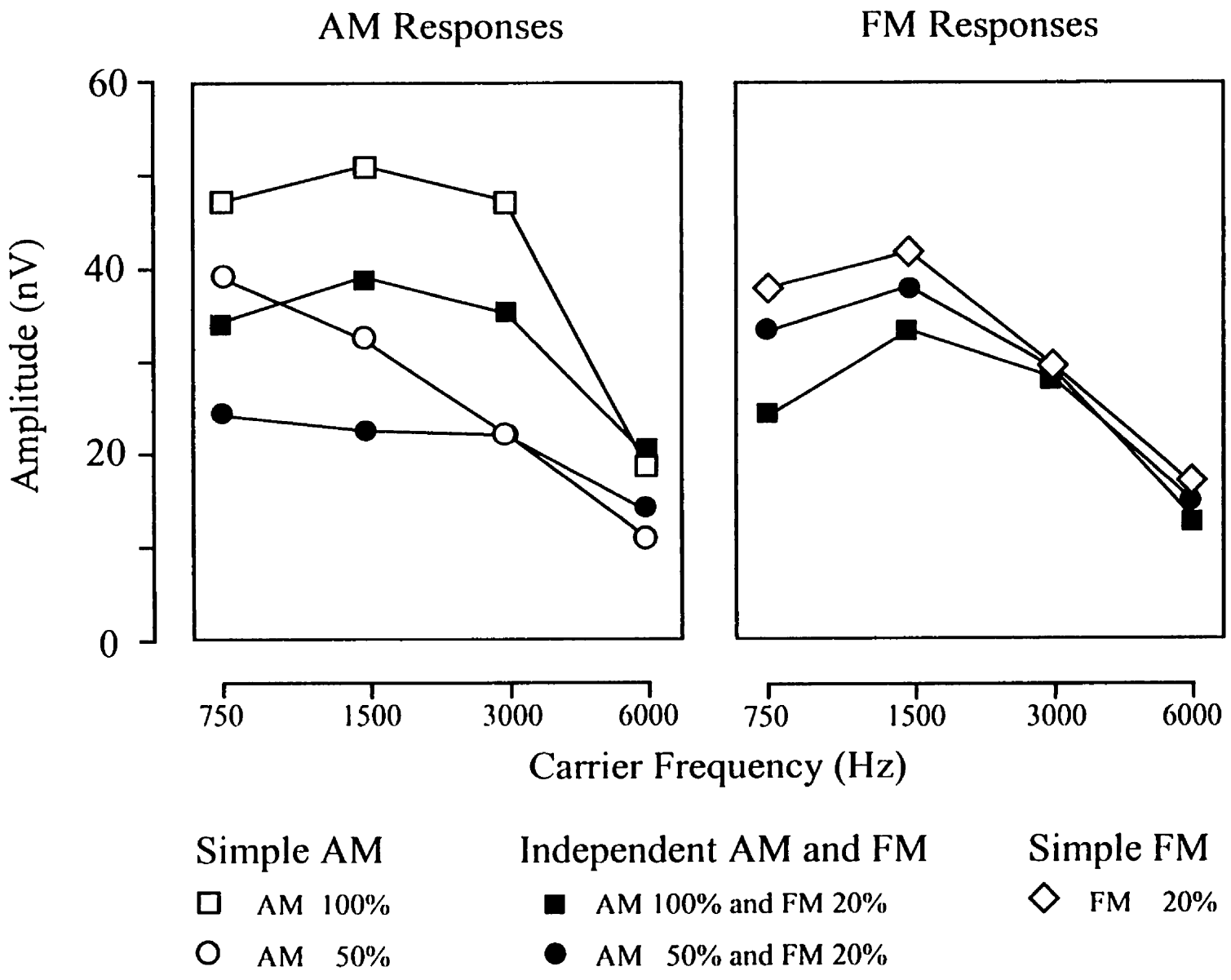
AM Responses
FM Responses
60
40
20
0
Amplitude (nV)
750
1500
3000
6000
750
1500
3000
6000
Carrier Frequency (Hz)
Simple AM
AM 100%
AM 50%
Independent AM and FM
AM 100% and FM 20%
AM 50% and FM 20%
Simple FM
FM 20%

**Table 3-5 Mixed modulation at a phase of 90°**

| | 100% AM | | 20% FM | | MM | | Predicted MM | |
|---|---|---|---|---|---|---|---|---|
| Carrier (Hz) | amplitude (nV) | phase delay(°) | amplitude (nV) | phase delay(°) | amplitude (nV) | phase delay(°) | amplitude (nV) | phase delay(°) |
| 750 | 37 | 224 | 31 | 109(199) | 29 | 195 | 37 | 173 |
| 1500 | 45 | 210 | 37 | 60(150) | 17 | 153 | 23 | 155 |
| 3000 | 42 | 189 | 28 | 41(131) | 17 | 161 | 23 | 149 |
| 6000 | 13 | 204 | 14 | 2(92) | 13 | 285 | 5 | 294 |

The values for the recorded amplitudes and phases (columns 2-7) were obtained by vector averaging across subjects. The amplitudes are therefore smaller than those shown in Figure 3-11 where the amplitudes were averaged without regard to phase. The values predicted in columns 8 and 9 were obtained by vector summation of the data represented in columns 2-5. The bracketed data in column 5 represent what the phase delay would be if the FM were at 0° relative to the AM (making the data homologous to the phase delays in preceding tables).

A second paradigm examined how effectively, compared to 100% AM stimuli, the IAFM stimuli could produce detectable responses as intensities approached threshold. Stimuli were presented to the subject's left ear using insert earphones. Two types of stimuli were used. The first were 100% AM carrier-frequencies of 500, 1000, 2000 and 4000 Hz that were modulated at 80.1, 85.0, 89.8, and 94.7 Hz, respectively. The second were IAFM carrier-frequencies that were both 50% AM, at the previously noted modulation-rates, and 20% FM at 78.1, 83.0, 86.9, and 91.8 Hz. An AM depth of 50%, rather than 100%, was used since the FM response may have been previously reduced in amplitude because the ability of FM to evoke a response may have been decreased during the periods when the amplitude envelope intermittently approached zero. There were nine experimental conditions: each type of stimulus was presented at 20, 30, 40, 50 dB SPL. A no-stimulus condition provided control estimates of detection probability. The detectability of the response for each of the stimuli was determined using the F-ratio test on each

of the three sub-averages collected in each condition, as well as on the overall average response. This under-estimated the final significance of the responses, but provided a better evaluation of the incidence of detectable responses (since 30 separate response probabilities were obtained for each stimulus and intensity rather than 10). For the IAFM responses, the probabilities of the significance of the AM and FM responses were combined using the Stouffer method.

The results are shown in Figure 3-13. A three-way (intensity, stimulus-type and carrier-frequency) repeated-measures ANOVA was used to assess the amplitudes. The amplitudes increased with increasing intensity ($F=22.9$; $df=4,36$; $p<.001$; $\epsilon=.30$). The 100% AM responses were significantly larger than either of the components of the IAFM response (stimulus-type main effect, $F=12.1$; $df=2,18$; $p<.01$; $\epsilon=.57$). The responses were larger at the middle frequencies (frequency main-effect: $F=9.5$; $df=3,27$; $p<.01$; $\epsilon=..66$), with a significant interaction between frequency and intensity ($p<.01$). The percentage of detected responses increased with increasing intensity. The combined detectability for the two responses to the IAFM stimulus was similar to the detectability for the 100% AM response and both were significantly larger than either of the IAFM components alone (comparing the four results over all intensities: $\chi^2=34.1$, $df=3$; $p<.001$). Based on the average results rather than the sub-averages, the average thresholds for 500, 1000, 2000 and 4000 Hz stimuli were 38, 30, 22, and 26 dB for the 100% AM stimuli and 31, 24, 24 and 27 dB SPL for the IAFM stimuli using the combined approach.

## DISCUSSION

### Physiological Processing of AM and FM

The results obtained in these experiments have clear implications about the physiological mechanisms underlying the perception of AM and FM. For the same carrier-frequency, the processes that mediate our perception of AM and FM seem quite independent. The response to MM stimulation is reasonably well explained by the vector-addition of the individual responses to AM and FM (Experiments 3, 4, and 6). The modeled results suggested a reduction in amplitude for the AM and FM responses of only 10-20% which would indicate little overlap of the neuronal generators of these responses. Furthermore, these reductions in amplitude may be reasonably explained by other mechanisms. The FM response is probably reduced somewhat in

*Please see next page for figure*

**Figure 3-13. Effects of stimulus intensity on IAFM responses.** This figure compares the responses to IAFM stimuli (50% AM and 20% FM) to the responses to 100% AM stimuli. The top set of graphs shows the amplitudes for each of the 4 carrier-frequencies. The dotted line represents the average noise level in the adjacent bins of the FFT. The response amplitudes for the no-sound (NS) condition are at the level of the residual background noise. The amplitude increases with increasing intensity above 20 dB SPL, with the amplitude being larger at the middle frequencies than at 500 or 4000 Hz, and with the amplitude for the 100% AM response being larger than either of the two components of the IAFM response. The lower graphs show the percentage of responses that were considered as significantly ($p<0.05$) different from the background noise. When there is no response present in the no-sound condition the probability of detecting a response is approximately 5% as would be expected from the statistics of the test. The response to the 100% AM stimulus is more readily detectable than the responses to either of the components of the IAFM response. The dashed line represents the percent of responses detected if the probabilities of the two responses to the IAFM stimulus were combined. The data in these graphs are based upon sub-averages of the response. The actual final percentages of responses detected on the basis of the full average would be significantly higher than that portrayed in these graphs.

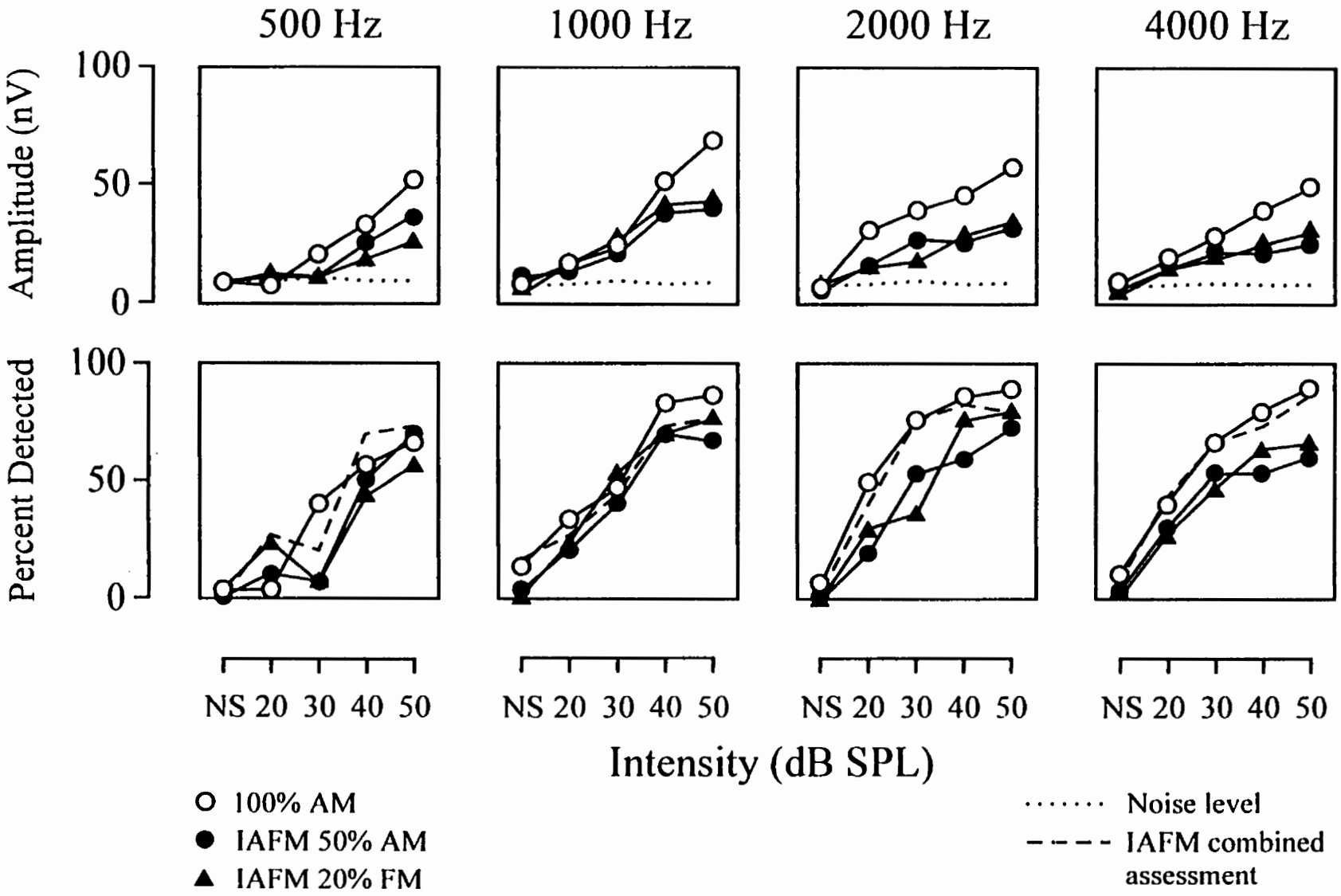
500 Hz
1000 Hz
2000 Hz
4000 Hz
Amplitude (nV)
100
50
0
Percent Detected
100
50
0
NS 20 30 40 50
NS 20 30 40 50
NS 20 30 40 50
NS 20 30 40 50
Intensity (dB SPL)
100% AM
IAFM 50% AM
IAFM 20% FM
Noise level
IAFM combined assessment

amplitude by the concomitant modulation of the amplitude of the stimulus, since it is not easy to follow the frequency of the stimulus when the amplitude intermittently goes to zero. Similarly, the compound AM response might be slightly reduced if the neuronal responses that contribute to the compound response come from different regions of the cochlea that are activated at slightly different latencies.

Probably the most convincing demonstration of the independence of these two processes occurs in the experiments that used one carrier-frequency with different modulation-frequencies for AM and FM – independent amplitude and frequency-modulation (Experiment 6). Despite the fact that the modulations are very close together and the peaks in the response spectra almost superimposed (Figure 3), the recorded responses show clearly defined steady-state components at each of the modulation-frequencies.

The usual explanation for how AM and FM stimuli are processed in the cochlea focuses upon the asymmetry of the cochlear activation pattern (Zwicker and Fastl, 1990). The general conclusion is that AM is mediated by neurons with characteristic frequencies that are higher than the carrier-frequency of the modulated tone, whereas FM is mediated by neurons most sensitive to frequencies lower than the carrier-frequency of the stimulus. However, the cochlear activation pattern does not always map directly onto neuronal discharge patterns. The discharge rate of auditory nerve fibers show non-linear relationships to changes in the intensity of the stimuli. There is saturation at high intensities, and the rate of discharge varies differently with intensity depending upon the frequency of the stimulus relative to the characteristic frequency of the responding fiber. Basically the response versus intensity slope is more rapid when the stimulus frequency is at or below the characteristic frequency of the fiber than when the stimulus frequency is higher (Geisler et al., 1974; Sachs and Abbas, 1974; Yates et al., 1990). Recent results have clearly demonstrated that the hair cells and the auditory fibers respond better at a lower frequency than the characteristic frequency when the intensity of the stimulus is increased (Zwislocki, 1991; Smith, 1998). FM stimuli are probably mediated best by hair cells and neurons with characteristic frequencies lower than the carrier-frequency of the stimulus. This occurs since the higher cut-off slope of the tuning curve makes the responding system particularly sensitive to frequency changes at stimulus frequencies above the characteristic frequency.

These concepts can be illustrated by referring to "iso-rate contours" for the auditory nerve fibers (Figure 3-14). These diagrams have unfortunately only occasionally been produced (e.g. Geisler et al., 1974) although they can be derived from the more commonly presented iso-intensity contours (e.g., Rose et al., 1971). Different fibers will show different slopes for the iso-rate contours (Winter et al., 1990) but the general idea shown in Figure 3-14 should be consistent across most fibers. The figure also shows how AM and FM stimuli can be mapped onto such a diagram. The lines representing the AM and FM stimuli are positioned at locations that show maximum neuronal activation. In the diagram, the stimulus lines cross the largest number of rate-contours. The best AM response occurs when the carrier is slightly below the characteristic frequency of the fiber, whereas the best FM response occurs when the carrier-frequency is slightly above. If the carrier-frequency of an FM stimulus were located within the neuronal response area so that the stimulus goes through iso-rate contours on both sides of the response area, the neuron would respond at twice the modulation-frequency (cf. Khanna and Teich (1989b).

The latency data that we obtained for the AM and FM responses do not easily fit with this view. The AM response occurs with a phase delay that is generally a little later than that of the FM response. This is confirmed by the estimated latencies in Table 3-4, which try to resolve some of the general ambiguities associated with determining latency from phase (see Chapter 4, *Figure 4-2*). If the travelling wave is a major determinant of the response latency, our results would suggest that the AM response is mediated at some more distant region of the cochlea than the FM response, a region concerned with lower frequencies. However, any phase measurement of the FM signal is arbitrary. We, and the literature, have defined the zero point of the FM stimulus relative to the high frequencies in the signal. We could just as easily have determined the phase relative to the low frequencies in the signal. This would have given a response that is a half-cycle earlier or later than what was measured. This could have shifted the latency that we measured using the "preceding cycles" technique. However, it should not have affected the latency as measured by the "apparent latency" or "group delay" technique, since this measurement is unaffected by where in the cycle the response is initiated. Here, the FM response

*Please see next page for figure*

**Figure 3-14. Mechanisms of processing AM and FM.** This figure shows a diagrammatic iso-rate contour plot for an auditory nerve fiber. The figure is loosely based on the data of Geisler et al. (1974). The fiber is most sensitive to low-intensity stimuli at the "characteristic frequency" (CF). Within the shaded response area of the fiber, the contours indicate increasing rates of discharge. The two straight lines on the figure represent stimuli used for AM or FM stimulation. These are positioned at the locations where they would elicit the largest response from the fiber at the frequency of modulation. The circles represent the carrier-frequencies of these optimal stimuli. The largest response to AM occurs when the carrier-frequency is less than the characteristic frequency of the fiber, whereas the largest response to FM occurs when the carrier-frequency is higher. The inset diagram shows optimally responding neurons for AM and FM of a particular carrier-frequency

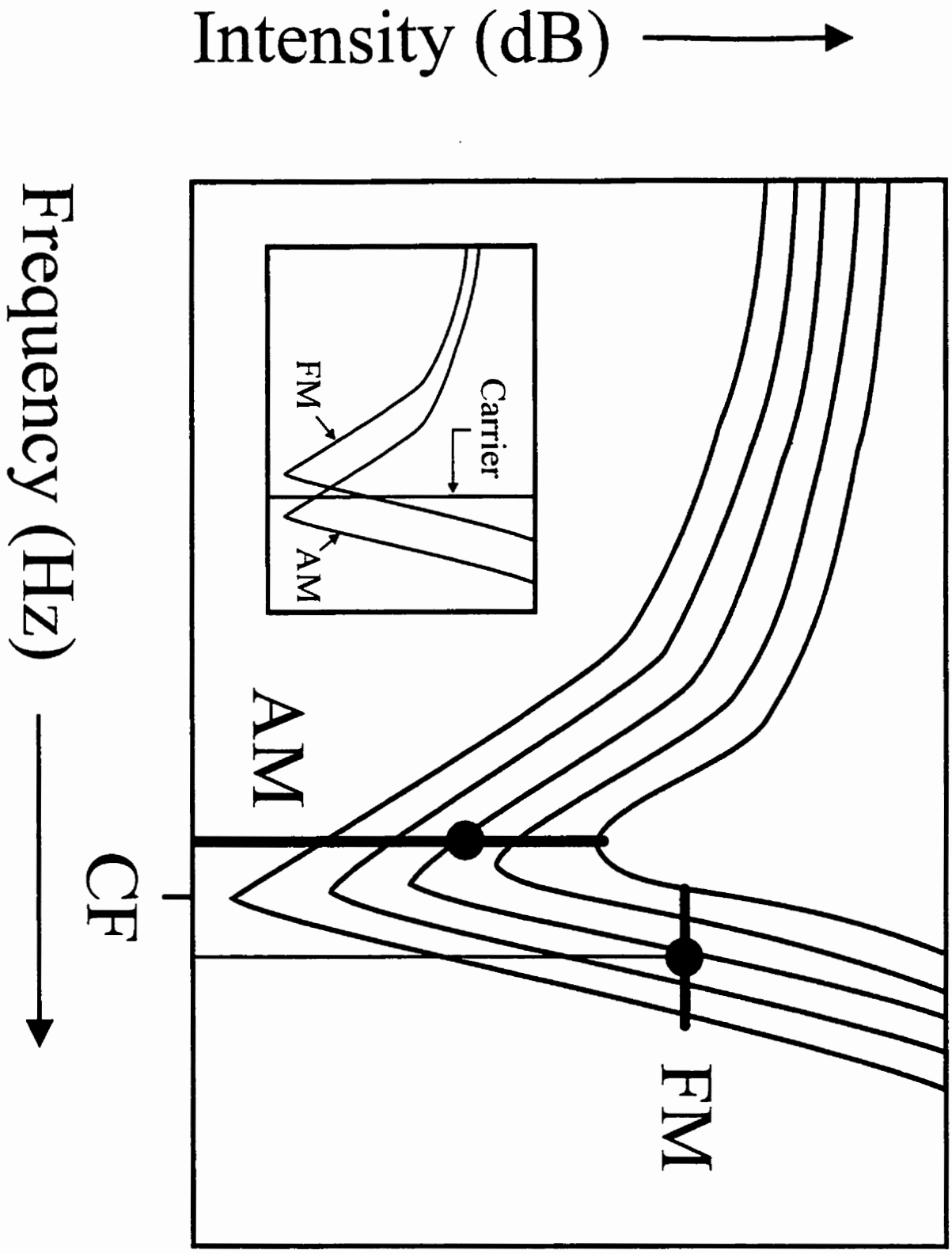
Intensity (dB)
Frequency (Hz)
CF
AM
FM
Carrier
FM
AM

also tends to be earlier than the AM response.

The latency of the response may, however, be determined as much by the filtering effect of the hair cell response-system as by the actual time to move along the basilar membrane. This idea is discussed more fully in Eggermont (1979), and reviewed in Chapter 4 of this thesis. If this filtering concept is true, then the response latency will be shorter when the activation occurs through the edges of a filter rather than at its center. This could explain the earlier latencies that we measured for the FM responses.

In effect, we are suggesting that the response to FM is mediated by means of AM with a varying location on the basilar membrane for the modulation. Saberi and Hafter (1995; and also Saberi, 1998) have demonstrated that the binaural integration of FM and AM signals can be explained on the basis of FM-AM conversion at the level of the cochlear bandpass filter. Although FM is coded mainly as a moving AM at the level of the cochlea, FM must later produce another set of effects or it would be perceived the same as AM. At the modulation-frequencies that we are using AM and FM are perceptually very similar, but at low frequencies they are quite different. The explanation for this used by Zwicker and Fastl (1990) is that the information about the phase of the sidebands occurs outside of the critical band mediating the carrier when the frequency of modulation is high. Although the sidebands are processed (through other critical bands) the relative phase between the sideband and the carrier (determining the AM or FM nature of the signal) cannot be perceived. This interpretation of the response in terms of the amplitude spectrum may be valid for perception where information is integrated over a period of time of 200 ms or more, but it is not very helpful when explaining a moment-to-moment following response like the steady-state response.

One reason for the independence of the AM and FM response from the same carrier-frequency would then be that the responses come from different regions of the cochlea. The AM response would be mediated at a more apical region than the FM response. It is possible that this might be investigated using AM and FM at different carrier-frequencies and bringing these close together to see where interference occurs. However, the multiple interactions between the carriers (beats, suppression, masking) would make the results very difficult to understand.

The steady-state responses we are recording probably represent activity at early stages in

the analysis of the auditory information. Despite the latencies of between 15 and 20 ms (preceding-cycles technique), the responses probably originate in the brainstem with the delay caused by several synapses. The responses are probably generated by modulation-sensitive neurons in the brainstem, generating compound fields that can be recorded at the scalp. We found no evidence for large interference between modulations of different carriers (Experiment 2). FM responses were susceptible to the presence of other stimuli, perhaps because they are more easily masked as they move over a wider range of the basilar membrane. The amplitude decrease in these FM responses was only about 20% and this still makes it possible to record multiple responses simultaneously. The majority of the neurons generating the steady-state responses probably do not integrate across spectral regions or across different types of modulation. This integration clearly must occur to explain the perceptual interference (Yost and Sheft, 1989; Wilson et al., 1990) but this is probably at later stages in processing (and might be detectable through slower steady-state responses). The steady-state responses that we record at high rates of modulation are similar to the unit responses reported in the dorsal cochlear nucleus where modulation phase-locking occurs for specific carriers (Zhao and Liang, 1997).

**Clinical Usefulness of the Steady-state Responses**

Cohen et al. (1991) reported that MM stimuli could evoke significantly larger steady-state responses than AM stimuli. We previously demonstrated that MM stimuli with 25% FM at 50 dB SPL intensity levels evoked responses that reached significance about twice as rapidly as the responses to 100% AM stimuli (Chapter 2, *Figure 2-6*). In the experiments of this chapter, we show that the enhancement of the response persists at 40 and 30 dB SPL (Figure 3-5). If a response is 30% larger, then the residual noise in the recording can be 30% larger for the same signal-to-noise ratio. Theoretically, this would occur when averaging $(1/1.3)^2$ or 59% as many responses. This fits with our results showing the responses to MM stimuli reach the same levels of significance in about 2/3 the time compared to the responses to simple AM stimuli. For AM stimuli presented at 50 dB SPL the MASTER technique currently requires between 3 and 6 minutes to obtain significant responses for all eight stimuli, in sleeping adult subjects. Less intense stimuli produce smaller responses, causing recordings for near-threshold stimuli (20 or 30 dB SPL) to require more time before reaching significance. The savings in time obtained by

using MM stimuli can therefore significantly improve testing efficiency.

At about 30 dB SPL the MASTER technique, using AM only stimuli, begins to fail to show significant responses even though subjects can hear the stimuli. In Experiment 6 we were able to estimate the electrophysiological thresholds and found levels close to 30 dB SPL. This fits with data reported previously by Lins et al (1996). These thresholds were 10-15 dB above the behavioral thresholds, both behavioral and electrophysiological recordings being obtained in a quiet room but not one properly sound-attenuated for audiometry. Herdman and Stapells (2000) found electrophysiological thresholds to AM stimuli near 20 dB SPL, again at about 10 dB above behavioral thresholds. Two factors may have accounted for their lower thresholds: their use of a properly sound-attenuated chamber, and their use of 5 dB steps. Because MM stimuli evoke larger responses than AM stimuli even at the near threshold (30 dB SPL) intensity levels, the use of MM stimuli when evaluating thresholds should make the technique more efficient and more accurate. The increases found in adults should also be found in infants since behavioral evidence has suggested that by 4-6 months infants have the ability to process frequency-modulation (Aslin, 1989; Colombo and Horowitz, 1986; Rickards et al, 1994). The hypothesized improvement in the MASTER technique for assessing thresholds in both infants and adults needs to be confirmed.

The MM responses are not always larger than those evoked by 100% AM stimuli. In order for the MM responses to be larger, the relative phase for the FM component of the MM stimulus should be between 270 (-90) and 0 degrees for stimuli between 750 and 4000 Hz. Different phases may be better for the 500 and 6000 Hz stimuli (for example, 35 and -208 respectively). Further study to see how to improve thresholds at these low and high frequencies is probably required. Different phases for the MM as well as different modulation-frequencies might be tested to see what parameters are optimal for the response. As discussed by Cohen et al (1991), a MM stimulus created by aligning the highest frequencies with the maximum amplitude will have its spectrum shifted to the higher frequency region (cf. top of Figure 3-2). This can be compensated in a clinical test by adjusting the carrier-frequency in order to keep the MM stimulus centered on the frequency of interest. However, it should also be noted that using only 20-25% FM the stimuli remain similar to the spectra produced by a 100% AM stimulus.

The IAFM stimuli produced 2 responses for each carrier-frequency. Due to the relative independence of the AM and FM responses we had anticipated that the two IAFM responses might provide a more efficient evaluation of responsiveness than the single response to 100% AM stimuli. However, this does not seem to be the case (Figure 3-13). The evaluation of these responses using the Stouffer method failed to show that this method would be more useful than simply using MM stimuli in creating a more rapid hearing test. A major problem was that the response to the FM component of the IAFM was larger when the AM was 50% than 100%, which produces a smaller AM response. Since the combined detectability of the IAFM responses did not differ significantly from the detectability of the 100% AM response, and since the MM response is more easily detected than the AM response, audiometry is probably best performed using MM stimuli.

A large amount of work with the auditory steady-state responses has examined at how well they can estimate hearing thresholds (e.g. Aoyagi, 1994; Rance et al.,1995; Lins et al., 1996; Herdman and Stapells, 2000). The modulation of a carrier tone provides a signature by which the system's response to the tone can be detected and the stimulus is then decreased in intensity until there is no response. The steady-state responses can also estimate how well the auditory system processes differences in frequency and intensity at supra-threshold intensities. Rather than using a set amount of modulation and decreasing the intensity of the stimulus, we can use a set intensity and decrease the amount of modulation to obtain a detection threshold (or limen) for FM or AM depth. The electrophysiological thresholds for detecting modulation using steady-state responses (Experiment 1) are close to those obtained behaviorally. These findings suggest that these responses to rapid AM and FM may provide useful measurements of frequency and intensity discrimination. Psychophysical studies using slow rates of modulation have found that FM but not AM can be impaired in hearing-impaired individuals (Lacher-Fourgère and Demany, 1998). These findings might also be demonstrable at higher modulation rates using physiological rather than psychophysical measurements. In assessing the suprathreshold discrimination of frequency and intensity, the IAFM technique may be very helpful, since it provides two independent measures of discrimination for each carrier.

The human auditory steady-state response is able to follow at high modulation-frequencies. Rickards and Clark (1984) recorded steady-state responses at modulation-

frequencies up to 450 Hz (although data are only graphed to 130 Hz). We have demonstrated reliable responses in the 160-190 Hz range (see next chapter). The amplitude is smaller than when the modulation-frequency is in the 80 to 100 Hz range but since the noise is also smaller, the responses remain significant. The ability of the auditory system to follow rapid changes in the frequency or amplitude of the sound is assessed psychophysically by means of temporal modulation transfer functions (Viemeister, 1979). These functions are abnormal in patients with sensorineural hearing loss, particularly for higher frequencies of modulation (Bacon and Viemeister, 1985; Formby, 1987). Evaluating the steady-state responses at faster rates may help detect individuals who have problems processing rapid formant-transitions in speech (Tallal et al., 1996). Since the temporal modulation of speech sounds may serve as cues to facilitate the recognition of consonants (Van Tasell et al., 1987; Shannon et al., 1995), it is possible that the ability of the steady-state responses to follow rapid modulation-frequencies may relate to the ability of the auditory system to accurately process speech.

## CONCLUSIONS

MM stimuli may be useful in clinical application of the MASTER technique by evoking larger responses than AM or FM alone at intensities as low as 30 dB SPL. The MM augmentation can be explained by the simple vector averaging of the AM and FM responses, which seem to be generated in largely independent systems. Audiometry using the steady-state responses is therefore best performed using MM stimuli. Stimuli with independent amplitude and frequency-modulation (IAFM) provide two separate responses from each carrier-frequency. They do not yield any better evaluation of threshold than using 100% AM tones, but they may become useful in objectively evaluating suprathreshold discrimination.

# CHAPTER 4

## AUDITORY STEADY-STATE RESPONSES:

## PHASE AND LATENCY MEASUREMENTS

A portion of this material has already appeared in M. S. John and T. W. Picton (2000) *Auditory steady-state responses: phase and latency measurements*. Hearing Research. 141; 57-79. *Reprinted with permission*

Some data, in alternative form, were also presented at the meeting of the Neuroscience Society, Los Angeles, November, 1998, and at the meeting of the International Electric Response Audiometry Study Group in Tromsø, Norway, June, 1999.

## ABSTRACT

Human auditory steady-state responses were recorded to four stimuli, with carrier-frequencies ($f_c$) of 750, 1500, 3000 and 6000 Hz, presented simultaneously at 60 dB SPL. Each carrier-frequency was modulated by a specific modulation-frequency ($f_m$) of 80.6, 85.5, 90.3 or 95.2 Hz. By using four different recording conditions, we obtained responses for all permutations of $f_m$ and $f_c$. The phase delays (P) of the responses were unwrapped and converted to latency (L) using the equation: $L = P/(360*f_m)$. The number of cycles of the stimulus that occurred prior to the recorded response was estimated by analyzing the effect of modulation-frequency on the responses. These calculations provided latencies of 20.7, 17.7, 16.1 and 16.1 ms for carrier-frequencies 750, 1500, 3000 and 6000 Hz. The latency-difference of about 4.5 ms, which exists between low and high carrier-frequencies, was also obtained when stimuli were presented with at faster modulation rates (160-180 Hz), both monaurally and binaurally, at different intensities, alone or in conjunction with other stimuli, and using modulation-frequencies that were separated by as little as 0.24 Hz. This frequency-related delay is greater than that measured using transient evoked potentials because of differences in how response-latencies are determined. Combining the latencies for steady-state responses with the latencies for oto-acoustic emissions might provide estimates for both transport-time and filter build-up in the human cochlea.

## INTRODUCTION

Physiological responses to auditory stimuli of high frequency generally occur at earlier latencies than responses to stimuli of low frequency. One reason for this is that auditory stimuli initiate a "traveling wave" in the basilar membrane of the cochlea (Von Békésy, 1960). This traveling wave distributes high frequencies of sound to the regions of the basilar membrane near the stapes and low frequencies to the regions near the apex of the cochlea. As well as thus mediating a frequency-to-place coding in the auditory system, the travelling wave also involves a delay since time is taken to move along the basilar membrane. This frequency-related delay or "transport-time" is the subject of some controversy (Dancer, 1992), although most evidence suggests that the delay is in the millisecond range, increases exponentially with increasing distance along the basilar membrane, and depends upon the passive properties of the basilar membrane being equivalent for living and dead preparations (Ruggero, 1994).

Another reason for frequency-related delays in the neurophysiological responses is the filtering that occurs during the transduction of the acoustic energy in the stimulus to electrical impulses in the auditory nerve fibers (Eggermont, 1979a). The more sharply a filter is tuned, the longer it takes for the output of the filter to reach maximum amplitude. Since the neural response is delayed by some fraction of this rise-time, the neural latency has a "filter-delay" added to the delay due to the travelling wave. The filter-related delay varies inversely with the frequency to which the filter is tuned. In the normal cochlea both the transport-time and the filter-delay (often considered together as the "travelling wave delay") contribute to the frequency-related delays of the physiological responses.

The latencies obtained from physiological measurements are sometimes converted to "traveling wave velocities" (e.g., Parker and Thornton, 1978; Kim et al., 1994) on the basis of the normal length of the basilar membrane and the hypothesized normal locations of frequency-specific regions on this membrane (von Békésy, 1963). Since the length of the human basilar membrane varies from subject to subject, for example being longer for males than females (Sato et al., 1991), and since the exact locations of the different frequency-regions on this membrane are not accurately known, it seems more valuable to report latencies rather than hypothetical velocities. In human subjects, these latencies can be measured using oto-acoustic emissions or evoked potentials.

Oto-acoustic emissions are small acoustic signals generated in the hair cells as they participate in the active filtering process of cochlea. The movements of the hair cells generate acoustic energy which is transmitted back along the basilar membrane and out through the middle ear to the ear canal. Several studies of human oto-acoustic emissions have shown delays of approximately 8 ms between 10 kHz and 1 kHz (Kimberley et al., 1993; O'Mahoney and Kemp, 1995; Bowman et al., 1997). Since the delay for the oto-acoustic emission represents an acoustical round trip, one half of the delay is usually taken to measure the travelling wave delay.

Recording auditory nerve action potentials or auditory brainstem responses can also provide a measure of the travelling wave delay. The auditory nerve responses contain an additional delay in the synapse between the inner hair cell and the afferent fiber. The auditory brainstem responses are affected by both this delay and a conduction delay between the auditory nerve and the generator of the response in the brainstem. Responses specific to particular regions of the cochlea can be obtained using clicks and derived-band masking (e.g., Don and Eggermont, 1978) or brief tones and notched noise masking (e.g., Picton et al., 1979). Frequency-related delays in the responses from the cochlear nerve and auditory brainstem are similar to those obtained with oto-acoustic emissions (Neely et al., 1988; Eggermont et al., 1996), indicating that the synaptic and conduction delays that occur between the cochlea and the generator of the brainstem response are not significantly affected by the frequency of the sound.

Auditory steady-state responses offer several advantages over transient evoked potentials (Galambos et al., 1981; Stapells et al., 1984). Auditory steady-state responses evoked by the sinusoidal modulation of the amplitude of a tone contain energy only at the carrier-frequency and sidebands separated from the carrier by the frequency of modulation. These responses are more frequency-specific than the responses to transient stimuli which show a broad smearing of frequencies. Another advantage is that multiple steady-state responses can be evaluated simultaneously, provided each stimulus has a different modulating frequency. The separate responses are then measured in the frequency domain at the frequencies equal to the different modulating frequencies (Lins and Picton, 1995).

A steady-state response is characterized by its amplitude and phase. Even though the phase data are always available, most experiments have focused only on amplitude. The most

frequent measurement of phase calculates "phase coherence" (Fridman et al., 1984; Stapells et al., 1987; Dobie and Wilson, 1993; Rance et al., 1995): a response is considered reliable if its phase remains stable over time rather than varying randomly. Phase is not much used otherwise, probably because of ambiguities inherent in its measurements. The first ambiguity derives from the fact that phase is a circular rather than linear measurement (Fisher, 1993). When phase crosses an upper or lower limit (e.g. from 359° to 0°), the discontinuities in the measurement make normal linear calculations inappropriate. For example, the average of two measurements with phases of 359° and 1° is 0° rather than 180°. The second ambiguity is due to the steady-state nature of the response. It is impossible, from one measurement, to determine how many cycles occurred between the stimulus and the measured evoked steady-state response. A delay equivalent to one, two or more cycles of the modulation-frequency might have intervened between the stimulus and the response. One approach to this ambiguity is the measurement of "apparent latency" (the slope of the phase versus frequency plot) introduced by (Regan, 1966). In the literature on auditory physiology, apparent latency is described as "group delay" (Goldstein et al., 1971) and has been used to measure the latency of the motion of the basilar membrane (Patuzzi, 1996), the cochlear microphonic (Dallos and Cheatham, 1971), the oto-acoustic emissions (Kimberley et al., 1993; Schneider, 1999), and the discharge of auditory nerve fibers (Gummer and Johnstone, 1984; Joris and Yin, 1992).

This chapter examines the phases of auditory steady-state responses to discover if they relate to the acoustic frequencies of the eliciting stimuli in an orderly and stable manner. If these phases can be sensibly converted into latencies, and if these latencies are related to frequency-related delays in the cochlea, then auditory steady-state responses might be useful in assessing travelling wave delays in normal and pathological ears. We used auditory steady-state responses evoked by tones modulated at rates greater than 75 Hz. As stated in previous chapters, since these can be reliably recorded in infants (Rickards et al., 1994; Lins et al., 1996) and since they do not change significantly with sleep (Cohen et al., 1991; Lins and Picton, 1995), these rapid steady-state responses are clinically more useful than the slower 40 Hz responses.

## METHODS

### Subjects

The 34 subjects (13 female) participating in these experiments were volunteers obtained

from laboratory personnel, colleagues, and friends. Their ages ranged between 15 and 36 years. All subjects were screened for normal hearing for pure tones (range 500-6000 Hz) at 20 dB HL. During the recordings the subjects lay in a comfortable reclining chair inside a quiet room. Subjects were encouraged to relax and fall asleep during the recordings in order to reduce the background noise levels in the EEG. Most subjects slept for the entire recording period. Eight subjects participated in Experiments 1 and 2. Six of the eight subjects in Experiment 2, had also been subjects in Experiment 1. Experiment 3 was performed concurrently with Experiments 1 and 2 and used the same subjects. Experiment 4 (10 subjects) and Experiment 5 (8 subjects) used data that had been recorded for the experiments discussed in Chapter 1. Experiment 6 evaluated the replicability of the results in 6 of the 8 subjects who had been studied in Experiment 5. In experiment 7, we increased the number of subjects to 16 (8 female) since we wanted to explore male/female differences. These experiments with human subjects, which formed part of a larger research project on "Evoked Potentials Audiometry", were approved by the Research Ethics Committee of the Baycrest Centre for Geriatric Care.

Auditory Stimuli

The stimuli were generated digitally and converted to analog form with 12-bit resolution. The digital-to-analog (DA) conversion was based on a 4 MHz clock and occurred at a rate of once every 100 clock ticks (0.025 ms) or 40 kHz (this was faster than the rate used in Chapter 1 due to the use of 6 kHz stimuli, which made a faster DA rate preferable). The analog waveforms were then low-pass filtered (48 dB/octave) at 10 kHz to remove digitization noise and high-pass filtered at 250 Hz to remove any possible electrical artifact at the modulating frequencies. The stimuli were amplified to a calibration-intensity and then attenuated to achieve the desired dB level. In Experiments 4-7, the stimuli were presented to the subject through an Eartone$^{TM}$ 3A insert earphone placed in the right ear. The stimuli were calibrated using a Brüel and Kjaer Model 2230 Sound Level Meter with a DB 0138 2-cm$^2$ coupler. For Experiment 1 to 3, TDH-50P headphones were used and calibration was performed using a Brüel and Kjaer Artificial Ear Type 4152. Both the ear inserts and the headphones show a relatively flat (±3 dB) intensity response for stimuli of 4000 Hz and below. Stimuli of 6000 Hz were reduced by 20 dB for the ear insert and by 5 dB for the headphone. (This large change in acoustic energy will be addressed

in the discussion.)

Each amplitude-modulated (AM) stimulus was created by multiplying together two sine waves, according to the formula and methods described in Chapter 1. As in Chapter 1, the stimuli for multiple stimulation were formed by summing the individual amplitude-modulated stimuli (Lins et al., 1995). We have described these signals in both the time and frequency domains (see Chapter 1, *Auditory Stimuli*).

The frequencies of both the carrier and modulation signals were adjusted so that an integer number of cycles occurred within each recording section (usually lasting 409.6 ms). This allowed the individual sections to be linked together without acoustic artifact and to be interchangeable during artifact rejection (see Chapter 2, *section 5.5*). As should now be apparent, a carrier-frequency of 1000 Hz was adjusted to 1000.98 Hz so that 410 complete cycles occurred within each section, and a modulation-frequency of 81 Hz was adjusted to 80.566 Hz so that 33 cycles occurred within a section. For simplicity, carrier-frequencies will be henceforth expressed to the closest 10 Hz and the modulation-frequencies with only one digit after the decimal point. Since we have found that the amplitudes of the individual responses are not significantly affected when adjacent carrier-frequencies are 1 octave apart (see Chapter 1, *Table 1-1*), the experiments used tone combinations having octave separations such as 750, 1500, 3000, and 6000 Hz (750 octave series), or 500, 1000, 2000, and 4000 Hz (500 octave series).

*Please see next page for figure.*

**Figure 4-1. Human auditory steady-state responses.** This figure presents the data from a single subject in one of the conditions of Experiment 1. Four tones were simultaneously presented. Each tone had its own specific carrier-frequency and modulation-frequency as shown at the top of the figure. The bottom section of the figure displays the amplitude spectrum of the averaged response up to 200 Hz. EEG alpha band activity and potentials related to movement and eye-blinks appear in the lower spectral frequency region. The peak indicated with the asterisk represents line noise at 60 Hz. The four peaks indicated with the filled triangles occur at the modulation-frequencies of the stimuli and represent the responses specific to each of the four simultaneously presented stimuli. The unfilled triangles point to responses that represent the second harmonics of these responses, which were particularly evident in this subject. Polar plots of the responses at the modulation-frequencies are shown in the center of the figure. The circles represent the $p<0.05$ confidence limits of the noise in the adjacent frequency bins. For this figure the phase angles of the polar plots have been rotated to compensate for the phase delays caused by the amplifiers and the 90° shift caused by the stimulus being coded sinusoidally and the onset phase of the response being measured as a cosine.

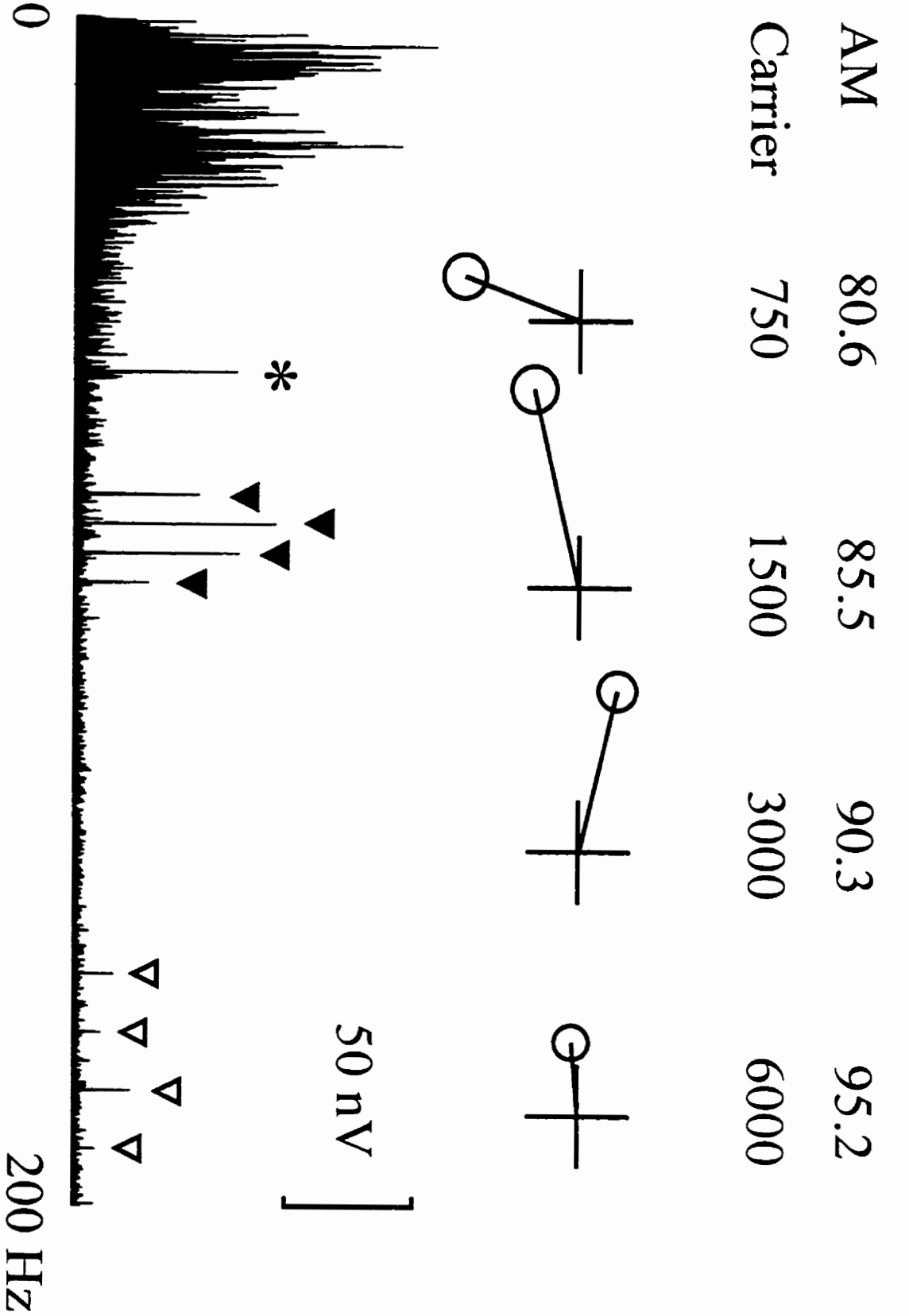
AM
80.6
85.5
90.3
95.2
Carrier
750
1500
3000
6000
0
200 Hz
50 nV

Recording

Gold-plated recording electrodes were placed at the vertex and at the posterior midline of the neck just below the hair line (7-8 cm below the inion). The ground electrode was placed on the right side of the neck. The skin beneath the electrodes was abraded to ensure that inter-electrode impedances were below 5 kOhm at 10 Hz. Electroencephalographic (EEG) signals were collected using a bandpass of 10 to 300 Hz (6dB/octave).

The timing for the analog-to-digital (AD) conversion was based on the same 4 MHz clock as controlled the DA conversion. Digitization of the EEG occurred every 3200 ticks of the clock (0.8 ms) at a rate of 1250 Hz (exactly 1/32 the rate of DA conversion).

Recordings continued over multiple sweeps each lasting 6.5536 seconds (8192 time-points). Averaging was performed over 64 sweeps. Each recording sweep consisted of 16 sections each lasting 409.6 ms. In order to allow reasonable artifact-rejection, a section (rather than an entire sweep) was rejected if the section contained any potentials with amplitudes greater than ±40 μV. If a section was rejected, that part of the recording sweep was filled in with the next recorded data. Between 0 and 20% of the sections were rejected. Each recording lasted from 7 to 8 minutes, depending on the number of rejections. Figure 4-1 shows data recorded from a typical subject.

The preceding details describe the recording setup for all experiments except the last (Experiment 7). This experiment used the newer MASTER system (Chapter 2) with the following settings: an AD conversion rate of 500 Hz, a section size of 2048 points, and 4 sections per sweep yielding a sweep duration of 16.384 seconds. The modulation-frequencies were chosen so that the numbers of cycles within a section (4.096 seconds) were adjacent integers (e.g., 328, 329, 330 and 331 giving modulation-frequencies of 80.078, 80.322, 80.566, and 80.811 Hz).

Amplitude and Phase Measurements

Responses were initially analyzed by averaging together the recorded sweeps in the time-domain. The resultant 6.5536-second (8192-timepoint) averaged sweep was then transformed into the frequency domain using a Fast Fourier Transform (FFT). The specific frequencies available from the FFT are integer multiples of the **1/(Nt)** resolution of the FFT where **N** is the number of time-points and **t** is the time per timepoint. For Experiments 1 to 6, the resolution of the FFT spectrum was 0.1526 Hz, and the resultant spectrum spanned from zero to 4096 times this amount or 625 Hz. (For Experiment 7 the resolution was 0.061 Hz)

For each frequency represented in the FFT spectrum, the X-Y (or real and imaginary) coordinates are then commonly transformed into polar coordinates as amplitude and phase. The amplitude is the length of the vector ($\sqrt{X^2 + Y^2}$) and the phase is the rotation of the vector in relation to the X axis as calculated by arctan (Y/X). All phase measurements were expressed in terms of degrees rather than radians. When combining values across subjects, vector averaging procedures were used: each data point was represented as X and Y, averaging was performed separately for the X and Y values, and the average X and Y values were then used to calculate the average amplitude and phase. In order to ensure that each subject contributed equally to the phase measurements, the data were normalized to unit amplitude before vector averaging.

Signal-to-Noise Assessments

As in the previous Chapters, the presence or absence of a response was assessed by an F-ratio (Zurek, 1992; Dobie and Wilson, 1996; Lins et al., 1996; Valdes et al., 1997), computed on the ratio between the power measured at the signal frequency and the average power in the neighboring frequency-bins. We again estimated the noise levels using 120 frequency measurements - 60 above and 60 below the signal frequency (i.e., about 10 Hz on each side of the signal for experiments 1-6). When using the multiple-stimulus technique those frequencies at which another signal is present were, of course, excluded from this calculation. For the data reported in this Chapter, 91% of the responses reached the $p<0.001$ level of significance and only

4% did not reach the $p<0.05$ level . Most of the responses that did not reach significance were evoked by the low carrier-frequencies (500 or 750 Hz). The data which did not reach significance were still included in the combined measurements, since we were interested in how well the results represented normal findings (noisy though they might be).

Experimental Design

**Experiment 1. Monaural Stimulation 80-100 Hz:** In this experiment we used a 750 Hz octave series of carrier-frequencies and four different modulation-frequencies in the 80-100 Hz range (80.6, 85.5, 90.3 and 95.2 Hz). The four different carrier-frequencies were presented simultaneously with each being modulated by a different modulation-frequency. Four separate recording conditions allowed us to measure the responses to each carrier-frequency as modulated by each of the modulating frequencies.

**Experiment 2. Monaural Stimulation 150-190 Hz:** This experiment was the same as Experiment 1 except modulation-frequencies in the 150 to 180 Hz range were used (158.7, 168.5, 178.2, and 187.9 Hz). Six of the eight subjects were the same as in Experiment 1.

**Experiment 3. Dichotic Stimulation:** Experiments 1 and 2 each had two additional conditions in which stimuli were presented dichotically. In the first dichotic testing condition a 500 Hz octave series was presented to the left ear using modulation-frequencies of 78.1, 83.0, 87.9, and 92.8 Hz (153.8, 163.6, 173.34, and 183.11 Hz in Experiment 2) while a 750 Hz octave series was presented to the right ear using modulation-frequencies of 80.5, 85.4, 90.3, and 95.2 Hz (158.7, 168.5, 178.2, and 187.9 Hz in Experiment 2). Similar to the monaural conditions, in the dichotic 500 and 750 conditions the adjacent modulation-frequencies differed by about 5 Hz in each ear. In the second dichotic testing condition, these stimuli were presented to the opposite ears. Hence, in each dichotic condition, eight stimuli were simultaneously presented to a subject.

**Experiment 4. Effects of Intensity:** Since latency increases with decreasing intensity occur with transient evoked potentials, we examined the effects of intensity on phase using a 500

Hz octave series modulated in the 80 Hz range which was presented at both 35 and 75 dB SPL. This experiment was described in Chapter 1 although the phase data were not examined.

**Experiment 5. Effects of Multiple Stimuli:** This experiment examined the changes in latency that might be caused by presenting several tones simultaneously, rather than separately, as has been previously done. Responses to a single 1000 Hz tone or a single 2000 Hz tone modulated in the 80 Hz range served as baseline measurements. These tones were then simultaneously presented with other tones in several conditions: two tones (the 1000 Hz and 2000 Hz tones together), four tones in one ear separated by one octave, four tones in one ear separated by one-half octave, and eight tones in one ear separated by one-half octave. Similar to Experiment 4, the amplitude data from this experiment were from the experiments described in Chapter 1

**Experiment 6. Stability Over Time:** In order to assess the stability of steady-state phase, 6 subjects were recorded at two separate times, 3 to 4 weeks apart, using the 750 Hz octave series at both the 80-100 Hz and 150-190 Hz modulation rates. (The first recording session was the same as that in Experiments 1 and 2).

**Experiment 7. Small Differences in Modulation-frequency**. In Experiments 1 through 6 we attempted to compensate for using different modulation-rates for each carrier. The effects of modulation-rate can be somewhat removed by a method which uses roughly identical modulation-rates for all the carriers being tested. In this experiment we used modulation-rates that were separated by only 0.244 Hz rather than the approximately 5 Hz used in the previous experiments. The was accomplished by increasing the sweep length in order to obtain 0.061 Hz resolution in the amplitude spectrum. The increased resolution caused adjacent modulation-frequencies to be separated by 3 other bins in the amplitude spectrum. A baseline, using only the 1500 Hz carrier-frequency (modulated at 80.322 or 160.156 Hz), was recorded in order to compare this response to that obtained using multiple stimuli with very small differences between adjacent modulation-frequencies. Condition 1 of this experiment used modulation-rates

in the 80 Hz range (750 Hz modulated at 80.078, 1500 Hz at 80.322 Hz, 3000 Hz at 80.566, and 6000 Hz at 80.811). Condition 2 used modulation-rates in the 160 Hz range (159.912, 160.156, 160.400, 160.645 Hz). Eight male and eight female subjects participated in this experiment.

Statistical Evaluations

The main analyses concerned changes in the latency or phase of the responses which occurred due to the experimental manipulations. *Prior to analysis, the measured data were arranged so that the rows of the data set corresponded to a carrier-frequency and the columns corresponded to modulation rate.* The statistical significance of the results was assessed by repeated-measures analyses of variance (ANOVA) with Greenhouse-Geisser corrections when appropriate (SPSS version 7.5). Because many of the post-hoc comparisons which occurred in a single experiment were independent we again chose to use the Fisher Least Significant Difference (LSD) test (GB-STAT version 5.0). Differences were considered significant at the $p<0.05$ level.

Converting Phase to Latency

The recorded phase measurements were adjusted in several steps in order to remove delays introduced into the recordings by the equipment that generated the stimuli and recorded the responses. First, there were small delays caused by the 250-Hz high-pass filter that was used to prevent possible contamination of the stimulus with energy at the modulation-frequencies. This delay varied with modulation-frequency. Second, there was an acoustic delay of about 0.9 ms, which varied slightly with carrier-frequency, in the tube connecting the speaker with the ear-insert. These time delays were originally measured in milliseconds, using the acoustic calibration equipment, and converted into phase by multiplying by 360 and then dividing by the period of the modulation-frequency. Third, the recording amplifiers caused changes in phase which could be measured by recording the response of the amplifier to a calibration-signal at the modulation-frequency. Fourth, the measured phase was then adjusted by 90° since the amplitude spectrum was computed in terms of cosine phase, whereas the stimulus was modulated using a

sine function.

These final phase values (θ) were converted into phase delay (Rodriguez et al., 1986) using the equation:

$$P=360-\theta \qquad (1)$$

Phase delay is more easily comprehensible than the onset phase, since it gets larger as the time of the response moves further away from the stimulus. The phase delays were maintained within the 0-360° limits by adding or subtracting 360 from measurements below or above this range, respectively.

Phase delay (**P**) can be converted to latency (**L**) according to the formula:

$$L=P/(360*f_m) \qquad (2)$$

This is equivalent to multiplying the period of a full cycle ($1/f_m$) by the fraction of the cycle (**P/360**) represented by the phase delay. Since this does not take into account two ambiguities in the measurements, the formula was adapted to:

$$L=(P+n*360+m*360)/(360*f_m) \qquad (3)$$

where **n** and **m** are integers selected to resolve the ambiguities associated with phase measurements.

The first ambiguity occurs because of the circularity of the phase measurement. When phase increases 1°, from 360° to 1°, the numerical measurement abruptly changes by 359°. This can be compensated for by "unwrapping" the measurements (which have been bundled together in one cycle) and allowing the measurements to enter an adjacent cycle when they cross a cycle boundary. This ambiguity is illustrated diagrammatically in the upper section of Figure 4-2. Figure 4-3 shows the ambiguity in real data measuring the phase delays for a 750 Hz carrier modulated at different frequencies for 8 subjects. The phase delay increases as the modulation-frequency increases and, in the original phase values of four of the subjects, the phase jumped

*Please see next page for figure.*

**Figure 4-2: Ambiguities in the measurement of phase.** The upper half of the figure shows the ambiguities that occur because phase is a circular rather than linear measurement. If the phase increases as some other parameter is varied, it may exceed 360° and revert to 0°, causing a sudden fall in the regularly increasing measurements. This can be handled by "unwrapping" the measurements by adding 360° (up-going arrow in the upper right section of the figure). The bottom half of the figure illustrates the ambiguities that occur because the response is recorded in steady-state. The cosine onset-phase of the response recorded in the second line was measured as 150°. Phase delay is measured as the phase difference from the stimulus waveform (onset at 0° cosine) to the same part of the response waveform. This is equivalent to 360° minus the measured phase or 210°. Translated to latency, this is 210/(360*100) or 5.8 ms. Unfortunately there is no way of knowing whether that 0° point of the ongoing stimulus is evoking that part of the response or the same part occurring one or two cycles later (at latencies 15.8 or 25.8 ms for 570° and 930° phase delays). If we record the response at another stimulus rate (and if we can assume that the response has the same latency for the two rates), then we can determine which of the possibilities is most likely. At 85 Hz the phase delay was 130°. This gives a latencies of 4.2, 16.0 and 27.8 ms. The measurements of 15.8 and 16.0 ms are the most similar between the two stimulus rates. An "apparent latency" can also be calculated from the slope of the phase with stimulus frequency divided by 360. For these measurements, this latency is 80/(15*360) or 14.8 ms.

# Circular Ambiguities

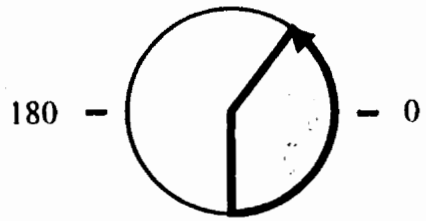


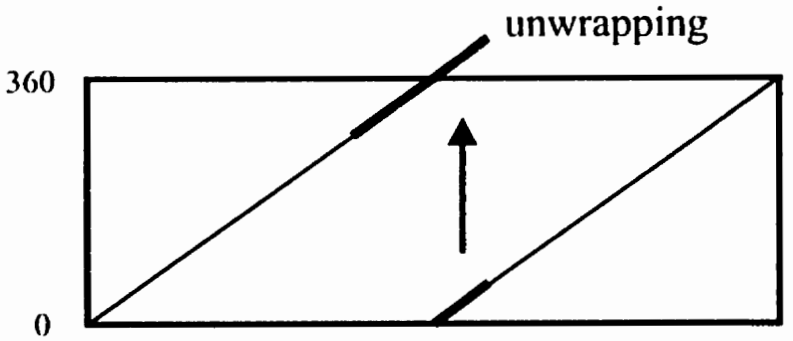


# Steady-State Ambiguities

Delay may include an unknown number of preceding cycles

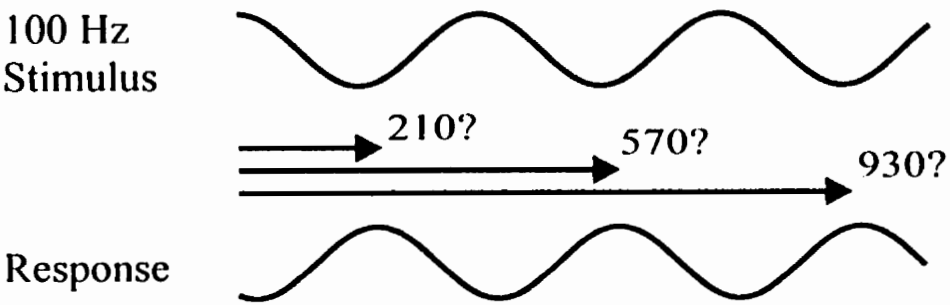


Responses at different stimulus rates help determine this number

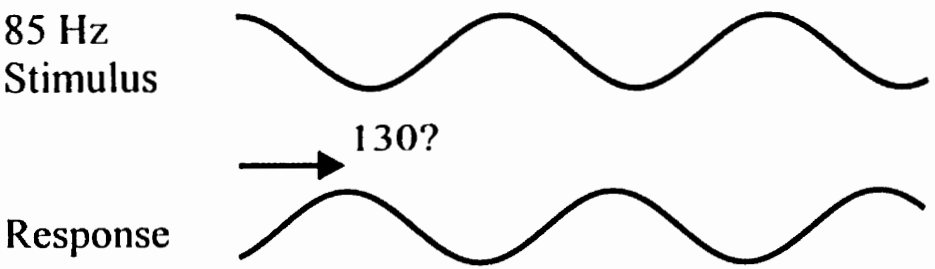

*Please see next page for figure.*

**Figure 4-3: Unwrapping of phase.** This figure shows the phase of the response to the 750 Hz tone at different modulation-frequencies in all 8 subjects studied in Experiment 1. The original measurements of phase delays were limited to the range 0-360°. In 4 of the subjects this caused a large discontinuities in the course of the lines graphs (dashed lines). These were compensated by adding 360° to the aberrant measurements. For example, in the subject identified using the circles the phase delay jumped from 310° at 85.5 Hz to 14° at 90.3 Hz and then continued to increase to 36° at 95.2 Hz. The latter two measurements were unwrapped to 374° and 396°. The figure also illustrates the inter-subject variability in the measurements.

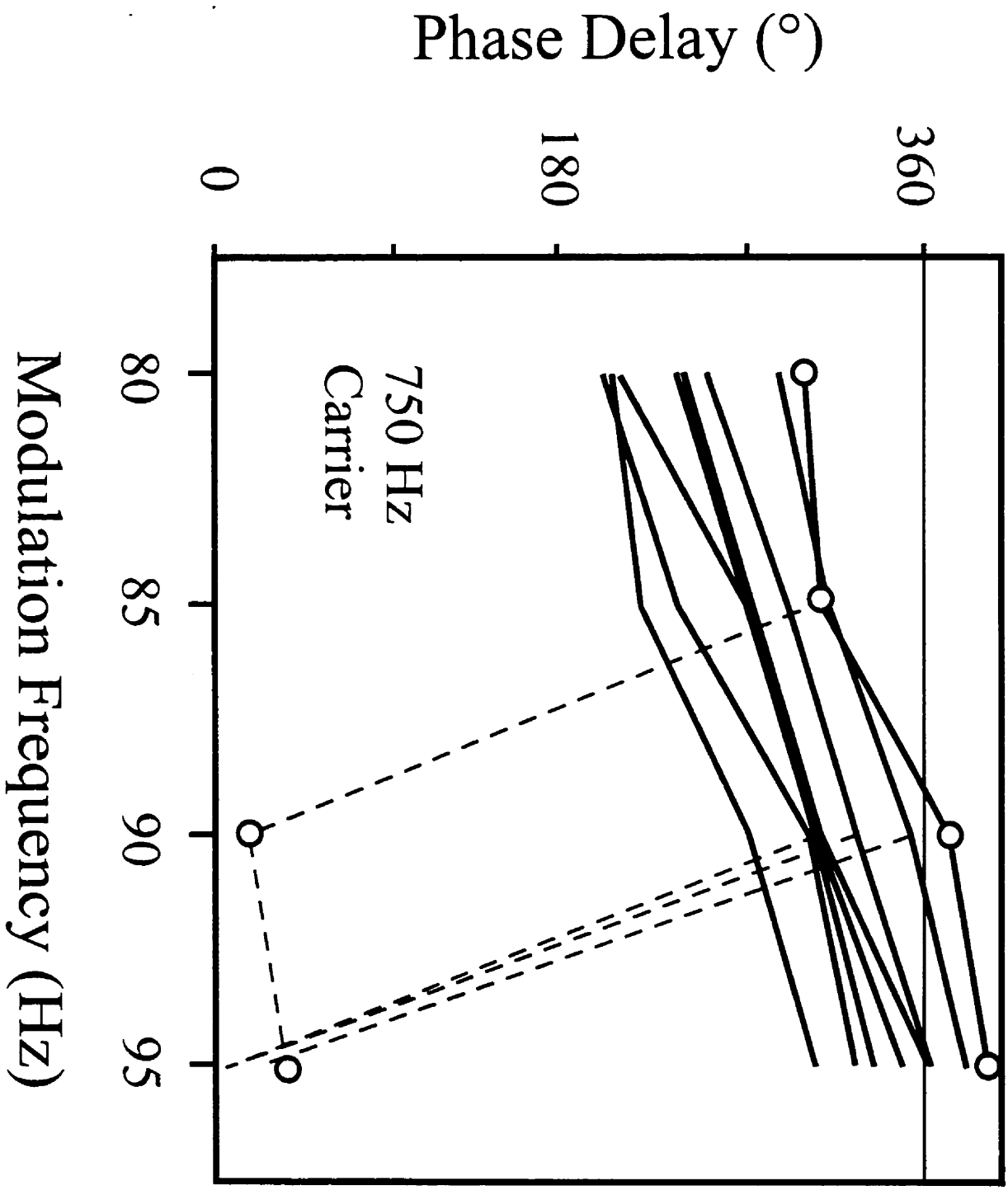
Phase Delay (°)
0
180
360
Modulation Frequency (Hz)
80
85
90
95
750 Hz
Carrier

back to values close to zero (dashed lines). These values are not far apart from the other values (between 270° and 360°) in terms of circular phase. This ambiguity can be removed by adding 360° to those measurements that were more than 180° lower than adjacent measurements (in formula (3) **n** is set to 1). We are effectively proposing that a delay corresponding to a full cycle of the modulation-frequency occurs before the measured responses in these subjects.

The second ambiguity arises from the steady-state nature of the response. Because the responses are the same from cycle to cycle, the number of cycles of the stimulus that might have occurred before the measured response is uncertain. The bottom section of Figure 4-2 illustrates this ambiguity. This ambiguity can be resolved by measuring the response phase when the same carrier-frequency (and, therefore, probably the same traveling wave latency) is modulated by several different modulation-frequencies (each in their own recording session). This is illustrated by the data graphed in Figure 4-4, which shows the effects of modulation-frequency on the responses at different carrier-frequencies. For a carrier-frequency of 1500 Hz the phase delay was 152° at a modulation-frequency of 80.6 Hz, and 245° at 95.2 Hz (open circles in left graph of Figure 4-4). If phase delays were directly converted into latencies according to formula (2) then latencies of 5.2 and 7.2 ms would be obtained since the period is 12.4 ms for an 80.6 Hz signal and 10.5 ms for a 95.2 Hz signal. The 2.0 ms difference is similar to the difference between the periods of the two modulation-frequencies (12.4-10.5=1.9 ms). If we therefore propose that a delay equivalent to one full cycle occurred before the cycle being measured (**m**=1 in formula (3)) the latencies become 17.6 ms (12.4 +5.2) and 17.7 ms (10.5 +7.2). The measurements are closer than with no preceding cycles and closer than what would be obtained if we postulated two preceding cycles (**m**=2), which would give latencies of 30.0 and 28.2 ms.

We based the choice of **m** on the goodness of fit of the collected data when multiple modulation-frequencies were used with the different carrier-frequencies. This is illustrated in Figure 4-5. The left graph assumes that no preceding cycles have occurred before the response. There are significant effects of both carrier-frequency and modulation-frequency. The middle graph shows the results of adding a cycle (**m**=1) to the data shown in the upper graph. In this graph, the different modulation rates yield approximately equivalent estimates of latency. As can be seen in the right graph, adding a further cycle (**m**=2) cause the data to diverge again with a significant effect of modulation-frequency. Once **m** has been decided on the basis of these

results, **m** can be applied to responses recorded using only one modulation-frequency for each carrier-frequency (e.g., Experiment 3). An ambiguity might arise if there is no clear difference in the effect of modulation-frequency for two adjacent values of **m**.

This approach is related to the "apparent latency" calculated by dividing the slope of phase-delay versus stimulus-frequency by 360 (Regan, 1966; Regan, 1989; van der Tweel and Verduyn Lunel, 1965). In this particular example, the apparent latency of the two responses to 1500 Hz carriers is (245-152)/(360*(95.2-80.6)) or 17.7 ms. A graphic way of calculating this measurement was proposed by (Diamond, 1977). The equivalence of these different measurements of latency is documented in Appendix B. In the auditory literature, apparent latency is equivalent to "group delay" (Goldstein et al., 1971).

Unfortunately, it is often difficult to interpret apparent latency since the phase shifts occurring in physiological filters are difficult to characterize (Bijl and Veringa, 1985) and the actual relation of apparent latency to physiological delay is not clear (Hari et al., 1989). A major problem occurs when the physiological response shows filter effects along the dimension of the modulation-frequency. The physiological system may only respond to a band of modulation-frequencies or may respond less to higher modulation-frequencies. A first order low-pass filter will show a phase shift equal to $\arctan(f_m/f_0)$ where $f_0$ is the cut-off frequency of the filter (Brown et al., 1982). It might be possible to estimate the effect of such filtering on the responses from the amplitudes of the responses at the different modulation-frequencies, and then compensate the phase measurements prior to latency calculations (Regan, 1989, pp29-30). We performed these calculations for our data based on estimated phase shifts of about 90° per octave, but these did not significantly alter the results. Another approach is to eliminate these effects by considering data (for different carrier-frequencies) only at one modulation-frequency. This can be done with multiple measurements (data from Experiments 1 and 2), or by using modulation-frequencies so close together that any effect of modulation-frequency would be negligible (Experiment 7).

*Please see next page for figure.*

**Figure 4-4 Phase-frequency plots.** This figure shows the average data from Experiments 1 and 2. As can be seen in the graphs the phase delay increases regularly with increasing modulation-frequency with a slope that increases with decreasing carrier-frequency. This slope can be used to estimate "apparent latency" or "group delay".

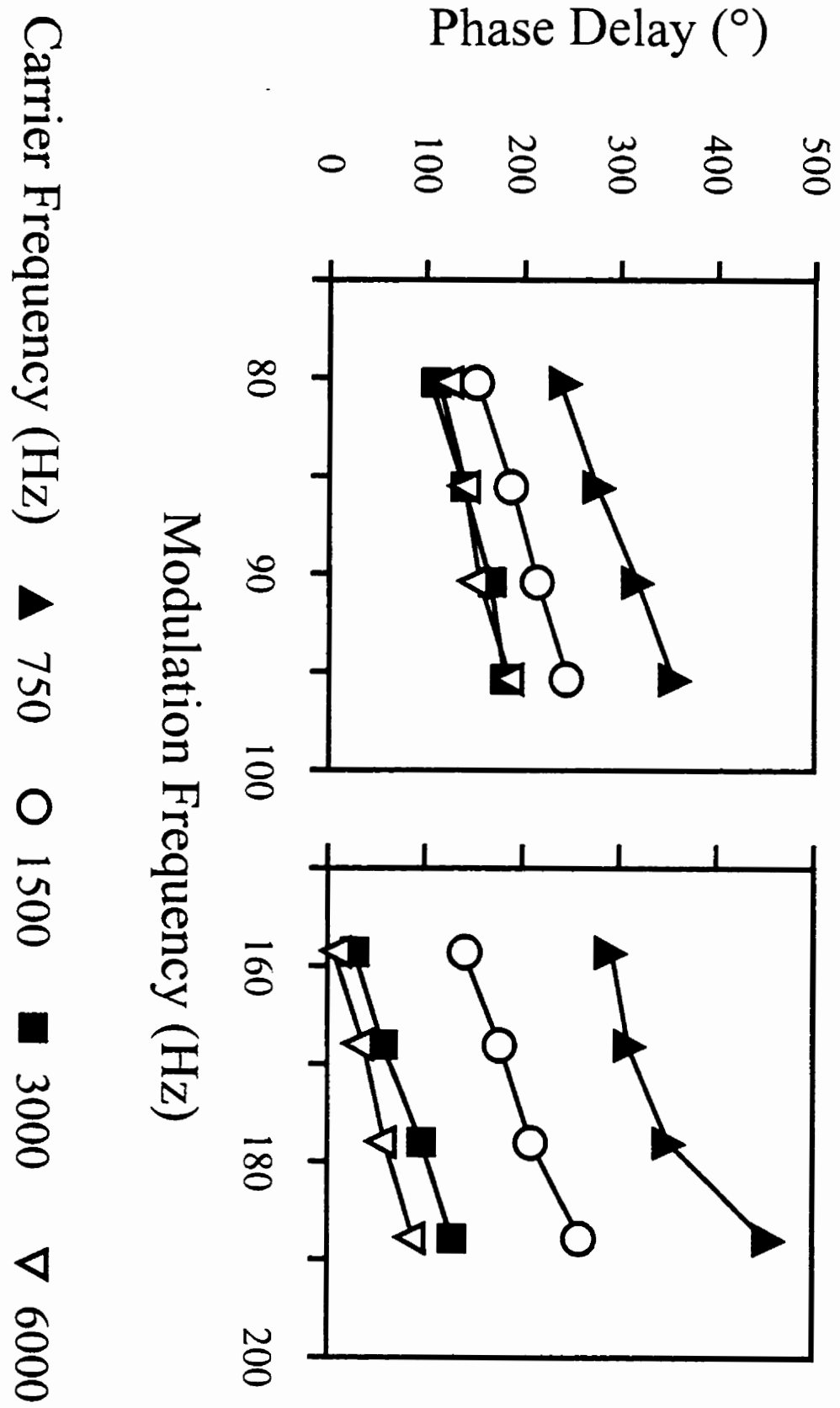
Phase Delay (°)
0
100
200
300
400
500
80
90
100
160
180
200
Modulation Frequency (Hz)
Carrier Frequency (Hz) ▲ 750 ○ 1500 ■ 3000 ▽ 6000

*Please see next page for figure.*

**Figure 4-5: Preceding cycles (80-100 Hz).** This figure illustrates a method by which the number of cycles preceding the recorded response can be estimated. The phase delay is converted to latency and then the actual latency from the stimulus is calculated by adding an integer number (m) of cycles of modulation to the estimated latency. Since carrier-frequencies are what should determine the delays in the cochlea, different modulation-frequencies should result in the same latency estimate. As can be seen in the figure, the delays related to each carrier-frequency are most consistent across the different experimental conditions when **m**=1.

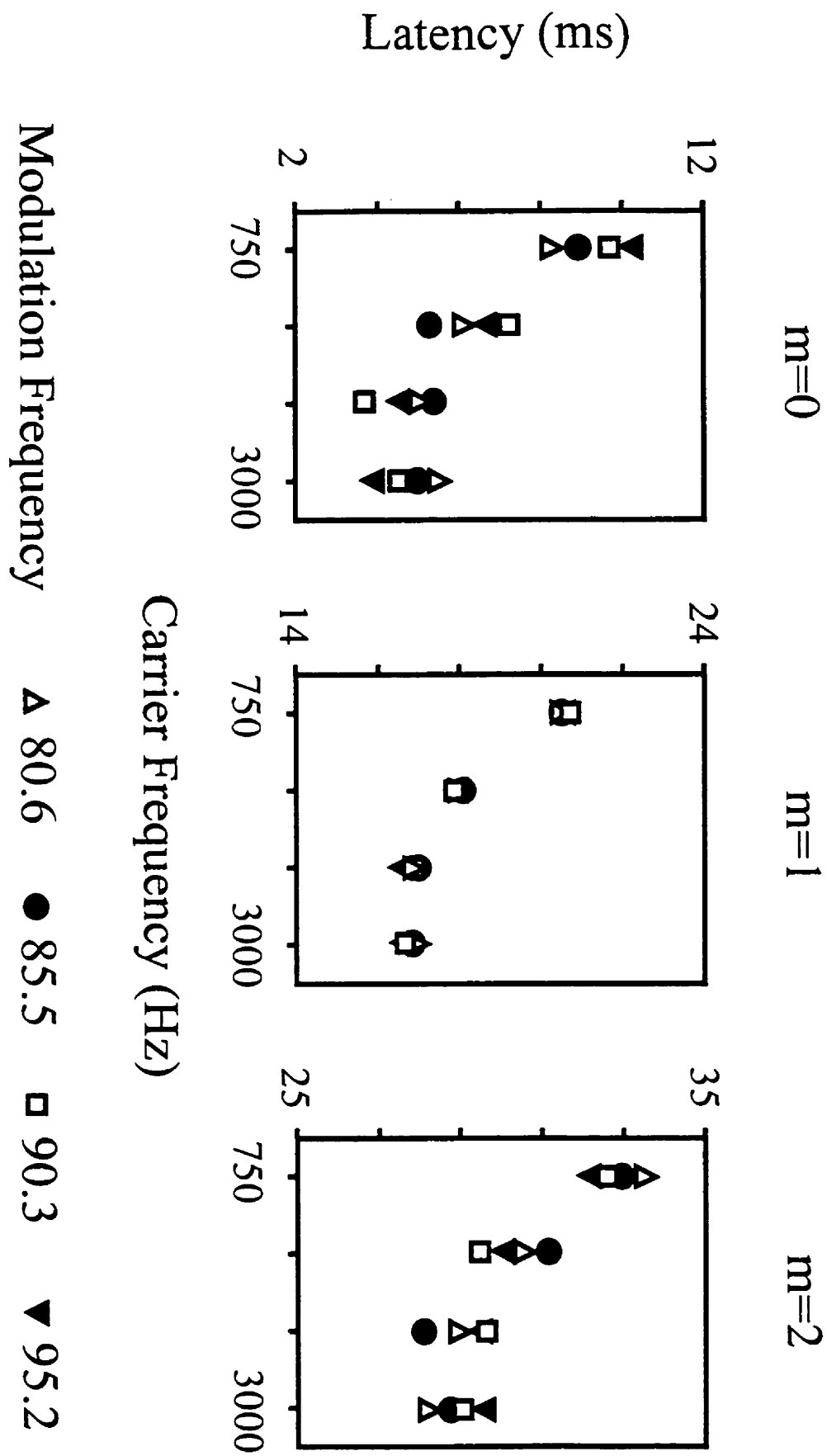
Latency (ms)
m=0
m=1
m=2
12
2
24
14
35
25
750
3000
Carrier Frequency (Hz)
Modulation Frequency
Δ 80.6
● 85.5
□ 90.3
▼ 95.2

## MODELING

Some simple modeling was undertaken to determine how the measured latencies might occur on the basis of known physiological processes. A MATLAB program was constructed to imitate the effects of four processes. First, the filtering that occurs at the level of the hair cells was modeled as a gammatone filter using the parameters from (Patterson, 1994), see also (Glasberg and Moore, 1990). Second, the filtered signal was rectified. For simplicity and since we were not interested in the effects of different intensities, no compression (e.g. Corey and Hudspeth, 1983; Dallos, 1985) was used in the rectification. Third, we modeled the refractoriness of the auditory nerve fiber discharges using the equations of Carney (1993; see also Eggermont, 1985) and parameters approximately equivalent to those recommended in that paper (an absolute refractory period of 1 ms and then a double exponential return with time constants of 1 and 25 ms). Since we were estimating population discharges rather than individual fiber discharges, the refractoriness was applied with a strength of 40%. This meant that only that portion of the neurons would fire at any one time and therefore be susceptible to being refractory the next time. Fourth, we estimated the compound field potentials generated from the population of neurons in the brain responsible for the scalp potentials. This involved imposing a latency jitter (arbitrarily set as a rectangular 2 ms function) to mimic the variability in the conduction times between the cochlea and the generator neurons. The field potential of a single fiber discharge was estimated using the "model unit reponse" of Elberling (1976; see also (Teas et al., 1962), without the secondary peak. This was then convolved with the estimated population discharge pattern to give the modeled field potentials.

The latencies of the modeled responses were measured by determining the latency of the maximum of the cross-correlation function between the original acoustic signal and the modeled field potential. Two acoustic signals were analyzed: an AM tone with a modulation-frequency of 80 Hz and carrier-frequencies between 500 and 8000 Hz, and a click with a duration of .2 ms presented a rate of 50/seconds.

## RESULTS

Experiment 1: Monaural Stimulation 80-100 Hz

Sample data from one subject in this experiment are shown in Figure 4-1. Figure 4-3 shows the inter-subject variability of the phase delays at 750 Hz. The left side of Figure 4-4 shows the mean phase delays for all 4 carrier-frequencies and all modulation-frequencies.

A 4 x 4 repeated-measures ANOVA for the phases of the responses to the 750 Hz octave series modulated at 80-100 Hz, which compared carrier-frequency and modulation-frequency, indicated significant effects of both carrier-frequency ($F=33.8$; df 3,21; $p<0.001$) and modulation rate ($F=111.2$; df 3,21; $p<0.001$), as well as a significant interaction ($F=3.9$; df 9,63; $p<0.05$, $\varepsilon=.31$) due to a flattening of slope as the carrier-frequencies increased.

When converting from phase delay into latency, the data can be modeled as having occurred after 0, 1 or 2 preceding cycles by altering the parameter **m** in equation (3). These calculations are shown in Figure 4-5. When **m**=0, the experimental analysis of the latency data showed main effects of both carrier-frequency ($F=152.8$; df 3,21; $p<0.001$, $\varepsilon=.43$) and modulation rate ($F=18.3$; df 3,21; $p<0.001$, $\varepsilon=.42$). When **m**=1, there was a significant change in latency with carrier-frequency ($F=101.2$; df 3,21; $p<0.001$, $\varepsilon=.43$) but not with modulation rate ($F=0.56$; df 3,21; $p=0.7$). By adding a further cycle, so that **m**=2, the data again became divergent, and a significant effect of modulation rate again emerged ($F=33.8$; df 3,21; $p<.001$, $\varepsilon=.43$).

The best fit for the data, when **m**=1, yields steady-state response latencies for the 750 Hz octave series of 20.7, 17.7, 16.1, and 16.1 ms. Post-hoc Fisher LSD tests showed that the differences in latency between carrier-frequencies were significantly different ($p<0.01$) except between 3000 Hz and 6000 Hz. Table 4-1 provides the latencies estimated for each carrier-frequency at each modulation rate when m=1. The apparent latency values for these data were 22.2, 17.5, 13.9, and 12.7 ms.

The amplitudes are plotted in Figure 4-6. There was a no significant effect of carrier-frequency ($F=3.57$; df 3,21; $p=0.058$, $\varepsilon=.64$) or of modulation-frequency ($F=2.54$; df 3,21; $p=0.13$, $\varepsilon=.50$). The 750 and 6000 Hz tones tended to produce smaller responses. Furthermore, the overall amplitudes across the different carrier-frequencies did show a slight decrease in

*Please see next page for figure.*

**Figure 4-6: Effects of modulation-frequency on amplitude.** This figure represents the mean data for the 8 subjects evaluated in Experiments 1 and 2. There is a slight decrease in amplitude with increasing modulation-frequency. This was not significant between 80-100 Hz but was significant between 150-190 Hz. This suggests a small low-pass filtering process.

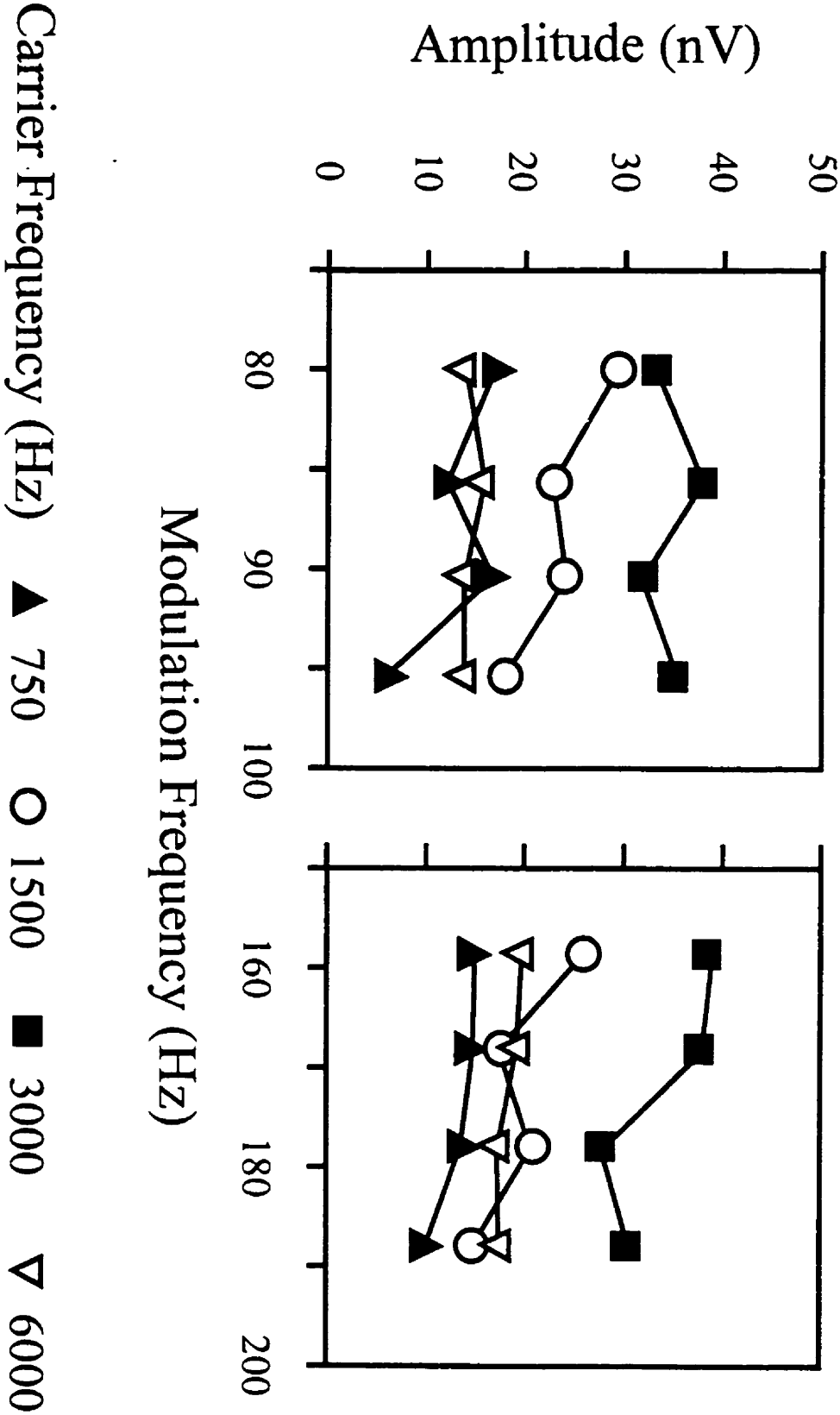
Amplitude (nV)
0
10
20
30
40
50
80
90
100
160
180
200
Modulation Frequency (Hz)
Carrier Frequency (Hz) ▲ 750 O 1500 ■ 3000 ∇ 6000

**Table 4-1. Estimated Latencies at Different Modulation-frequencies (Data from Experiments 1 and 2)**

| Rate (Hz) | Latency (ms) | | | |
|---|---|---|---|---|
| | 750 | 1500 | 3000 | 6000 |
| 80.6 | 20.6 | 17.6 | 16.1 | 16.4 |
| 85.5 | 20.6 | 17.8 | 16.3 | 16.2 |
| 90.3 | 20.8 | 17.7 | 16.1 | 15.9 |
| 95.2 | 20.8 | 17.7 | 15.8 | 15.9 |
| 158.7 | 11.3 | 8.6 | 6.6 | 6.3 |
| 168.5 | 11.0 | 8.8 | 6.8 | 6.5 |
| 178.2 | 10.9 | 8.8 | 7.0 | 6.5 |
| 190.0 | 12.0 | 9.0 | 7.0 | 6.5 |

amplitude (5nV from 80 to 95) with increasing modulation-frequency that was equivalent to about 6 dB/octave. Assuming that this may have been associated with a phase shift of 90° per octave, the phase measurements were adjusted and latencies recalculated. The differences caused by these calculations were less than 0.2 ms.

Experiment 2: Monaural Stimulation 150-190 Hz

The mean phase measurements are shown on the right of Figure 4-4. The data are plotted with different values of **m** in Figure 4-7. In the case of the 150 Hz series, for **m**=0, a 4 x 4 repeated-measures ANOVA showed a main effect of latency for carrier-frequency ($F=165.5$; df 3,21; $p<.001$, $\varepsilon=.48$) and also for modulation rate ($F=59.6$; df 3,21; $p<.001$, $\varepsilon=.48$). When **m**=1, there was a significant change in latency with carrier-frequency ($F=96.4$; df 3,21; $p<.001$, $\varepsilon=.48$), but not for modulation rate ($F=1.2$; df 3,21; $p=.3$). After adding a further cycle so that **m**=2, the data again became divergent across both carrier-frequency ($F=165.5$; df 3,21; $p<.001$) and modulation-frequency ($F=8.9$; df 3,21; $p<.01$).

The mean latencies for the 750 Hz octave series 150-180 Hz modulated data were 11.3, 8.9, 6.9, and 6.4 ms. Post-hoc Fisher LSD tests within each modulation-frequency showed significantly ($p<0.01$) different latencies across the different carrier-frequencies except for the difference between 3000 and 6000 Hz. However, these latencies were significantly different if the data were collapsed across all modulation rates ($F=6.9$; df 1,14; $p<0.001$). The apparent latencies for these data were 15.1, 10.9, 9.5, and 7.5 ms.

The mean amplitudes of these responses are plotted in the right half of Figure 4-6. The trends seen in the 80 Hz data again appeared here, but now there was a significant effect of carrier-frequency ($F= 8.04$; df 3,21; $p<.05$) and also modulation rate ($F=6.74$; df 3,21; $p<.05$). As in the case of the 80 Hz data, there again was a decrease in the amplitudes of the 750 and 6000 Hz responses and a roughly linear decrease in amplitude as modulation rate increased (7 nV from 155 to 185 Hz). Again, recalculation of the latencies after compensating the phases for a possible 90°/octave shift did not significantly alter the latencies.

Experiment 3 Dichotic Stimulation

In the first dichotic condition, a 750 Hz octave series was presented to the right ear while a 500 Hz octave series was presented to the left ear, and in the second condition these stimuli were presented to the opposite ears. In order to analyze the data, the results were combined to

provide latency estimates at ½-octave steps in each ear. The mean data compared between the ears are plotted in Figure 4-8. The mean and standard deviations across the subjects are provided in Table 4-2. There are minor differences between Figure 4-7 and the Table 4-2 data since vector averaging was used to calculate the mean phases for the latencies in the Figure 4-but ordinary arithmetic averaging was used to calculate the latencies for the table (to allow us to obtain measurements of inter-subject variability).

The responses to the 80 Hz dichotic AM tones showed significant effects for carrier-frequency ($F=71.2$; df 7,49; $p<.001$) and no significant effect of ear ($F=2.15$; df 1,7; $p=.19$). Post-hoc Fisher-LSDs indicated that the differences in latency between all adjacent carrier-frequencies (½-octave steps) were significant at the .001 level up to the 3000 Hz level. The responses to the 160 Hz dichotic AM tones showed significant effects for carrier-frequency ($F=91.8$; df 7,49; $p<.001$) and, again, the responses for the left and right ears failed to show any significant differences ($F=.07$; df 1,7; $p=.8$). Post-hoc Fisher-LSDs again indicated that the differences in latency between all adjacent carrier frequencies (½-octave steps) were significant at the .001 level up to the 3000 Hz level. We also compared the responses recorded when stimuli were presented to the left ear in the monaural condition to those recorded in the left ear during the dichotic condition. There were no significant differences between monaural and dichotic response latencies.

Experiment 4: Effects of Intensity. (N=8)

When the intensity of the stimuli increased from 35 dB SPL to 75 dB SPL (Figure 4-9), the latency of the response in the 80-100 Hz range decreased by an average of 2.4 ms (2.6, 2.5, 2.8, and 1.7 ms for the 500, 1000, 2000, 4000 Hz carrier frequencies). A comparison between 35 and 75 dB SPL response indicated a significant decrease in latency ($F=30.9$; df 1,7; $p<.001$) and across carrier frequency ($F=33.6$; df 3,21; $p<.001$). Although there was a smaller decrease at the 4 kHz response there were no significant interactions between loudness and carrier frequency with respect to latency. Post-hoc LSD comparisons indicated that this decrease was significant for all frequencies at the .05 level.

Experiment 5: Effects of Multiple Stimuli (N=10)

In the other experiments presented in this chapter, multiple (4) stimuli were presented in

each ear. Here, we examined the latencies obtained by a 1000 Hz or 2000 Hz tone presented alone, compared to the latencies obtained when multiple stimuli were used. The latencies of the 1000 Hz and 2000 Hz tones in the different stimulus conditions are shown in Table 4-3. A two-way (carrier frequency by number of simultaneously presented stimuli) repeated-measures ANOVA showed a significant main effect for carrier frequency ($F=103.2$, $df=1,9$; $p<.001$) but not for number of stimuli ($F=2.13$; df 4,36; $p=.10$). However, there was a significant interaction between carrier frequency and number of stimuli ($F=7.96$; df 4,36; $p<.001$). Compared to the single stimulus condition, when adjacent stimuli were separated by less than 1 octave, increased latency was seen, although post-hoc testing showed this effect was only significant ($p<.05$) in the case of the 1000 Hz tone.

Experiment 6: Stability of Phase (N=6)

In order to assess the stability of steady-state phase we tested 6 subjects and then tested them again 3-4 weeks later, at both 80 Hz and 150 Hz modulation rates. In the 80 Hz condition the average change was -0.11 ms (range: -0.66 to +0.67ms). In the 150 Hz condition the average change was only -0.04 ms (Range: -0.49 to +0.31 ms). The results for each carrier frequency are provided in Table 4-4. For the 80 Hz responses, the change for the difference between 750 and 6000 Hz changed from one recording to the next by 0.15 ms (range: -0.71 to +1.14 ms). For the 150 Hz responses, this measurement changed by -0.06 ms (range: -0.255 to +0.05 ms).

*Please see next page for figure.*

**Figure 4-7: Preceding cycles (150-190 Hz).** This figure shows how the number of preceding cycles of modulation were estimated for the data recorded with modulation-frequencies of 150-190 Hz. The figure is similar to Figure 4-4. Again, the data are most consistent across the recording condition when the number (**m**) of preceding cycles of modulation equals one.

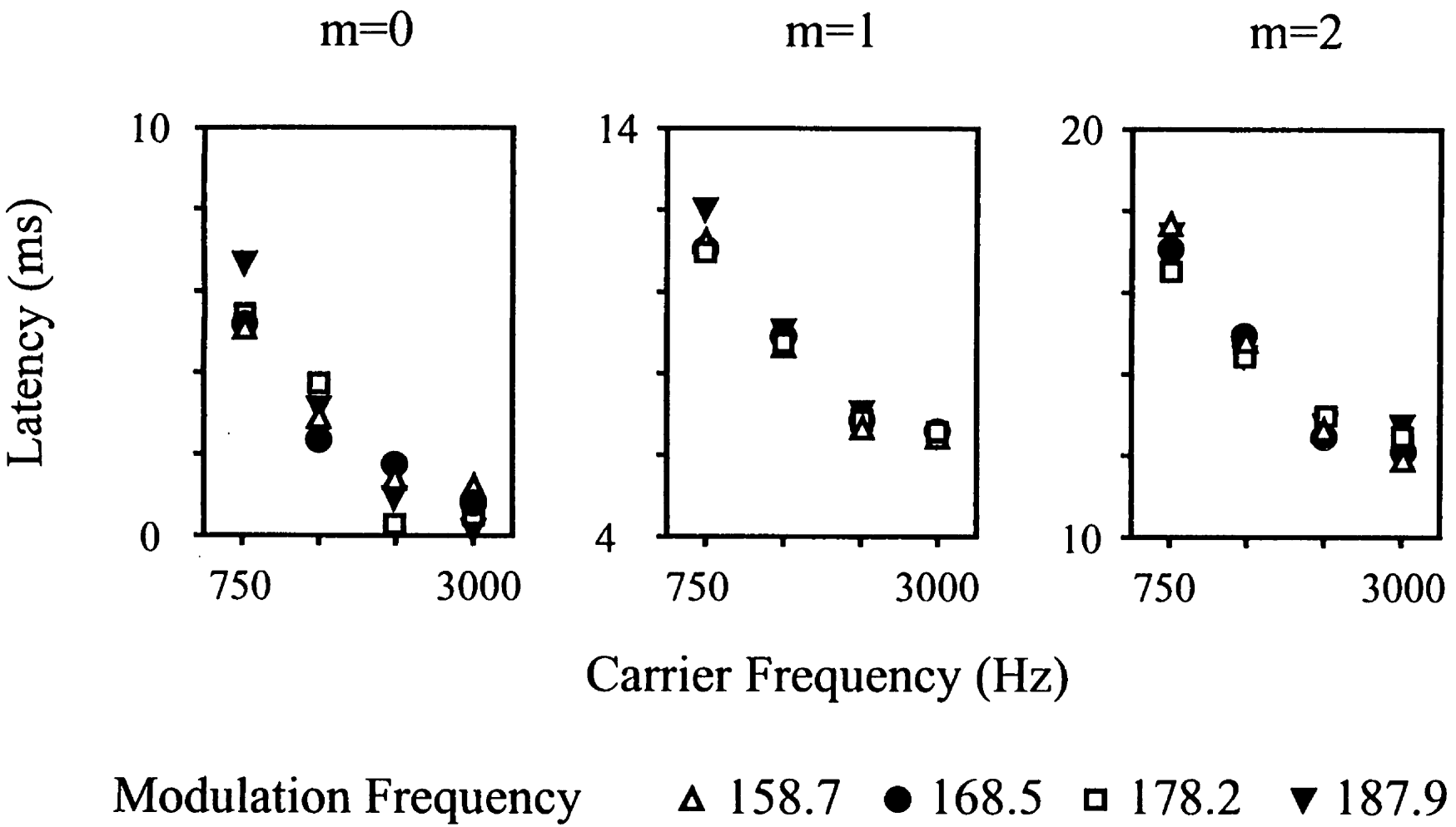
m=0
m=1
m=2
Latency (ms)
10
0
14
4
20
10
750
3000
750
3000
750
3000
Carrier Frequency (Hz)
Modulation Frequency
158.7
168.5
178.2
187.9

*Please see next page for figure.*

**Figure 4-8: Dichotic stimulation.** This figure shows the results of Experiment 3. Four stimuli with carrier frequencies separated by an octave were presented to one ear and four stimuli at intervening carrier frequencies were presented to the other ear. The data are the latencies derived using m=1 from the vector-averaged phase delays across the 8 subjects recorded in this experiment.

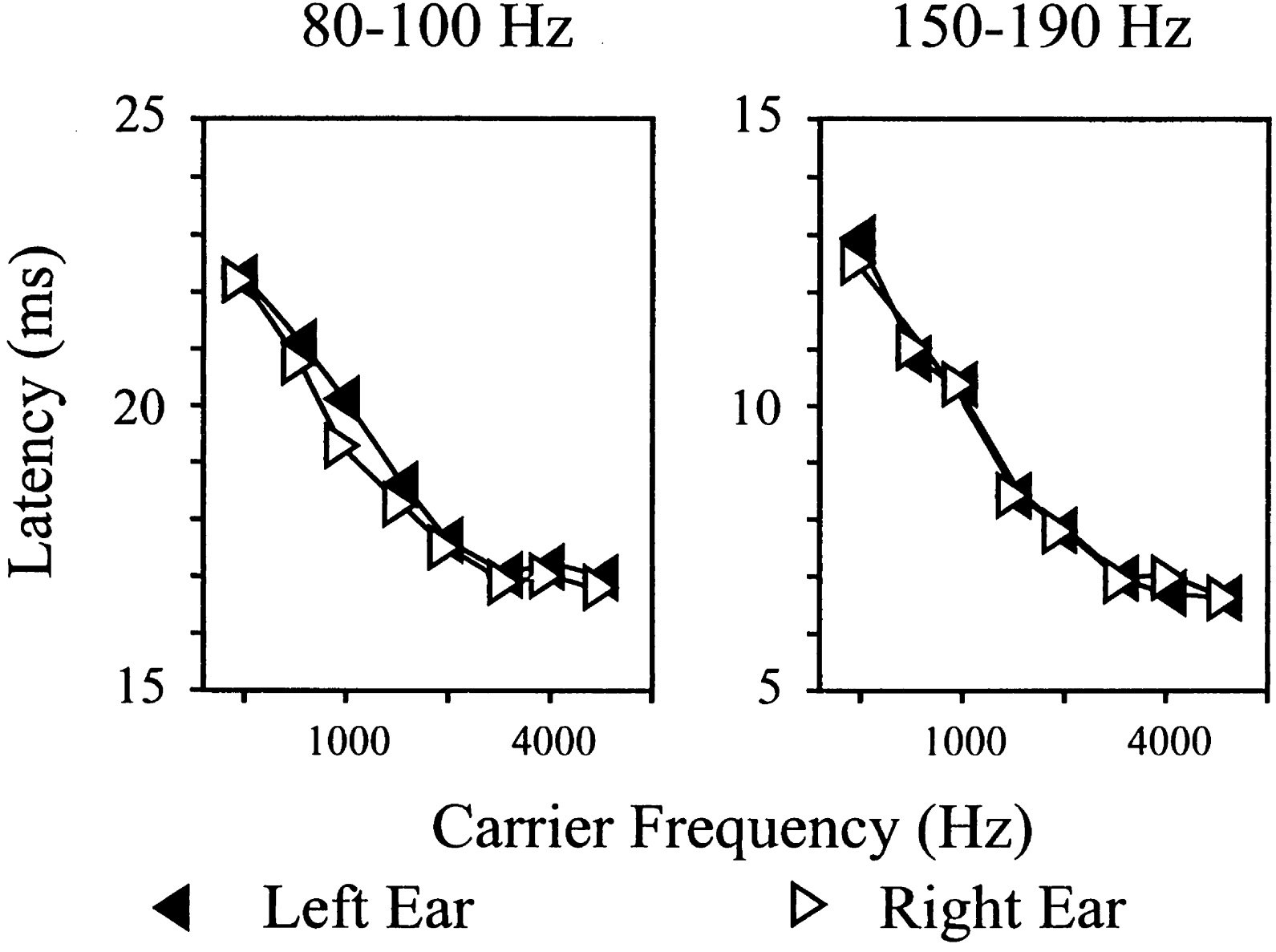
80-100 Hz
150-190 Hz
25
20
15
15
10
5
1000
4000
1000
4000
Latency (ms)
Carrier Frequency (Hz)
Left Ear
Right Ear

*Please see next page for figure.*

**Figure 4-9: Effects of intensity on response latency.** These data represent the average results across the 8 subjects participating in Experiment 4. They show the decrease (approximately 2 ms) in the estimated latency with increasing intensity.

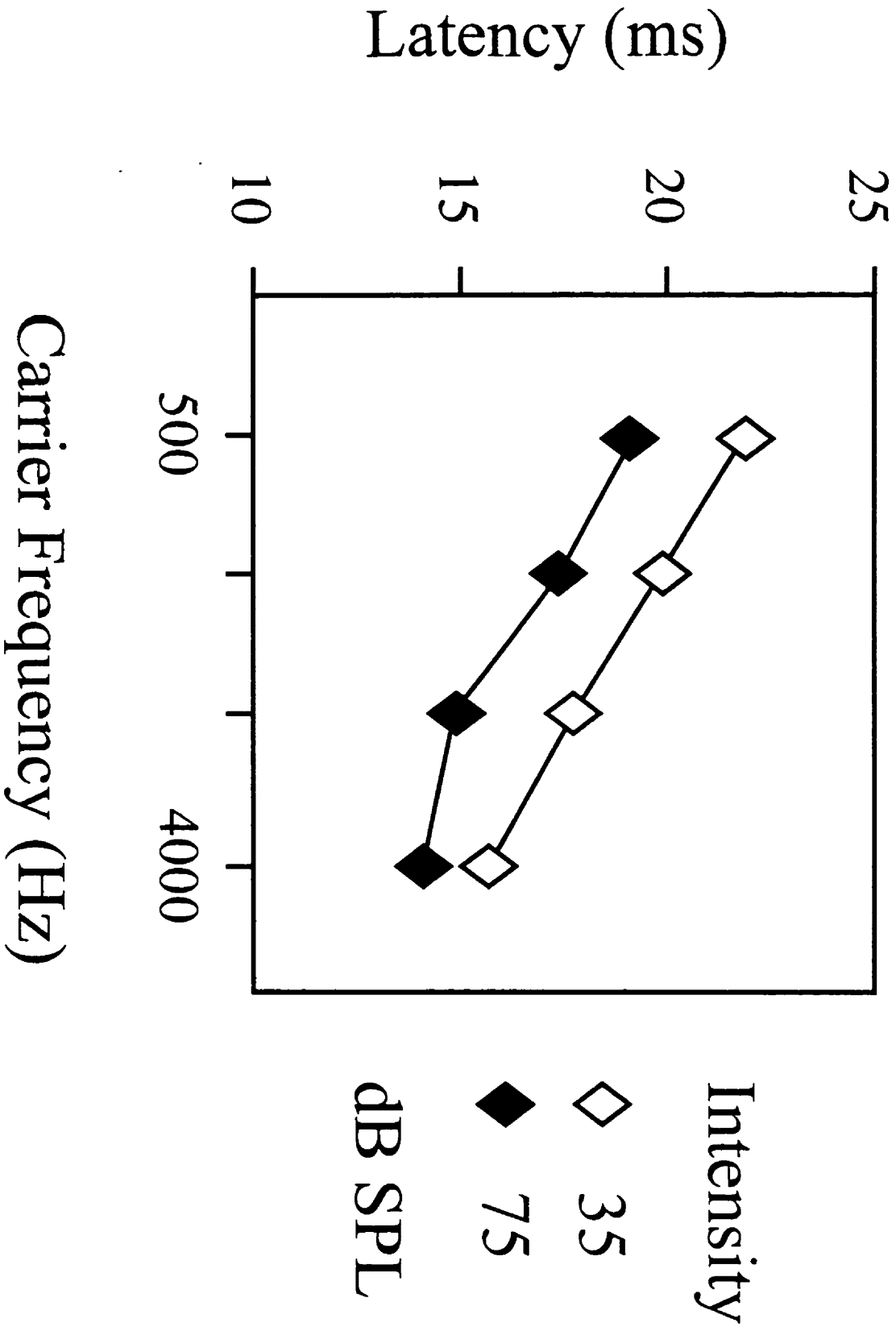
Latency (ms)
10
15
20
25
500
4000
Carrier Frequency (Hz)
Intensity
35
75
dB SPL

Experiment 7. Small Differences in Modulation-frequency (N=16)

The latencies for this experiment are plotted in Figure 4-10. The differences between the latency for the 750-Hz carrier and the latency for the 6000-Hz carrier were 3.5 and 4.5 ms for the 80 Hz and 160 Hz series, respectively. Like Experiments 1, 2, and 3 the 80 Hz data failed to show any decrease in latency between the 3000 to 6000 Hz responses, while in the 160 Hz data, a decrease was apparent. An ANOVA of the all of the data indicated highly significant effects for carrier frequency ($F=107.7$; df 3,42; $p<.001$) and between the 80 and 160 Hz modulation rates ($F=2840.0$; df 1,14; $p<.001$). There was also a significant effect of gender ($F=4.6$; df 1,14; $p=0.05$) with the male subjects showing latencies which were delayed, on average, by 0.78 ms compared to the female subjects. There was no significant interaction between gender and carrier frequency although the difference between 750 and 6000 Hz was slightly greater for males than for female subjects in the 80 Hz data.

The amplitude and phase of the 1500 Hz tone presented alone was compared to its amplitude when it was presented simultaneously with the 3 other tones. For the 80-Hz response the amplitudes were smaller (92%) when the stimulus was presented with the other tones, while in the case of the 160-Hz the amplitude was larger (140%). For both modulation-frequencies the responses were slightly earlier by 0.4 ms (same for both) when the stimulus was presented with the other tones.

Results of Modeling

The basic parameters of the model are illustrated in Figure 4-11. Figure 4-12 shows how the model processes two different inputs – an 80-Hz AM tone and a click presented at a rate of 50 Hz. Figure 4-13 graphs the latencies estimated using cross-correlation for these two kinds of stimuli. The carrier frequency of the AM tone and the characteristic frequency of the hair cell filter were varied in octave steps form 500 to 8000 Hz. The latency changes over the complete range were 5.4 ms for the AM tone and 3.2 ms for the click-evoked potential. Estimates of the difference between 750 and 6000 Hz were 3.7 ms and 2.4 ms.

**Table 4-2. Effects of Carrier Frequency on Response Latency**

**(Data from Experiment 3)**

| | | Carrier(Hz) | | | | | | | |
|---|---|---|---|---|---|---|---|---|---|
| Modulation Range (Hz) | | 500 | 750 | 1000 | 1500 | 2000 | 3000 | 4000 | 6000 |
| 80 Hz | mean | 21.5 | 20.2 | 18.9 | 17.6 | 16.7 | 16.0 | 16.1 | 15.8 |
| | sd | 1.6 | 1.5 | 0.8 | 0.6 | 0.5 | 0.5 | 0.7 | 0.8 |
| 160 Hz | mean | 12.2 | 11.1 | 10.3 | 8.9 | 7.8 | 6.8 | 6.9 | 6.6 |
| | sd | 1.7 | 1.0 | 1.1 | 1.4 | 0.7 | 0.3 | 0.4 | 0.5 |

**Table 4-3. Effects of Multiple Stimuli on Latency Estimates**

**(Data from Experiment 4: means and standard deviations)**

| Carrier (Hz) | 1 Tone (1 Octave) | 2 Tones (1 Octave) | 4 Tones (1 Octave) | 4 Tones (1/2 Octave) | 8 Tones (1/2 Octave) |
|---|---|---|---|---|---|
| **1000** | 20.9±2.9 | 21.5±2.8 | 21.3±2.7 | 22.4±2.8 | 21.9±2.9 |
| **2000** | 18.9±2.7 | 18.3±2.5 | 18.7±2.7 | 19.1±2.9 | 19.9±2.8 |

**Table 4-4. Stability of the Responses over Two Separate Recording Sessions**

**(Data from Experiment 6)**

| Modulation | Carrier | Latency | | Difference between Sessions | | | |
|---|---|---|---|---|---|---|---|
| | | mean | sd | mean | sd | min | max |
| 80-100 Hz | 750 | 19.9 | 0.8 | 0.1 | 0.4 | -0.5 | 0.5 |
| | 1500 | 17.0 | 0.6 | 0.1 | 0.4 | -0.3 | 0.7 |
| | 3000 | 15.4 | 0.9 | 0.2 | 0.4 | -0.4 | 0.6 |
| | 6000 | 15.5 | 0.6 | 0.0 | 0.6 | -0.7 | 0.7 |
| 150-190 Hz | 750 | 10.8 | 0.8 | 0.0 | 0.1 | -0.2 | 0.1 |
| | 1500 | 8.8 | 0.8 | 0.0 | 0.2 | -0.3 | 0.3 |
| | 3000 | 6.3 | 0.4 | 0.0 | 0.2 | -0.3 | 0.2 |
| | 6000 | 6.1 | 0.4 | -0.1 | 0.2 | -0.5 | 0.1 |

*Please see next page for figure.*

**Figure 4-10: Small differences in modulation-frequency.** This figure shows the results of Experiment 7. The estimated latencies were slightly shorter for the 8 female subjects than for the 8 male subjects.

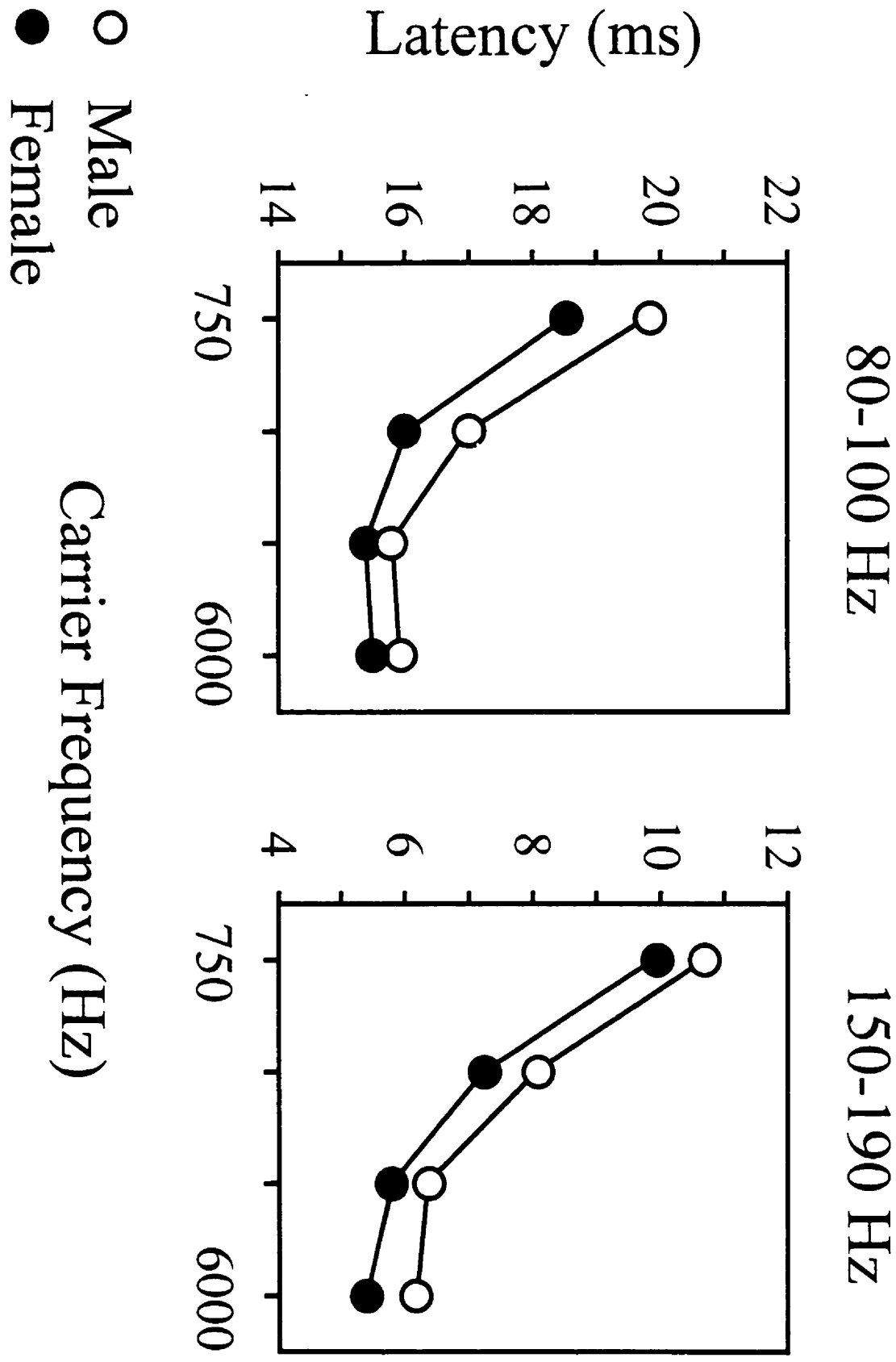
Latency (ms)
80-100 Hz
150-190 Hz
14
16
18
20
22
4
6
8
10
12
750
6000
Carrier Frequency (Hz)
Male
Female

## DISCUSSION:

Auditory Steady-State Responses

Human auditory steady-state responses can be recorded using stimulus rates up to several hundred Hz (Rickards and Clark, 1984). The amplitude of these responses is larger at rates near 40 Hz (Galambos et al., 1981) and 80 Hz (Cohen et al., 1991; Lins et al., 1995). Responses at both these rates have been used as an objective measurement of hearing thresholds (Rance, 1995; Lins, 1996; Dobie and Wilson, 1998). The more rapid responses are less affected by changes in sleep or maturation (Cohen et al., 1991; Levi et al., 1993; Lins and Picton, 1995) and might therefore provide more reliable measurements in children and other difficult-to-test patients. The results of this chapter indicate that responses in the 150-190 Hz range might also provide reliable measurements.

The nature of human auditory steady-state responses has been mainly studied with the responses evoked at stimulus rates near 40 Hz (Galambos et al., 1981; Stapells et al., 1984). If they largely arise from the same neurons that generate transient evoked potentials, the steady-state responses can be predicted from the superposition of multiple overlapping transient responses (Galambos et al., 1981; Hari et al., 1989; Plourde et al., 1991). However, it is also possible that rapid stimulation might elicit a separate response from neurons that are specifically responsible for rhythmic activity and that resonate at the frequency of stimulation (Basar et al., 1987). These generators might be responsible for spontaneous cortical gamma rhythms. Discrepancies between the steady-state response and the response predicted by superposition (Azzena et al., 1995) and the persistence of the response beyond the time when the stimuli are presented (Santarelli et al., 1995) support the idea of resonance. However, by modeling the refractory effects and considering multiple generators, one can still explain most of the 40-Hz response findings on the basis of the superposition of the transient response waveforms (Gutschalk et al., 1999). We think that it is unlikely that independent rhythmic generators might account for the steady-state responses at frequencies above 80 Hz. We therefore consider the responses to be generated by neurons in the brainstem (and possibly cortex) that become locked to the envelopes of amplitude-modulated tones.

The estimated latencies for the 150-190 Hz responses were about half the latencies for the 80-100 Hz responses (e.g. Table 4-4, Figure 4-8). Our latencies (17.7 and 9.0 ms at 1500 Hz) are

similar to those of Cohen et al. (1991) who reported latencies at 1000 Hz (55 dB HL) of 24.8 ms for modulation-frequencies of 30-60 Hz and 13.0 ms for 90-125 Hz, given that the latencies decrease with increasing modulation-frequencies (Rickards and Clark, 1984). Previous work in our laboratory had provided an apparent latency of 19 ms for 1000 Hz tones modulated between 71-100 Hz. The latencies at 150-190 Hz suggest that the generators might be at about the same level of the brainstem as those generating wave V of the auditory brainstem response. The latencies for the 80-100 Hz responses suggest a generator higher in the brainstem.

Latency of Steady-State Responses

The phase of a steady-state response is related to delay. Unfortunately, this relationship is ambiguous and phase cannot be directly translated into latency. By assessing phase at different stimulus rates, it is often possible to resolve the ambiguities and arrive at a clear estimate of "apparent latency" (Regan, 1966) or "group delay" (Goldstein et al., 1971).

The distorting effect of physiological filters operating across the different rates of stimulation remains a problem (Bijl and Veringa, 1985). This is analogous to estimating the delays related to filter slopes when studying the group delays of tuning curve (Goldstein et al., 1971). The effects of such filters can only be estimated. In the data presented here, these effects appear small since similar results were obtained when the latency estimates were based on the same modulation-frequencies rather than different modulation-frequencies. Supporting data were obtained on separate recordings for the different carrier frequencies with each carrier frequency being modulated by exactly the same modulation-frequency (Experiments 1 and 2, and Table 4-1), and using modulation-frequencies that were sufficiently close together during multiple stimulation that any filter-effect would be negligible (Experiment 7).

The physiological interpretation of the latencies of the steady-state responses remains difficult. The main problem is that the recorded response may not derive from a single generator. Many different regions of the auditory nervous system from the auditory nerve to the auditory cortex generate responses that follow the modulation signal of an amplitude-modulated tone. Each of these regions can create a response that has a specific phase and latency relationship to the stimulus. All these responses will overlap to make up the response recorded from the scalp. The phase and latency characteristics of the scalp-recorded response may be very complex unless

*Please see next page for figure.*

**Figure 4-11: Modeling parameters.** This figure shows the parameters used in the four processes for modeling the latencies of the responses to amplitude-modulated tones and clicks. The first process is the cochlear filter which is modeled as a gammatone filter using the parameters of (Patterson, 1994). The second process is synaptic rectification. The third process is to estimate the fiber discharge rates. For this estimation the refractoriness of the fibers was estimated using parameters from (Carney, 1993). The fourth process in the model was to estimate the field potentials generated from the responding units. As well as a jittering of the latency (not illustrated) the response pattern was then convolved with an estimated unit field potential using parameters similar to those of (Elberling, 1976).

## 1. Hair Cell Filter

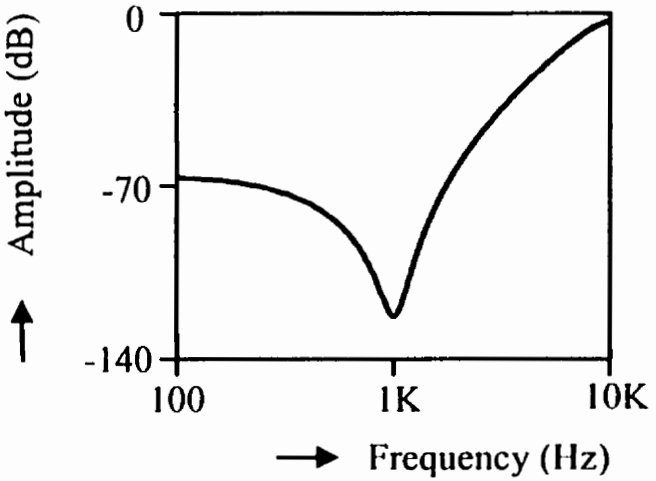


## 3. Nerve Fiber Firing

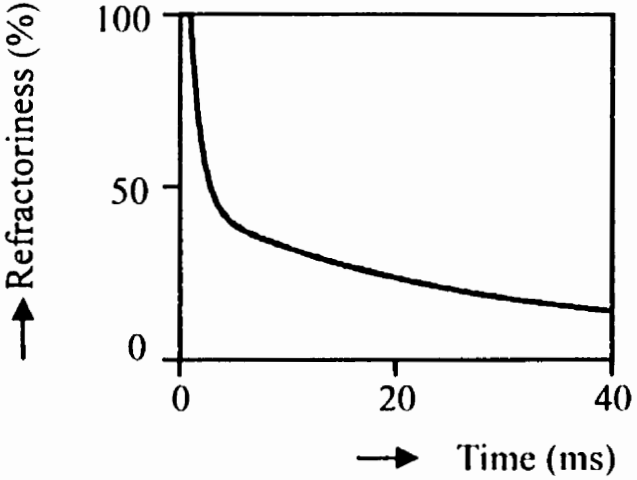


## 2. Synaptic Rectification

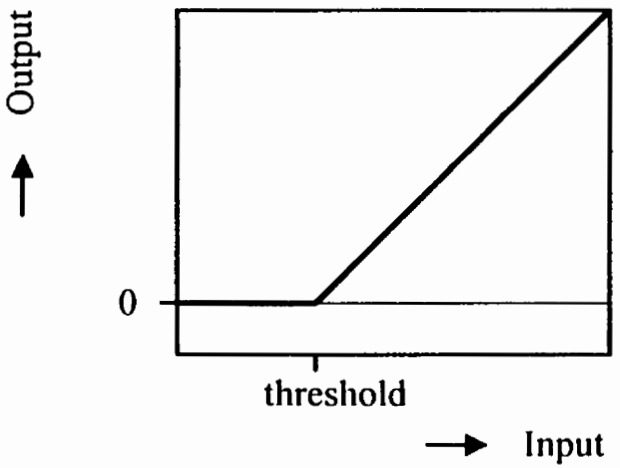


## 4. Unit Field Potentials

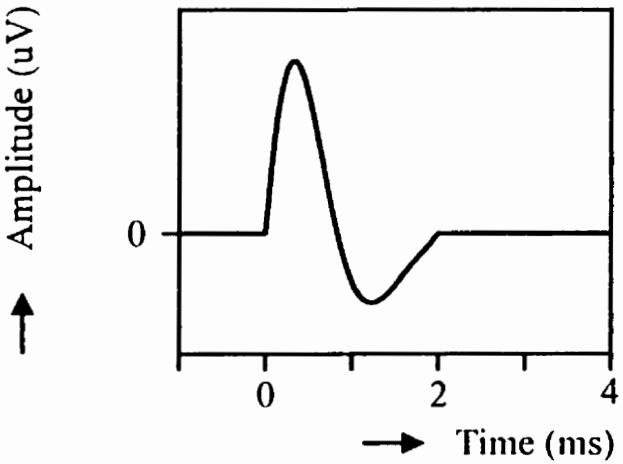

*Please see next page for figure.*

**Figure 4-12: Modeling the physiological processes.** This figure illustrates the processing of acoustic stimuli through the various steps in the model. The hair cell filter intervenes between the acoustic stimulus and the hair cell potential. Rectification then occurs to give the synaptic potential. The refractoriness of the nerve fibers determines the fiber discharge pattern. The scalp potentials are then determined by both the jitter and the field pattern of the unit discharges.

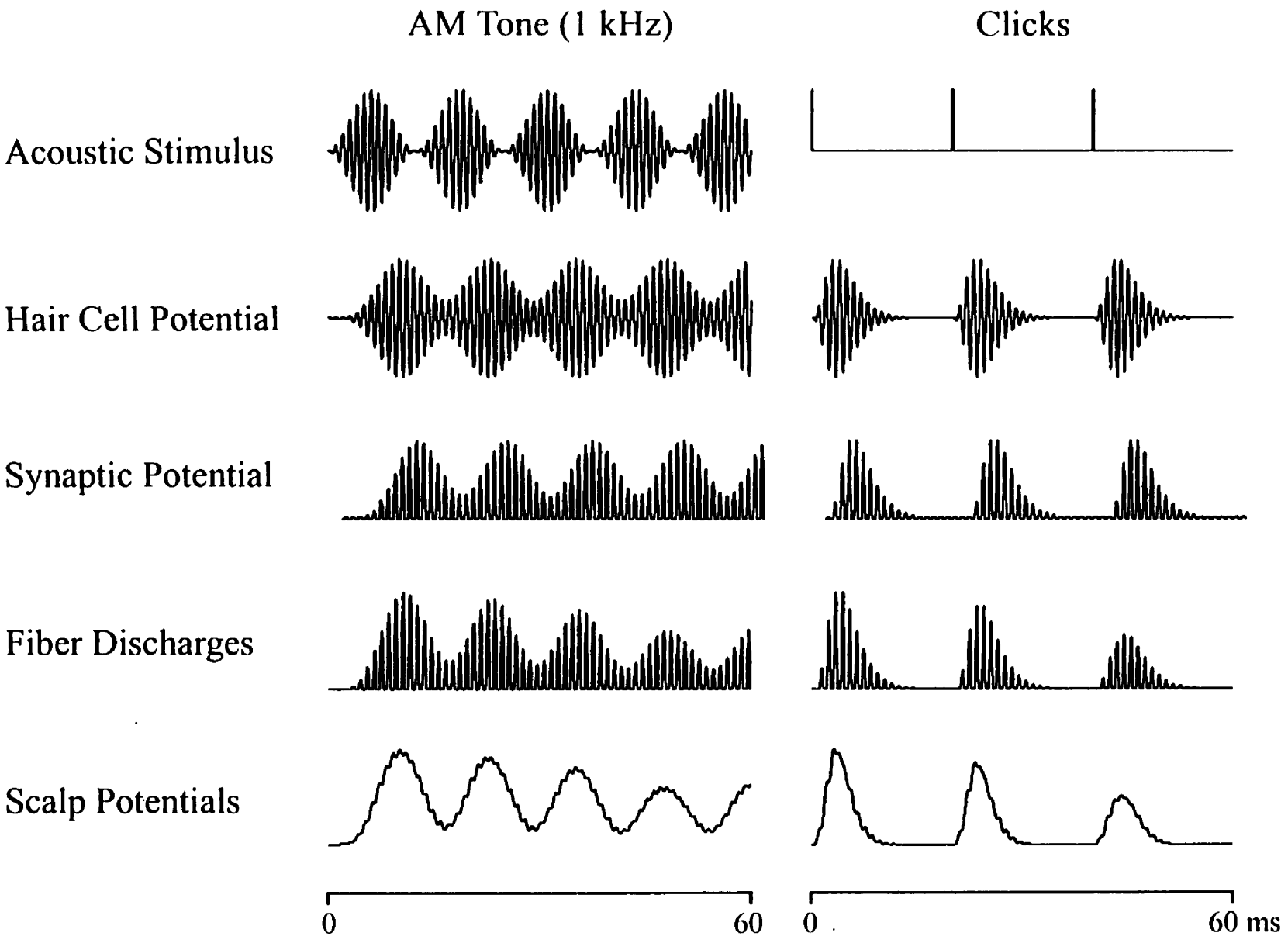
AM Tone (1 kHz)
Clicks
Acoustic Stimulus
Hair Cell Potential
Synaptic Potential
Fiber Discharges
Scalp Potentials
0
60
0
60 ms

*Please see next page for figure.*

**Figure 4-13: Modeled latencies.** This figures graphs the latencies obtained for the steady-state response to a pure tone amplitude-modulated (AM) at 80Hz and a click stimulus presented at a rate of 50Hz. The latency change of the steady-state response with changing carrier frequency is almost double that of the click response.

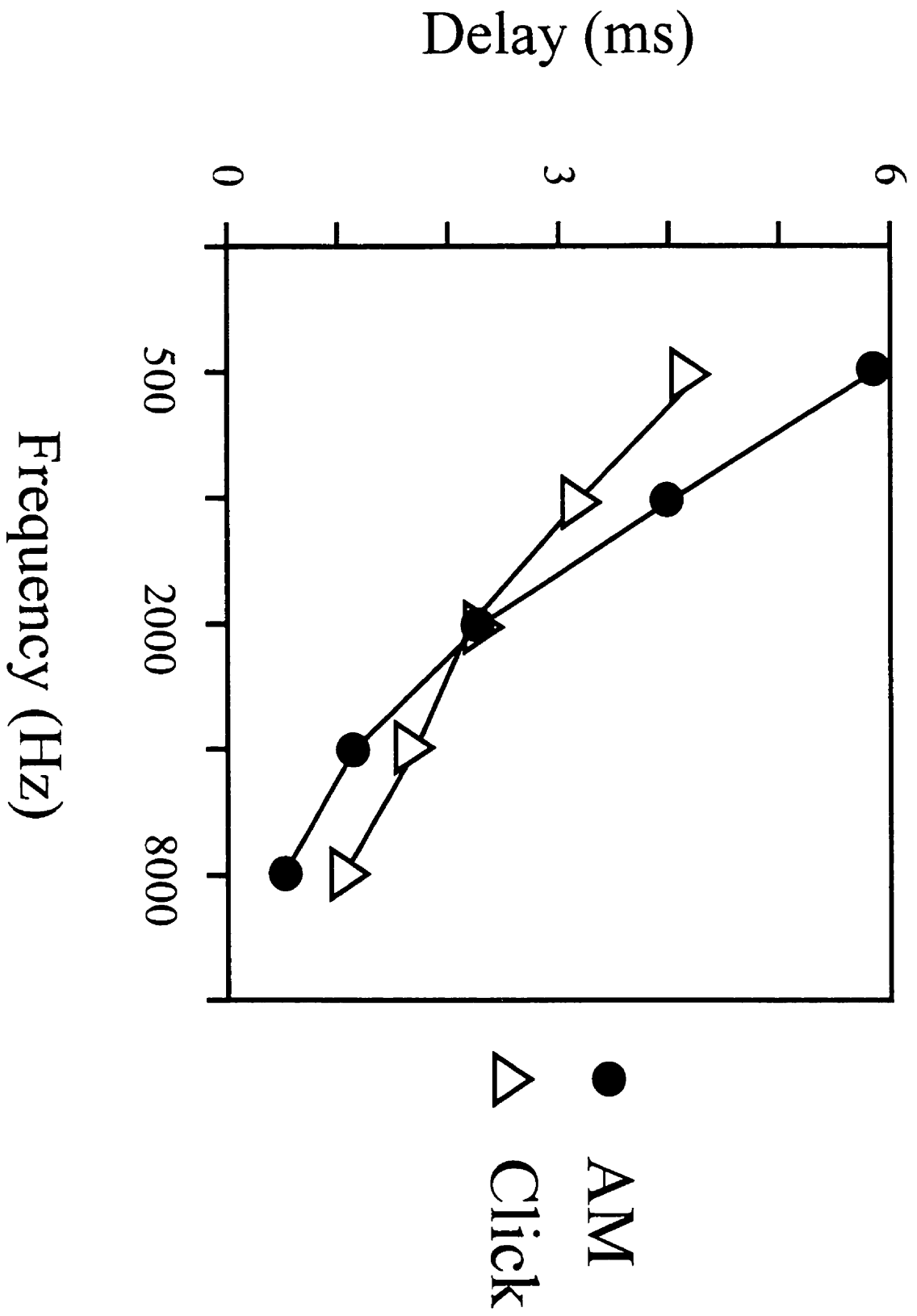
Delay (ms)
0
3
6
500
2000
8000
Frequency (Hz)
AM
Click

one of the generators is clearly dominant.

An example may be possible changes in the phase of the steady-state response with changes in the level of arousal. In a waking subject, the dominant response at 40 Hz may be from the auditory cortex. With sleep, this response may attenuate and the scalp- recorded response may reflect only those potentials generated in the brainstem. The response during sleep is therefore much smaller than during wakefulness and occurs earlier (Lins and Picton, 1995).

In our particular case, the amplitude of the responses from different generators may vary differently with the carrier-frequency. If so, the phase of the scalp-recorded response that combines potentials from the different brain generators, may not show a clear and regular relationship to carrier frequency. Furthermore, such data might provide an apparent latency that does not fit with an integer number of cycles prior to the recorded response. It is best only to calculate the apparent latency over regions where there is no change in the slope of the phase-frequency curve, since this suggests one dominant generator. Different generators at different frequencies could cause the slope to change (e.g., 750 Hz on the right of Figure 4-4). Another reason for non-integer preceding cycles would be some undetermined filter delay in the system. These factors (multiple generators and unknown filters) may explain some of the discrepancies between our measurements of apparent latency and the estimated latencies obtained by postulating an integer number of cycles of modulation prior to the recorded response. Although the latencies were generally concordant, the apparent latencies measured for the 750 Hz carrier were longer than those estimated using preceding cycles (22.2 versus 20.7 ms at 80-100 Hz and 15.1 versus 11.3 ms at 150-190 Hz).

The advantages of using the "preceding cycles" approach over apparent latency is that once the number of preceding cycles is estimated by using multiple modulation rates, then only one rate is needed to make subsequent latency measurements. The disadvantage is that it has no clear way to handle the possibility of multiple generators, which could then lead to a non-integer number of preceding cycles. However, although the group delay or apparent latency measurements allow for such non-integer effects, the interpretation of the results in such a situation is not clear. In our results, the apparent latency measurements differed slghtly from the latencies obtained with the preceding cycles approach, particularly for the low-frequency stimuli

(750 Hz). In this situation, one must consider the possibility of overlapping responses with different latencies, e.g., from different brainstem neurons.

We feel that the scalp-recorded potential in response to tones amplitude-modulated at frequencies 80-100 Hz probably derives mainly from a generator in the high brainstem. Preliminary source analyses in our laboratory support this idea (cf. Mauer and Döring, 1999). If this generator is clearly dominant over other generators, for example in the auditory nerve or lower brainstem, the derived latencies should be quite accurate. The relations of the response phase to carrier frequency should then reflect the effects of transport-time and filter build-up in the cochlea. For the stimulation rates of 150-190 Hz, the responses that we are recording may reflect approximately equal contributions from generators in both the high brainstem and lower brainstem.

Latencies in the Auditory System

Five main factors contribute to the latency of a neurophysiological response to an auditory stimulus:

(i) Acoustic delay. This is the delay between the production of the stimulus and its arrival at the oval window after transmission through the air and the middle ear to the tympanic membrane. This was 0.9 ms for the ear inserts and was instantaneous for the headphones.

(ii) Transport time. This is the delay between the arrival of the acoustic energy at the oval window and the beginning of activity at the location on the basilar membrane where transduction occurs for a stimulus of that particular frequency. High frequencies of sound maximally activate the basilar membrane close to the oval window and low frequencies maximally activate the regions of the basilar membrane at some distance from the oval window. The transport time therefore depends upon the frequency of the stimulus. Eggermont (1979b) estimated this "mechanical time" as $\mathbf{f}^{-0.5}$ where **f** is the characteristic frequency.

(iii) Filter built-up time. This is the time taken for the acoustic energy to pass through the active filtering process ("cochlear filter") of the hair cells that are sensitive to the frequencies of sound in the stimulus. This time will depend upon the sharpness of the filter, a parameter that can be measured by the Q10 dB parameter which is the characteristic frequency of the filter divided

by the bandwidth of the filter at an intensity 10dB above the threshold intensity for the filter. Values for Q10dB in mammalian cochleae vary between 1 and 15 with the filters for lower frequency sounds having lower values (Eggermont, 1979b; Ruggero, 1992). The filter delay is usually measured in terms of the number of cycles to maximum amplitude and this varies with the Q10dB, with delays increasing by 2-3 ms as the stimulus frequency increases from 1 to 10 kHz (Eggermont, 1979b, data compensated by removing ß as discussed later).

(iv) Synaptic delay. As the hair cells react to the sounds they synaptically activate the afferent nerve fibers. The transmission time across the synapse requires somewhere between 0.5 and 1.0 ms. This delay is not frequency-dependent.

(v) Conduction delay. This is the time taken for the neural responses to travel from their point of origin on the afferent fiber terminals to the location from which they are recorded. For human evoked potentials this time includes some additional synaptic and conduction delays as the impulses travel to the place where they generate the response recorded from the scalp. The conduction time can be estimated from studies wherein the auditory nerve fibers are electrically stimulated. Shirane and Harrison (1991) found a delay of below 1 ms in the colliculus' response as the characteristic frequency of the chinchilla afferent fiber being electrically stimulated decreased from 10 kHz to 1 kHz (compared to about 2 ms when using acoustic clicks).

The latency of the neural response is unfortunately not just a simple sum of these five delays. The problem centers on the temporal characteristics of neural responsiveness, particularly refractory times, and the way in which field potentials are generated. When presented with a transient stimulus the nerve fibers will respond more to the initial cycles of activation and less to later cycles. This complex relationship becomes even more complicated if one measures the combined responses of multiple neurons, such as the compound action potential of the auditory nerve. The neurons contributing to this combined response will show a significant variance in their response patterns and this can make the compound response quite different from the individual responses. One of the main effects is to accentuate the response at the onset of a stimulus. The discharges of many of the neurons will be relatively synchronous at the beginning of the stimulus and will become less synchronous as the stimulus continues (Elberling, 1976).

Because of these factors, the latency of the neurophysiological response to a transient

stimulus is not as long as the delay caused by the filter build-up. The response occurs sometime during the build-up of the filter response and this time can vary with other parameters such as stimulus intensity. In order to account for this effect, Eggermont, (1979b) multiplied the delay by a factor ß between 0 and 1.0, in general estimating ß at 0.5.

When recording steady-state responses, the neural response patterns have reached a balance between reactivity and refractoriness and this balance remains constant during the recording. We therefore suggest that for the steady-state response ß is effectively equal to 1.0. If so, the frequency-related delay of the steady-state response is exactly equal to the sum of the transport time and the filter build-up time for stimuli with frequencies equal to the carrier frequency.

Most studies of the neuronal responses to AM stimulation in animals (e.g. Rees and Palmer, 1989; Langner, 1992) have not considered the phase of the response patterns. Other studies (e.g Møller, 1973; Rees and Møller, 1983) have measured changes in the phase of the discharge patterns with modulation-frequency and how this relates to the temporal modulation transfer function of the neurons. Joris and Yin (1992) measured the phases of the neuronal responses to AM tones in the auditory nerve of the cat and found group delays related to carrier frequency increasing about 3 ms from 10 kHz to 500 Hz. This was similar to the changes in group delay estimated from the phase locked responses to pure tones (e.g., Goldstein et al., 1971; Gummer and Johnstone, 1984). Our data show a change of 5-6 ms over these frequencies, the larger delays probably being related to species-differences in the basilar membrane and the travelling wave velocity, or some frequency-related change in conduction time (see (v) above).

Relations to Oto-acoustic Emissions

Kimberley et al. (1993) studied frequency-related delays in cochlear processing using distortion product oto-acoustic emissions (DPOAE). The latency of these responses is usually considered in terms of a "round-trip" delay: the acoustic signal must first reach the hair cells and then the acoustic energy generated by the hair cells must travel back to the external ear canal to be recorded up by the microphone. Dividing the DPOAE latency by 2 provides latencies that are roughly equivalent to the latencies of the neurophysiological responses. However, as Kimberley et al. (1993) clearly state, this is a simplified view. They point out that the latency of the DPOAE

"consist[s] of (a) the actual traveling-wave delay to the f2 frequency place, (b) the cochlear filter delay at the site of generation, near f2, and (c) the backward travel time of the DPOAE from the generation site to the oval window." The reason for the rough equivalence between ½ of the DPOAE latency and the frequency-related latency of the evoked potentials is that ß is approximately 0.5 and the transport time (a and c) is small relative to the filter delay (b).

If the travelling wave delay is equal to the backward travel time, the latency of the DPOAE ($t_e$) can be represented by:

$$t_e = t_f + 2t_b$$

where $t_f$ is the filter delay and $t_b$ is the transport time on the basilar membrane. We are proposing that the frequency-related delay in the steady-state response ($t_s$) is represented by:

$$t_s = t_f + t_b$$

Combining these measurements could provide separate estimates for the transport time and the filter time. The latencies of the oto-acoustic emissions change approximately 7 ms from 10 kHz to 1 kHz (Kimberley et al., 1993; Moulin and Kemp, 1996a). Our data indicate that the latencies of the steady-state responses would change by about 5 ms over the same frequency range. This would suggest that filter build-up causes frequency-related delays of up to 3 ms in the cochlea and that the transport time varies up to 2 ms.

Although illustrating how latency data for emissions and steady-state responses might be related, this analysis overly simplifies the nature of the DPOAE delay. Firstly, the forward and backward transport times are not necessarily equal. Brown et al. (1994) review several different physiological models in the context of how DPOAE latencies change with development. The backward travel time may be very brief if it is based on a compression wave (cf., Sutton and Wilson, 1983). Moulin and Kemp (1996b) have presented evidence supporting the idea that the return time of the DPOAE is significantly shorter than its forward latency. A second major difficulty in the analysis concerns the location on the basilar membrane responsible for generating the DPOAE s. Moulin and Kemp (1996b) demonstrated that different DPOAE s (e.g., $2f_1$-$f_2$ or 2F2-F1) are likely generated in different cochlear locations. Third, it is not clear that the return path is direct. Shera and Fuinan (1999) have recently reviewed our understanding of the delays measured for the DPOAE s. They suggest that the 'sources' of the backward traveling

waves are locations on the basilar membrane characterized by non-linear electromechanical distortion. In this view, both stimulus frequency and distortion product emissions ultimately arise from linear reflection at these locations. The reflected energy derives from the stimulus-evoked travelling wave for stimulus-evoked emissions and from the nonlinear processing at regions of overlap between the $f_1$ and $f_2$ sounds for distortion product emissions.

Clearly, we shall have to understand the nature of DPOAE latency more fully before we can combine it with the latency of the steady-state response to determine the relative contributions of transport and filtering to cochlear delays. Using the same stimuli to evoke both the emissions and the steady-sate responses might decrease the number of variables and simplify the relations between these physiological responses. This approach would lead to examining the steady-state responses to cochlear distortion products (e.g., Chertoff and Hecox, 1990; Rickman and Chertoff, 1991) or the emissions evoked by amplitude-modulated tones.

Effects of Intensity

The latency of wave V of the click-evoked auditory brainstem response increases from 5.5 ms to 8.5 ms as the intensity is decreased from 70 dB to 20 dB above threshold. Eggermont and Don (1980) considered this latency change in light of derived response studies. Part of the change can be attributed to a shift in the region of the cochlea that contributes most prominently to the response. At high intensities the basal end of the cochlea dominates but at low intensities the region of the cochlea mediating frequencies near 1000 Hz dominates. However, this can only account for about 1 ms of the change and there remains an intensity-related change about 2 ms that occurs for each derived band response. Several factors contribute to this residual latency change. There might be a small place shift within the narrow band of frequencies responsible for the response. There might also be some change in the ß parameter such that the higher intensity clicks evoke responses earlier on the rise time of the synaptic activation. There might be further effects of refractoriness and synchronization (cf. steps 3 and 4 in our model). Finally, there might be some increased latency in the brainstem pathways due to decreased efficiency of synaptic transmission when fewer afferent fibers are activated and firing of the postsynaptic cells is nearer threshold. The steady-state responses show a latency change of 2.4 ms from 75 to 35 dB SPL (roughly equivalent to 65 and 25 dB HL). We have suggested that steady-state responses are little affected by the ß parameter and the effects of refractoriness and synchronization. This

leaves synaptic transmission in the brainstem as a likely cause of the intensity-related delay.

A place shift in the cochlea probably contributes significantly to the change in our latencies with intensity. Our stimuli were pure tones rather than broad-band stimuli and we did not try to eliminate the effects of pace shift by using derived response masking techniques (which would be problematic with the multiple stimulus approach). Studies using the cochlear microphonic (Honrubia and Ward, 1968) and intracellular recordings from the hair cells (Zwislocki, 1991) have clearly shown that the activation pattern of a pure tone on the basilar membrane shifts towards the stapes with increasing intensity.

Latency changes with intensity can also be mediated by changes in rise time of the post-synaptic potential. With louder sounds, the synaptic potential rises more rapidly either because the release of synaptic transmitter at each synapse is greater or because of more synapses being simultaneously activated. The effects of intensity on the latency means that close attention must be paid to calibrating the stimuli. This is a particular problem when using ear-inserts since the intensities of the stimuli with carrier frequencies of 6000 Hz are 20 dB lower than those of with lower carrier frequencies. In Experiment 7, the data at 6000 Hz (Figure 4-1) probably over-estimate the actual latencies by 0.5-1.0 ms. One way to eliminate the confounds of intensity might be to use continuous tones which are partially amplitude-modulated (Moller, 1975,1985). The ongoing tone maintains the post-synaptic neuron near threshold and the modulation brings it immediately over or under the threshold. The latency then does not change significantly wit the intensity of the tone since the post-synaptic neuron does not have to reach threshold from a resting level. Responses to transient stimuli show much larger latency effects because the silence between the stimuli allows the post-synaptic membrane to return to resting polarization levels. Our tones were 100% AM and may have been similar to transient stimuli in this regard. It will be interesting to see if we can decrease or remove the intensity effects using 30% amplitude-modulated tones.

The responses with carrier frequencies 500 and 750 Hz tended to be lower in amplitude than the others. We have obtained similar results in other experiments (Chapters 1 and 2). Part of this might be caused by the lower effective intensity of these stimuli (since HL thresholds are a little higher at 500 and 750 Hz than at the higher frequencies). Another contributing factor may be the fact that these low carrier frequencies evoke an activation pattern on the basilar membrane that covers a greater spatial extent than the higher carrier frequencies. Because neurons along a

broad area of the basilar membrane all respond to the same low carrier frequency, some of the neurons responding might be activated significantly earlier than others. The resultant latency-jitter of the responses might attenuate the amplitude of the compound response.

Gender effects

The auditory brainstem response shows consistent latency differences with gender. Wave V elicited by clicks is in general 0.2 ms later in males subjects than in female subjects. When considering derived responses, male subjects show a longer latency difference between the responses of the basal turn and the responses from the apical turn. Don et al. (1993) interpreted these gender-differences in terms of two effects. The first was related to faster cochlear delay times in females caused by the shorter length (and greater stiffness) of the basilar membrane (Sato et al., 1991). For the 700-Hz derived response this would account for 0.5 ms difference between male and females subjects. The second process accounting for a further 0.2 ms difference could be explained by gender-differences in the size or the length of the auditory nerve, or by changes in the synchronization of the responses caused by the faster travelling wave velocity. Our findings for Experiments 5 and 7 also suggested a gender-related difference in latency with male subjects having longer latencies than female subjects; however, the data contained considerable inter-subject variability and did not show any clear differences in this effect across the different carrier-frequencies.

Effects of Pathology

Measuring the phase and latency of auditory steady-state responses should increase our understanding of the underlying cochlear and neuronal mechanisms. It is also possible that such measurements may help evaluate patients with cochlear dysfunction. A main problem in such applications will be the reliability of the data. Close attention to relaxing the subjects and to eliminating artifacts improves the quality of the data. With experience, our inter-subject variance has gone down (compare the standard deviations of Table 4-3 from earlier studies with those of Table 4-2). The latency estimates are quite stable from one measurement to the next (Table 4-4). However, the limits of normal (a normal subject may change up to 0.5 ms or more from one measurement to another) may be greater than the changes that occur due to changing clinical conditions. For example, Munro et al. (1995) suggested that changes in the range of 0.3 ms may need to be detected in the case of endolymphatic hydrops—in the treatment of hydrops the

change in latency would be in the other direction.

In patients with endolymphatic hydrops there may be decreases in the transport time due to increased pressure levels across the basilar membrane. The general idea is that the increased stiffness of the basilar membrane will decrease the transport time. Thornton and Farrell (1991) used the derived auditory brainstem response to measure the latency (and hence the travelling wave velocity) at different locations on the basilar membrane. They found that the velocity was greater than normal in the high frequency regions of the cochlea. However, it should also be noted that sensorineural hearing loss causes a broadening of the tuning curves of the auditory nerve fibers (e.g., Dallos and Harris, 1978) and this will decrease the filter-time and cause an earlier response (Eggermont, 1979a; Don et al., in press). It is therefore important in Meniere's Disease to disentangle the effects of transport time (hydrops) and filter time (hair cell damage). The latency changes in the physiological responses in patients with Meniere's Disease seem to occur independently of filter changes that might be caused by hair cell damage (Thornton and Farrell, 1991; Kim et al., 1994; Donaldson and Ruth, 1996). Nevertheless, reliably measuring the small latency changes with the ABR is technically very difficult (Munro et al., 1995) and electro-cochleographic measurements of the relative size of the summating potential and the action potential (e.g., Margolis et al., 1995) remains the most commonly used electrophysiological aid to the diagnosis of Meniere's Disease. It is possible that measuring the latencies of the steady-state responses might provide some diagnostic help in patients with Meniere's Disease. It is also likely that the application of MASTER to pathological cases will result in both amplitude and phase abnormalities in the responses, and that these effects can be disassociated. However, we have not yet determined whether the measurements will be sufficiently reliable for clinical use.

## SUMMARY

The latencies of the human auditory steady-state responses to AM tones change significantly and consistently with the carrier frequency, with the latencies being shorter for higher carrier frequencies. The latency changes 5.5-6.0 ms when the carrier changes from 500 to 6000 Hz (e.g. Table 4-2). This change appears to be mainly due to two cochlear processes: the transport time for the acoustic energy to reach the responsive region of the basilar membrane and the filter buildup time of the hair-cell transduction process.

# SUMMARY & FUTURE CONSIDERATIONS

## SUMMARY

The research reported in this thesis provides a strong foundation which should enable researchers in both the clinical and research communities to rapidly advance the MASTER technique. Several areas of this material may been seen as major contributions to the field.

The literature contains an increasing number of articles that report larger responses, for MM compared to AM stimuli, as initially found by Cohen et al. in 1991. Since this initial study, there has been little insight into the mechanisms behind this augmentation of response amplitude. The demonstration that the MM response can be deconstructed into the vector sum of the individual responses to AM and FM stimuli, should now enable researchers to use MM stimuli more successfully (by choosing appropriate phase-values for the carrier-frequencies being tested).

The introduction of IAFM stimuli enables the simultaneous, and relatively independent, testing of both the AM and FM processing systems. Since AM, FM, and IAFM stimuli can be presented at rates that approximate the formant transitions found in natural human speech, it is likely that we will soon be able to develop objective measures of the processing deficiencies that lead some individuals to experience difficulties in the discrimination of speech. These objective measurements should help in accurately diagnosing the pathology of a patient, in monitoring the function of hearing aids, and in designing better hearing aids, based upon the added knowledge that we may gain with respect to whether certain types of pathology (e.g., deficiencies in particular bands) are more related to processing-problems than others.

The latency data of Chapter 4, similarly, are very useful since many authors treat the issue of phase superficially: making brief references to the phase values, and returning to the amplitude data as quickly as possible. This is the only study that has extensively explored the issue of phase with respect to steady-state responses since the initial studies by Regan, Diamond, and Bijl, which occurred over 15 years ago.

Researchers may now more sensibly evaluate the phase values that exist in their data and thereby obtain more useful information from their studies. Clinically, this chapter may also be useful if it is found that the frequency-specific latencies of the steady-state potentials can be used, similarly to the stacked derived-band ABR technique, to more accurately detect changes in latency which often occur in the case of acoustic neuromas and Meniere's disease (Thornton and Farrell, 1991; Don et al. 1997). However, this may be somewhat difficult as described later in this section.

The most important contribution of this thesis was undoubtedly the creation of the user-friendly MASTER data collection system using LabVIEW software, as described in Chapter 2. The ability to easily create various experiments, which would have taken many additional months of programming only 5 years ago, enabled us to investigate many aspects of the steady-state technique as fast as we could come up with the ideas for the experiments. Additionally, the technological capacities of today's PCs easily enabled us to store the raw data for subsequent analysis rather than having to iteratively change our programs and repeat experiments.

Further, the system has enabled us to begin to disseminate a valuable tool into the hands of a larger scientific community. Rather than fitting inside a PC, the original MASTER data collection system existed in a large metal rack and was, by far, the largest piece of hardware in our laboratory: it used a considerable amount of specialized hardware to do what we now can do much more cost-effectively and efficiently in software. The creation of a system which is small, inexpensive, and uses commercially available hardware has enabled us to provide over 9 MASTER data collection systems to researchers located around the world. As hoped, the technique has already benefited from the unique talents and specialization of other researchers, and has been used to investigate such topics as cortical re-organization due to hearing-loss in animal models, and to evaluate the hearing of various clinical populations.

## FUTURE CONSIDERATIONS

The work in this thesis has formed the foundations for this young technique. The Do's and Don'ts are well established. There are obviously many directions that future research may follow. Several of these are of primary interest to me.

### *Biomedical Engineering Challenges*

A major challenge of the technique is to reduce the recording time even further. Currently, determination of threshold requires about 30 minutes. The likelihood that this technique would be used clinically in a more routine manner, or even as a screening test, would be greatly increased if the time required was reduced to the 10 or 15 minute range. Several approaches may possibly work well in this regard. Initial results in our laboratory indicate that weighting the epochs according to their noise levels seems to shorten the time required to obtain significant responses.

Another challenge is to design automatic threshold seeking algorithms for the technique that are sensitive to the statistical problems of multiple comparisons. Currently, by using a pre-determined amount of time, for example 6 minutes, the statistical test does not suffer from the same problems as if the test results were evaluated 18 times over that 6 minute duration. In other words, we do not have to correct for the issue of multiple comparisons by using something akin to a Bonferroni correction factor. Since the responses are evaluated using running averages, rather than relying on separate data sets, the statistical objections may possibly be less pronounced, yet these still have to be addressed satisfactorily.

Within the context of a threshold seeking technique another issue immediately arises. What if a particular stimulus becomes significant prior to the responses to other stimuli that are being tested? For example, what if the 1000 Hz stimuli evokes a significant response prior to the 2000 and 4000 Hz stimuli? What is the next step? If the intensity of the different stimuli were controlled independently, and physically combined prior to their arrival at the acoustic transducer, then the intensity of stimuli, which had already produced a significant response, could be independently decreased. However,

presenting the 1000 Hz tone at 30 dB SPL while the 2000 Hz and 4000 Hz stimuli are presented at 50 dB SPL may increase the probability of interaction between stimuli due to, for example, masking. Appropriate studies investigating these possible interactions are easy to design and will quickly show whether or not these sorts of interactions will hinder the independent modulation of the intensity of a single tone, within the multiple-tone stimulus, using the MASTER technique.

*Non-Linearities*

The topic of non-linearities is addressed in this thesis mostly with respect to the compressive rectification which occurs in the cochlea and causes responses to appear at the frequencies of modulation. Chapter 1 further delves into the issue of non-linearities by highlighting the fact that non-linearities may act to reduce steady-state response amplitudes due to interference by energy related to the distortion products (see Figures 1-1 and 1-10). The modulation of multiple narrow-band noise-stimuli, rather than tone-stimuli, may be less prone to the destructive effects of energy from distortion products, since these will be minimized and will be spread across the spectrum. Accordingly, even though a single narrow-band noise-stimulus produced a slightly smaller response than the use of a single pure tone, response amplitudes produced when multiple noise stimuli are presented simultaneously, may be larger than those evoked by a multiple-tone stimulus.

Additionally, while some of our models incorporate non-linear mechanisms, the ways in which the components interact is linear, for example, the values from each stage are added or multiplied together (See Figures 1.7 and 4.1). While our models provided useful insights, the factors that led to our results may have been further clarified by a greater consideration of non-linear systems theory. For example, the enhancement that we noted for upward sweeps over downward sweeps may have possibly been explained by the phenomenon of non-linear resonance: equal driving forces (for example, the energy of the upward an downward sweeps) produced two different "solutions" (i.e., the response amplitudes). Since non-linear resonance occurs due to the history of the stimulus, the instantaneous energy of the stimulus in the middle of the sweep may have

resulted in a large amplitude or small amplitude response due to the bi-stability of the system.

Nevertheless, the findings may be well explained using a linear rather than nonlinear analysis. Firstly, the vector addition of the AM and FM response seems to reasonably predict the MM response, in other words it is *having the correct phase, rather than the largest amplitude* that is the characteristic of the upward sweep FM stimulus that seems to cause the MM response to be bigger for the upward rather than downward sweep (See Figures 3-7 and 3-8). Secondly, as is shown in Figure 3-5, the MM stimulus (where the upward FM sweep was aligned with the maximum of the AM envelope) created a larger response at all frequencies, except for 6000 Hz. If the upwards FM sweep was causing the MM stimulus to activate the higher "well" of resonance, then it seems unlikely that this could occur within each of the rather limited frequency ranges activated by the 7 carrier-frequencies (each of which demonstrated a larger response for the upward sweep). Additionally, the results shown in Figure 3-4 of Chapter 3, obtained to FM depths being decreased from 20% to 2% shows a roughly linear decrease with modulation depth. The role of non-linear resonance in the processing of FM stimuli would ostensibly be demonstrated by an exponential decay, or a peak in the amplitude response curve. In other words, a 20% FM stimulus would have an increased chance of activating a non-linear resonant response (either in the cochlea or the brainstem), compared to a stimulus presented at only 2% FM. However, physiologically, upward sweeps produce larger responses than downward sweeps, and behaviourally, facilitation is often found. Since upward and downward sweeps contain the same frequency content, the phenomenon has the classic signature of a non-linear resonant system. Accordingly, further investigation of this area is merited.

*Caveats*

Prior to discussing several clinical areas where the MASTER technique may be applied, some mention should be made about the differences between studying normal and pathological hearing systems. As discussed in the introduction of this thesis, the data presented here were collected using individuals with normal hearing. Accordingly, the

data often accurately reflected quite subtle changes in stimulation parameters, such as small changes in FM or AM depth. When applying the MASTER technique to clinical populations, the effects of various experimental manipulations may not be as clear (i.e., robust) as were obtained in this thesis, using subjects with healthy ears. The statistical software packages used here provided us with power analyses for each of our experiments. In investigations concerning pathology, where smaller effects may be expected, attention should be paid to these power values in order to ensure that negative results are not occurring due to insufficient sample sizes.

Additionally, in patients with hearing loss, pathological characteristics such as broad tuning curves may cause their responses to be different than those presented here. Possibly, the MASTER technique may not perform as well in some patient populations. If the interactions between stimuli are large, incorrect information, such as false negative responses, may result. As pointed out in the introduction, in an initial study on young subjects with normal and aided hearing some responses recorded using the MASTER technique indicated an effect of interaction between stimuli (Picton et al, 1998). However, as discussed by these authors, since natural sounds normally have multiple frequencies, the results obtained using MASTER may reflect what is occurring when a subject hears sounds outside of the clinic.

Further, dichotic stimulation were used in a number of experiments in this thesis. For each set of experiments that used dichotic stimulation, we ensured that the parameter being tested was similar when stimuli were presented to a single ear or to both ears. In studies of pathology, binaural interaction or the lack thereof, must be determined prior to simultaneous testing of both ears. The use of dichotic stimulation in patients with pathological hearing systems, especially if more central mechanisms may be affected, should be approached with caution.

Lastly, the use of higher intensity stimuli should be approached with caution. During a pilot investigation of the technique, we recorded responses from a patient with acoustic neuroma in order to investigate changes in phase (i.e., latency) that may accompany the presence of a tumor. Several of the patient's responses at 65 dB SPL did not reach significance, and thus latency data could not be computed on those responses.

Because steady-state stimuli are continuous, the simple solution of increasing the intensity to 80 dB SPL or more should be approached with caution since presenting multiple stimuli at this level for prolonged periods might cause both discomfort to the subject, and could also lead to threshold shifts. Additionally, in order to compare pathological responses to normal values, data for healthy subjects would also have to be collected at these relatively high intensity levels. While the MASTER technique is clearly very powerful, its development as a clinical assessment tool will likely present some interesting challenges in the case of certain disorders.

*Clinical Applications*

Several exciting clinical applications of the MASTER technique should be evaluated. For example, the work in this thesis showed that the AM and FM channels are relatively independent and can therefore give us two different types of meaningful information about the processing of the auditory system. In addition to thresholds of intensity, thresholds which rely on depth of modulation, using supra-threshold stimuli, may prove as useful measure in objective evaluations of both AM and FM sensitivity.

In Chapter 3, Figure 3-11 shows that AM and FM for a particular carrier frequency region can both be presented together at different rates. It is attractive to think about using this type of information, for example, for developing population norms for a type of FM/AM ratio. Since both responses are recorded at the same time, under identical stimulus conditions, this type of ratio would not be prone to the problems inherent in recording these responses separately where small changes, such as the position of an earphone, might cause significant changes in the recorded response. Using both AM and FM stimuli may enable us to obtain objective information which may be related to processing of speech, especially at faster rates of modulation or different modulation depths.

Chapter 4 showed that the phase of the steady-state responses could be reasonably converted into latency using our proposed preceding-cycles technique. The intra-subject variability, of the latencies of various carrier frequencies, was fairly low and could serve as normative values by which to compare clinical populations. Because transient

techniques, using derived band responses, have been used to detect small acoustic neuromas (where the latencies are increased, for example, due to associated demyelination) and Meniere's disease (where the latencies are decreased due to compression of the basilar membrane), it is obviously interesting to speculate that the MASTER technique might be able to demonstrate some success in these areas as well. Various issues related to these clinical applications of the technique were discussed in Chapter 4, in the section entitled "Effects of Pathology".

Lastly, as discussed in Chapter 4, we have recorded steady-state responses at rates near 200 Hz. Although not described in the thesis, a pilot study has provided preliminary evidence that indicates that, at faster modulation rates, older subjects with hearing loss show decreased responses. The generation of age related modulation-rate transfer functions for both AM and FM may prove to be clinically useful in assessing different kinds of hearing pathology, which currently are studied using such techniques as gap detection.

Clearly, there are several areas in which the MASTER technique may now be evaluated relatively easily. While the MASTER technique was originally investigated as a method of evaluating thresholds for AM stimuli, during the course of this thesis, we have obtained results that have additionally suggested several equally important applications of the technique. It is likely that the MASTER technique will continue to generate exciting findings both inside and outside of the laboratory for some time, and will soon come to serve as an exciting tool of objective audiometry.

# Appendix A

## MODELING THE DATA FROM EXPERIMENT 3 OF CHAPTER 1.

In this appendix we provide additional information concerning the modeling done in Chapter 1, Figure 1-7. The figure plots the results obtained in Experiment 1, for a probe tone at 1 kHz, when a masker was presented at different frequencies. We attempted to understand the results by dividing the curve into components based on known physiological and physical phenomena. In order to do this we entered data from the experiment into the first 2 rows of an excel spreadsheet, as is shown in Table A-1. Rows 4-7 contain the values that would result given an input of 1. As the input passes through each process, the effect was mimicked by letting each value have a multiplicative effect.

**Table Appen-1**

| CF | **0.5** | **0.75** | **0.9** | **0.95** | **1** | **1.05** | **1.1** | **1.2** | **1.35** | **1.5** | **2** |
|---|---|---|---|---|---|---|---|---|---|---|---|
| DATA | 1.39 | 1.22 | 1.12 | 0.51 | 0.79 | 0.48 | 0.51 | 0.66 | 0.80 | 1.05 | 0.99 |
| INPUT | 1 | 1 | 1 | 1 | 1 | 1 | 1 | 1 | 1 | 1 | 1 |
| BM | 0.9 | 0.83 | 0.79 | 0.37 | 0.46 | 0.84 | 0.95 | 0.98 | 1 | 1 | 1 |
| INT | 0.79 | 0.79 | 0.79 | 0.79 | 1 | 0.79 | 0.79 | 0.79 | 0.79 | 0.79 | 0.79 |
| SUP | 0.9 | 0.98 | 1 | 1 | 1 | 0.43 | 0.41 | 0.53 | 0.66 | 0.91 | 0.97 |
| RES | 2.17 | 1.91 | 1.80 | 1.76 | 1.71 | 1.68 | 1.65 | 1.60 | 1.53 | 1.46 | 1.29 |
| MODEL | 1.39 | 1.22 | 1.12 | 0.51 | 0.79 | 0.48 | 0.51 | 0.66 | 0.80 | 1.05 | 0.99 |

KEY:

CF = carrier-frequency(kHz) AMP = amplitude of probe INPUT = input

INT = interference effects BM = basilar membrane SUP = suppression

RES = residual MODEL =Result of input with each cell of column.

Table A-1: The amplitude values obtained for the probe at different values of the masker carrier-frequency are shown. The cells were set up in Excel and the cells of the columns were allowed to have a multiplicative affect. Using the first column of data as an example, 0. 9 * 0.79 * 0.9 * 2.17 results in a final value of 1.39, which is the value of the data obtained for the probe when the masker was at 0.5 kHz.

The aim of the model is to explain the empirical data by inserting reasonable values for each row, so that the modeled response will agree with the empirically obtained data. The first component of the model takes into account the effects of the mechanical motion of the basilar membrane (e.g., due to the activation pattern of the traveling wave). The activation pattern of the traveling wave is asymmetrical. Its amplitude decreases rapidly toward the low frequency regions of the basilar membrane and more slowly towards the high frequency regions. When the activation patterns of two stimuli overlap, the envelopes of their traveling waves add together. The inner hair cells located in an area of overlap will respond to the result of the interaction between the two stimuli in that area.

The decrease seen for the response to the probe will depend on the differences between the frequencies of the masker and the probe. Since the traveling wave is asymmetrical the resultant curve will also be asymmetrical: it should resemble a horizontal mirror image of the activation pattern of the traveling wave as is suggested by the mirror image responses of the masker and probe response seen in the noise data of Figure 1-6. Considering only the effect of the basilar membrane component, the lowest point on the traveling wave function (the largest decrease in the amplitude of the probe) should occur when the masker tone has the same frequency as the probe since that will cause the greatest interference in the synchronicity. The probe amplitude is modeled as decreasing to about 65% of the amplitude of the responses obtained when the probe stimulus was presented alone.

The second component of the model considers the effect of interference between the acoustic stimuli. It is likely that tones of 0.95, 1 and 1.05 kHz stimulate quite similar groups of inner hair cells in the basilar membrane. Why might there be a decrease in the response when the masker is in this range? A possible mechanism is the phenomenon of wave interference. When two sine waves of different frequencies are added together, the area occupied by the resultant wave contains beats, and is therefore smaller then the area occupied by two equal waves of the same frequency and phase added together. In other words, there will be less energy to be modulated since this has been transferred to the beat frequency. For two tones added together, the decrease is about 71% as is shown in this simple MATLAB program.

```
%program to calculate energy of beat compared to pure tone.
t=1:.0001:20;                          %define sr of 1000 Hz;
%Define 2 sine waves
sig1=sin(2*pi*98*t);                   %98Hz sine wave
sig2=sin(2*pi*100*t);                  %100 Hz sine wave

%Plot sine waves
subplot(3,1,1),plot(t(1:8000),sig1(1:8000));
subplot(3,1,2),plot(t(1:8000),sig2(1:8000));

%create beat
sig3=sig1+sig2;                        %create beat by adding sine waves
subplot(3,1,3),plot(t(1:8000),sig3(1:8000));

v1=sqrt(var(sig1));                    %RMS of sine wave=.7071
v2=sqrt(var(sig2));                    %RMS of sine wave=.7071
v3=sqrt(var(sig3));                    %RMS of beat wave=1
v4=v3/(v1+v2);                         % RMS of a beat is 1 rather than
                                       2*0.071 or 1.4142, and 1/1.4142=.071.
```

As more tones are added together there will be further decreases in the energy to be modulated, since more beats are created. For example, in Chapter 1, Figure 1-1 (column 2, bottom row), some effects of rectification on the energy of a multiple-steady-state stimulus were modeled: the formation of beats due to the interaction of two (or four) carrier-frequencies causes the energy at the frequencies of modulation to be decreased. However, since the experiment done in Chapter 1 only used a probe and a single masker, the effect can reasonably be set at 71%. In our model, we set this interference effect at 79% (about 20% attenuation), rather than 71% (about 30% attenuation), since the compression that occurs, as the intensity of a stimulus increases, would act to decrease this attenuation.

The third effect that is considered is the well-known effect of two-tone suppression which is defined as a reduction in the response to a tone due to the presence of a second tone (Galambos and Davis, 1943; Sachs and Kiang, 1968). As discussed in the chapter, two-tone suppression is likely a cochlear phenomenon since it persists after sectioning the auditory nerve central to the site of recording (Kiang et al, 1965). Two-tone suppression is also a frequency-specific phenomenon. Although, maskers with frequencies either

above or below the frequency of the probe can suppress the response to the probe, at moderate intensities, the suppression is greater when the suppressing tone is higher in frequency (Harris, 1979; Arthur 1971).

3. **Residual**

When comparing (i.e., subtracting) the data from the three components discussed above to the actual data, a residual effect persists. The general characteristics of the effect is of an amplification. This effect is larger for maskers with frequencies lower then the probe as opposed to two-tone suppression. It appears to be less frequency specific in that it is characterized by a wider frequency range than two-tone suppression. As discussed in Chapter 1, synchrony enhancement has been postulated by other researchers who have obtained similar results (Dolphin, 1994).

# Appendix B

## THE EQUIVALENCE OF DIFFERENT METHODS FOR MEASURING LATENCY.

The basic technique of apparent latency is to measure the slope of the phase versus frequency plot (Regan, 1966; Regan, 1989, p 42). The only constraints are that the slope should be consistent across the stimulus frequencies examined, and that effects of physiological filtering on the response phase should be compensated prior to the calculations (Regan, 1989, p 29). Diamond (1977) proposed a simple graphic way to estimate apparent latency. This is illustrated schematically in Figure Appen-1 using modeled data. The latency of a particular peak in the steady-state response is plotted as **T** along the x-axis against the interstimulus interval plotted as **t** along the y-axis. A line joining the latencies is then extended to intercept the x-axis at a latency **L** equivalent to the apparent latency. Using two points (A and B) for simplicity, the slope of the line is:

$$(t_B-t_A)/(T_B-T_A)$$

and the equation for the intercept is

$$L = T_B-t_B(T_B-T_A)/(t_B-t_A)$$

If we substitute into this equation

$$T_X=\theta_X/(360F_X)$$

and

$$t_X=1/F_X$$

where $\theta$ is the phase delay of the response at the chosen peak and **F** is the frequency of stimulation, we can simplify the equation to obtain:

$$L=(\theta_A-\theta_B)/(360(F_A-F_B))$$

which is the definition of apparent latency.

The technique described in Chapter 4 measures the latency as:

$$L=\theta_A/(360F_A)+N/F_A$$

where N is an integer chosen so that both measurements (A and B) give the same value

$$\theta_A/(360F_A)+N/F_A = \theta_B/(360F_B)+N/F_B$$

This equation can be recast by bringing both phases over to the left, adding $\theta_B(F_A-F_B)/360$ to both sides and then dividing by $F_B(F_A-F_B)$ to give:

$$(\theta_A-\theta_B)/(360(F_A-F_B)) = \theta_B/(360F_B)+N/F_B$$

This makes the measured latency (on the right) equal the apparent latency. The only difference between the two techniques is that apparent latency allows non-integer values of N.

---

*Please see next page for figure.*

**Figure Appen-1: Graphic estimation of apparent latency.** This figure illustrates the technique used by Diamond (1977) to estimate the apparent latency of a steady-state response. The responses are plotted on the Y-axis according to the inter-stimulus interval. A line drawn between homologous peaks in these responses, e.g., A and B, is extended to the X-axis, and the apparent latency (L) is estimated at the intercept.

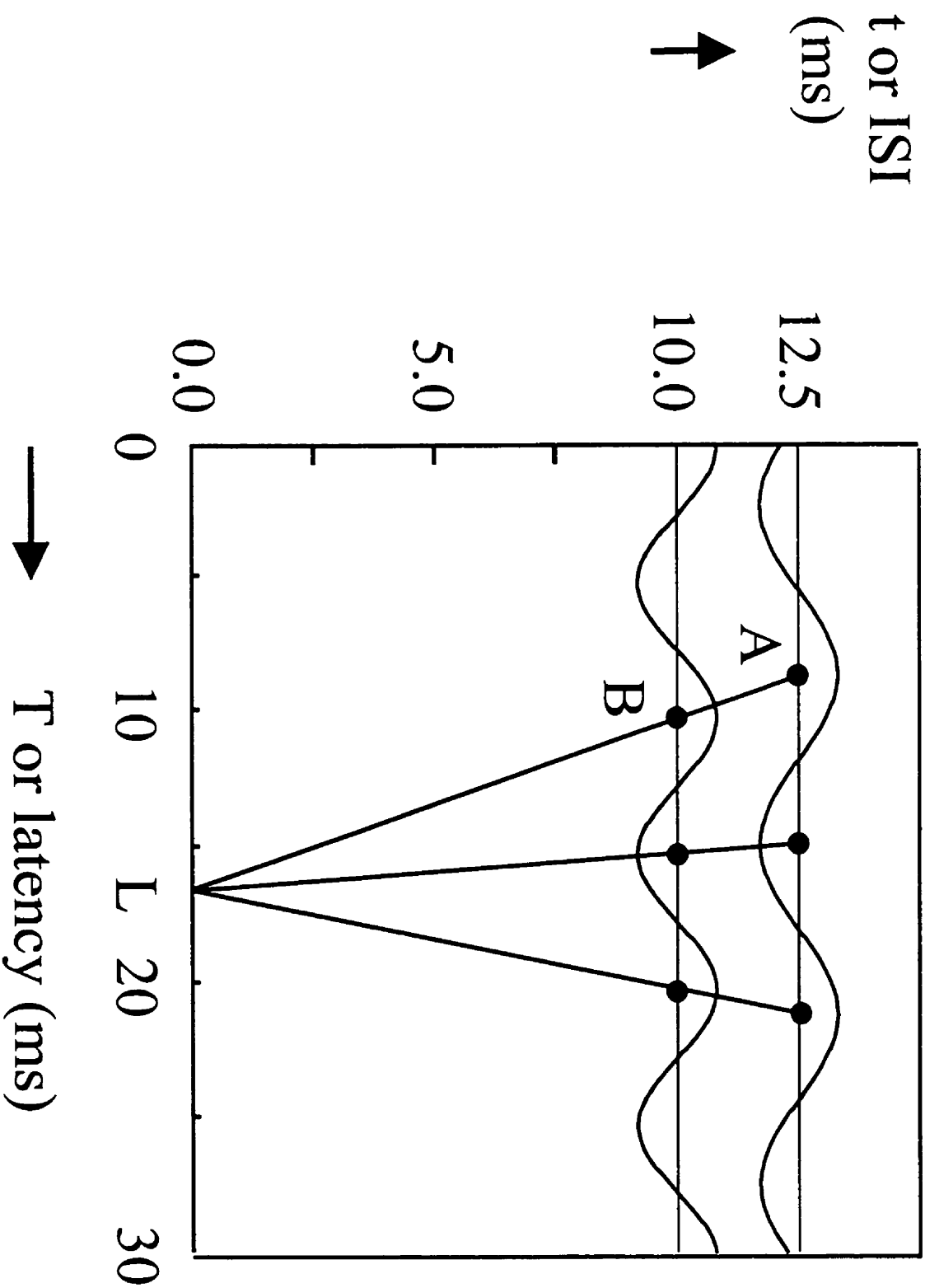
t or ISI
(ms)
12.5
10.0
5.0
0.0
0
10
L 20
30
T or latency (ms)
A
B

THIS PAGE INTENTIONALLY LEFT BLANK

# REFERENCES


Aoyagi, M, Yoshinori, K, Suzuki, Y, Fuse, T, and Koike, Y., (1993). Optimal modulation frequency for amplitude-modulation following response in young children during sleep. *Hear Res*;65:253-261.

Aoyagi, M., Kiren, T., Furuse, H., Fuse, T., Suzuki, Y., Yokota, S., and Koike, Y., (1994). Pure-tone threshold prediction by 80-Hz amplitude-modulation following response. *Acta Otolaryngol Suppl*; 511:7-14.

Arthur, RM, Pfeiffer, RR, and Suga, N., (1971). Properties of 'two-tone inhibition' in primary auditory neurones. *J Physiol;* 212:593-609.

Aslin, R. N. (1989). Discrimination of frequency transitions by human infants. *JASA* 86, 582-590.

Azzena, G.B., Conti, G., Santarelli, R., Ottaviani, F., Paludetti, G., and Maurizi, M., (1995). Generation of human auditory steady-state responses (SSRs). I: Stimulus rate effects. *Hear. Res.;* 83, 1-8.

Bacon, S.P., and Viemeister, N.F. (1985). Temporal modulation transfer functions in normal-hearing and hearing-impaired listeners. *Audiology;* 24, 117-134.

Bardt, T.F., Unterberg, A.W., Kiening, K.L., Schneider, G.H., and Lanksch, W.R., (1998). Multimodal cerebral monitoring in comatose head-injured patients. *Acta Neurochirurgica*; 140, 357-365.

Basar, E., Rosen, B., Basar-Eroglu, C., and Greitschus, F., (1987). The associations between 40 Hz-EEG and the middle latency response of the auditory evoked potential. *Int. J. Neurosci.*; 33, 103-117.

Bijl, G.K., and Veringa, F., (1985). Neural conduction time and steady-state evoked potentials. *Electroencephalogr. Clin. Neurophysiol.*; 62, 465-467.

Bowman, D.M., Brown, D.K., Eggermont, J.J., and Kimberley, B.P., (1997). The effect of sound intensity on f1-sweep and f2-sweep distortion product otoacoustic emissions phase delay estimates in human adults. *JASA*; 101, 1550-1559.

Brown, P.B., Franz, G.N., and Moraff, H., (1982). *Electronics for the modern scientist*. Elsevier, Amsterdam.

Budai, D., Kehl, L.J., Poliac, G.I., and Wilcox, G. L.,(1993). An iconographic program for computer-controlled whole-cell voltage clamp experiments.

*Journal of Neuroscience Methods*; 48, 65-74.

Carney, L.H., (1993). A model for the responses of low-frequency auditory-nerve fibers in cat. *JASA*; 93, 401-417.

Cohen, L.T., Rickards, F.W. and Clark, G.M., (1991). A comparison of steady-state evoked potentials to modulated tones in awake and sleeping humans. *JASA;* 90, 2467-2479.

Colombo, J., and Horowitz, F. D. (1986). Infants' attentional responses to frequency modulated sweeps. *Child Dev.;* 57, 287-291.

Cooper, NP., (1996). Two-tone suppression in cochlear mechanics. *JASA*; 99:3087-3098.

Corey, D.P., and Hudspeth, A.J., (1983). Analysis of the microphonic potential of the bullfrog's sacculus. *J. Neurosci.*; 3, 942-961.

Dallos, P., (1973). Nonlinear distortion. In: *The auditory periphery.* New York: Academic Press, 1973 391-464.

Dallos, P., (1985). Response characteristics of mammalian cochlear hair cells. *J. Neurosci.*; 5, 1591-1608.

Dallos, P., and Cheatham, M.A., (1971). Travel time in the cochlea and its determination from cochlear- microphonic data. *JASA* 49, Suppl 2:1140+.

Dallos, P., and Harris, D., (1978). Properties of auditory nerve responses in absence of outer hair cells. *J. Neurophysiol.*; 41, 365-383.

Dancer, A., (1992). Experimental look at cochlear mechanics. *Audiology*; 31, 301-312.

Dauman, R., Szyfter, W., Charlet de Sauvage, R., and Cazals, Y., (1984). Low frequency thresholds assessed with 40 Hz MLR in adults with impaired hearing. *Arch Oto-Rhino-Laryngol* ;240:85-89.

Davis, C., Mazzolini, A., and Murphy, D., (1997). A new fibre optic sensor for respiratory monitoring. *Australasian Physical and Engineering Sciences in Medicine*; 20, 214-219.

Delgutte, B., (1990). Physiological mechanisms of psychophysical masking: Observations from auditory-nerve fibers. *JASA*; 87:791-809.

Delgutte, B., (1996). Physiological models for basic auditory percepts. In:

Hawkins HL, McMullen TA, Popper AN, Fay RR, eds. *Auditory Computation.* Springer: New York, 1996:157-220.

Demany, L., and Clement, S. (1998).The perceptual asymmetry of frequency modulation. In *Psychophysical and Physiological Advances in Hearing,* edited by A. R. Palmer, A. Rees, A. Q. Summerfield, and R. Meddis, (Whurr, London, UK, 1998), pp. 571-577.

Diamond, A.L., (1977). Latency of the steady state visual evoked potential. *Electroencephalogr. Clin. Neurophysiol.*; 42, 125-127.

Dobie, R.A., and Wilson, M.J., (1998). Low-level steady-state auditory evoked potentials: effects of rate and sedation on detectability *JASA*; 104, 3482-3488.

Dobie, R.A., and Wilson, M.J., (1996). A comparison of t test, F test, and coherence methods of detecting steady-state auditory-evoked potentials, distortion-product otoacoustic emissions, or other sinusoids. *JASA*; 100, 2236-2246.

Dobie, R.A., (1993). Objective response detection. *Ear and Hearing*; 14, 31-35.

Dobie, RA, and Wilson MJ. (1993). Objective response detection in the frequency domain. *Electroenceph Clin Neurophysiol*; 88:516-524.

Dolphin, W.F., (1996). The envelope following response to multi-envelope component stimuli. *Audiology* ;35:113.

Dolphin, W.F., (1997). The envelope following response to multiple tone pair stimuli. *Hear. Res.*; 110, 1-14.

Dolphin, WF, and Mountain, DC., (1993). The envelope following response (EFR) in the Mongolian gerbil to sinusoidally amplitude-modulated signals in the presence of simultaneously gated pure tones. *JASA*; 94:3215-3226

Dolphin,W.F., Chertoff, M.E., and Burkard, R., (1994). Comparison of the envelope following response in the Mongolian gerbil using two-tone and sinusoidally amplitude-modulated tones. *JASA*; 96, 2225-2234.

Don, M., and Eggermont, J.J., (1978). Analysis of the click-evoked brainstem potentials in man unsing high- pass noise masking. *JASA*; 63, 1084-1092.

Don, M., Eggermont, J.J., and Brackmann, D.E., (1979). Reconstruction of the audiogram using brain stem responses and high- pass noise masking. *Annals of Otology, Rhinology, and Laryngology Suppl;* 57, 1-20.

Don, M., Ponton, C.W., Eggermont, J.J., and Masuda, A., (1993). Gender

differences in cochlear response time: an explanation for gender amplitude differences in the unmasked auditory brain-stem response. *JASA*; 94, 2135-2148.

Don M, Masuda A, Nelson R, and Brackmann D., (1997). Successful detection of small acoustic tumors using the stacked derived-band auditory brain stem response amplitude. *Am J Otol*;18(5):608-21; discussion 682-5.

Don, M., Ponton, C.W., Eggermont, J.J., and Kwong, B., (1998). The effects of sensory hearing loss on cochlear filter times estimated from ABR latencies. *JASA*.;104(4),2280-9.

Donaldson, G.S., and Ruth, R.A., (1996). Derived-band auditory brain-stem response estimates of traveling wave velocity in humans: II. Subjects with noise-induced hearing loss and Meniere's disease. *J. Speech Hear. Res.*; 39, 534-545.

Edwards, B. W., and Viemeister, N. F. (1994). Frequency modulation versus amplitude modulation discrimination: evidence for a second frequency modulation encoding mechanism. *JASA* 96, 733-740.

Egan JP, and Hake HW., (1950). On the masking pattern of a simple auditory stimulus. *JASA*; 22,622-630.

Eggermont, J. J. (1979-1979b). Narrow-band AP latencies in normal and recruiting human ears. *JASA* 65, 463-470.

Eggermont, J.J., (1979a). Compound action potentials: tuning curves and delay times. *Scand. Audiol. Suppl.*; 9, 129-139.

Eggermont, J.J., Brown, D.K., Ponton, C.W., and Kimberley, B.P., (1996). Comparison of distortion product otoacoustic emission (DPOAE) and auditory brain stem response (ABR) traveling wave delay measurements suggests frequency-specific synapse maturation. *Ear Hear.;* 17, 386-394.

Eggermont, J.J., and Don, M., (1980). Analysis of the click-evoked brainstem potentials in humans using high- pass noise masking. II. Effect of click intensity. *JASA* 68, 1671-1675.

Elberling, C., (1976). Modeling action potentials. *Rev. Laryngol. Otol. Rhinol. (Bord.) Suppl.*; 97, 527-537.

Erulkar, S.D., Butler, R.A., and Gerstein, G.L. (1968). Excitation and inhibition in cochlear nucleus. II. Frequency-modulated tones. *J. Neurophysiol.;* 31, 537-548.

Fisher, N.I., (1993). *Statistical analysis of circular data*. Cambridge University

Press, Cambridge.

Fisher, R.A., (1929). Tests of significance in harmonic analysis. *Proceedings of the Royal Society (London) Series A*; 125, 54-59.

Formby, C., (1987). Modulation threshold functions for chronically impaired Meniere patients. *Audiology;* 26, 89-102.

Fridman, J., Zappulla, R., Bergelson, M., Greenblatt, E., Malis, L., Morrell, F., and Hoeppner, T., (1984). Application of phase spectral analysis for brain stem auditory evoked potential detection in normal subjects and patients with posterior fossa tumors. *Audiology;* 23, 99-113.

Frisina RD, Smith RL, and Chamberlain SC., (1990). Encoding of amplitude modulation in the gerbil cochlear nucleus: I. A hierarchy of enhancement. *Hear Res;* 44:99-122.

Frisina RD, Smith RL, and Chamberlain SC., (1990). Encoding of amplitude modulation in the gerbil cochlear nucleus: II. Possible neural mechanisms. *Hear Res*; 44:123-142.

Galambos, R., Makeig, S., and Talmachoff, P.J., (1981). A 40-Hz auditory potential recorded from the human scalp. *Proc. Natl. Acad. Sci. U.S.A.*; 78, 2643-2647.

Gardner, R. B., and Wilson, J. P. (1979). Evidence for direction-specific channels in the processing of frequency modulation, *JASA*; 66, 704-709.

Geisler, C. D., Rhode, W. S., and Kennedy, D. T. (1974). Responses to tonal stimuli of single auditory nerve fibers and their relationship to basilar membrane motion in the squirrel monkey. *J. Neurophysiol.;* 37, 1156-1172.

Geisler, C.D., (1998). *From sound to synapse: physiology of the mammalian ear.* New York: Oxford University Press, 1998. pp 169-228

Glasberg, B.R., and Moore, B.C., (1990). Derivation of auditory filter shapes from notched-noise data. *Hear. Res.*; 47, 103-138.

Goldstein, J. L., Baer, T., and Kiang, N. Y. S. (1971) A theoretical treatment of latency, group delay, and tuning characteristics for auditory-nerve responses to clicks and tones. In *Physiology of the auditory system* edited by M. B. Sachs, (National Educational Consultants, Baltimore, MD, 1971), pp. 133-141.

Gordon, M., and O'Neill, W. E. (1998). Temporal processing across frequency channels by FM selective auditory neurons can account for FM rate

selectivity. *Hear. Res.*; 122, 97-108.

Green DM., (1976). *An introduction to hearing.* New York: Wiley, 1976, Nonlinear distortion: pp 182-184 and 235-252.

Gummer, A.W., and Johnstone, B.M., (1984). Group delay measurement from spiral ganglion cells in the basal turn of the guinea pig cochlea. *JASA*; 76, 1388-1400.

Gutschalk, A., Mase, R., Roth, R., Ille, N., Rupp, A., Hähnel, S., Picton, T.W., and Scherg, M., (1999). Deconvolution of 40 Hz steady-state fields reveals two overlapping source activities of the human auditory cortex. *Clin. Neurophysiol.*; 110, 856-868.

Hari, R., Hamalainen, M., Joutsiniemi, S.L., (1989). Neuromagnetic steady-state responses to auditory stimuli. *JASA*; 86, 1033-1039.

Harris, DM., (1979). Action potential suppression, tuning curves and thresholds: comparison with single fiber data. *Hear Res*;1:133-154.

Harrison, R.V., Aran J.M., and Erre, J.P., (1981). AP tuning curves from normal and pathological human and guinea pig cochleas. *JASA*; 69, 1374-1385.

Harrison, RV, (1988), The Biology of Hearing and Deafness, Illinois, Charles C Thomas, 1988, pp 70, 217-219.

Hartmann, W. M., (1998). Signals, Sound, and Sensation (Springer-Verlag, New York).

Hartmann, W.M., (1997). Signals, Sound and Sensation. pp 393-467 (American Institute of Physics, Woodbury, New York, 1997).

Hartmann, W.M., and Hnath, G.M., (1982). Detection of mixed modulation. *Acustica*; 50, 297-312.

Herdman, A.T., and Stapells, D.R. (2000). Thresholds determined using the monotic and dichotic auditory steady-state response technique in normal-hearing subjects. *Scandinavian Audiology.*(In press)

Heyer, E.J., Wald, A., and Mencke, A., (1995). Intraoperative data acquisition for the study of cerebral dysfunction following cardiopulmonary bypass. *Journal of Clinical Monitoring*; 11, 305-310.

Jerger J, Chmiel R, Frost, JD Jr, and Coker, N., (1986). Effect of sleep on the auditory steady state evoked potential. *Ear Hear*; 7, 240-245.

Jerger, J., and Jerger, S. (1970). Evoked response to intensity and frequency change. *Arch. Otolaryngol.*; 91, 433-436.

John, M. S., and Picton, T. W. (2000a). MASTER: A Windows program for recording multiple auditory steady-state responses. *Comput. Methods Programs Biomed.*; 61, 125-150.

John, M. S., and Picton, T. W. (2000b). Human auditory steady-state responses to amplitude-modulated tones: Phase and latency measurements. *Hear. Res.*; 141, 57-79.

John, M.S., Lins, O.G., Boucher, B.L., and Picton., T.W. , (1998). Multiple auditory steady-state responses (MASTER): stimulus and recording parameters. *Audiology*; 37, 59-82.

Johnson G.W., (1997). LabView Graphical Programming: Practical Applications in Instrumentation and Control. 2 ed. (McGraw-Hill, New York, 1997).

Joris, P.X., and Yin, T.C., (1992). Responses to amplitude-modulated tones in the auditory nerve of the cat. *JASA*; 91, 215-232.

Kay, R. H., and Matthews, D. R. (1972). On the existence in the human auditory pathway of channels selectively tuned to the modulation present in FM tones. *J. Physiol. (Lond.)*; 255, 657-677.

Khanna, S. M., and Teich, M. C. (1989a). Spectral characteristics of the responses of primary auditory-nerve fibers to amplitude-modulated signals. *Hear. Res.*; 39, 143-157.

Khanna, S. M., and Teich, M. C. (1989b). Spectral characteristics of the responses of primary auditory-nerve fibers to frequency-modulated signal *Hear. Res.*; 39, 159-175.

Kiang NYS, Liberman MC, and Levine RA., (1976). Auditory-nerve activity in cats exposed to ototoxic drugs and high intensity sounds. *Ann Otol Rhinol Laryngol*; 85,752-768.

Kiang NYS, Watanabe T, Thomas EC, and Clark LF., (1965). *Discharge patterns of single fibers in the cat's auditory nerve*. MIT Monograph No. 35. Cambridge: MIT Press, 1965.

Kim, Y., Aoyagi, M., and Koike, Y., (1994). Measurement of cochlear basilar membrane traveling wave velocity by derived ABR. *Acta Otolaryngol. Suppl.*; 511, 71-76.

Kimberley, B.P., Brown, D.K., and Eggermont, J.J., (1993). Measuring human

cochlear traveling wave delay using distortion product emission phase responses. *JASA*; 94, 1343-1350.

Kohn M, Lifshitz K, and Litchfield D., (1978) Averaged evoked potentials and frequency modulation. *Electroencephalogr Clin Neurophysiol*; 45(2):236-43.

Kunov, H., Madsen, P.B., and Sokolov, Y., (1997). Single system combines five audiometric devices. *Hearing Journal*; 50(3), 32-34.

Kuwada, S., Batra, R., and Maher, V.L., (1986). Scalp potentials of normal and hearing-impaired subjects in response to sinusoidally amplitude-modulated tones. *Hearing Research*; 21, 179-192.

Lacher-Fougère, S., and Demany, L. (1998). Modulation detection by normal and hearing-impaired listeners. *Audiology*; 37, 109-121.

Langner, G, and Schreiner, CE., (1988). Periodicity coding in the the inferior colliculus of the cat. I. Neuronal mechanisms. *J Neurophysiol*; 60:1799-1822.

Langner, G., (1992). Periodicity coding in the auditory system. *Hear. Res.*; 60, 115-142.

Langner, G., and Schreiner, C.E., (1988). Periodicity coding in the inferior colliculus of the cat. *JASA*; 63, 1799-1822.

Langner, G., Schreiner, C. E., and Biebel, U. W., (1998). Functional implications of frequency and periodicity coding in the auditory midbrain. *In Psychophysical and Physiological Advances in Hearing.* edited by A. R. Palmer, A. Rees, A. Q. Summerfield, and R. Meddis, (Whurr, London, UK, 1998), pp. 277-285.

Levi, E.C., Folsom, R.C., and Dobie, R.A., (1993). Amplitude-modulation following response (AMFR): effects of modulation rate, carrier frequency, age, and state. *Hear. Res.*; 68, 42-52.

Linden, R.D., Campbell, K.B., Hamel, G., and Picton, TW., (1985). Human auditory steady state evoked potentials during sleep. *Ear Hear* ;6,167-174.

Lins OG, Picton TW, Boucher B, Durieux-Smith A, Champagne SC, Moran LM, Perez-Abalo, MC, Martin V, Savio G., (1996). Frequency-specific audiometry using steady-state responses. *Ear Hear* ;17: 81-96.

Lins, O.G., and Picton, T.W., (1995). Auditory steady-state responses to multiple simultaneous stimuli. *Electroencephalogr. Clin. Neurophysiol.*; 96, 420-432.

Lins, O.G., Picton, P.E., Picton, T.W., Champagne, S.C., Durieux-Smith, A., (1995). Auditory steady-state responses to tones amplitude-modulated at 80-110 Hz. *JASA*; 97, 3051-3063.

Lütkenhöner, B., (1991). Theoretical considerations on the detection of evoked responses by means of the Rayleigh test. *Acta Otolaryngologica Supplement;* 491, 52-60.

Madler, C, and Pöppel, E., (1987). Auditory evoked potentials indicate the loss of neuronal oscillations during general aneasthesia. *Naturwissenschaften;* 74:42-43.

Maiste, A., and Picton, T., (1989). Human auditory evoked potentials to frequency-modulated tones. *Ear and Hearing;* 10, 153-160.

Margolis, R.H., Rieks, D., Fournier, E.M., and Levine, S.E., (1995). Tympanic electrocochleography for diagnosis of Meniere's disease. *Arch. Otolaryngol. Head Neck Surg.*; 121, 44-55.

Mauer, G., and Döring, W.H., (1999). Generators of amplitude modulation following response (AMFR). Paper presented at the June 1999 meeting of the International Evoked Response Audiometry Study Group, Tromsø, Norway

Mendelson, J.R., Schreiner, C.E., Sutter, M.L., and Grasse, K.L. (1993). Functional topography of cat primary auditory cortex: responses to frequency-modulated sweeps. *Exp. Brain Res.*; 94, 65-87.

Møller, A.R., (1972). Coding of amplitude and frequency modulated sounds in the cochlear nucleus of the rat. *Acta Physiol. Scand.*; 86, 223-238.

Møller, A.R., (1974). Response of units in the cochlear nucleus to sinusoidally amplitude-modulated tones. *Exp Neurol* ;45:104-107.

Møller, A.R., (1974). Coding of sounds with rapidly varying spectrum in the cochlear nucleus. *JASA*; 55, 631-640.

Møller, A.R., (1977). Coding of time-varying sounds in the cochlear nucleus. *Audiology*; 17, 446-468.

Møller, A.R., and Jannetta. (1985). Neural Generators of the Auditory Brainstem Resonse. In: Jacobson, JT, ed. *The Auditory Brainstem Response*, 1985: 13-31.

Moore, B.C., (1995), Frequency analysis and masking. In: Moore BCJ, ed. *Hearing. Handbook of Perception and Cognition*, Second Edition. New York: Academic Press:161-205.

Moore, B.C., and Sek, A., (1994). Effects of carrier frequency and background noise on the detection of mixed modulation. *JASA*; 96, 741-751.

Moore, B.C., and Sek, A., (1996). Detection of frequency modulation at low modulation rates: evidence for a mechanism based on phase locking. *JASA*; 100, 2320-2331.

Moulin, A., and Kemp, D.T., (1996a). Multicomponent acoustic distortion product otoacoustic emission phase in humans. I. General characteristics. *JASA*; 100, 1617-1639.

Moulin, A., and Kemp, D.T., (1996b). Multicomponent acoustic distortion product otoacoustic emission phase in humans. II. Implications for distortion product otoacoustic emissions generation. *JASA*; 100,1640-1662.

Munro, K.J., Smith, R., and Thornton, A.R., (1995). Difficulties experienced in implementing the ABR travelling wave velocity (Delta V) technique with two commercially available systems. *Br. J. Audiol.*; 29, 23-29.

Neely, S.T., Norton, S.J., Gorga, M.P., and Jesteadt, W., (1988). Latency of auditory brain-stem responses and otoacoustic emissions using tone-burst stimuli. *JASA*; 83, 652-656.

Nomoto M, Suga N, and Katsuki Y., (1964). Discharge pattern and inhibition of primary auditory nerve fibers in the monkey. *J Neurophysiol*; 27:768-787.

Nordstrom, M.A, Mapletoft E.A., and Miles,T.S., (1995). Spike-train acquisition, analysis and real-time experimental control using a graphical programming language (LabView). *Journal of Neuroscience Methods*; 62, 93-102.

O'Mahoney, C., and Kemp, D.T., (1995). Distortion product otoacoustic emission delay measurement in human ears. *JASA*; 97, 1-15.

Ozimek, E., and Sek, A. (1987). Perception of amplitude and frequency modulated signals (mixed modulation. *JASA*; 82, 1598-1603.

Parker, D.J., and Thornton, A.R., (1978). Cochlear travelling wave velocities calculated from the derived components of the cochlear nerve and brainstem evoked responses of the human auditory system. *Scand. Audiol.*; 7, 67-70.

Patterson, R., (1994). The sound of a sinusoid: spectral models. *JASA*; 96, 1409-1418.

Patuzzi R, and Sellick PM., (1983). A comparison between basilar membrane and inner hair cell receptor potential input-output functions in the guinea pig

cochlea. *JASA*; 74,1734-1741.

Patuzzi, R., (1996). Cochlear micromechanics and macromechanics. In: Dallos, P., Popper, A.N., Fay, R.R. (Eds.), *Springer handbook of auditory research*. Springer, New York, pp. 187-223.

Phillips, D. P., Mendelson, J. R., Cynader, M. S., and Douglas, R. M. (1985). Responses of single neurones in cat auditory cortex to time-varying stimuli: frequency-modulated tones of narrow excursion. *Exp. Brain Res.* 58, 443-454.

Picton, T.W., Durieux-Smith, A., Champagne, S.C., Whittingham, J., Moran, L.M., Giguère, C., and Beauregard,Y.,(1998). Objective evaluation of aided thresholds using auditory steady-state responses. *Journal of the Ameriademy of Audiology;* 9, 315-331.

Picton, T.W., Linden, R.D., Hamel, G., and Maru, J.T., (1983) . Aspects of averaging. *Seminars in Hearing*; 4, 327-341.

Picton, T.W., Ouellette, J., Hamel, G., and Smith, A.D., (1979). Brainstem evoked potentials to tonepips in notched noise. *J. Otolaryngol.*; 8, 289-314.

Picton, T.W., Skinner, C.R., Champagne, S.C., Kellett, A.J., and Maiste, A.C. (1987). Potentials evoked by the sinusoidal modulation of the amplitude or frequency of a tone. *JASA*; 82, 165-178

Picton,T.W., Vajsar, J., Rodriguez, R., and Campbell, K.B., (1987). Reliability estimates for steady-state evoked potentials. *Electroencephalography and Clinical Neurophysiology*; 68, 119-131.

Plourde G, and Picton TW., (1990). Human auditory steady-state responses during general anaesthesia. *Anaest Analg*; 71,460-468.

Plourde, G., Stapells, D.R., and Picton, T.W., (1991). The human auditory steady-state evoked potentials. *Acta Otolaryngol. Suppl.* 491, 153-159.

Poindessault, J.P., Beauquin, C., and Gaillard, F., (1995). Stimulation, data acquisition, spikes detection and time/rate analysis with a graphical programming system: an application to vision studies. *Journal of Neuroscience Methods;* 59, 225-235.

Poon, P.W., Chen, X., and Cheung, Y.M., (1992). Differences in FM response correlate with morphology of neurons in the rat inferior colliculus. *Exp. Brain Res.* 91, 94-104.

Press, W.H, Teukolsky, S.A., Vetterling, W.T., and Flannery, B.P., (1992).

*Flannery Numerical recipes in C: the art of scientific computing*. 2nd ed. pp. 623-626. (Cambridge University Press, Cambridge, 1992)

Preuss, A., and Muller-Preuss P., (1990) Processing of amplitude-modulated sounds in the medial geniculate body of squirrel monkeys. *Exp Brain Res*; 79,207-211.

Rance, G., Rickards,F.W., Cohen,L.T. , De Vidi, S., and Clark, G.M. (1995). The automated prediction of hearing thresholds in sleeping subjects using auditory steady-state evoked potentials. *Ear and Hearing;* 16, 499-507.

Rance,G., Dowell, R.C., Rickards, F.W., Beer, D.E., and Clark.G.M., (1998). Steady-state evoked potential and behavioral hearing threshold in a group of children with absent click-ABR. *Ear and Hearing*; 19, 48-61.

Rees, A., and Møller, R., (1983). Responses of neurons in the inferior colliculus of the rat to AM and FM tones. *Hear. Res.*; 10, 301-330.

Rees, A., and Palmer, A.R., (1989). Neuronal responses to amplitude-modulated and pure-tone stimuli in the guinea pig inferior colliculus, and their modification by broadband noise. *JASA*; 85, 1978-1994.

Regan D, and Cartwright RF., (1970). A method for measuring the potentials evoked by simultaneous stimulation of different retinal regions. *Electroenceph Clin Neurophysiol*; 28,314-319.

Regan, D, and Regan, MP., (1988). The transducer characteristics of the hair cells in the human inner ear: A possible objective measure. *Brain Res*; 438,363-365.

Regan, D., (1966). Some characteristics of average steady-state and transient responses evoked by modulated light. *Electroencephalogr. Clin. Neurophysiol.*; 20, 238-248.

Regan, D., (1989). *Human Brain Electrophysiology: Evoked Potentials and Evoked Magnetic Fields in Science and Medicine*. Amsterdam: Elsevier, 1989: pp 34-43, 70-134 and 275-278.

Regan, D., and Heron, J.R., (1969). Clinical investigation of lesions of the visual pathway: a new objective technique. *Journal of Neurology, Neurosurgery and Psychiatry*;32, 479-483.

Regan, D., Heron, J.R., and Cartwright, R.F., (1970). Simultaneous analysis of potentials evoked by focal illumination of two retinal areas by flicker and pattern stimuli; application to migraine and to visual field investigations. *Electroencephalography and Clinical Neurophysiology*; 29, 105-106.

Regan, M.P., (1994). Linear half-wave rectification of modulated sinusoids. *Appl Math Comput*;62,61-79.

Rhode W.S., NS Greenberg S., (1992). Physiology of the cochlear nuclei. In: Popper AN, Fay RR, eds. *The Mammalian Auditory Pathway: Neurophysiology*. New York: Springer Verlag,:94-152

Rhode, W.S., Robles, L., (1974). Evidence from Mössbauer experiments for nonlinear vibration in the cochlea. *JASAer*; 55,588-596.

Rickards, F.W., Tan, L.E., Cohen, L.T., Wilson, O.J., Drew, J.H., and Clark, G.M.,(1994), Auditory steady-state evoked potential in newborns. *British Journal of Audiology;* 28, 327-337.

Rickards, F.W., and Clark, G.M., (1984). *Steady state evoked potentials to amplitude-modulated tones, in Evoked Potentials II*, eds. R.H. Nodar and C.Barber, pp. 163-168 (Butterworth, Boston, 1984)

Ricketts, C., Mendelson, J. R., Anand, B., and English, R., (1998). Responses to time-varying stimuli in rat auditory cortex. *Hear. Res.*; 123, 27-30.

Robles, L., Ruggero, M.A., and Rich, N.C., (1986). Basilar membrane mechanics at the base of the chinchilla cochlea. I. Input-output functions, tuning curves, and response phases. *JASA*; 80,1364-1374.

Rodriguez, R., Picton, T., Linden, D., Hamel, G., and Laframboise, G., (1986). Human auditory steady state responses: effects of intensity and frequency. *Ear Hear.*; 7, 300-313.

Rose, J.E., Hind, J.E., Anderson, D.J., and Brugge, J.F. (1971). Some effects of stimulus intensity on response of auditory nerve fibers in the squirrel monkey. *J. Neurophysiol.* 34, 685-699.

Rosenthal, R., (1991). *Meta-Analytic Procedures for Social Research* (Sage, London, UK, 1991), Chap. 6, pp. 59-88.

Ruggero, M.A., (1992). Physiology and coding of sound in the auditory nerve. In: Popper, A.N., Fay, R.R. (Eds.), *Springer handbook of auditory research*. Springer-Verlag, New York,pp. 35-93.

Ruggero, M.A., (1994). Cochlear delays and traveling waves: comments on 'Experimental look at cochlear mechanics'. *Audiology*; 33, 131-142.

Rupert A, Moushegian G, and Galambos R. (1963). Unit response to sound from auditory nerve of the cat. J Neurophysiol; 26,449-465.

Russell, IJ, and Sellick, PM., (1978). Intracellular studies of hair cells in the mammalian cochlea. *J Physiol* ;284:261-290.

Saberi, K., (1998). Modeling interaural-delay sensitivity to frequency modulation at high frequencies. *JASA*; 103, 2551-2564.

Saberi, K., and Hafter, E.R., (1995). A common neural code for frequency- and amplitude-modulated sounds. *Nature*; 374, 537-539.

Sachs, M.B., and Abbas, P.J. (1974). Rate versus level functions for auditory-nerve fibers in cats: tone- burst stimuli. *JASA* 56, 1835-1847.

Sachs, MB, and Kiang NY-S.,(1968). Two-tone inhibition in auditory nerve fibers. *JASA*; 43:1120-1128.

Santarelli, R., Maurizi, M., Conti, G., Ottaviani, F., Paludetti, G., and Pettorossi, V.E., (1995). Generation of human auditory steady-state responses (SSRs). II: Addition of responses to individual stimuli. *Hear. Res.* 83, 9-18.

Sato, H., Sando, I., and Takahashi, H., (1991). Sexual dimorphism and development of the human cochlea. Computer 3-D measurement. *Acta Otolaryngol.;* 111, 1037-1040.

Schuster, A., (1898). On the investigation of hidden periodicities with application to a supposed 26 day period of meteorological phenomena. *Terrestrial Magnetism & Atmospheric Electricity;* 3, 13-41.

Sek, A., and Moore, B. C. (1996). Detection of auditory "events" based on amplitude and frequency modulation. *JASA*; 100, 2332-2340.

Shannon, R. V., Zeng, F. G., Kamath, V., Wygonski, J., and Ekelid, M. (1995). Speech recognition with primarily temporal cues. *Science*; 270, 303-304.

Sheft,S. and Yost, W.A., (1990). Temporal integration in amplitude modulation detection. *JASA*; 88, 796-805.

Shirane, M., and Harrison, R.V., (1991). The effects of long and short term profound deafness on the responses of inferior colliculus to electrical stimulation of the cochlea. *Acta Otolaryngol. Suppl.*; 489, 32-40.

Sinex, D. G., and Geisler, C. D. (1981). Auditory-nerve fiber responses to frequency-modulated tones. *Hear. Res.*; 4, 127-148.

Smith RL., M.L. Brachman, and R.D Frisnina (1985). Sensitivity of auditory-nerve fibers to changes in intensity: a dichotomy between decrements and

increments. *JASA;* 78,1310-1316.

Smith, R.L. (1998). Auditory-nerve responses to amplitude modulation: Some implications for synaptic transmission. In *Psychophysical and Physiological Advances in Hearing.* edited by A. R. Palmer, A. Rees, A.Q. Summerfield, and R. Meddis, (Whurr, London, UK, 1998), pp. 162-169.

Spoor, A., Timmer, F., and Odenthal, D. (1969). The evoked auditory response (ear) to intensity modulated and frequency modulated tones and tone bursts. *Audiology*; 8, 410-415.

Stanley, W.D., (1982). *Electronic Communication Systems*. pp 141-213 (Reston Publishing, Reston, Virginia, 1982).

Stapells, D.R., Linden, D., Suffield, J.B., Hamel, G., and Picton, T.W., (1984). Human auditory steady state potentials. *Ear Hear.*; 5, 105-113.

Stapells, D.R., Makeig, S., and Galambos, R., (1987). Auditory steady-state responses: threshold prediction using phase coherence. *Electroencephalogr. Clin. Neurophysiol.*; 67, 260-270.

Stapells, D.R., Picton, T.W., and Durieux-Smith, A., (1993). *Electrophysiologic measures of frequency-specific auditory function In Principles and Applications of Auditory Evoked Potentials* ed. J.T. Jacobson, pp. 251-283 (Allyn and Bacon, New York, 1993).

Stapells, DR, Galambos R, Costello JA, and Makeig S., (1988). Inconsistency of auditory middle latency and steady-state responses in infants. *Electroenceph Clin Neurophysiol*; 71:289-295.

Starr A., and Don M. (1988). Brain Potentials Evoked by Acoustic Stimuli. In *Human Event-Related Potentials, EEG Handbook (revised series, vol 3)* edited by T.W. Picton (Elsevier, Amserdam-New York-London, 1988) p 97-157.

Tallal, P. Miller, S. L., Bedi, G., Byma, G. Wang, X., Nagarajan, S. S., Schreiner, C., Jenkins, W. M., and Merzenich, M. M. (1996). Language comprehension in language-learning impaired children improved with acoustically modified speech. *Science*; 271, 81-84.

Tansley, B. W., and Regan, D. (1979). Separate auditory channels for unidirectional frequency modulation and unidirectional amplitude modulation. *Sens Processes*; 3, 132-140.

Tansley, B. W., and Suffield, J. B. (1983). Time course of adaptation and recovery

of channels selectively sensitive to frequency and amplitude modulation. *JASA*; 74, 765-775.

Teas, D.C., Eldredge, D.H., and Davis, H., (1962). Cochlear responses to acoustic transients: an interpretation of whole-nerve action potentials. *JASA*; 34, 1438-1459.

Thornton, A.R., and Farrell, G., (1991). Apparent travelling wave velocity changes in cases of endolymphatic hydrops. *Scand. Audiol.*; 20, 13-18.

Tian, B., and Rauschecker, J. P. (1994). Processing of frequency-modulated sounds in the cat's anterior auditory field. *J. Neurophysiol.*; 71, 1959-1975.

Valdes, J. L., Perez-Abalo, M. C., Martin, V., Savio, G., Sierra, C., Rodriguez, E., and Lins, O. (1997). Comparison of statistical indicators for the automatic detection of 80 Hz auditory steady state responses. *Ear Hear.* 18, 420-429.

Van der Tweel, L.H., and Verduyn Lunel, H.F.E., (1965). Human visual responses to sinusoidally modulated light. *Electroencephalogr. Clin. Neurophysiol.*;18, 587-598.

Van Tasell, D. J., Soli, S. D., Kirby, V. M., and Widin, G. P. (1987). Speech waveform envelope cues for consonant recognition. *JASA* 82, 1152-1161.

Victor, J.D. and Mast, J., (1991). A new statistic for steady-state evoked potentials. *Electroencephalography and Clinical Neurophysiology*; 78, 378-388. published erratum appears in Electroencephalography and Clinical Neurophysiology 83 (1992) 270.

Viemeister, N.F., (1979). Temporal modulation transfer functions based upon modulation thresholds. *JASA*; 66, 1364-1380.

Von Békésy, G., (1960). *Experiments in hearing.* McGraw-Hill, New York.

Von Békésy, G., (1963). Hearing theories and complex sounds. *JASA* 35, 588-601.

Wada S.I., and Starr A., (1983). Generation of auditory brain stem responses (ABRs). III. Effects of lesions of the superior olive, lateral lemniscus and inferior colliculus on the ABR in guinea pig. *Electroencephalogr Clin Neurophysiol;* 56(4),352-66

Wei, WWS., (1990). Time series analysis: Univariate and multivariate methods. Redwood City, CA: Addison-Wesley, 1990, Estimation of the spectrum: 256-287.

Whitfield, I.C., and Evans, E.F., (1965). Responses of auditory cortical neurons to stimuli of changing frequency. *J. Neurophysiol.*; 28, 655-672.

Wilson, A. S., Hall, J. W., and Grose, J. H. (1990). Detection of frequency modulation (FM) in the presence of a second FM tone. *JASA* 88, 1333-1338.

Winter, I.M., Robertson, D., and Yates, G.K. ,(1990). Diversity of characteristic frequency rate-intensity functions in guinea pig auditory nerve fibers. *Hear. Res.*; 45, 191-202.

Yates, G.K., (1987). Dynamic effects in the input/output relationship of auditory nerve. *Hear. Res.* 27, 221-230.

Yates, G.K., (1995). Cochlear structure and function. In: Moore BCJ, ed. *Hearing. Handbook of Perception and Cognition*, Second Edition. New York: Academic Press, 1995:41-74.

Yates, G.K., Winter, I.M., and Robertson, D., (1990). Basilar membrane nonlinearity determines auditory nerve rate-intensity functions and cochlear dynamic range. *Hear. Res.* 45, 203-219.

Yost, W. A., and Sheft, S. (1989). Across-critical-band processing of amplitude-modulated tones. *JASA*; 85, 848-857.

Zhao, H. B., and Liang, Z. A. (1997). Temporal encoding and transmitting of amplitude and frequency modulations in dorsal cochlear nucleus. *Hear. Res.* 106, 83-94.

Zurek PM, and Rabinowitz, WM.,(1995). System for testing adequacy of human hearing. United States Patent 5,413,114. May 9, 1995.

Zurek, P. M. (1992). Detectability of transient and sinusoidal otoacoustic emissions. *Ear Hear.*; 13, 307-310.

Zwicker, E. (1962). Direct comparisons between the sensations produced by frequency modulation and amplitude modulation. *JASA*; 34, 1425-1430.

Zwicker, E., and Fastl, H. (1990). *Psychoacoustics: Facts and Models* (Springer-Verlag, New York).

Zwislocki, J.J., (1991). What is the cochlear place code for pitch. *Acta Otolaryngol. (Stockholm)*; 111, 256-262.

**And they lived happily ever after...**

**The End.**